

**Mammalian *m*-AAA Proteases as
Key Regulators of Mitochondrial Function –
Analysis of Dominant Negative Mutant Variants**

Inaugural-Dissertation

zur

Erlangung des Doktorgrades

der Mathematisch-Naturwissenschaftlichen Fakultät

der Universität zu Köln



vorgelegt von

Ines Raschke

aus Hildesheim

Köln, 2009

**Mammalian *m*-AAA Proteases as
Key Regulators of Mitochondrial Function –
Analysis of Dominant Negative Mutant Variants**

Inaugural-Dissertation

zur

Erlangung des Doktorgrades
der Mathematisch-Naturwissenschaftlichen Fakultät
der Universität zu Köln



vorgelegt von

Ines Raschke

aus Hildesheim

Köln, 2009

ये निभन्थ प्यरे विन्स को समर्पि है

Berichtersteller:

Professor Dr. Thomas Langer

Professor Dr. Mats Paulsson

Tag der mündlichen Prüfung: 15. Mai 2009

Abstract

To ensure the removal of excess and non-assembled proteins, mitochondria require a protein quality control system which is constituted by several proteases located in different compartments of mitochondria. *m*-AAA proteases, oligomeric ATP-dependent metallopeptidases, are key components of this system active at the matrix side of the inner membrane. Human *m*-AAA proteases build up homo- and hetero-oligomeric complexes composed of AFG3L2 and SPG7. Mice express a third subunit, Afg3l1, resulting in a variety of possible isoenzymes. Interestingly, mutations or deletions of one subunit of mammalian *m*-AAA proteases cause neurodegeneration in distinct regions of the central and peripheral nervous system in mouse and human, indicating that different tissues, in particular neurons, require a specific subset of isoenzymes. The yeast *m*-AAA protease can also act as a processing enzyme regulating mitochondrial biogenesis, raising the question which activity is linked to the pathogenesis of the associated diseases. Which molecular functions of mammalian *m*-AAA proteases contribute to different disease states are poorly understood. Mammalian *m*-AAA proteases have been linked to the processing of the dynamin-like GTPase OPA1 implying a role of mammalian *m*-AAA proteases in mitochondrial fusion. Therefore, to further elucidate the function of mammalian *m*-AAA proteases it was necessary to identify more substrates of the proteases.

In this study, a mutation in the Walker B motif of the ATPase domain of Afg3l2/AFG3L2 was identified as dominant negative substrate trap. Using this novel approach, expression of dominant negative mutant variants in human cells, interacting partners and putative substrates have been identified providing further insights into the molecular functions of mammalian *m*-AAA proteases in mitochondria. These proteases were demonstrated to be present in a supercomplex with prohibitins together regulating cell proliferation and mitochondrial fusion by stabilizing I-OPA1. In parallel, *m*-AAA proteases interact with SLP2 and control stress induced mitochondrial hyperfusion pointing to the formation of another supercomplex containing the proteases and SLP2. The precursor of AFG3L2 itself and MICS1, an inner membrane protein crucial for cristae organization and apoptosis, were identified as possible substrates.

Linking *m*-AAA protease functions to mitochondrial fusion, cristae organization and apoptosis may help to unravel the molecular mechanisms underlying neurodegeneration associated with mutations in human *m*-AAA proteases.

Table of contents

ABSTRACT	5
1. INTRODUCTION	10
1.1. Mitochondria in life and pathogenesis	10
1.2. Oxidative phosphorylation system (OXPHOS)	11
1.2.1. Defects of the oxidative phosphorylation system	12
1.3. Mitochondrial dynamics	14
1.3.1. Mitochondrial division	16
1.3.2. Mitochondrial fusion	17
1.3.3. Inner membrane dynamics	20
1.3.3.1. The ATP synthase and cardiolipin as cristae organizers?	20
1.3.3.2. Cristae remodelling during apoptosis	21
1.3.3.3. Interfering with OPA1 processing – a trigger for apoptosis?	22
1.3.4. Pathogenic alterations of mitochondrial dynamics	23
1.3.5. Regulation of mitochondrial dynamics	25
1.3.5.1. Regulation by post-translational modifications	25
1.3.5.2. Regulation by the lipid milieu	25
1.3.5.3. Regulation by degradation and processing events	26
1.4. Protein quality control in mitochondria	28
1.4.1. AAA proteases as key regulators of protein quality control and mitochondrial biogenesis	29
1.4.2. <i>m</i> -AAA proteases and prohibitins – highly conserved supercomplexes in the inner mitochondrial membrane	32
1.4.3. Mammalian <i>m</i> -AAA proteases	34
1.4.3.1. Phenotypes associated with defects in mammalian <i>m</i> -AAA protease subunits	35
1.4.4. What determines a substrate? How is it recognized by AAA-proteases?	37
1.5. Aims of the thesis	39
2. MATERIAL AND METHODS	40
2.1. Material	40
2.1.1. Chemicals	40
2.1.2. <i>E. coli</i> strains	40
2.1.3. Mammalian cell lines	40
2.1.4. Generation of expression plasmids	41
2.1.5. Oligonucleotides	42
2.1.6. Antibodies	42
2.2. Molecular biological methods	43
	6

2.3. Cell biological methods	44
2.3.1. Cell culture	44
2.3.2. Transfections	44
2.3.3. FlpIn T-REx system and selection of stable transformants	44
2.3.4. β -galactosidase activity assay	45
2.3.5. Cell proliferation assay	45
2.3.6. Measurement of respiratory activities	46
2.3.6.1. Oxygen consumption in intact cells	46
2.3.6.2. Assessment of mitochondrial membrane potential	46
2.3.6.3. Measurement of cellular ATP contents	47
2.3.7. Monitoring mitochondrial morphology using fluorescence microscopy	47
2.3.8. Analysis of cellular apoptosis	48
2.3.9. Isolation of mitochondria from tissue culture cells	48
2.3.10. Analysis of mitochondrial phospholipid composition	49
2.3.10.1. Phospholipid extraction	49
2.3.10.2. Phosphate determination	49
2.3.10.3. Thin-layer chromatography (TLC)	49
2.4. Protein biochemistry methods	50
2.4.1. Preparation of protein lysates from tissue culture cells	50
2.4.2. Crosslinking of OPA1	50
2.4.3. Polyacrylamide gel electrophoresis (PAGE)	51
2.4.3.1. SDS-PAGE	51
2.4.3.2. BN/CN-PAGE and in-gel-activity stainings	51
2.4.3.3. 2D-electrophoresis: BN-SDS-PAGE and dSDS-PAGE	52
2.4.4. Metal affinity chromatography of His-tagged AFG3L2	53
2.5. Immunological methods	54
2.5.1. Immunoblotting	54
2.5.2. Co-immunoprecipitation	54
3. RESULTS	56
3.1. Mutational analysis of mammalian <i>m</i>-AAA proteases	56
3.2. Generation of stable cell lines expressing mouse or human AFG3L2 variants	58
3.2.1. The FlpIn T-REx system	58
3.2.2. Selection for AFG3L2 overexpressing cell lines	60
3.3. Mutation of the Walker B motif has a dominant-negative effect on cell proliferation	61
3.4. Mammalian <i>m</i>-AAA proteases are required for mitochondrial fusion	63
3.4.1. <i>m</i> -AAA proteases regulate the stability of long OPA1 isoforms	65
3.4.1.1. Expression of a dominant negative Walker B mutant leads to an accumulation of short OPA1 isoforms	67
3.4.1.2. The energy metabolism is not impaired in cells expressing dominant negative Walker B mutants	67
3.4.1.3. Dominant-negative mutation in Walker B induces destabilization of respiratory chain supercomplexes	70

3.4.1.4.	Induced OPA1 processing at site S1 and increased turnover of non cleavable OPA1 variants	74
3.4.1.5.	OPA1 co-immunoprecipitates with overexpressed Afg3L2	75
3.4.1.6.	Analysis of the OPA1 complex and apoptotic sensitivity	76
3.4.2.	<i>m</i> -AAA proteases play a role in stress induced hyperfusion via interaction with Stomatin-like protein 2	79
3.5.	<i>m</i>-AAA proteases interact with MICS1	82
3.5.1.	AFG3L2 harboring a mutation in the Walker B motif as a substrate trap	82
3.5.2.	MICS1 is not processed by <i>m</i> -AAA proteases	84
4.	DISCUSSION	86
4.1.	Dominant-negative Walker B mutation – a novel approach to study mammalian <i>m</i>-AAA proteases	86
4.2.	Mammalian <i>m</i>-AAA proteases affect the stability of respiratory chain supercomplexes	88
4.3.	The <i>m</i>-AAA protease-prohibitin complex is indispensable for cell proliferation	90
4.4.	<i>m</i>-AAA proteases are essential for mitochondrial fusion activity by stabilizing I-OPA1	92
4.5.	Identification of novel interacting partners or putative substrates of mammalian <i>m</i>-AAA proteases	96
4.5.1.	<i>m</i> -AAA proteases and SLP2 are crucial for mitochondrial hyperfusion	96
4.5.2.	<i>m</i> -AAA proteases interact with MAIP1 (<i>m</i> -AAA protease interacting protein 1)	99
4.5.3.	AFG3L2 is autocatalytically processed	100
4.5.4.	MICS1 is a putative substrate of mammalian <i>m</i> -AAA proteases	101
4.6.	<i>m</i>-AAA proteases and prohibitins – highly conserved complexes with overlapping functions?	103
4.7.	Translating cellular phenotypes to neurodegenerative diseases	104
5.	REFERENCES	108
6.	APPENDIX	129
6.1.	List of abbreviations	129
6.2.	Mass spectrometric analysis	131
6.3.	Protein sequence analysis	134
6.3.1.	<i>m</i> -AAA proteases	134
6.3.2.	MAIP1 and JHEbdp29	138
6.3.3.	MICS1 and YccA	138

7.	ZUSAMMENFASSUNG	139
8.	DANKSAGUNG	141
9.	EIDESSTATTLICHE ERKLÄRUNG	142
10.	LEBENS LAUF	143

1. Introduction

1.1. *Mitochondria in life and pathogenesis*

It is widely believed that the mitochondrion was originally derived from a free-living α -prokaryotic organism which explains the presence of a compact mitochondrial DNA (mtDNA). The genome encodes for key subunits of the electron transport chain and RNA components needed for mitochondrial translation (Falkenberg *et al.*, 2007). Mitochondria are double-membrane bound organelles that are indispensable for the viability of a eukaryotic cell. It is therefore not surprising that numerous proteins involved in the biogenesis of these organelles are encoded by essential genes (Neupert and Herrmann, 2007). Mitochondria perform a variety of functions in anabolism and catabolism, energy conversion, apoptosis, calcium signaling and reactive oxygen production (Pinton *et al.*, 2008; Scheffler, 1999). In the yeast *Saccharomyces cerevisiae*, none of these functions determine the essential character of the organelles. For instance, the citric acid cycle or oxidative phosphorylation can be inactivated by targeted gene deletions or by the loss of mitochondrial DNA without affecting the viability of yeast cells in the presence of fermentable carbon sources. However, the essential function of mitochondria is the Iron-sulfur (Fe/S) protein biogenesis (Lill *et al.*, 2005). Fe/S proteins are involved in a wide variety of cellular processes such as respiration, cofactor biosynthesis, ribosome biogenesis, regulation of gene expression, and DNA-RNA metabolism (Lill and Muhlenhoff, 2008). Therefore, it is not surprising that a loss-of-function mutation in one of the genes involved in iron-sulfur cluster biogenesis *FXN* (*frataxin*) leads to the clinical syndrome Friedreich ataxia (FRDA) which is characterized by impaired mitochondrial iron storage and metabolism (Campuzano *et al.*, 1997; Campuzano *et al.*, 1996).

Mitochondria are complex organelles whose dysfunction are responsible for a broad spectrum of human diseases (DiMauro and Schon, 2008). Mitochondrial dysfunctions cause over 50 diseases ranging from neonatal fatalities to adult onset neurodegeneration and are probably contributing to cancer and type II diabetes (DiMauro, 2004; DiMauro and Schon, 2003; Lowell and Shulman, 2005; Wallace, 2005).

1.2. Oxidative phosphorylation system (OXPHOS)

The mitochondrial oxidative phosphorylation system (OXPHOS) is the final biochemical pathway for the vast majority of eukaryotes to produce the principal fuel of the cell – ATP (Saraste, 1999). The essential constituents are commonly shared and localized in the inner mitochondrial membrane, i.e., the four major protein complexes of the standard respiratory chain and the FoF₁-ATP synthase (complex V), together designated as **OXPHOS complexes** (Figure 1).

The complexes I (NADH: ubiquinone oxidoreductase), III (ubiquinol:cytochrome c oxidoreductase), and IV (cytochrome c oxidase, also referred to as COX) transduce the energy of nutritional compounds by vectorial proton translocation across the inner membrane. This energy is used by the FoF₁-ATP synthase to produce ATP from ADP and inorganic phosphate as well as a driving force for other processes like import of nuclear-encoded proteins into mitochondria. The two mobile redox components ubiquinone (Coenzyme Q) and cytochrome c act as cosubstrates in the respiratory chain. The smallest and most hydrophilic respiratory chain complex, succinate:ubiquinone oxidoreductase (complex II), incorporates the heterodimeric succinate dehydrogenase of the matrix-located citric acid cycle and feeds electrons from succinate oxidation into the respiratory chain without proton pumping [for review (Krause, 2007)].

However, there is substantial evidence that complexes I, III and IV in mitochondria of mammals and other organisms are organized as **supramolecular networks** in the inner membrane (Schägger and Pfeiffer, 2000). This view is strengthened by the fact that the mitochondrial inner membrane is structurally subdivided into two main areas, the **inner boundary membrane and the cristae**, which are separated from each other by cristae junctions (Frey *et al.*, 2002; Mannella, 2006; Reichert and Neupert, 2002; Zick *et al.*, 2009). In fact, the OXPHOS complexes are predominantly located in the protein-rich cristae and represent the most abundant protein components, thermodynamically favouring the aggregation into large supramolecular structures (Gilkerson *et al.*, 2003; Helms, 2002; Vereb *et al.*, 2003; Vogel *et al.*, 2006; Wurm and Jakobs, 2006). It is speculated that these supramolecular arrangements facilitate the channelling of the substrates ubiquinone and cytochrome c or similar enzymatic advantages. Metabolites can be directly delivered from one enzyme to the next. Experimental evidence is given by the fact that supercomplexes display an increased activity of complex I (Schägger and Pfeiffer, 2000). Therefore, supercomplexes are called respirasomes or metabolons

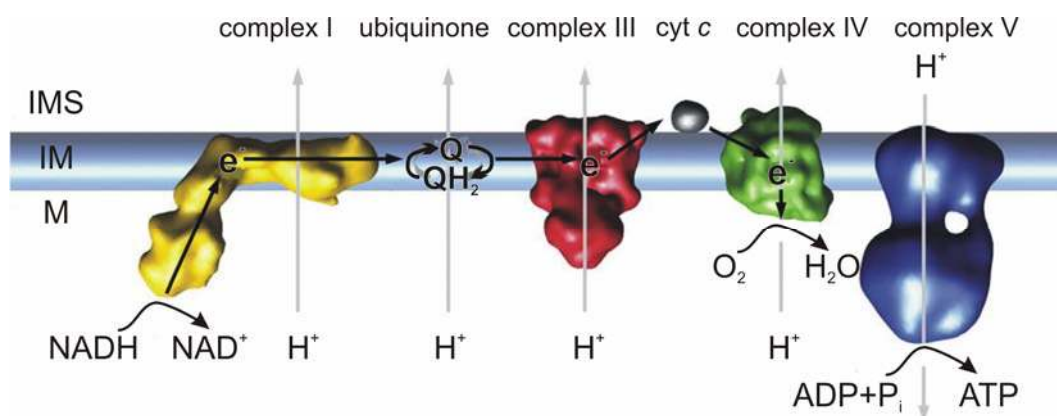


Figure 1: The mitochondrial respiratory chain.

The OXPHOS complexes generate an electrochemical gradient over the mitochondrial inner membrane (IM). NADH is oxidized to NAD⁺. The electrons (e⁻) are transferred from NADH via complex I (CI) and ubiquinone (Q) to CIII. Afterwards they pass through the peripheral e⁻-carrier cytochrome (cyt) c and CIV to the terminal acceptor oxygen, which is reduced to water. The electrochemical proton gradient is used by CV. Modified from (Vonck and Schäfer, 2009). IMS, intermembrane space; M, matrix; H⁺, proton.

(Krause, 2007; Krause *et al.*, 2004; Marques *et al.*, 2007; Schägger, 2001; Schägger and Pfeiffer, 2000; Wittig *et al.*, 2006; Wittig and Schägger, 2009). Another crucial function of respiratory chain supercomplexes appears to be the assembly or stabilization of complex I, the largest and most intricate respiratory complex. It is suggested that complex III and IV are involved to various extents in the assembly or stabilisation of complex I in mammals (Diaz *et al.*, 2006; McKenzie *et al.*, 2006; Schägger *et al.*, 2004). The mitochondrial ATP synthase dimerizes and forms higher oligomeric structures. These dimer ribbons enforce a strong local curvature on the membrane which is hypothesized to increase the local proton concentration and to thereby optimize its own performance (Strauss *et al.*, 2008). Notably, supercomplexes are necessary to keep cells and organisms in healthy condition (Wittig and Schägger, 2009).

1.2.1. Defects of the oxidative phosphorylation system

It is not surprising that a pathological change of the OXPHOS activity has definite consequences for the cell and the body. The OXPHOS can be directly or indirectly affected. A direct influence is characterized by mutations in genes which interfere either with the structure or the assembly of the various subunits and their prosthetic groups of the respiratory chain complexes and supercomplexes. Human OXPHOS diseases or mitochondrial encephalomyopathies are often characterized by multiple deficiencies of two or more respiratory complexes (Wittig and Schägger, 2009). They are especially

interesting from the genetic point of view because the respiratory chain is the only metabolic pathway in the cell that is under dual control of the mtDNA and the nuclear DNA (nDNA) (DiMauro, 2004). There remains a considerable lack of understanding of the pathogenic mechanism involved in the development of clinical symptoms and the deterioration seen in many patients. The central role of OXPHOS in metabolism suggests that many of these features are related to abnormal metabolic consequences of the defects (Munnich *et al.*, 1992; Smeitink *et al.*, 2006).

Of the approximately 90 proteins that build up the respiratory chain, 13 are encoded by mtDNA (Falkenberg *et al.*, 2007). Human mitochondrial DNA is a 16.569-kb circular, double stranded molecule, which contains 37 genes: besides the 13 structural genes, 2 rRNA and 22 tRNA genes (DiMauro and Schon, 2008; Falkenberg *et al.*, 2007). Disease related mutations are therefore not only found in protein coding genes, but also in genes which affect mitochondrial protein synthesis due to mutations in tRNA or rRNA genes. Most common diseases associated with protein-coding genes are NARP (neuropathy, ataxia, retinitis pigmentosa), MILS (maternally inherited Leigh syndrome, see below) and LHON (Leber's hereditary optic neuropathy). NARP and MILS are associated with mutations in the *ATPase6* gene (DiMauro, 2004; DiMauro and Davidzon, 2005). However, the mtDNA has lost more than 99 % of its original genes and most of its autonomy (DiMauro and Schon, 2008). Mitochondria now depend on nuclear factors for all basic functions. Disorders due to mutations in nDNA are very numerous since most respiratory chain subunits are nucleus-encoded – and, more importantly – because correct structure and functioning of the respiratory chain requires many steps, all of which are under the control of nDNA (DiMauro, 2004). Most mutations in nDNA encoded complex I or complex II subunits, cause Leigh syndrome (LS) which is characterized by neuropathological lesions already during early childhood caused by defective oxidative metabolism on the developing nervous system (DiMauro and Schon, 2008). Most mutations in complex I subunits cause LHON which is linked to mutations in both, mtDNA and nDNA. It leads to blindness in young adults. The pathology is linked to degeneration of retinal ganglion cells (Carelli *et al.*, 2007).

OXPHOS function and activity does not only depend on protein components but on the lipid environment as well. Complexes of the respiratory chain are embedded in the lipid milieu of the inner mitochondrial membrane (Wittig and Schägger, 2009). **Cardiolipin** (bisphosphatidyl glycerol) belongs to a subclass of phospholipids, in which backbones and head groups are formed from repeating units of phosphoryl and glycerol moieties (polyglycerophospholipids) (Schlame, 2008). It has a dimeric structure, i.e. it contains four

fatty acid chains. It is ubiquitous in eukaryotes and predominantly found in the mitochondrial inner membrane where it constitutes about 20% of the total lipids (Kent, 1995; Schlame *et al.*, 2000). It seems that the physical properties of cardiolipin allow a number of interactions that may have implications for the structural organization of biological membranes (Schlame, 2008). Loss of cardiolipin in yeast correlates with structural lability of the respiratory supercomplexes and with functional deficiency of the complex IV moiety that was found to be in an almost inactive but reversible resting state (Pfeiffer *et al.*, 2003). Milder defects in the cardiolipin (CL) biosynthesis pathway had similar effects. Deletion of Taz1 (tafazzin), the cardiolipin transacylase or cardiolipin remodeler, reduces the stability of yeast respirasomes. This mutant contained a modified cardiolipin with altered fatty acid chain length and changed degree of unsaturation on position C2 (Brandner *et al.*, 2005). Yeast Taz1 physically assembles in complexes with the ATP synthase and ADP/ATP carrier. In the absence of CL, the interaction is reduced compared to when CL is present (Claypool *et al.*, 2008).

Similarly, studies of Barth syndrome patients with deficient cardiolipin-remodeling due to mutations in the *tafazzin* gene, showed reduced stability of human respiratory supercomplexes (McKenzie *et al.*, 2006). McKenzie observed an enhanced release of complex IV from I₁III₂IV_n supercomplexes. This means that the altered cardiolipin affected specifically the stability of the complex III–IV interaction in yeast and human respirasomes. Thus, the devastating effects of Barth syndrome, clinically characterized by cardioskeletal myopathy, neutropenia and abnormal growth (Barth *et al.*, 1983), can be explained by a reduced amount of respiratory complexes which is due to the decreased respirasome stability (Schlame and Ren, 2006; Wittig and Schägger, 2009).

1.3. Mitochondrial dynamics

The view of mitochondria constituting a bean-like structure is still found in textbooks for students in school and university. However, this structure is restricted to certain mammalian tissues, e.g. skeletal muscle. Meanwhile, experimental evidences favor the existence of dynamic interconnected networks that acquire specialized shapes, undergo changes in number and intracellular distribution and reorganize their morphology, often in response to the metabolic needs of the cell (Cervený *et al.*, 2007; Detmer and Chan, 2007; Hoppins *et al.*, 2007; Suen *et al.*, 2008; Westermann, 2008). The change of mitochondrial morphology rapidly adapting to cellular demands is critical for a number of important processes including calcium signaling, ROS protection, mtDNA maintenance

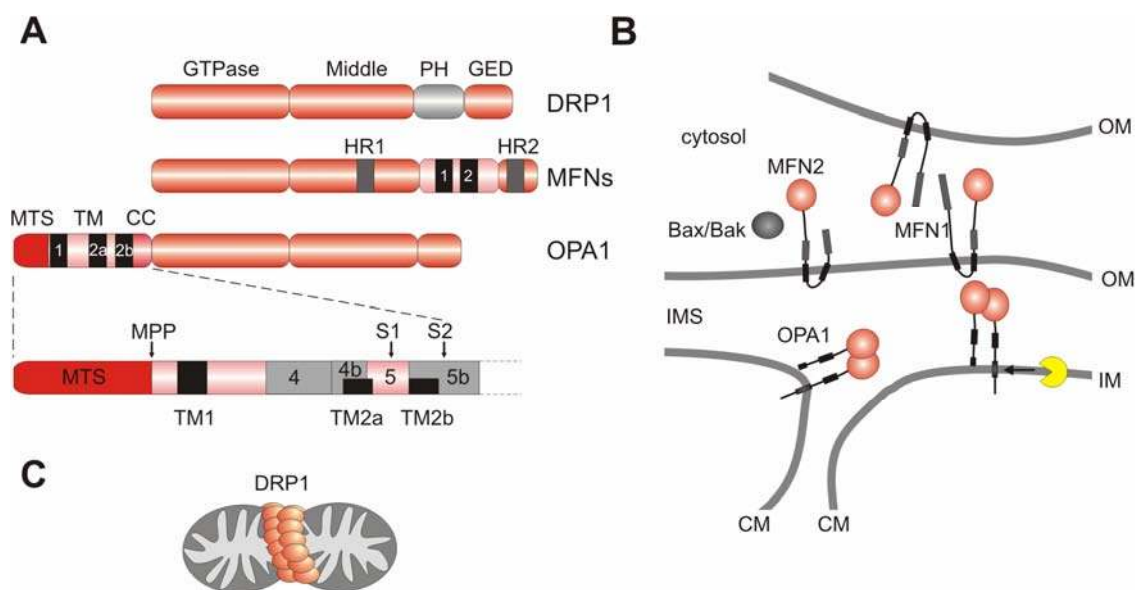


Figure 2: Human dynamin-related proteins (DRPs) involved in mitochondrial dynamics.

(A) All DRPs contain a GTPase domain that binds and hydrolyses GTP, a middle domain and a GTPase effector domain (GED) that are involved in oligomerization and stimulation of GTPase activity. All contain a lipid interacting domain, either a pleckstrin-homology (PH) domain or transmembrane domains (TM, black). The mRNA of OPA1 is alternatively spliced. Involved exons are indicated in grey.

(B) The core fusion machinery. The heptad regions (HR) of mitofusins (MFNs) are important for tethering of mitochondrial outer membrane. Bax/Bak control assembly of MFN2. OPA1 and MFN1 mediate inner membrane fusion. OPA1 is regulated by proteolytic processing and is also important for the cristae structure.

(C) Model of mitochondrial fission mediated by DRP1. DRP1 undergoes GTP-driven assembly into a helical structure which drives the constriction of the mitochondrial tubule.

MTS, mitochondrial targeting signal; CC, coiled coil region; IMS, intermembrane space; OM, outer membrane; IM, inner membrane; CM, cristae membrane.

Modified from (Delettre *et al.*, 2001; Hoppins and Nunnari, 2009; Lackner and Nunnari, 2009; Praefcke and McMahon, 2004; Zhang and Chan, 2007).

and aging, developmental processes and apoptosis (Balaban *et al.*, 2005; Chen *et al.*, 2003; Szabadkai *et al.*, 2006; Tang *et al.*, 2009; Youle and Karbowski, 2005). But, the fundamental functions of mitochondrial fusion are thought to be content mixing and to distribute mtDNA within the mitochondrial population and maintain respiratory competent and energized organelles, on the one hand. On the other hand, fission is required to efficiently distribute organelles to distal parts of the cell and is crucial for quality control by mitophagy and apoptosis (Hoppins *et al.*, 2007; Lackner and Nunnari, 2009; Twig *et al.*, 2008).

Mitochondrial morphology is maintained by two opposing events: fusion on the one hand, and division on the other hand. Much progress has been made in analyzing the components of fission and fusion machineries, but understanding the complex physiological functions of mitochondrial dynamics is just at its beginning. Intriguingly, major key players in fission and fusion belong to the same protein family, the dynamin

superfamily or dynamin-related protein family (DRPs) that mediate a variety of cellular processes [reviewed in (Praefcke and McMahon, 2004)]. The dynamins are structurally similar but functionally diverse GTP-binding proteins with sizes ranging from 70 to 100 kD. More precisely, fission and fusion proteins belong to a subgroup called dynamin-like GTPases [reviewed in (Hoppins *et al.*, 2007; Hoppins and Nunnari, 2009; Lackner and Nunnari, 2009; Praefcke and McMahon, 2004; Suen *et al.*, 2008)]. All DRPs possess a highly conserved GTPase domain that adopts the core fold common to all regulatory GTPases and certain additional regions predicted to adopt coiled-coil structures, referred to as middle domain and GTPase effector domain (GED) (Lackner and Nunnari, 2009; Praefcke and McMahon, 2004). Figure 2 A shows the domain architecture of the dynamin-like GTPases involved in fusion and fission of mammalian mitochondria. Middle domain and GED domain participate in intra- and inter-molecular interactions that are required for self assembly and assembly stimulated hydrolysis (Sever *et al.*, 1999; Smirnova *et al.*, 1999).

1.3.1. Mitochondrial division

Yeast Dnm1 and its human homologue **Drp1** drive mitochondrial fission (Otsuga *et al.*, 1998; Smirnova *et al.*, 1998) (see Figure 2). Yellow fluorescent protein targeted Drp1 was shown to cycle between mitochondria and the cytosol. Only a small fraction associated with mitochondrial outer membranes indicating continuous exchange of subunits between cytosolic and assembled Dnm/Drp1 (Legesse-Miller *et al.*, 2003; Wasiak *et al.*, 2007). In analogy to yeast, it is assumed that Drp1 assembles into spirals at constriction sites of mitochondrial division which is needed for its function (Ingerman *et al.*, 2005; Jensen *et al.*, 2000). GTP-driven Dnm1 self-assembly drives mitochondrial membrane constriction and is therefore necessary for mitochondrial fission (Hinshaw and Schmid, 1995; Naylor *et al.*, 2006) (Figure 2 C). Dnm1/Drp1-dependent mitochondrial division requires additional players to target the mitochondrial division dynamin to the mitochondrial surface, most notably **Fis1**, which is anchored to the outer mitochondrial membrane via a C-terminal transmembrane domain (Mozdy *et al.*, 2000). However, Drp1 recruitment is not altered in mammalian cells lacking Fis1 suggesting additional mechanisms to target Drp1 (Lee *et al.*, 2004). Upon stimulation of apoptosis Drp1 gets massively recruited to mitochondria indicating that those additional factors also increase following the induction of apoptosis (Breckenridge *et al.*, 2003; Frank *et al.*, 2001; Germain *et al.*, 2005). Drp1 participates not only in the fission of mitochondria, but also in the regulation of the shape of other organelles, such as peroxisomes (Schrader, 2006).

1.3.2. Mitochondrial fusion

Mitochondrial fission is balanced by fusion. *In vitro* fusion assays provided evidence that inner and outer membrane fusion events are separable and have distinct energy requirements (Malka *et al.*, 2005; Meeusen *et al.*, 2004). However, both processes are certainly linked and the idea of communication between these machineries resulting in coupled outer and inner membrane fusion is favoured (Hoppins *et al.*, 2007). The first protein identified to be involved in mitochondrial outer membrane fusion was the *fuzzy onions* gene (Fzo1) (Hales and Fuller, 1997). Subsequently, homologues in other species including mammals and yeast could be defined. Interestingly, mammals express two Fzo1 homologues which were termed the mitofusins, **mitofusin 1** and **mitofusin 2**, Mfn1 and Mfn2, respectively (Hermann *et al.*, 1998; Rojo *et al.*, 2002; Santel and Fuller, 2001) (see Figure 2 A). Mitofusins are essential for embryonic development: lacking either Mfn1 or Mfn2 in mice is embryonic lethal (Chen *et al.*, 2003). In cell culture models, it has been shown that mitofusins are essential for mitochondrial fusion: knockout mouse embryonic fibroblasts of Mfn1 or Mfn2 show predominantly fragmented mitochondria and have greatly reduced mitochondrial fusion *in vivo* (Chen *et al.*, 2005; Chen *et al.*, 2003). They share an N-terminal GTPase domain and a bipartite transmembrane domain at the C-terminus which spans the outer membrane of mitochondria, resulting in an orientation to the cytosol of both amino- and carboxy-termini (Fritz *et al.*, 2001; Rojo *et al.*, 2002). Two hydrophobic heptad repeats flank the transmembrane domains which are thought to form helical coiled-coil structures (Brown *et al.*, 1996; Hoppins *et al.*, 2007). Intermolecular as well as intramolecular assemblies exist within mitofusins and are crucial for fusion activity (Griffin and Chan, 2006) (see Figure 2 B). Additionally, *in vitro* experiments showed that Mfn1, and to a lesser extent Mfn2, can form homo-oligomeric complexes *in trans*, indicating that mitofusins and Fzo1 enable the GTP dependent tethering of outer membranes through complexes formed by molecules derived from opposing membranes (Hoppins *et al.*, 2007; Ishihara *et al.*, 2004). Human *MFN2* is linked to Charcot-Marie-Tooth (CMT2A – see chapter 1.3.4) disease (Züchner *et al.*, 2004). Interestingly, homo-oligomeric complexes formed by many Mfn2 disease mutants are non-functional for mitochondrial fusion. Notably, wild-type Mfn1, but not Mfn2, complements mutant Mfn2 through the formation of hetero-oligomeric complexes, including complexes that form *in trans* between mitochondria (Detmer and Chan, 2007). This might explain the susceptibility of tissues with low expression of Mfn1 in CMT2A pathogenesis. A conditional knockout of mitofusins in the cerebellum of mice revealed a requirement of Mfn2, but not of Mfn1, for Purkinje cells (Chen *et al.*, 2007). This underlines a close interplay of both mitofusins (Amiott *et al.*, 2008; Detmer and Chan, 2007). In summary,

analysis of the functions of Mfn1 and Mfn2 and their kinetic properties reveal differences, indicating that their exact roles in fusion may not be completely redundant (Ishihara *et al.*, 2004). Intriguingly, de Brito and Scorrano showed recently that Mfn2 is enriched at contact sites between the endoplasmic reticulum (ER) and mitochondria, thereby regulating both, the morphology of the ER and mitochondria and tethering both organelles to each other. This function of Mfn2 is important for mitochondrial calcium uptake (de Brito and Scorrano, 2008).

Interestingly, the proapoptotic Bcl-2 family members **Bax and Bak** also effect mitochondrial dynamics (Karbowski *et al.*, 2002; Karbowski *et al.*, 2006) (Figure 2 B). Bax colocalizes with Drp1 and Mfn2 proteins during programmed cell death (Karbowski *et al.*, 2002). Additionally, in non-apoptotic cells Bax and Bak regulate the assembly of Mfn2 into high molecular weight complexes allowing fusion (Karbowski *et al.*, 2006).

Outer and inner membrane fusion are separable events, but nevertheless, are interconnected (Malka *et al.*, 2005; Meeusen *et al.*, 2004). In yeast, one of the essential components of mitochondrial fusion is **Ugo1** (Sesaki and Jensen, 2001; Sesaki *et al.*, 2003; Wong *et al.*, 2003). Ugo1 is an outer membrane protein with its N-terminus in the cytosol and the C-terminus inside of mitochondria (Sesaki and Jensen, 2001). Since it physically interacts independently with both, the inner and outer membrane fusion machineries, it is proposed to function as an adaptor, creating a two membrane spanning fusion complex (Sesaki and Jensen, 2001; Sesaki and Jensen, 2004; Wong *et al.*, 2003). Ugo1, a modified member of the mitochondrial transporter family, has three transmembrane domains acting as a dimer in outer and inner membrane fusion. Hoppins *et al.* suggested that it acts after membrane tethering, indicating its operation at the lipid-mixing step of fusion (Coonrod *et al.*, 2007; Hoppins *et al.*, 2009).

However, neither a mammalian homologue of Ugo1 exists nor an analogue of Ugo1 has been identified so far. Hoppins hypothesized that one of the approximately 50 members of the transport/carrier protein family in humans might be one Ugo1 analogue (Hoppins *et al.*, 2009). However, direct interaction of Mfn1, Mfn2 and OPA1 has been demonstrated by co-immunoprecipitation experiments (Guillery *et al.*, 2008). Whether this interaction is sufficient to mediate correlated inner and outer membrane fusion is not understood. However, OPA1 is involved in the inner membrane fusion, and interestingly, this depends on Mfn1, but not on Mfn2 (Cipolat *et al.*, 2004). **OPA1 (as its yeast homologue Mgm1)** is a large GTPase of the DRP family which is attached to the inner membrane facing the GTPase domain to the intermembrane space (Olichon *et al.*, 2003;

Olichon *et al.*, 2002; Wong *et al.*, 2000; Wong *et al.*, 2003) (Figure 2 B). Lacking either Mgm1 or OPA1 in cells results in fragmented mitochondria (Sesaki *et al.*, 2003; Wong *et al.*, 2000). Both proteins harbor an N-terminal mitochondrial targeting sequence (MTS), two consecutive hydrophobic segments, a coiled coil domain, a GTPase domain, and a GED (GTPase effector domain: middle and a C-terminal coiled-coil domain) (Hoppins *et al.*, 2007; Hoppins and Nunnari, 2009; Zhang and Chan, 2007) (see Figure 2 A).

It has been shown that **yeast Mgm1** mediates fusion through oligomerization, GTP hydrolysis and binding to negatively charged phospholipids (like cardiolipin, phosphatic acid, phosphatidylserine, and phosphatidylinositol 3,4-bisphosphate) (Meglei and McQuibban, 2009). Yeast Mgm1 gives rise for an alternative topogenesis. At steady state two isoforms exist. A long isoform is attached to the inner membrane (l-Mgm1), whereas a short isoform, generated by ATP-dependent processing of l-Mgm1 by the inner membrane **rhomboid protease Pcp1**, is soluble in the intermembrane space (s-Mgm1) (Herlan *et al.*, 2004; Herlan *et al.*, 2003; McQuibban *et al.*, 2003). Both isoforms are important for fusion activity and mtDNA maintenance, although l-Mgm1 can support reduced levels of fusion in cells (Herlan *et al.*, 2003; Sesaki *et al.*, 2003). Interestingly, *in vitro* fusion assays by Meeusen *et al.* with temperature sensitive mutants of Mgm1 revealed functional outer membrane fusion whereas inner membrane fusion was abolished, although membranes stayed in close contact. More precisely, authors demonstrated that a functional GTPase domain and GED *in trans* enable tethering on opposing membranes. Thus, in addition to fusion of inner membranes to single lipid bilayers, Mgm1 promotes the tethering of membranes which is needed prior to fusion (Meeusen *et al.*, 2006).

OPA1 is also present as l-OPA1 and s-OPA1 isoforms, but the human OPA1 gene encodes 31 exons of which exon 4, 4b and 5b are involved in tissue and cell type specific alternative splicing resulting in the generation of eight different mRNA variants (Delettre *et al.*, 2001; Olichon *et al.*, 2002; Satoh *et al.*, 2003) (Figure 2 A). Alternative splicing and subsequent processing results in the accumulation of five apparent isoforms of the OPA1 protein, two long and three short isoforms, of which both are needed for full fusion activity indicating that the balance between both isoforms regulates mitochondrial fusion (Delettre *et al.*, 2001; Duvezin-Caubet *et al.*, 2007; Ishihara *et al.*, 2006; Olichon *et al.*, 2003; Olichon *et al.*, 2007; Song *et al.*, 2007). In addition to the mitochondrial processing peptidase (MPP) processing site, the polypeptides encoded by each mRNA splice form contain an S1 cleavage site, and some also contain a more C-terminal S2 cleavage site (Ishihara *et al.*, 2006) (Figure 2 A). S2 cleavage is carried out by the *i*-AAA protease facing the inter membrane space (Yme1), whereas the protease cleaving at site S1 is not known (Griparic *et al.*, 2007; Song *et al.*, 2007). The mammalian homologue of yeast Pcp1,

presenilin-associated rhomboid-like (PARL), and **Paraplegin** (see chapter 0), a subunit of the *m*-AAA protease, have been implicated in this processing (Cipolat *et al.*, 2006; Frezza *et al.*, 2006; Ishihara *et al.*, 2006). Interestingly, reconstituted OPA1 in yeast can be processed by the *m*-AAA protease but not by PARL (Duvezin-Caubet *et al.*, 2007). OPA1 and Mgm1 were linked to apoptosis via its role of cristae maintenance besides mitochondrial fusion (Frezza *et al.*, 2006; Meeusen *et al.*, 2006), which is discussed in the next paragraph.

1.3.3. Inner membrane dynamics

The inner membrane of mitochondria is organized in two morphologically distinct domains, the **inner boundary membrane (IBM)** and the **cristae membrane (CM)** which are connected by narrow tubular **cristae junctions (CJ)** (Frey *et al.*, 2002; Mannella, 2006; Mannella *et al.*, 2001; Reichert and Neupert, 2002; Vogel *et al.*, 2006). Electron tomography revealed that cristae are not simply random folds in the inner membrane but rather internal compartments formed by invaginations of the membrane (Mannella, 2006). Furthermore, the ultrastructure of mitochondria varies considerably between tissues, organisms and the physiological state of the cell (Zick *et al.*, 2009). For instance, dependent on the energy status of the cell two conformations have been observed: a “condensed” conformation (condensed matrix) characterized by a large swollen intra-cristal space volume (respiratory state III – high ADP), and an “orthodox” state, where the volume was considerably smaller (respiratory state IV – low ADP) (Zick *et al.*, 2009). Due to different functions the IBM and the CM are distinct from each other, e.g. the CM is enriched in proteins involved in oxidative phosphorylation, iron/sulphur cluster biogenesis, protein synthesis and transport of mtDNA-encoded proteins, whereas the IBM is enriched in proteins involved in fusion and protein transport of nuclear-encoded proteins. Interestingly, the observed distribution of proteins has been shown to change upon variations of the physiological state, further underlining a dynamic organization of the inner membrane (Vogel *et al.*, 2006).

1.3.3.1. The ATP synthase and cardiolipin as cristae organizers?

Several proteins or protein complexes have been implicated in cristae structure or organization. Influencing the oligomeric state or the proton channel ATP6 of the **F₁F₀-ATP synthase** revealed disarranged cristae [reviewed in (Zick *et al.*, 2009)]. It is discussed that dimerization and oligomerization of this complex generates a certain membrane curvature to the CM, increasing locally the proton concentration and thereby optimizing the performance of the ATP synthase (Dudkina *et al.*, 2006; Minauro-Sanmiguel *et al.*, 2005;

Strauss *et al.*, 2008). Additionally, stability of the F₁F₀-ATP synthase affects the membrane potential pointing to a role for organization of specific microdomains of OXPHOS complexes in the CM resulting in optimized respiration (Bornhovd *et al.*, 2006). Interestingly, lymphoblast mitochondria from Barth syndrome patients having mutations in the cardiolipin remodeler **tafazzin** have abnormalities involving adhesions of inner mitochondrial membranes with subsequent collapse of the intracristae space (Acehan *et al.*, 2007). Cristae density is reduced and the structure is altered suggesting that tafazzin affects cristae morphogenesis caused by reduced cardiolipin (or cardiolipin derivative) levels. However, it is not clear whether the observed effects are caused by a yet unknown structural role of tafazzin on CMs or by an indirect effect due to reduced stability of the supercomplexes of the respiratory chain (Acehan *et al.*, 2007). Nevertheless, this study links alterations in levels of specific phospholipids to inner membrane dynamics.

1.3.3.2. Cristae remodelling during apoptosis

Alterations and remodelling of inner membrane structures are evident in numerous human disorders and during apoptosis (Zick *et al.*, 2009). A central step in the mitochondrial apoptotic pathway is the release of soluble proteins upon selective permeabilization of the outer membrane including **cytochrome c** (cyt c) or apoptosis inducing factor (AIF) (Green and Kroemer, 2004). Cristae remodelling upon apoptosis is widely believed but the answer to the question “*what comes first? – cyt c release or the changes of the cristae structure?*” is highly controversial. Sun *et al.* proposes that cristae remodelling and, in particular, the widening of the cristae junctions are necessary to release cyt c. Additionally, it was shown that **caspases** seemed to remodel cristae and to widen the CJ independent of the release of cyt c and the loss of the mitochondrial membrane potential (Sun *et al.*, 2007). Interestingly, Frezza stated that the tightness of CJ correlated with oligomerization of the long (membrane anchored) and short (soluble) OPA1 isoforms. Widening of CJ induced by the truncated BH3-only protein Bid (tBid) facilitated cyt c release (Frezza *et al.*, 2006; Scorrano *et al.*, 2002).

Conversely, Yamaguchi observed a narrowing of CJ which goes along with the disassembly of **OPA1 complexes** and increased availability of cyt c at the outer membrane (Yamaguchi *et al.*, 2008). It is hypothesized that in the Bcl-2 inhibitable Bax/Bak-dependent intrinsic pathway of apoptosis the release of cyt c from mitochondria is a consequence of two carefully coordinated events: formation of outer membrane pores and opening of cristae junctions triggered by OPA1 oligomer disassembly. Both steps are necessary for the complete release of cyt c (Yamaguchi and Perkins, 2009). Interestingly, both, mitochondrial outer membrane permeabilization and CJ opening were caspase independent events speaking against caspase induced late and gross changes of cristae

morphology like it was suggested by Sun (Sun *et al.*, 2007; Yamaguchi *et al.*, 2008). Notably, a disassembly mutant of OPA1 blocked cyt c release and apoptosis, but not Bax activation (Yamaguchi *et al.*, 2008).

Three candidate proteins have been implicated in CJ formation: OPA1, mitofilin and the prohibitins (Zick *et al.*, 2009). OPA1 is discussed above. Deletion of the inner membrane protein **Mitofilin** demonstrated disorganized cristae. Closely packed stacks of concentric sheets without visible CJs have been observed, with no effect on mitochondrial morphology but an increased sensitivity towards apoptotic stress (John *et al.*, 2005). Prohibitins have been reported to form large ring-like complexes with a diameter fitting well to those reported for CJs (Tatsuta *et al.*, 2005) (see 1.4.2). Mammalian prohibitins are linked to OPA1 processing and will be discussed in the next chapter.

1.3.3.3. Interfering with OPA1 processing – a trigger for apoptosis?

Distinct triggers of apoptosis induce the processing of OPA1 (Guillery *et al.*, 2008; Ishihara *et al.*, 2006) (see chapter 1.3.5.3) which causes an altered cristae morphogenesis. **Prohibitins** exert essential function for cristae morphogenesis by controlling the stability of long OPA1 isoforms (Merkwirth *et al.*, 2008). Loss of function of prohibitins leads to fragmentation of mitochondria, disorganized mainly vesicular cristae and an increased sensitivity towards apoptotic stimuli (see chapter 1.4.2). **LETM1 (yeast Mdm38)**, whose downregulation and overexpression has been linked to mitochondrial morphology and cristae aberrations which has been implicated in regulating OPA1 processing and to sensitize cells to apoptosis triggered by certain inducers (Dimmer *et al.*, 2008; Piao *et al.*, 2009; Tamai *et al.*, 2008). LETM1 is an inner-membrane protein with a large domain extruding into the matrix. It interacts with the mitochondrial AAA-ATPase BCS1L which is important for respiratory complex III assembly. Indeed, siRNA of both BCS1L and LETM1 interfered with assembly of certain respiratory complexes and supercomplexes. Downregulation leads to a swollen matrix, overexpression to an opposite phenotype – swollen cristae (Tamai *et al.*, 2008). The morphological changes upon siRNA were fully reversible upon treatment with the K^+/H^+ ionophore nigericin, suggesting a role for Mdm38/LETM1 as a K^+/H^+ antiporter. Whether the effect on cristae is due to its proposed transporter activity or to the stabilizing function of LETM1 on respiratory chain complexes remains open. Another protein interfering with mitochondrial cristae morphogenesis and resistance to apoptosis is **MICS1**, a protein residing in the inner membrane (Oka *et al.*, 2008). SiRNA mediated downregulation of this seven transmembrane domains spanning protein causes fragmentation, disorganized cristae and stimulates release of proapoptotic proteins. Cristae appeared less and became curved visualized by ring-like structures. Overexpression induced mitochondrial aggregation and partially inhibited cyt c release

during apoptosis, regardless of Bax activation. OPA1 processing is not impaired in general but was enhanced upon induction of apoptosis.

However, whether LETM1 or MICS1 directly control cristae via OPA1 is not clear. Moreover, whether LETM1, MICS1 or the prohibitins affect the OPA1 complex or CJ opening remains elusive. In addition, the mechanism of how cristae and CJs are formed is also completely unknown. In conclusion, studying inner membrane dynamics is a complicated field, since observed phenotypes can probably not be explained by simply one specific or direct function of one protein or lipid. Future analyses will have to reveal the exact roles of the involved proteins OPA1, prohibitins, LETM1, MICS1, or mitofilin in determining cristae morphology, CJ opening and its link to apoptosis.

1.3.4. Pathogenic alterations of mitochondrial dynamics

Mitochondria constantly fuse and divide and must be distributed to reach areas of high energy demands, e.g. synaptic endings in neurons (Cervený *et al.*, 2007; Detmer and Chan, 2007; Knott *et al.*, 2008). Interfering with these balanced mechanisms has severe consequences on cellular and organism level. Therefore, it is obvious that several human diseases are associated with mutations in genes that are essential for mitochondrial dynamics. Notably, the majority of these diseases involve the degeneration of specific nerves, indicating that neurons are particularly prone to defects in mitochondrial dynamics (Bossy-Wetzell *et al.*, 2003; Chen and Chan, 2006; Knott and Bossy-Wetzell, 2008; Knott *et al.*, 2008).

Heterozygous mutations in the fusion protein **OPA1** cause **autosomal dominant optic atrophy (ADOA)**, the Mendelian counterpart of LHON. It is the most common heritable form of optic neuropathy and is characterized by the degeneration of retinal ganglion cells, the axons of which form the optic nerve (Alexander *et al.*, 2000; Delettre *et al.*, 2000; DiMauro and Schon, 2008). The large majority of mutations in the OPA1 gene described to date is predicted to lead to a truncated OPA1 protein and to haploinsufficiency (Ferre *et al.*, 2005). Classic DOA usually begins before 10 years of age, with a large variability in the severity of clinical expression, which may range from non-penetrant unaffected cases up to very severe, early onset cases, even within the same family carrying the same molecular defect (Amati-Bonneau *et al.*, 2008; Carelli *et al.*, 2007; Delettre *et al.*, 2002). Recently, OPA1 has been linked to autophagy, the selective elimination of organelles. Before autophagy, mitochondria lose membrane potential ($\Delta\Psi_m$) and OPA1. Overexpression of OPA1 decreases mitochondrial autophagy (Twig *et al.*, 2008).

Table 1: The genetic diseases of mitochondrial shaping proteins.

Disease	Major phenotype	Gene affected	Mitochondrial morphology	Involvement of other organelles
ADOA	loss of retinal ganglion cells	OPA1	probably fragmented	not known
CMT2A	loss of sensorimotor axons	MFN2	probably fragmented	yes, ER
CMT4A	loss of sensorimotor axons	GDAP	probably fragmented	not known
WHS	seizures	LETM1	probably fragmented	not known
Lethal metabolic syndrome	metabolic and CNS problems	DRP1	elongated	yes, peroxisomes

Major pathological, genetic and mitochondrial features of genetic diseases associated with mutations in genes coding for mitochondria-shaping proteins are shown. See text for more detail. DOA, dominant optic atrophy; CMT, Charcot-Marie-Tooth type; WHS, Wolf-Hirschhorn syndrome; CNS, central nervous system.

Additionally, *OPA1*^{+/-} heterozygous mice have increased numbers of autophagosomes in the retinal ganglion cell layer indicating that ADOA is caused by an increase in abnormal mitochondria which are subjected to degradation by autophagy (White *et al.*, 2009).

Another fusion gene, **MFN2 or mitofusin 2** is linked to **Charcot-Marie-Tooth (CMT)** disease (Züchner *et al.*, 2004). CMT is one of the most common hereditary neuropathies. It is caused by mutations in at least 30 different genes. Patients suffer from progressive distal motor and sensory impairments that start in feet and the hands as a result of the degeneration of the long peripheral nerves. Depending on the type of CMT, these diseases are caused by either a primary defect in the Schwann cells that myelinate the peripheral nerves or by a defect in the neurons themselves (Detmer and Chan, 2007; Züchner and Vance, 2005). 40 mutations have been associated with *MFN2* or **CMT2A**, leading to an axonopathy affecting neurons (Züchner *et al.*, 2004). Although most patients with *MFN2* mutation don't have optic atrophy and most patients with *OPA1* mutation do not have CMT, some families harboring mutations in *MFN2* show up phenotypes characterized by the coexistence of peripheral neuropathy and optic atrophy, like in ADOA (Züchner *et al.*, 2006). This **CMT type 6** phenotype is presumably caused by deficient mitochondrial movement (DiMauro and Schon, 2008). Another form of CMT is associated with defects in mitochondrial dynamics. Ganglioside-induced differentiation-associated protein-1 (*GDAP1*) is mutated in **CMT4A**, one of the recessive forms (Niemann *et al.*, 2005).

The **Wolf-Hirschhorn syndrome (WHS)** is caused by a partial deletion of the short arm of one chromosome 4 resulting in severe pre- and post-natal growth retardation, impairment of muscle tone, severe mental retardation, developmental delay with

microcephaly, and in all cases, seizures (Zollino *et al.*, 2003). The gene **LETM1** (leucine zipper EF-hand-containing transmembrane protein 1 – homologue of yeast Mdm38) is deleted in all patients with seizures, suggesting a role for haploinsufficiency in the pathogenesis of seizures (Endele *et al.*, 1999; Schlickum *et al.*, 2004; Zollino *et al.*, 2003).

An infant patient with a dominant-negative fission gene **DRP1** allele has been reported. This patient died at 1 month of age and had abnormalities, including reduced head growth, increased lactic acid and optic atrophy. Isolated fibroblasts from this patient showed elongated mitochondria and peroxisomes (Waterham *et al.*, 2007).

1.3.5. Regulation of mitochondrial dynamics

Several steps of regulation have been already described above, e.g. the high molecular weight complex formation of mitofusin 2 which is dependent on Bax and Bak (Karbowski *et al.*, 2006). However, recent studies have uncovered additional regulatory mechanisms that control the activity, assembly, distribution and stability of the key components for mitochondrial fusion and division.

1.3.5.1. Regulation by post-translational modifications

Post-translational modifications have been shown mainly for Drp1/Dnm1. Two **phosphorylation** events have been demonstrated in the GED of Drp1, which results dependent on the site in opposing effects for mitochondrial shape. Phosphorylation on site S616 promotes mitochondrial fission during mitosis. Conversely, dephosphorylation on S637 by the calcium-dependent phosphatase calcineurin promotes fission and is involved in the propagation of apoptosis (Chang and Blackstone, 2007; Cribbs and Strack, 2007; Jahani-Asl and Slack, 2007; Taguchi *et al.*, 2007). Additionally, mitochondrial dysfunction, characterized by depolarization and increased cytosolic calcium levels, activates Drp1-bound calcineurin. Calcineurin dephosphorylates Drp1 thereby recruiting Drp1 to mitochondria (Cereghetti *et al.*, 2008).

1.3.5.2. Regulation by the lipid milieu

Downstream of the tethering of mitochondrial outer membranes in the fusion process acts **mitochondrial phospholipase D (MitoPLD)**. This protein belongs to a superfamily of lipid-modifying enzymes. It targets to the mitochondrial surface and promotes trans-mitochondrial membrane adherence in an Mfn-dependent manner by hydrolysing cardiolipin to generate the phosphatic acid (Choi *et al.*, 2006). In addition to serving as a membrane anchoring site, phosphatic acid has been proposed to act as a fusogenic lipid in biophysical modeling studies by lowering the activation energy for membrane bending

during generation and expansion of fusion pores (Kooijman *et al.*, 2003; Kozlovsky *et al.*, 2002).

An interesting study by Osman *et al.* revealed a link between the lipid composition of mitochondrial membranes and the regulation of mitochondrial dynamics. Deletion of yeast **Ups1**, which has been previously shown to be involved in the alternative topogenesis of Mgm1, results in the loss of Cardiolipin and an accumulation of l-Mgm1. In contrast, knockout of **Gep1** (homologue of Ups1) significantly impairs the formation of s-Mgm1, but results in decreased stability of phosphatidylethanolamine (Osman *et al.*, 2009). Like Tafazzin, deletion of Gep1 leads to aberrant cristae morphogenesis. The authors suggest a novel mechanism, namely that an altered phospholipid composition of the inner membrane impairs Mgm1 cleavage. In line, yeast Mgm1 mediates fusion by binding to negatively charged phospholipids like cardiolipin (Meglei and McQuibban, 2009). In conclusion, these findings imply a role of a certain lipid environment for divergent forms of membrane fusion (Cervený *et al.*, 2007; Choi *et al.*, 2006; Osman *et al.*, 2009; Zhang and Chan, 2007). Intriguingly, cardiolipin, previously shown to participate in mitochondria-dependent apoptosis, provides an essential activating platform for caspase-8 on mitochondria (Gonzalez *et al.*, 2008). Thus, interfering with cardiolipin might directly affect programmed cell death pathways.

1.3.5.3. Regulation by degradation and processing events

Drp1 has been shown to get desumoylated by SENP5 (**SUMO** specific protease) dependent on Bax/Bak stimulation (Wasiak *et al.*, 2007; Zunino *et al.*, 2007). This modification correlates with the stable association of Drp1 with mitochondrial membranes (Wasiak *et al.*, 2007). MARCH5, a mitochondrial E3 **ubiquitin** ligase, regulates the subcellular trafficking of Drp1, likely by impacting the correct assembly at scission sites or the disassembly step of fission complexes (Karbowski *et al.*, 2007). However, whether sumoylation or ubiquitinylation targets Drp1 for degradation is unclear.

The yeast mitofusin **Fzo1** is an unstable protein and its steady state level is critical to maintain mitochondrial morphology. Either deletion or overexpression of Fzo1 alters mitochondrial fusion resulting in abnormal aggregated mitochondria (Escobar-Henriques *et al.*, 2006; Fritz *et al.*, 2003; Hermann *et al.*, 1998; Rapaport *et al.*, 1998). Two independent proteolytic pathways regulate Fzo1 steady state protein levels. During non-vegetative growth, which is mimicked by adding the mating factor alpha to cells, Fzo1 is subjected to proteasome dependent degradation, and this subsequently leads to mitochondrial fragmentation (Escobar-Henriques *et al.*, 2006; Neutzner and Youle, 2005). During vegetative growth, Fzo1 is degraded in a constitutive manner which depends on the F-box protein Mdm30 (Escobar-Henriques *et al.*, 2006). F-box proteins are generally

thought to serve as substrate recognition elements of ubiquitin ligases of the Skp1-Cullin-F-box (SCF) family (Petroski and Deshaies, 2005; Willems *et al.*, 2004). However, in the absence of Mdm30, the steady state concentration of Fzo1 is increased and yeast cells accumulate aggregated and fragmented mitochondria (Fritz *et al.*, 2003). Fzo1 gets ubiquitinated by an SCF ubiquitin ligase that includes Mdm30 as a substrate recognition factor, thereby identifying a critical regulatory outer membrane protein being a target of the cytosolic ubiquitin-proteasome system (Cohen *et al.*, 2008).

Mgm1 and the mammalian **OPA1** are cleaved to maintain mitochondrial fusion activity (Herlan *et al.*, 2003; Ishihara *et al.*, 2006; Olichon *et al.*, 2003; Sesaki *et al.*, 2003; Song *et al.*, 2007). Long isoforms of Mgm1/OPA1 get processed upon import into mitochondria to create the short isoforms which, together with the long isoforms, assemble into fusion active OPA1 complexes (see chapter 1.3.2). This processing event is termed constitutive processing. However, it is distinct from an induced cleavage. In fact, processing of l-OPA1 to s-OPA1 is stimulated to rapid completion by dissipation of the membrane potential with CCCP, subsequently followed by the fragmentation of the mitochondrial network (Duvezin-Caubet *et al.*, 2006; Griparic *et al.*, 2007; Guillery *et al.*, 2008; Ishihara *et al.*, 2006; Song *et al.*, 2007). Moreover, apoptosis induction and MOMP (mitochondrial outer membrane permeabilization) induce OPA1 cleavage as well (Guillery *et al.*, 2008; Ishihara *et al.*, 2006) (see 1.3.3.3). On a molecular level Baricault *et al.* hypothesized that decreased mitochondrial ATP levels, either generated by apoptosis induction, membrane potential dissipation or inhibition of ATP synthase, is the common and crucial stimulus that controls OPA1 processing. In addition, it has been reported that ectopic iron addition can activate OPA1 cleavage, whereas zinc inhibits this process (Baricault *et al.*, 2007). In line, this processing event seems to be metalloprotease-mediated (Guillery *et al.*, 2008). The induced processing is carried out at site S1 by a yet unknown protease (Song *et al.*, 2007). Meanwhile, Loucks *et al.* identified a metal-independent fourth cleavage site in the N-terminal region of cerebellar granule cell OPA1 which seem to be under the indirect control of certain caspases upon induction of apoptosis (Loucks *et al.*, 2009). They claim that the truncated protein lacks a specific lysine residue within the GTPase domain which contributes to mitochondrial fragmentation. The protease cleaving at site S1 during constitutive processing of OPA1 to generate a balanced equilibrium of long and short OPA1 isoforms is unknown. Likewise, which protease/s cleave/s at site S1 upon induced processing and at the caspase-dependent processing site remains to be identified. Notably, as mitochondrial morphology depends on both long and short isoforms of OPA1, proteolytic processing is an important process regulating mitochondrial dynamics and apoptosis.

1.4. ***Protein quality control in mitochondria***

Most mitochondrial proteins are encoded by nuclear genes, whose unfolded protein products are imported into mitochondria by translocases in the inner and/or outer membrane (Neupert and Herrmann, 2007). Other mitochondrial proteins, which are encoded in the mitochondrial genome, are synthesized in the mitochondrial matrix which subsequently assemble into respiratory chain complexes in the inner membrane (Fontanesi *et al.*, 2008; Rak *et al.*, 2009). It is not surprising that the organization of the expression of two genomes and arrangement of all proteins and complexes in the four compartments of the highly dynamic mitochondria requires strict quality control surveillance. Indeed, this is maintained by a network of molecular pathways that include quality control machineries, such as chaperones and proteases (Broadley and Hartl, 2008).

During protein import, the mitochondrial processing peptidase (MPP) (Brunner *et al.*, 1994), the intermediate peptidase (MIP) (Isaya *et al.*, 1994; Kalousek *et al.*, 1992) and the innermembrane peptidase (IMP) (Behrens *et al.*, 1991; Esser *et al.*, 1996; Schneider *et al.*, 1991) are responsible for the cleavage of targeting presequences of nuclearly encoded proteins. Molecular chaperone proteins of the Hsp70 and Hsp100 family stabilize misfolded proteins against aggregation or mediate the dissolution of protein aggregates and thereby ensure proteolysis (Bateman *et al.*, 2002; Röttgers *et al.*, 2002; Wagner *et al.*, 1994). Eukaryotic cells respond to the accumulation of unfolded proteins by sensing perturbations of protein homeostasis in a cellular compartment and, in turn, activate genes that enhance the protein-handling capacity of the compartment (Benedetti *et al.*, 2006; Ron and Walter, 2007). This process is named unfolded protein response (UPR) which has been identified in the cytosol, in the ER (UPR^{ER}) and also within mitochondria (UPR^{mt}) (Benedetti *et al.*, 2006; Lindquist, 1986; Martinus *et al.*, 1996; Ron and Walter, 2007; Ryan and Hoogenraad, 2007; Yoneda *et al.*, 2004; Zhao *et al.*, 2002). The UPR^{mt} induces nuclear genes encoding the mitochondrial matrix chaperones Hsp60 and Hsp10 as well as MPP, the matrix serine protease ClpP and the inner membrane AAA protease Yme1 (Aldridge *et al.*, 2007; Zhao *et al.*, 2002). Proteases involved in the degradation of misfolded and non-assembled proteins to peptides, which are subsequently either exported from the organelle or degraded further to amino acids, are derived from ATP-dependent bacterial proteases and highly conserved in eukaryotes (Koppen and Langer, 2007). ClpP, together with its AAA⁺ chaperone ClpX, and the Lon protease are active in the matrix of mitochondria (Koppen and Langer, 2007; Tatsuta and Langer, 2008). In *E. coli*, ClpXP can recognize its substrates which get unfolded by ClpX and then threaded into the ClpP proteolytic chamber through the narrow axial pores for degradation (Yu and Houry, 2007). Only the

unfolding and threading by the chaperone require ATP binding and hydrolysis, while proteolysis by ClpP is energy independent.

The mitochondrial membrane is the protein-richest cellular membrane and contains the respiratory chain. Therefore, protein homeostasis is of major importance to maintain mitochondrial function. Membrane anchored ATP-dependent AAA proteases conduct the quality control surveillance in the inner membrane.

1.4.1. AAA proteases as key regulators of protein quality control and mitochondrial biogenesis

AAA (ATPases associated with various cellular activities) was first used to describe a class of ATP-hydrolyzing enzymes with a range of functional roles (Kunau *et al.*, 1993). Subsequent work showed that AAA proteins are actually a subset of a much larger superfamily of ATPases, now referred to as AAA⁺ protein family (Neuwald *et al.*, 1999). These P-loop NTPases are defined by the presence of the nominal P-loop, a conserved nucleotide phosphate-binding motif, also referred to as the Walker A motif, and a second, more variable region, called the Walker B motif. The Walker A motif is important for binding of nucleotides, which are typically ATP or GTP, and Mg²⁺ (Saraste *et al.*, 1990; Snider and Houry, 2008; Walker *et al.*, 1982). The glutamate side chain in the Walker B motif is thought to activate a water molecule for attack on the γ -phosphate of bound ATP, and therefore, is important for ATP hydrolysis (Baker and Sauer, 2006; Hersch *et al.*, 2005) (Figure 3 B). It has been shown that specific residues in the pore of the ATPase are in contact with the substrate molecule (Martin *et al.*, 2008). ATP binding and hydrolysis enable the moving of these residues thereby unfolding and pulling the substrate into the proteolytic chamber of the protease (Martin *et al.*, 2008).

In all organisms, many vital cellular processes, including membrane fusion, cell cycle regulation, organelle biogenesis, protein repair and degradation, are controlled by members of the AAA⁺ superfamily (Beyer, 1997; Mogk *et al.*, 2008; Neuwald *et al.*, 1999; Ogura and Wilkinson, 2001). The activity of AAA⁺ proteins relies on their ability to use the energy of ATP hydrolysis to generate a mechanical force, leading to the remodelling of bound substrates. ATP binding and hydrolysis is mediated by the conserved AAA domain, which additionally drives the oligomerization of AAA⁺ proteins, leading to the formation of barrel-shaped oligomers with a central channel (Mogk *et al.*, 2004; Mogk *et al.*, 2008; Sauer *et al.*, 2004) (Figure 3). AAA proteases are a group of ATP-dependent metalloproteases which are highly conserved membrane anchored protein complexes present from bacteria to human (Koppen *et al.*, 2007; Langer *et al.*, 2001).

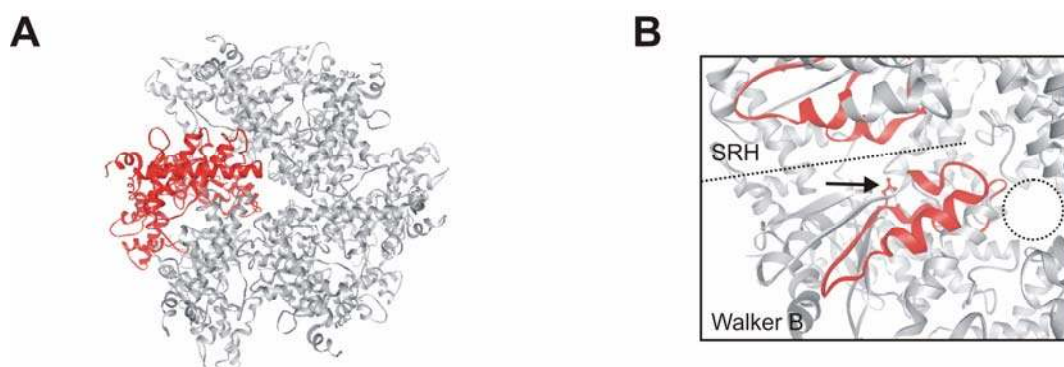


Figure 3: Structural features of AAA proteases.

(A) FtsH crystal structure from *Thermus thermophilus*. AAA proteases presumably form a hexameric structure, one subunit is highlighted in red. View from the cytosolic site to the membrane (view on the proteolytic domain of FtsH).

(B) The Walker B motif with adjacent SRH region of the neighboring subunit. Both regions are highlighted in red. The arrow indicates the critical glutamate in the Walker B motif. The dashed line indicates the subunit border and the dashed circle the pore of the hexameric complex.

The AAA domain at the aminoterminal end contains the Walker A and B motif and the conserved second region of homology (SRH). SRH residues function as intrasubunit (asparagin) and intersubunit (two arginines) sensors of the ATP γ -phosphate, the latter called an arginine finger. This arginine finger is only present in AAA proteins and not in other subgroups of AAA⁺ proteins (Ogura *et al.*, 2004). It stimulates ATP hydrolysis needed for the activity of the enzyme (Hanson and Whiteheart, 2005; Ito and Akiyama, 2005; Karata *et al.*, 1999; Korbel *et al.*, 2004; Snider and Houry, 2008). AAA proteases belong to the M41 metallopeptidase family characterized by the canonical metal binding HExxH motif (Rawlings and Barrett, 1995) (see Figure 4).

The bacterial protease **FtsH** is a cytoplasmic membrane protein that has N-terminally located transmembrane segments and a main cytosolic region consisting of AAA-ATPase and Zn²⁺-metalloprotease domains. It forms a homo-hexamer, which can be further complexed with an oligomer of the membrane-bound modulating factor HflKC, that is a homologue of the prohibitins (Browman *et al.*, 2007; Ito and Akiyama, 2005) (see chapter 1.4.2). FtsH degrades a set of short-lived proteins, enabling cellular regulation at the level of protein stability [reviewed in (Ito and Akiyama, 2005)]. FtsH also degrades some mis-assembled membrane proteins, contributing to their quality maintenance. It is an energy-utilizing and processive endopeptidase with a special ability to dislocate membrane protein substrates out of the membrane, for which its own membrane-embedded nature is essential.

Targeted to the eukaryotic inner membrane of mitochondria by a sorting sequence at the N-terminus at least two AAA proteases exist, which face their active centers to opposing sites of the membrane. Yeast homo-oligomeric **i-AAA protease** built up by Yme1 subunits is active in the intermembrane space, whereas the hetero-oligomeric **m-AAA protease** complex of Yta10 and Yta12 exposes its catalytic site to the matrix of yeast mitochondria (Koppen and Langer, 2007; Langer, 2000; Leonhard *et al.*, 1996) (see Figure 4). Several *m*-AAA protease isoenzymes are present in mammals (see below.)

m- and *i*-AAA protease exert overlapping substrate specificity and conduct mitochondrial **protein quality control surveillance** (Lemaire *et al.*, 2000; Leonhard *et al.*, 2000). They recognize the folding state of solvent-exposed domains and degrade non-native and non-assembled membrane polypeptides (Arlt *et al.*, 1996; Leonhard *et al.*, 1996; Leonhard *et al.*, 1999). Some substrates of the *m*-AAA protease are known: subunits 1 and 3 of cytochrome *c* oxidase (COX), cytochrome *b* (*Cob*) and the subunits 6, 8 and 9 of the ATP-synthase (Arlt *et al.*, 1996; Guélin *et al.*, 1996). In addition to these integral membrane proteins, the *m*-AAA protease has also been demonstrated to degrade peripheral membrane proteins such as Atp7 (Korbel *et al.*, 2004). In the absence of a functional *i*-AAA protease, yeast cells are characterized by a respiratory deficiency at high temperature, an inability to grow on glucose rich medium at low temperature, an increased rate of mtDNA escape to the nucleus, and a petite-negative phenotype, i.e. strongly impaired growth in the absence of mtDNA (Thorsness and Fox, 1993; Weber *et al.*, 1995). Only a limited number of protein quality control substrates of the yeast *i*-AAA protease has been identified including non-assembled Cox2, unassembled prohibitin subunits PHB1 and PHB2, as well as external NADH dehydrogenase (Nde1) (Augustin *et al.*, 2005; Kambacheld *et al.*, 2005; Nakai *et al.*, 1995; Pearce and Sherman, 1995; Weber *et al.*, 1996).

Intriguingly, the yeast *m*-AAA protease, in addition to its quality control function, has been shown to **specifically process** MrpL32, a subunit of the large mitochondrial ribosomal particle (Nolden *et al.*, 2005). The phenotypes associated with deletions of either Yta10 or Yta12, namely the inability to grow on non-fermentable carbon sources and deficiencies in the synthesis of Cox1 and *Cob*, can be fully explained by an impaired MrpL32 processing: dysfunctional ribosomes fail to translate mitochondrial DNA and cause deficiency in the assembly of respiratory chain complexes (Arlt *et al.*, 1998; Nolden *et al.*, 2005).

However, AAA proteases exert also **functions independently of their proteolytic activity**. The yeast *m*-AAA protease dislocates the nuclear encoded cytochrome *c* peroxidase (Ccp1) thereby allowing its processing by the inner membrane rhomboid

protease Pcp1. This two-step processing of the ROS scavenger is important for the proper release of Ccp1 into the intermembrane space upon import into mitochondria (Esser *et al.*, 2002; Kwon *et al.*, 2003; Tatsuta *et al.*, 2007). Regarding this import function of the yeast *m*-AAA proteases, it is not surprising that Ccp1 processing takes place preferentially at the inner boundary membrane of mitochondria (Suppanz *et al.*, 2009). A similar non-proteolytic role has been suggested for the *i*-AAA protease during import of polynucleotide phosphorylase (PNPase) (Rainey *et al.*, 2006). PNPase contains an N-terminal targeting signal that is cleaved off by MPP in the matrix followed by translocation of mature PNPase into the IMS. Import of mammalian PNPase into yeast mitochondria was shown to depend on the presence of the *i*-AAA protease subunit Yme1. However, PNPase is neither processed nor degraded by the *i*-AAA protease suggesting a non-proteolytic function of Yme1 in the translocation of PNPase across the inner membrane.

Interestingly, AAA proteases have been linked to proteins important for the **lipid environment**. In fact, their deletions affect the integrity of cell and mitochondrial membranes. Bacterial FtsH is the sole, ATP-dependent and essential *E. coli* protease. It maintains the proper lipopolysaccharide/phospholipids ratio by degrading LpxC, a deacetylase for the biosynthesis of lipid A, the membrane embedded lipid moiety of lipopolysaccharides (Ogura *et al.*, 1999). Impaired degradation results in lethal overaccumulation of lipopolysaccharides. In yeast, the majority of phosphatidylethanolamine (PE), an essential component of yeast mitochondria, is synthesized by phosphatidylserine decarboxylase 1 (Psd1), a component of the inner mitochondrial membrane (Voelker, 1997). Deletion of the *i*-AAA protease Yme1 enhanced Psd1 stability and increased slightly PE levels (Nebauer *et al.*, 2007). Deletions of the subunits of the *m*-AAA protease either Yta10 or Yta12 diminish both, cardiolipin and PE levels (Osman *et al.*, 2009). However, mechanisms causing these phenotypes are not understood.

1.4.2. *m*-AAA proteases and prohibitins – highly conserved supercomplexes in the inner mitochondrial membrane

The *m*-AAA protease exists in a large supercomplex together with prohibitins, PHB1 and PHB2 (Steglich *et al.*, 1999). The prohibitins are ubiquitously expressed in eukaryotes and highly conserved among species (Merkwirth and Langer, 2009; Mishra *et al.*, 2006; Nijtmans *et al.*, 2002; Steglich *et al.*, 1999; Tatsuta *et al.*, 2005). Prohibitin 1 and 2 face

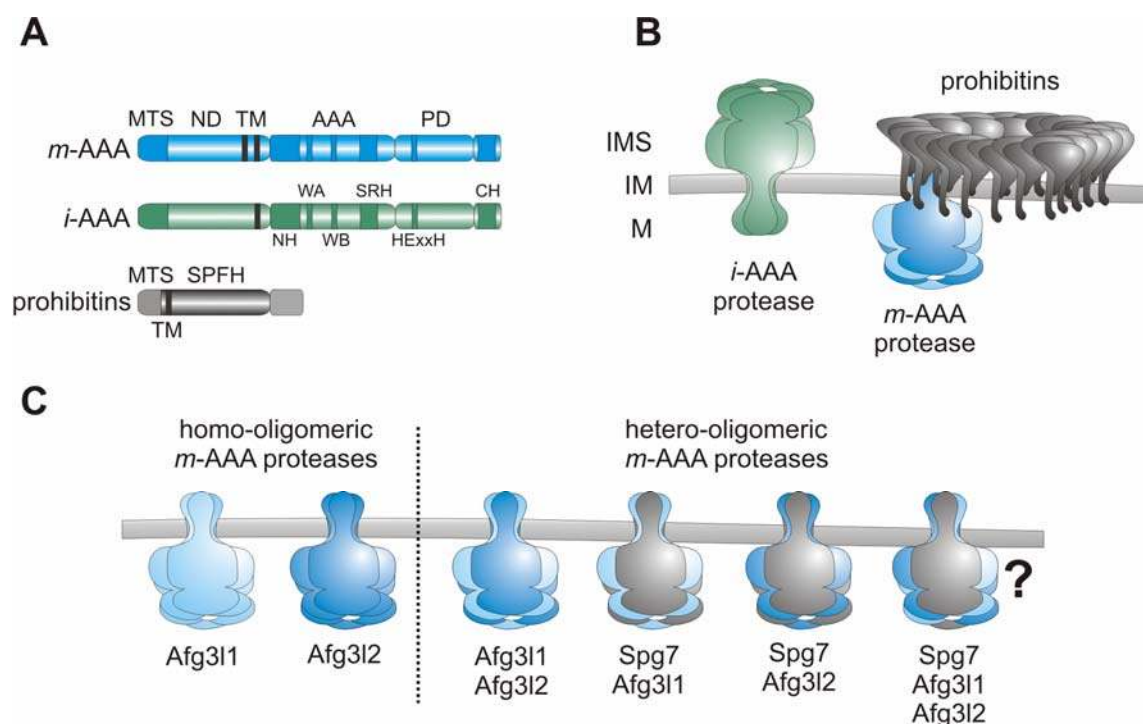


Figure 4: Domain structure and topology of AAA proteases and prohibitins.

(A) Domain structure of AAA proteases and prohibitins. *m*- and *i*-AAA proteases as well as prohibitins are targeted to mitochondria via their mitochondrial targeting signal (MTS). The aminoterminal domain (ND) is followed by the ATPase domain (AAA) and a carboxy-terminal proteolytic domain (PD). One (*i*-AAA) or two (*m*-AAA) hydrophobic regions anchor the protein in the inner membrane of mitochondria (IM) resulting in opposing topology. Aminoterminal helical (NH) region and C-terminal helical domain have been shown to be involved in substrate binding to yeast Yme1. Walker motifs A and B (WA, WB) are important for ATP binding and hydrolysis, respectively. The second region of homology (SRH) contains the arginine finger that stimulates ATP hydrolysis. The PD contains the canonical metal binding site of Zn²⁺-dependent metallopeptidases. Prohibitins contain one TM region and a domain which is characteristic for members of the SPFH-family (stomatin/prohibitin/flotillin/HflKC).

(B) The *i*-AAA protease exposes its active site to the intermembrane space (IMS) whereas the *m*-AAA protease is active at the matrix (M) site. The carboxy-terminal end of prohibitins is in the IMS. Prohibitins form ring-like structures which interact with *m*-AAA proteases to form a supercomplex.

(C) Potential murine *m*-AAA protease isoenzymes. "?" indicates no experimental evidence.

their carboxy-terminal end to the intermembrane space of mitochondria and form large ring-shaped complexes in the mitochondrial inner membrane (Tatsuta *et al.*, 2005). Figure 4 shows the topology of the supercomplex in the inner membrane of mitochondria. Their putative structural role in cristae junction formation is discussed in chapter 1.3.3.3. Prohibitins have been proposed to exert chaperone activity (Nijtmans *et al.*, 2000). Additionally, they are suggested to work as membrane scaffolds since they are homologous to members of the SPFH-family (for stomatin/prohibitin/flotillin/HflKC), which have been found in association with lipid rafts or directly interact with lipids (Browman *et al.*, 2007; Merkwirth and Langer, 2009; Tavernarakis *et al.*, 1999).

The high molecular weight complex of prohibitins and the *m*-AAA protease of approximately 2 MDa was first described for the bacterial homologues HflK and HflC (together HflKC) and FtsH (Kihara *et al.*, 1996), however, later also in yeast and in the mammalian system (Metodieiev, 2005; Steglich *et al.*, 1999; Tatsuta *et al.*, 2005). The role of this supercomplex is as unclear as the function of the prohibitins. The *hflKC* null mutation accelerates the degradation of SecY, a substrate of FtsH, *in vivo* (Kihara *et al.*, 1996). In line, purified HflKC protein inhibits the SecY-degrading activity of purified FtsH protein *in vitro* (Kihara *et al.*, 1996). In yeast, depletion of the prohibitins in strains which contain an increased amount of an unfolded/instable substrate of the *m*-AAA protease results in an accelerated processing of this substrate (Steglich *et al.*, 1999). Therefore, Steglich and Kihara hypothesized that prohibitins or HflKC negatively regulate the proteolytic activity of the protease (Kihara *et al.*, 1996; Steglich *et al.*, 1999). Depletion of prohibitins in mammals has severe effects on cell proliferation, cristae morphogenesis and mitochondrial morphology, all of which were linked to an induced processing of OPA1 (see 1.3.3.3) (Merkwirth *et al.*, 2008). Thus, in line with results from Steglich and Kihara, Merkwirth proposed that the absence of prohibitins in mammalian cells may promote OPA1 processing by *m*-AAA proteases (Merkwirth and Langer, 2009).

1.4.3. Mammalian *m*-AAA proteases

Homologues of the yeast *m*-AAA protease subunits exist in mammals which, when present as an active complex, can functionally substitute for the yeast *m*-AAA protease (Atorino *et al.*, 2003; Koppen *et al.*, 2007; Nolden *et al.*, 2005). Human subunits **paraglegin** and **AFG3L2** share 36-56 % sequence identity with their yeast counterparts and 39 % with each other (Banfi *et al.*, 1999; Casari *et al.*, 1998). A phylogenetic tree is found in the appendix chapter 6.3.1. Interestingly, a third subunit **Afg3l1** is expressed in mice but encoded by a pseudogene in humans (Kremmidiotis *et al.*, 2001; Shah *et al.*, 1998).

The complex composition of mammalian *m*-AAA proteases differs from yeast. Active **hetero- and homo-oligomeric assemblies** can be formed by human and murine Afg3l2 and Afg3l1 subunits except for paraglegin which assembles only with the other subunits. As a consequence, a set of diverse *m*-AAA protease isoenzymes exist (Koppen *et al.*, 2007) (Figure 4 C). Considering the variety of *m*-AAA protease complexes, expression level and assembly of the subunits might alter enzymatic properties or substrate specificity of the protease (Koppen and Langer, 2007; Koppen *et al.*, 2007; Martinelli *et al.*, 2009). The situation may become even more complex considering different substrate compositions in certain cell types or tissues (Mootha *et al.*, 2003). Therefore, it is not surprising that loss-of-

function mutations in paraplegin or Afg3l2 lead to different phenotypes in mouse and human. Both human subunits are linked to different neurodegenerative diseases. Strikingly, like for diseases associated with mitochondrial dynamics, phenotypes observed are highly tissue-specific.

1.4.3.1. Phenotypes associated with defects in mammalian *m*-AAA protease subunits

Mutations in *paraplegin* or *SPG7* are associated with an autosomal recessive form of **hereditary spastic paraplegia (HSP)** (Casari *et al.*, 1998). HSP is a heterogeneous group of genetic disorders in which the main feature is progressive spasticity in the lower limbs due to pyramidal tract dysfunction. This also results in brisk reflexes, extensor plantar reflexes, muscle weakness and urinary urgency. These symptoms are the result of a 'dying back' degeneration of the cortico-spinal tracts. The longest fibers, innervating the lower extremities, are most affected (Depienne *et al.*, 2007). The molecular mechanisms leading to axonal degeneration are probably as diverse and complex as the genetics of HSPs. It is believed, on the one hand, that cellular trafficking, and more particularly axonal transport –especially of mitochondria – is impaired. The first mitochondrial motility defect was identified in a family with autosomal dominant hereditary spastic paraplegia type 10 (SPG10) and mutations in a gene encoding one of the kinesins, affecting regions involved in microtubule binding and subsequently mitochondrial transport (Fichera *et al.*, 2004). On the other hand, mitochondrial dysfunction is the second process that leads to HSPs, and is exemplified by SPG13 and SPG7 (Depienne *et al.*, 2007; Rugarli and Langer, 2006). HSP type 13 or SPG13 is caused by mutation in the chaperonin HSP60 (Hansen *et al.*, 2002). However, HSP primary fibroblasts lacking SPG7 show reduced complex I activity and increased sensitivity to oxidant stress (Atorino *et al.*, 2003).

Mice lacking paraplegin (*Spg7*^{-/-}) are affected by a distal axonopathy of spinal cord and peripheral axons characterized by axonal swelling and degeneration resembling the human disease (Ferreirinha *et al.*, 2004). However, the phenotype is progressive and mice behave comparable to control littermates directly after birth. The earliest pathologic event in paraplegin-deficient mice at 4.5 month is the appearance of hypertrophic mitochondria with disrupted and swollen cristae in synaptic terminals. Later, axonal swellings occur through massive accumulation of organelles and neurofilaments, suggesting an impairment of anterograde axonal transport. Also retrograde axonal transport is delayed.

Dominant mutations in the *AFG3L2* gene cause **spinocerebellar ataxia** type 28 (SCA28) (Cagnoli *et al.*, 2008; DiBella *et al.*, 2008). Autosomal dominant cerebellar ataxias are a clinically and genetically heterogeneous group of neurodegenerative disorders primarily characterized by imbalance, progressive gait and limb ataxias, and dysarthria

(Harding, 1982). It is often associated with poor coordination of hands, speech, and eye movements (ophthalmoparesis). Pathogenesis mechanisms involve the degeneration of the cerebellum and the spinal cord (Cagnoli *et al.*, 2006; Mariotti *et al.*, 2008). Interestingly, mice having truncations in *Afg3l2*, leading to the loss of the protein (***Afg3l2*^{Emv66/Emv66}**), and mice having a critical mutation in the AAA domain (R389G) (***Afg3l2*^{par/par}**), show an extremely severe neuromuscular syndrome beginning at postnatal day 7 (P7) with hindlimbs paraparesis which progresses until complete tetraparesis and death, generally at P16 (Maltecca *et al.*, 2008). Mouse models are characterized by delayed myelination and impairment of axonal radial growth in both the central nervous system (CNS) and peripheral nervous system (PNS). Mitochondrial morphology abnormalities are detected in motor and sensory neurons, more frequently in proximity of the nucleus. Mitochondria isolated from brains and spinal cord reveal reduced activity as well as reduced levels of complex I and complex III (Maltecca *et al.*, 2008). However, non-neuronal tissues are not significantly affected in *Afg3l2* mutant mice. These findings raise the possibilities that the phenotypes associated with *Afg3l2* and paraplegin mutations reflect functional differences of *m*-AAA isoenzymes or might result from a tissue-specific expression of *m*-AAA protease subunits (Koppen *et al.*, 2007).

Further crossing of the *Spg7*^{-/-} mice with the *Afg3l2*^{Emv66/Emv66} mice and further backcrossing with *Spg7*^{-/-} mouse resulted in heterozygous *Afg3l2* mice (Martinelli *et al.*, 2009). ***Spg7*^{-/-} *Afg3l2*^{Emv66/+}** mice show an early-onset severe neurological phenotype, characterized by loss of balance, tremor, and ataxia. These mice display acceleration and worsening of the axonopathy observed in paraplegin-deficient mice. In addition, they exhibit a prominent cerebellar degeneration with loss of Purkinje cells and parallel fibers, and reactive astrogliosis. Mitochondria from affected tissues are prone to lose mtDNA, have unstable respiratory complexes, and display an impaired maturation of MrpL32. These data demonstrate genetic interaction between the *m*-AAA isoenzymes and suggest that different neuronal populations have variable thresholds of susceptibility to reduced levels of the *m*-AAA protease. Moreover, they implicate impaired mitochondrial proteolysis as a novel pathway in cerebellar degeneration (Martinelli *et al.*, 2009).

In conclusion, different mouse models exist which all aim to understand the molecular mechanisms causing the human diseases. However, HSP and SCA clearly demonstrate that mitochondrial dysfunction has emerged as a hallmark of neurodegenerative diseases (Lin and Beal, 2006). Mitochondria are regionally organized within some nerve cells, with higher accumulation in the nerve terminal. Synapses particularly need mitochondria to regulate calcium and ATP levels, thereby maintaining synaptic transmission and structure (Chen and Chan, 2006). But, what is the primary molecular effect within mitochondria in

the synaptic terminals lacking paraplegin? And why are in particular the neurons of the cortico-spinal tract affected? On the one hand, a reduced amount of *m*-AAA protease isoenzymes might fail to degrade non-assembled or misfolded polypeptides which accumulate and lead to certain stress stimuli, e.g. ROS. On the other hand, they could be incapable of processing a specific protein which interferes with the morphology of mitochondria. Giant mitochondria and swollen cristae have been observed. Is there any link to the mitochondrial dynamics machineries?

Strikingly, *m*-AAA proteases have been linked to OPA1. Ishihara *et al.* showed that overexpression of Spg7 (paraplegin) in mouse embryonic fibroblasts leads to accelerated OPA1 processing and subsequently to fragmentation of mitochondria indicating that the *m*-AAA protease might cleave OPA1 (Ishihara *et al.*, 2006). However, mouse embryonic fibroblasts lacking paraplegin exhibit a wild type OPA1 pattern (Duvezin-Caubet *et al.*, 2007). Additionally, the different tissue-specificities of both disorders, ADOA (chapter 1.3.4) and HSP, suggest that tissue specific consequences of a paraplegin-deficiency cannot simply be reconciled with an impaired OPA1 function itself (Koppen and Langer, 2007).

Certainly, to unravel HSP and SCA pathogenesis substrates of the mammalian *m*-AAA proteases must be identified. Tissue-specific, cellular and subcellular-specific organization of mitochondria as well as varying levels of different isoenzymes have to be considered.

1.4.4. What determines a substrate? How is it recognized by AAA-proteases?

AAA proteases recognize the folding state of solvent-exposed domains (Leonhard *et al.*, 2000). Degradation initiation regions of a substrate polypeptide like a degradation tag may be first recognized by the outer surface of the helical subdomain of the ATPase domain (Niwa *et al.*, 2002). This is the simplest way of recognizing a substrate which is thought to be independent of ATP hydrolysis. This first step is then followed by nucleotide-dependent conformational changes which drive translocation of the peptide tag through the central pore for successive events of endoproteolysis (Ito and Akiyama, 2005). The substrate has to be unfolded upon translocation. Different ATP-dependent proteases share distinct unfoldase activities, e.g. FtsH has been reported to be less powerful than other AAA⁺ proteases (Herman *et al.*, 2003). Studies on the *i*-AAA protease subunit Yme1 of yeast allowed the identification of two helical binding regions, which form a lattice-like structure at the surface of the proteolytic cylinder and mediate the initial encounter of substrate proteins with the protease (Graef *et al.*, 2007; Leonhard *et al.*, 1999): helices C-terminal of the proteolytic domain (CH) and N-terminal helices of the AAA domain (NH), which are

located in close proximity to the membrane surfaces and highly negatively charged. Thus, substrate proteins initially interact with the *i*-AAA protease at the outer surface of the proteolytic cylinder, before they enter the proteolytic chamber (Graef *et al.*, 2007). Evidence for substrate translocation into a proteolytic chamber through the central pore of mitochondrial AAA proteases has been obtained by mutational analysis of a conserved loop motif YVG (aromatic-hydrophobic-glycine) in Yme1 (Graef and Langer, 2006), which has been localized to the central pore of other hexameric AAA⁺ ring complexes (Wang *et al.*, 2001).

Furthermore, AAA protease-mediated degradation of inner membrane proteins involves the extraction of the substrate from the membrane bilayer (Leonhard *et al.*, 2000). For FtsH, it is proposed that the first event in the recognition of a membrane protein substrate occurs within the membrane through interaction of a transmembrane segment of the substrate and the transmembrane regions of FtsH as well as with HflKC (Ito and Akiyama, 2005). However, it is completely unknown what kind of features of the transmembrane region are recognized by FtsH/HflKC. The ability of the *m*-AAA protease to mediate vectorial membrane dislocation of proteins in an ATP-dependent reaction has been directly demonstrated (Tatsuta *et al.*, 2007). This membrane extraction of substrate proteins is likely to be facilitated by the membrane-embedded parts of AAA protease subunits which might form a pore-like structure or provide at least a more hydrophilic environment (Korbel *et al.*, 2004).

An example for a signal of degradation is the membrane protein YccA, a substrate of the bacterial AAA protease. A mutant of the YccA protein with a shortened cytosolic tail at the N terminus is stable but it still remains associated with FtsH indicating the N-terminus of this protein is the signal for degradation (Karata *et al.*, 2001; Kihara *et al.*, 1998). Binding of YccA was not affected by this truncation, indicating that the binding to FtsH is mediated by another region of the protein. Therefore, it is most likely that also other substrates bind to the protease which cannot be degraded or processed due to mutations in the protease. In fact, that has been shown for the yeast *m*-AAA protease. Although neither the binding regions in Mrp132, nor within the *m*-AAA protease are known, it traps Mrp132 when the enzyme is in an proteolytical inactive state (Nolden *et al.*, 2005).

1.5. *Aims of the thesis*

Yeast *m*-AAA proteases have been identified to be crucial regulators of mitochondrial quality control by degrading non-assembled and non-native polypeptides (Leonhard *et al.*, 2000). Additionally, they control mitochondrial biogenesis by processing of MrpL32, a subunit of the mitochondrial ribosome (Nolden *et al.*, 2005). The processing explains the pleiotropic phenotypes associated with the loss of the *m*-AAA protease. Mammalian *m*-AAA protease subunits are linked to neurodegenerative diseases whose pathogenesis' underlying molecular mechanisms are poorly understood. To analyze the cellular and molecular role of mammalian *m*-AAA proteases, stable cell lines expressing dominant-negative variants of mammalian *m*-AAA protease subunits were generated.

One putative substrate has been identified, the dynamin-related protein OPA1, which has been shown being important for mitochondrial fusion and cristae morphogenesis (Cipolat *et al.*, 2006; Duvezin-Caubet *et al.*, 2007; Frezza *et al.*, 2006; Ishihara *et al.*, 2006; Song *et al.*, 2007). Therefore, initial experiments were aiming at analyzing the link between *m*-AAA proteases and OPA1 processing. However, impaired processing of OPA1 is believed to not fully contribute to the phenotypes observed in the mammalian system (Koppen and Langer, 2007). Additionally, considering a tissue or cell type specific expression of *m*-AAA protease subunits and variations of the mitochondrial proteome even in single cells, most likely, also other substrate proteins in particular in different tissues or cell types may exist (Hollenbeck and Saxton, 2005; Mootha *et al.*, 2003). In regard of this hypothesis, the dominant-negative mammalian *m*-AAA protease subunits were fused to an affinity purification tag. Considering the yeast data, these proteolytically inactive complexes should work as a substrate traps allowing the co-purification of substrates and interacting partners of *m*-AAA protease isoenzymes. Finding substrate proteins should provide further insights into the pathogenesis of the neurodegenerative diseases hereditary spastic paraplegia or spinocerebellar ataxia.

2. Material and Methods

2.1. Material

2.1.1. Chemicals

Chemicals were purchased from Sigma, Merck or Roth unless stated otherwise. All buffers and solutions were prepared using ultrapure water (Milli-Q, Millipore).

2.1.2. *E. coli* strains

XL1-Blue (Stratagene)	<i>recA1 endA1 gyrA96 thi-1 hsdR17 supE44 relA1 lac</i> [F' <i>proAB lacI^qZΔM15 Tn10</i> (Tet ^r)]
XL10-Gold® (Stratagene)	Tet ^r Δ(<i>mcrA</i>)183 Δ(<i>mcrCB-hsdSMR-mrr</i>)173 <i>endA1 supE44 thi-1 recA1 gyrA96 relA1 lac Hte</i> [F' <i>proAB lacI^qZΔM15 Tn10</i> (Tet ^r) Amy Cam]

2.1.3. Mammalian cell lines

FlpIn™ T-REx™-293	Invitrogen; expresses the Tet repressor from pcDNA6/TR; contains a single integrated Flp Recombination Target (FRT) site from pFRT/lacZeo; derived from 293 human embryonic kidney cells (Graham <i>et al.</i> , 1977), for more information about the 293 parental cell line, see the ATCC Web site (www.atcc.org) and refer to ATCC number CRL-1573.
T-REx™-HeLa	Invitrogen; expresses the Tet repressor from pcDNA6/TR, derived from human cervical adenocarcinoma cells for more information about the HeLa parental cell line, see the ATCC Web site (www.atcc.org) and refer to ATCC number CCL-2.

2.1.4. Generation of expression plasmids

For expression of human *m*-AAA protease subunits in FlpIn T-REx-293 cells (see 2.1.3), constructs consisting of the ORF of human *SPG7* (*paraplegin*) (corresponding to amino acids 1-795) or human *AFG3L2* (amino acids 1-797) fused to a C-terminal hexahistidine epitope tag were excised from the yeast multicopy plasmids YEplac118 ADH or YEplac112 ADH (Gietz and Sugino, 1988), respectively (Mirko Koppen, unpublished). *SPG7* was cloned using restriction enzymes XbaI and Sall and cloned into EcoRV and XhoI cut mammalian expression vector pcDNA5 FRT/TO (Invitrogen) enabling expression under the control of a tetracycline-inducible CMV promoter. The open reading frame of *AFG3L2* was excised by KpnI and XhoI and ligated into KpnI and XhoI digested pcDNA5 FRT/TO. Murine *Afg3l2* (amino acids 1-802) was amplified from murine cDNA and subcloned into pGEM[®]-T Easy (Promega). NotI restriction sites and a C-terminal *Strep*[®]II-tag (Schmidt *et al.*, 1996) fused to an octahistidine epitope tag were introduced by PCR using the oligonucleotides listed in Table 3. Mouse *Afg3l2* was cloned by a NotI digest into pcDNA5 FRT/TO.

m-AAA protease subunits were mutated to substitute the catalytically active glutamate residues within the proteolytic centres (PC) and Walker B motifs (WB) in the ATPase domain by glutamine residues using the QuikChange[®] Site-Directed Mutagenesis Kit (Stratagene). Oligonucleotides used are listed in Table 3. The respective codons of the human and murine expression constructs were mutated from GAA to CAG or GAG to CAA, respectively. The mutated amino acids correspond to the following positions: human *SPG7* (PC, *SPG7*^{E575Q}; WB, *SPG7*^{E409Q}), human *AFG3L2* (PC, *AFG3L2*^{575Q}; WB, *AFG3L2*^{E408Q}), mouse *Afg3l2* (WB, *Afg3l2*^{E407Q}). All expression constructs were verified by DNA sequencing.

Table 2: List of plasmids used in this study

Plasmid	Reference
YEplac181 ^{ADH1} - <i>SPG7</i> (1-795)-6His	Mirko Koppen, unpublished
YEplac112 ^{ADH1} - <i>AFG3L2</i> (1-797)-6His	Mirko Koppen, unpublished
pCMV14- <i>rat Opa1 splice variant 1</i> -3FLAG	(Ishihara <i>et al.</i> , 2006)
pCMV14- <i>rat Opa1 splice variant 1ΔS1</i> -3FLAG	(Ishihara <i>et al.</i> , 2006)
pcDNA5 FRT/TO ^{CMVTetO₂} - <i>SPG7</i> (1-795)-6His	this study
pcDNA5 FRT/TO ^{CMVTetO₂} - <i>SPG7</i> ^{E575Q} (1-795)-6His	this study
pcDNA5 FRT/TO ^{CMVTetO₂} - <i>SPG7</i> ^{E409Q} (1-795)-6His	this study
pcDNA5 FRT/TO ^{CMVTetO₂} - <i>AFG3L2</i> (1-797)-6His	this study

Plasmid	Reference
pcDNA5 FRT/TO ^{CMVTetO} ₂ - AFG3L2 ^{E575Q} (1-797)-6His	this study
pcDNA5 FRT/TO ^{CMVTetO} ₂ - AFG3L2 ^{E408Q} (1-797)-6His	this study
pcDNA5 FRT/TO ^{CMVTetO} ₂ - Afg3l2 (1-802)-Strep [®] II-8His	this study
pcDNA5 FRT/TO ^{CMVTetO} ₂ - Afg3l2 ^{E407Q} (1-802)-Strep [®] II-8His	this study
pcDNA5 FRT/TO ^{CMVTetO} ₂ - MICS1 (1-345)-4HA	this study

2.1.5. Oligonucleotides

Table 3: List of oligonucleotides used in this study

Oligo	Description	Sequence
TL1048	3'-SPG7 ^{E575Q}	5'-GGCGTGGCCCGACTGATGAAACGCAACCAC-3'
TL1049	5'-SPG7 ^{E575Q}	5'-GTGGTTGCGTTTCATCAGTCGGGCCACGCC-3'
TL1050	3'-AFG3L2 ^{E575Q}	5'-CCGCATGGCCTGCTTGGTGGTATGCCACAG-3'
TL1051	5'-AFG3L2 ^{E575Q}	5'-CTGTGGCATAACCACCAAGCAGGCCATGCCG-3'
TL3795	3'-Ascl-8His- Strep-tag [®] II- Afg3l2	5'-GGCGCGCCTTAGTGATGGTGGTGGTGGTGGT GCTCGAGTTTTTCGAAGTCCGGGTGGCTCCAGCTGAC AACCTTCTCATT-3'
TL3796	5'-Ascl-Afg3l2	5'-GGCGCGCCACATGGCCCACCGCTGCCTGC-3'
TL3895	5'-Afg3l2 ^{E407Q}	5'-TCTCTTCATTGATCAGATTGATGCTGTGGG-3'
TL3896	3'-Afg3l2 ^{E407Q}	5'-CCCACAGCATCAATCTGATCAATGAAGAGA-3'
TL4280	5'-SPG7 ^{E409Q}	5'-TCGTCTACATCGATCAGATCGACGCGGTG-3'
TL4281	3'-SPG7 ^{E409Q}	5'-CACCGCGTCGATCTGATCGATGTAGACGA-3'
TL4284	5'-AFG3L2 ^{E408Q}	5'-TTGCATCCTCTTCATCGATCAAATCGATGCGGT-3'
TL4285	3'-AFG3L2 ^{E408Q}	5'-ACCGCATCGATTTGATCGATGAAGAGGATGCAA-3'
TL4896	3'-NotI- HindIII-4HA- MICS1	5'-AGCGGCCGCAAGCTTTAAGCGTAATCTGGAACA TCGTATGGGTAAGCGTAATCTGGAACATCGTATGG GTAAGCGTAATCTGGAACATCGTATGGGTAAGCGT AATCTGGAACATCGTATGGGTATTTCTTTCTGTTGC CTCCAGTTG-3'
TL4899	5'-KpnI-MICS1	5'-GGTACCGCCACCATGTTGGCTGCAAGGCTG-3'

2.1.6. Antibodies

Table 4: List of immunoreagents used in this study.

Antibody	Antigen	Dilution	Reference; comments
α-AFG3L2	Amino acids 413-828 of human AFG3L2	1:8000	F. Taroni, unpublished

Antibody	Antigen	Dilution	Reference; comments
α -AFG3L2	Amino acids 413-828 of human AFG3L2	1:500	this study; used for CO-IP
α -Afg3l2	Amino acids 90-103 of Afg3l2	1:200	(Koppen <i>et al.</i> , 2007)
α - β -actin	Actin N-terminal peptide	1:2000	Sigma
α -CI	Bovine complex I 30 kDa subunit	1:1000	Molecular Probes
α -CII	Bovine complex II 70 kDa subunit	1:1000	Molecular Probes
α -CIII	Bovine complex III core 2 subunit	1:1000	Molecular Probe
α -CIV	Bovine complex IV subunit II	1:1000	Molecular Probe
α -DLP1	Amino acids 601-722 of rat DLP1 (Drp1)	1:500	BD Biosciences
α -FLAG	Synthetic FLAG peptide DYKDDDDK	1:1000	Sigma
α -HA	Synthetic HA peptide YPYDVPDYA	1:3000	Roche
α -MrpL32	Amino acids 83-98 of murine MrpL32	1:500	(Nolden <i>et al.</i> , 2005)
α -OPA1	Amino acids 708-830 of human OPA1	1:900	BD Biosciences
α -PARP1	Synthetic peptide corresp. to the caspase cleavage site in PARP1.	1:1000	Cell Signaling Technology
α -PHB1	Recombinant C-terminus of human PHB1	1:500	BioLegend
α -PHB2	Recombinant C-terminus of human PHB2	1:500	BioLegend
α -SLP2	Amino acids 171-356 of human Stomatin-like 2 (SLP2)	1:2000	GenWay Biotech

2.2. Molecular biological methods

Standard methods in molecular biology were performed according to protocols published in (Sambrook and Russell, 2001). Restriction enzymes were purchased from NEB (New England Biolabs). PCRs were carried out using the High Fidelity PCR Master (Roche). For isolation of plasmid DNA from *E. coli* the NucleoSpin Plasmid QuickPure® and NucleoBond® PC100 kits were used, for extraction of DNA from agarose gels the NucleoSpin® Extract II kit (all Machery Nagel) was used, all according to instructions of the manufacturer.

2.3. Cell biological methods

2.3.1. Cell culture

FlpIn T-REx-293 (FITR293) and T-REx-HeLa cells were cultured in high-glucose and stable glutamine containing Dulbeccos Modified Eagle's Medium (DMEM+glutamax, PAA) supplemented with 7.5% [v/v] tetracycline-free fetal bovine serum (FBS, BIOCHROM), 100 U/ml penicillin (PAA), 100 µg/ml streptomycin (PAA), 100 µM non-essential amino acids (PAA) and 1 mM sodium pyruvate (PAA). 15 µg/ml blasticidin (Invivogen) was added to maintain the Tet repressor. Cells were cultured at 37 °C, 5 % CO₂ and 90 % humidity. Complete growth medium containing 10 % [v/v] DMSO was used for stepwise cryofreezing from -80 °C to -200 °C. After thawing FITR293 cells were cultivated without any selective reagent for 2 days. Detaching cells for splitting was performed by addition of 1 x trypsin/EDTA (PAA) for 5 min at 37 °C.

2.3.2. Transfections

Transient transfections were performed using the GeneJuice[®] Transfection Reagent (Novagen) according to the manufacturer's instructions. Unless otherwise noted cells were grown on 6-well plates and transfected with 1 µg of plasmid DNA followed by a second transfection 4 h later under identical conditions. Stable transformations were carried out using the FlpIn T-REx system (Invitrogen) (see 2.3.3).

2.3.3. FlpIn T-REx system and selection of stable transformants

The FlpIn T-REx system (Invitrogen) allows tetracycline-inducible and stable overexpression of a gene of interest in mammalian cell culture (see Figure 6). It is in detail explained in chapter 3.2.1. FITR293 cells expressing the Tet-repressor and harboring a genomically integrated FRT-site were grown on 6-well plate format with medium containing 100 µg/ml Zeocin[™] (Invivogen). The FITR293 cell line was transfected twice with GeneJuice[®] Transfection Reagent (Novagen). In total, 3 µg DNA of pcDNA5 FRT/TO constructs containing the genes of interest (see 2.1.4) and Flp-recombinase expressing pOG44 plasmid with a ratio of 1:5 was used for transfection. Flp mediates site-directed recombination of the FRT-sites in the pcDNA5 FRT/TO vector and in the genome of the FITR293 cell line thereby allowing the stable integration of the gene of interest. During this process cells lose their resistance to Zeocin which was excluded from the growth medium by the time of transfection. By contrast, after recombination cells become resistant to

hygromycin B. After 48 h cells were transferred to a 10 cm plate to reach 25 % confluency, and selection with 150 $\mu\text{g/ml}$ hygromycin B (Invivogen) was started. Growing clones were picked after 18-24 days and expanded to test for β -galactosidase activity and ZeocinTM sensitivity. Growth medium containing 100 $\mu\text{g/ml}$ ZeocinTM was changed daily. Positive clones died after 7-14 days of this treatment. Expression was induced with 1 $\mu\text{g/ml}$ tetracycline for 24 h (Fluka).

2.3.4. β -galactosidase activity assay

The β -galactosidase activity assay was performed to monitor the stable integration of the gene of interest into the genome of the FITR293 cells. Positive insertion results in the loss of β -galactosidase activity. The enzyme promotes lactose utilization. β -galactosidase hydrolyzes X-gal (5-bromo-4-chloro-3-indolyl-beta-D-galactopyranoside) (PEQLAB) into colorless galactose and 4-chloro-3-brom-indigo which forms an intense blue precipitate. Cells expressing β -galactosidase appear therefore blue under the light microscope. To visualize activity FITR293 cells were cultivated in 6 or 24 well plate format to a cell density of 60-80 %. Cells were washed twice with 1 x PBS (PAA) and fixed with 0.2 % [v/v] glutaraldehyde and 2 % [v/v] formaldehyde in 1 x PBS for 5 min at 4 °C. After two washing steps with 1 x PBS, 1000 μl (6-well) and 200 μl (24 well) of the X-gal- solution was added to the cells and incubated 30 min at 37 °C.

X-gal-solution:	1 mg/ml X-gal
	5 mM $\text{K}_3\text{Fe}(\text{CN})_6$
	5 mM $\text{K}_4\text{Fe}(\text{CN})_6$
	2 mM MgCl_2
	0.02 % [v/v] NP-40
	0.01 % [w/v] SDS

2.3.5. Cell proliferation assay

The CellTiter 96[®] AQueous One Solution Cell Proliferation Assay (Promega) is an optimized MTT-derived colorimetric method for determining the number of viable cells in proliferation, cytotoxicity or chemosensitivity assays (Alley *et al.*, 1988). The solution contains a tetrazolium compound [3-(4,5-dimethylthiazol-2-yl)-5-(3-carboxymethoxy-phenyl)-2-(4-sulfophenyl)-2H-tetrazolium, inner salt; MTS] and an electron coupling reagent. The yellow MTS gets reduced by active dividing cells to produce the purple formazan product. 5×10^3 cells were seeded onto poly-L-lysine-coated 96-well plates and

expression was induced by 1 $\mu\text{g}/\text{ml}$ tetracycline daily. Assays were performed by adding 20 μl of the CellTiter 96[®] AQ_{ueous} One Solution Reagent directly to culture wells containing 100 μl of growth media, incubating for 1–4 hours and then recording absorbance at 490 nm with a 96-well plate reader. The quantity of formazan product as measured by the absorbance at 490 nm is directly proportional to the number of living cells in culture. Assays were measured in quadruplicates and, unless otherwise stated, at least three independent experiments were performed.

2.3.6. Measurement of respiratory activities

2.3.6.1. Oxygen consumption in intact cells

Respiration of intact cells was measured at 37°C with a Clark-type electrode oxygraph (Hansatech Inc.) in a heated water-jacketed chamber connected to a circulating water bath. The chamber volumes were set to 500 μl . The measurement with 2.5×10^6 cells started with recording the routine endogenous respiration. After observing steady state respiratory flux, ATP synthase was inhibited with 2 μM oligomycin for 5 min. This was followed by uncoupling of oxidative phosphorylation using stepwise titration of cyanide *m*-chlorophenylhydrazine (CCCP) with concentrations in the range of 250–750 nM. After 5 min recording, cellular respiration was inhibited with 2 mM KCN and was corrected to KCN-insensitive respiration. The respiratory control ratio was obtained dividing the rates of oxygen consumption measured before and after the addition of CCCP.

Respiration buffer:	250 mM sucrose
	20 mM HEPES pH7.4
	10 mM KH_2PO_4
	4 mM MgCl_2
	1 mM EDTA
	5 mM glucose
	2 mM pyruvate
	4 mM glutamate

2.3.6.2. Assessment of mitochondrial membrane potential

Mitochondrial membrane potential is an important parameter of mitochondrial function and was measured by fluorescence-activated cell sorting (FACS, FACSCalibur equipped with CellQuest software (Becton Dickinson)) after staining of FITR293 cells with JC-1 (Molecular Probes) (Salvioli *et al.*, 1997). JC-1, a lipophilic, cationic dye exhibits potential-dependent accumulation in mitochondria, indicated by a fluorescence emission

shift from green (~529 nm) to red (~590 nm). Consequently, mitochondrial membrane potential dissipation is indicated by a decrease in the red/green fluorescence intensity ratio. In healthy cells with high mitochondrial membrane potential, JC-1 spontaneously forms complexes known as J-aggregates with intense red fluorescence. On the other hand, in apoptotic or unhealthy cells with low membrane potential, JC-1 remains in the monomeric form, which shows only green fluorescence. Analysis of JC-1 fluorescence was examined with an excitation at 488 nm and emission was recorded at 535 nm and 590 nm. Staining was performed according to manufacturer's instructions in growth medium (2.3.1) and membranes were depolarized by adding 100 μ M CCCP as a positive control.

2.3.6.3. Measurement of cellular ATP contents

FITR293 cells were grown in glucose containing growth medium (see 2.3.1). 48 h before the induction of protein expression with tetracycline, growth medium was changed to medium containing 1 mM galactose. 1.5×10^6 FITR293 cells were harvested after 24 h induction with 1 μ g/ml tetracycline and lysed immediately in 10% dichloric acid, neutralized in KOH and centrifuged at 15,000 x g for 15 min. ATP content was measured by a luminometric assay using luciferase. Based on an ATP standard curve and normalized on the total protein concentration the ATP basal level: nmol ATP/ μ g protein was obtained.

Luciferase buffer:	150 mM KCl
	25 mM Tris pH 7.4
	10 mM KH ₂ PO ₄
	2 mM MgCl ₂
	1 mM EDTA
	2.5 μ g/ml luciferase
	15 μ M luciferine

2.3.7. Monitoring mitochondrial morphology using fluorescence microscopy

To analyze mitochondrial morphology, cells were grown on poly-L-lysine coated coverslips and transfected with pDsRed2-Mito (Clontech). pDsRed2-Mito is a mammalian expression vector that encodes a fusion of *Discosoma sp.* red fluorescent protein (DsRed2) and the mitochondrial targeting sequence from subunit VIII of human cytochrome c oxidase (Mito). Sterile glass coverslips were incubated for 2 h with 0.01 % poly-L-lysine solution (Sigma) and rinsed twice with 1 x PBS (PAA). One day before transfection 1.2×10^5 FITR293 cells were seeded on coated coverslips in 6-well plates. 24-48 h after

transfection expression was induced with 1 $\mu\text{g/ml}$ tetracycline and 24 h later cells were fixed with 3 % [w/v] paraformaldehyde in 1 x PBS (PAA) for 15 min at 37°C. After 2 washing steps with 1 x PBS cells were incubated for 5 min at 37°C in 1 $\mu\text{g/ml}$ 4',6-Diamidino-2-phenylindole (DAPI) (Roche) in 1 x PBS to visualize nuclear DNA. The DAPI staining solution was removed by rinsing twice with 1 x PBS and samples were mounted in ProLong® Gold Antifade Reagent (Molecular Probes). Fluorescently labeled mitochondria were examined using the DeltaVision microscope system and the Softworx software (Applied precision). Images were deconvolved and further edited using CORELDRAW™ 12 Graphics Suite software (Corel Corporation).

2.3.8. Analysis of cellular apoptosis

To monitor apoptotic sensitivity FITR293 cell lines were treated with TNF- α which activates the death receptor pathway. $2-4 \times 10^5$ FITR293 cells were seeded one day before induction with 1 $\mu\text{g/ml}$ tetracycline onto 6 well plates. After 24 h, medium was replaced with medium containing 0-20 ng/ml human TNF- α , 2 $\mu\text{g/ml}$ cycloheximide and 1 $\mu\text{g/ml}$ tetracycline. Cells were further incubated for 24 h, harvested in the medium, pelleted by centrifugation (1,200 x g, 5 min, RT) and washed twice with 1 x PBS (PAA). Total cell lysates were size fractionated by SDS-PAGE (2.4.3.1) and analyzed by immunoblotting (2.5.1) using antibodies directed against PARP, one of the main cleavage targets of caspase-3 *in vivo* (Nicholson *et al.*, 1995; Tewari *et al.*, 1995).

2.3.9. Isolation of mitochondria from tissue culture cells

Mitochondria were isolated from FITR293 cells after inducing the expression of AFG3L2 variants with 1 $\mu\text{g/ml}$ tetracycline. Cell cultured in 10 x 15 cm dishes were washed once with ice cold 1 x PBS (PAA) and removed from the tissue culture plate with cell scrapers (Sarstedt). After pelleting at 1,200 x g at 4 °C for 5 min and two washing steps with 5-10 ml ice cold 1 x PBS, cells were resuspended in 8 ml homogenization buffer and homogenized using the Potter S (Braun) moving the Teflon potter 10 times up and down. Homogenates were then differentially centrifuged: a first step of 1,200 x g at 4 °C for 5 min served to remove intact cells and nuclei and a second step at 10,000 x g (20 min, 4 °C) to obtain mitochondrial pellets. After washing mitochondrial enriched membranes with homogenization buffer and centrifuging step at 10,000 x g at 4 °C for 20 min mitochondria were resuspended in resuspension buffer. Protein concentration was assessed by the Bradford protein assay (BioRad) using IgG as standard. The mitochondrial fractions were diluted with resuspension buffer to a final protein concentration of 10 mg/ml.

Homogenization buffer:	220 mM mannitol 70 mM sucrose 10 mM HEPES pH 7.4 1 x Complete Protease Inhibitor Cocktail (Roche)
Resuspension buffer:	homogenization buffer with 1 mM EDTA

2.3.10. Analysis of mitochondrial phospholipid composition

2.3.10.1. Phospholipid extraction

Phospholipids were extracted from mitochondria isolated from FITR293 cells induced with 1 $\mu\text{g/ml}$ tetracycline for 24 h using protocols described for isolation of yeast phospholipids (Vaden *et al.*, 2005). The mitochondrial membrane fraction (1 mg) was mixed with 2.5 ml chloroform/methanol [2:1, v/v] and vigorously shaken for 1 h in a 15 ml glasstube at RT. Samples were vortexed for 1 min after the addition of 300 μl water and centrifuged at 1,000 rpm for 5 min. The aqueous phase was removed and the organic phase was washed with 250 μl methanol/H₂O [1:1, v/v]. Then, the samples were dried in 1 ml glasstubes under a constant stream of air and lipids were dissolved in 100 μl chloroform.

2.3.10.2. Phosphate determination

To monitor the concentration of phospholipids a phosphate determination was performed (Rouser *et al.*, 1970). 10 μl and 5 μl of the sample, and 2.5 nmol, 5 nmol, 10 nmol, 20 nmol, 40 nmol of a 10 mg/ml phosphatidylcholine (PC) standard solution were transferred to separate 1 ml glasstubes. Phospholipids were dried under a continuous air stream. Then, 150 μl of a 70 % [v/v] perchloric acid were added, shortly vortexed and incubated for 40 min at 180 °C. At RT, 500 μl of H₂O, 200 μl of 1.25% [w/v] ammonium molybdate-solution and 200 μl of 5% [w/v] ascorbic acid were combined with the sample with always shortly vortexing in between and incubated for 5 min at 80°C. Subsequently, the absorption at a wavelength of 797 nm was measured to produce a standard curve of PC in order to calculate the amount of mitochondrial phospholipids.

2.3.10.3. Thin-layer chromatography (TLC)

TLC analysis was performed using 10 cm TLC plates (HPTLC Silica gel 60 F254, MERCK) which were activated in 1.8% [w/v] boric acid/ethanol by heating to 80 °C for at least 30 min. Samples and standards (phosphatidylcholine, -ethanolamine, -serine, -glycerol, -inositol and cardiolipin) were loaded using the robot Linomat 5 (LAMAG). The silica plates were dried after running and developed with chloroform/methanol/water [65:35:5, v/v/v]

and chloroform/ethanol/water/triethylamin [30:35:7:35, v/v/v/v] and stained with 470 mM CuSO₄ in 8.5 % *o*-phosphoric acid. Finally, incubation at 180 °C visualized the phospholipids on the plate.

2.4. Protein biochemistry methods

2.4.1. Preparation of protein lysates from tissue culture cells

For isolation of total cell lysates FITR293 cells were harvested by either trypsinization or by scraping (cell scraper, Sarstedt), pelleted at 1,200 x g at 4 °C and rinsed twice with 1 x PBS (PAA). Afterwards, cells were lysed in modified RIPA buffer by gentle shaking at 750 rpm and 4°C for 2 h. Lysates were centrifuged for 20 min at 16,000 x g to remove insolubilized material. Protein concentration was determined with a Bradford protein assay (BioRad) using IgG as standard and cell lysates were diluted with RIPA buffer to a final protein concentration of 10 mg/ml.

RIPA buffer:

- 10 mM Tris/HCl pH 7.4
- 150 mM NaCl
- 1 mM EDTA
- 1% [v/v] Triton X-100
- 0.5% [w/v] sodiumdeoxycholate
- 0.1% [w/v] sodium dodecyl sulphate (SDS)
- 1 mM phenylmethylsulphonyl fluoride (PMSF)
- 1 x Complete Protease Inhibitor Cocktail (Roche)

2.4.2. Crosslinking of OPA1

To test the ability of OPA1 to form a complex crosslinking with EDC (1-Ethyl-3-[3-dimethylaminopropyl]carbodiimide hydrochloride) (Pierce) was performed (Frezza *et al.*, 2006; Yamaguchi *et al.*, 2008). EDC is a zero-length crosslinking agent used to couple carboxyl groups to primary amines. It reacts with a carboxyl to form an amine-reactive *O*-acylisourea intermediate. For protein crosslinking, 150-200 μ g isolated mitochondria were treated with EDC. Mitochondrial membranes were spun for 5 min at 12,000 x g and 4 °C, and resuspended in 10 mM EDC in 1 x PBS (PAA) and incubated at 37 °C for 30 min to enable crosslinking. Then, mitochondria were pelleted at 12,000 x g for 5 min and dissolved in SDS-PAGE sample loading buffer. Tris in the sample buffer quenched the

crosslinking reaction. Complexes were separated by 6-12 % [w/v] Tris-glycine SDS-PAGE, transferred onto nitrocellulose membranes, and probed using the OPA1 specific antibody (see Table 3).

2.4.3. Polyacrylamide gel electrophoresis (PAGE)

2.4.3.1. SDS-PAGE

Besides standard Tris-glycine SDS-PAGEs (Laemmli, 1970) Tris-tricine SDS-PAGE was performed allowing better resolution of smaller proteins (Schägger, 2006; Schägger and von Jagow, 1987). The Protein Marker, Broad Range (2-212 kDa) (NEB) and the SeeBlue® Plus2 Pre-Stained Standard (Invitrogen) were used as molecular weight standards.

2.4.3.2. BN/CN-PAGE and in-gel-activity stainings

Blue native (BN)-PAGE was developed for the separation of mitochondrial membrane proteins and complexes in the mass range of 10 kDa to 10 MDa (Schägger and von Jagow, 1991). Nonionic detergents are used for solubilization of biological membranes. The choice of a specific nonionic detergent depends on the detergent stability of the protein complexes of interest. One of the mildest detergents is digitonin. It has been used to isolate supramolecular associations of multiprotein complexes, thus identifying physiological protein-protein interactions without using chemical crosslinking (Schägger *et al.*, 1994). CN- (clear- or colorless-) native PAGE offers general advantages for in-gel catalytic activity assays compared to blue native electrophoresis [reviewed in (Krause and Seelert, 2008)].

Isolated mitochondria (150 μ g) were solubilized using 10 g digitonin / g protein. Mitochondria were pelleted at 10,000 \times g at 4 °C for 10 min and resuspended in resuspension (see chapter 2.3.9) or solubilization buffer. 15 μ l of a 10 % [w/v] digitonin solution in solubilization buffer was added to the mitochondria. Samples were vigorously mixed at 1,400 rpm at 4° C and cleared by centrifugation for 30 min with 35,000 \times g. Addition of 50 U benzonase (Novagen) diluted in solubilization buffer and addition of MgCl₂ to a final concentration of 5 mM resulted in the degradation of interfering nucleic acids. To remove remaining insoluble material which disturbs the running behaviour of the protein complexes an additional centrifugation step at 35,000 \times g was performed before loading the gel. Next, complexes were separated according to their native molecular mass within a 3 %-13 % [w/v] native polyacrylamide gel with a 3 % [w/v] stacking gel using the Hoefer gel systems S400 or S600. Gel running was started with constant 100 V, followed by an increase to 500 V after samples entered the separation gel. A native molecular weight marker containing 10 μ g catalase (Serva), alcohol

dehydrogenase, apoferritin, thyroglobulin, carbonic anhydrase and albumin (all Sigma) was used.

Solubilization buffer: 50 mM NaCl
 50 mM imidazole pH 7.0
 5 mM 6-aminohexanoic acid
 10% (w/v) glycerol

Activity of individual OXPHOS (oxidative phosphorylation) complexes was visualized directly in the CN-PAGE gels. CN-PAGE gels were rinsed with water and incubated in the respective solution for analyzing the activity of Complex I (NADH dehydrogenase complex) (Kuonen *et al.*, 1986) and IV (cytochrome c peroxidase complex) (Thomas *et al.*, 1976). After appropriate staining, gels were scanned and fixed in 50 % [v/v] methanol.

NADH staining 100 mM Tris/HCl pH 7.4
 768 mM glycine
 0.08 % [w/v] nitro blue tetrazolium (NBT)
 0.014 % [w/v] NADH

Cox staining 50 mM NaPi pH 7.4 (or KPi)
 0.05% [w/v] 3,3'-Diaminobenzidine(DAB)-Tetrahydrochlorid
 0.05 % [w/v] cytochrome c
 1 % [w/v] Katalase
 7.5 % [w/v] sucrose

2.4.3.3. 2D-electrophoresis: BN-SDS-PAGE and dSDS-PAGE

Mitochondrial complexes separated on a BN/CN-PAGE were analyzed further on a second dimensional denaturing polyacrylamide electrophoresis. The gel stripe was cut and incubated for 4 x 15 min in freshly prepared 2 % [w/v] SDS and 2 % [w/v] β -mercaptoethanol in 66 mM NaHCO₃. The stripe was then subjected to a 13 % [w/v] Tris-tricine SDS-PAGE. Pouring and running of this gel was performed essentially as described previously (Krause and Seelert, 2008). BN/CN-SDS-PAGEs were either silver stained according to protocols that are optimized for staining sensitivity and compatibility with protein digestion and mass spectrometric analysis (Blum *et al.*, 1987; Tebbe *et al.*, 2005), or proteins were transferred on a PVDF membrane for immunoblotting (see chapter 2.5.1).

In addition to BN/CN-SDS-PAGE a doubled SDS-PAGE (dSDS-PAGE) was performed: a Tris-glycine SDS-PAGE containing 6 % [w/v] urea in the first dimension was combined with a Tris-tricine SDS-PAGE in the second dimension. These gel systems are reviewed in

(Rais *et al.*, 2004; Schägger, 2006). To increase resolution of proteins in the high molecular weight range, Niederquell modified the published protocol: a 12 % [w/v] acrylamide concentration for the first dimension was used followed by a 10 % [w/v] acrylamide gel in the second dimension (Niederquell, 2008). Gel stripes were incubated in equilibration buffer for 30 min and 5 min in overlay buffer with gentle agitation at RT.

Equilibration buffer: 0.12 M Tris/HCl pH 6.8
 1% [w/v] SDS
Overlay buffer: 0.15 M Tris/HCl pH 7.4
 + a few grains bromphenol blue (Serva)

2.4.4. Metal affinity chromatography of His-tagged AFG3L2

To identify interaction partners or putative substrates of human AFG3L2 the protein was purified using a carboxy terminal hexahistidine epitope tag. All steps were performed at 4 °C. Mitochondria were isolated as described above (2.3.9) and centrifuged at 16,000 x g for 10 min. 5-10 mg mitochondrial pellets were washed once with binding buffer without digitonin and solubilized in binding buffer containing 3 % [w/v] digitonin to generate a final protein concentration of 5 mg/ml by mixing at 1,400 rpm (6 g digitonin/ g protein). In parallel, Ni²⁺-beads (Ni Sepharose™ High Performance, GE) were pre-equilibrated with binding buffer. The solubilized fraction of the mitochondrial solution was then separated from insoluble material by ultracentrifugation at 45,000 x g and incubated with 30 µl of the Ni²⁺-beads for 1-2 h by gently rotating. 20-fold bead volumes of binding buffer containing increasing concentration of imidazol were used during the following washing steps: 2 x 20 mM, 2 x 50 mM, 1 x 70 mM imidazol. Bound material was eluted by incubation with binding buffer including 300 mM imidazol. Samples were analyzed by gradient Tris-tricine gel electrophoresis or a dSDS-PAGE approach (see chapters 2.4.3.1 and 2.4.3.3, respectively). Gels were stained with colloidal coomassie (Neuhoff *et al.*, 1990).

Binding buffer: 50 mM Tris/HCl pH 8.0
 150 mM NaCl
 20 mM imidazol
 10 % [w/v] glycerol
 0.5 % [w/v] digitonin
 1 mM PMSF
 1 x protease inhibitor cocktail without EDTA (Roche)

2.5. Immunological methods

2.5.1. Immunoblotting

Protein samples were size-fractionated by SDS-or BN/CN-PAGE and transferred to nitrocellulose (PROTRAN®, Whatman) or PVDF membranes (BioTrace™, PALL Life Sciences) according to an established protocol (Towbin *et al.*, 1979). After transfer of proteins, membranes were incubated for 30-60 min at RT in blocking solution (5% [w/v] milk powder in 1 x TBS-Tween). Immunodecoration with a specific antiserum diluted in blocking solution was carried out for at least 60 min at RT or overnight at 4°C. Nitrocellulose membranes were washed three times for 5-10 min at RT with 1 x-TBS-Tween. To detect bound primary antibodies, horseradish peroxidase-conjugated antibodies specific for immunoglobulin G of rabbit, mouse (BioRad) or chicken (Abcam) were applied in a dilution of 1:3,000-1:10,000 in blocking solution for 60 min. After washing the membranes three times with 1 x TBS-Tween, the chemiluminescence reagents ECL solution 1 and 2, were added in a mixture of 1:1. Chemiluminescence was detected by exposing the membranes to light-sensitive X-ray films (Super RX, Fuji). Stainings for OPA1 antibodies were carried out using 1 x TBS in all washing steps, and for the detection of the secondary antibody the Lumi-Light^{PLUS} Western Blotting Substrate (Roche) was used according to manufacturer's instructions.

1 x TBS:	10 mM Tris/HCl pH 7.4 150 mM NaCl
1 x TBS-Tween	1 x TBS + 0.05 % [v/v] Tween 20
ECL-solution 1:	100 mM Tris/HCl pH 8.5 250 µM luminol 400 µM p-coumaric acid
ECL solution 2:	100 mM Tris/HCl pH 8.5 0.02% [v/v] H ₂ O ₂

2.5.2. Co-immunoprecipitation

The protocol was modified from the published protocols for *m*-AAA protease subunit immunoprecipitation (IP) (Koppen *et al.*, 2007; Metodiev, 2005). All steps were performed at 4 °C. Mitochondrial membranes isolated from FITR293 cells (500 µg) were lysed in Co-IP buffer containing 2 % [w/v] digitonin and the total protein concentrations were adjusted to 1 mg/ml (20 g digitonin/ g protein) and mixed vigorously for 30 min. After centrifugation

with 35,000 x g for 15 min, 450 μ l of the supernatant were applied onto 50 μ l Protein A Sepharose™ CL-4B (GE) slurry (100 mg/ml) that were coupled with 12 μ l antiserum directed against AFG3L2 (see 2.1.6) or preimmune antisera for 1 h and then further incubated with gentle rotation for 4 h. The beads were washed three times with binding buffer including 0.5 % [w/v] digitonin followed by a washing step with 10 mM Tris/HCl pH 7.4. Antibody-antigen complexes were eluted from the beads by incubation of the beads with 1 x Laemmli buffer (Laemmli, 1970) and boiling for 5 min.

The monoclonal HA-antibody (20 μ l) was coupled onto 30 μ l Protein G Sepharose™ 4 Fast Flow (GE). Co-IP of transiently transfected HA-tagged MICS1 and AFG3L2 from FITR293 cells expressing the distinct AFG3L2 variants was carried out using digitonin solubilized whole cells: 0.5-1.0 x 10⁸ cells were washed twice with ice cold 1 x PBS (PAA) and resuspended in 2 ml Co-IP buffer containing 4 % [w/v] digitonin. Samples were lysed, bound to the HA-antibody-coupled protein G sepharose and treated as described above for the IPs using protein A beads.

Co-IP buffer	50 mM NaCl
	50 mM potassium phosphate buffer (KPi) pH 7.0
	4 mM Mg-acetate
	10% [w/v] glycerol
	1 mM PMSF
	1 x protease inhibitor cocktail (Roche)

3. Results

3.1. *Mutational analysis of mammalian m-AAA proteases*

The yeast *m*-AAA protease has been demonstrated as an important regulator of mitochondrial function. It is involved in protein quality control and mitochondrial biogenesis by degrading non-assembled polypeptide and specific processing of MrpL32, respectively [reviewed in (Arnold and Langer, 2002; Koppen and Langer, 2007; Langer, 2000; Nolden *et al.*, 2006)]. MrpL32 is a nuclear encoded subunit of the large mitochondrial ribosomal particle and is processed upon import into mitochondria by the yeast *m*-AAA protease. This leads to the assembly of functional ribosomes and efficient mitochondrial translation (Nolden *et al.*, 2005).

The identification of MrpL32 as a substrate of the yeast *m*-AAA protease can explain the respiratory deficiency of *m*-AAA protease mutant yeast cells, preventing the growth on non-fermentable carbon sources (Nolden *et al.*, 2005). However, MrpL32 processing in mammalian cells lacking subunits of the *m*-AAA protease is not as drastically impaired as it has been observed in yeast cells (Martinelli *et al.*, 2009; Nolden *et al.*, 2005). Therefore, it is hypothesized that mitochondrial dysfunction associated with the absence or mutation of mammalian *m*-AAA protease subunits is caused by an impaired processing of a yet unknown substrate or by an accumulation of misfolded polypeptides (Rugarli and Langer, 2006). Consequently, the identification of new substrates of mammalian *m*-AAA proteases might help to elucidate the role of mammalian isoenzymes within mitochondria and the whole cell.

Human *m*-AAA proteases constitute homo- and hetero-oligomeric complexes composed of AFG3L2 alone or together with paraplegin (SPG7) (Koppen *et al.*, 2007). In contrast, the yeast *m*-AAA protease subunits Yta10 and Yta12 exclusively form hetero-oligomeric complexes (Arlt *et al.*, 1996). It has been shown that mutations in the canonical metal binding site (HExxH motif) in the proteolytic domain in both yeast subunits from glutamate to glutamine residues (PS-mutants) (see Figure 5) lead to respiratory deficiency resembling the $\Delta yta10$ and $\Delta yta12$ phenotype (Arlt *et al.*, 1998). Interestingly, complex assembly and substrate binding properties were not affected (Arlt *et al.*, 1998). Furthermore, substrate proteins which cannot be processed by the proteolytically inactive yeast *m*-AAA protease are trapped by the complex *in vivo* (Nolden *et al.*, 2005), although

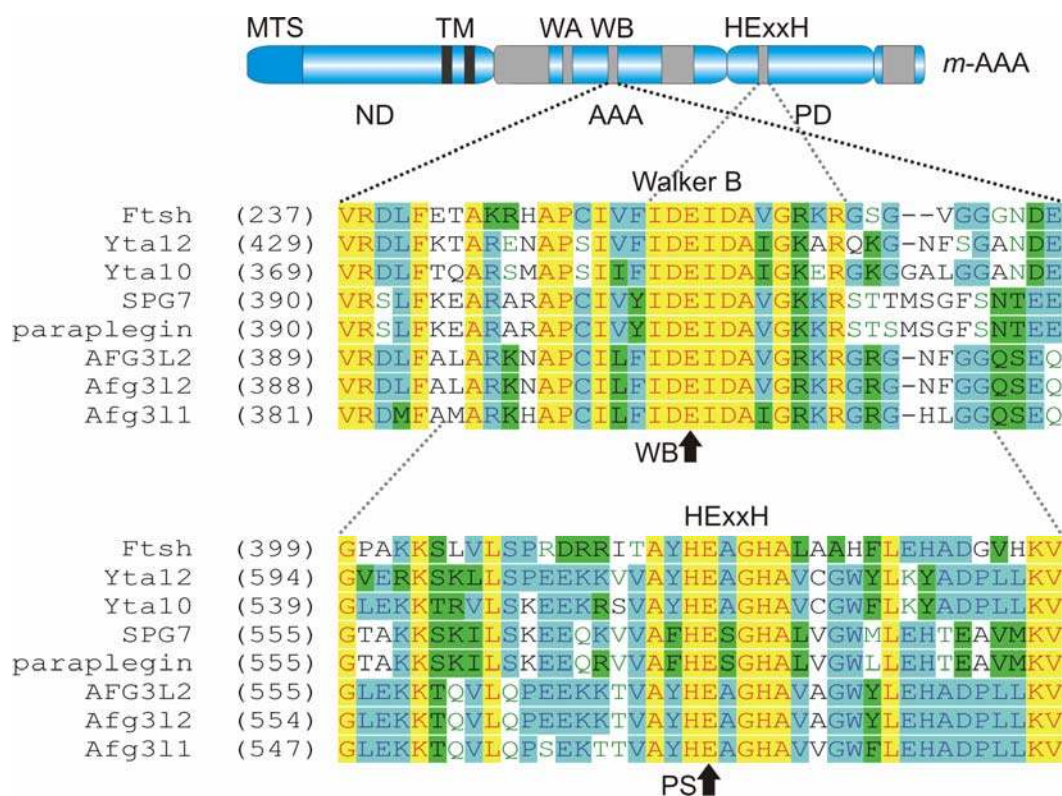


Figure 5: Domain structure and conservation of residues within Walker B and HExxH motifs of *m*-AAA proteases.

The *m*-AAA proteases contain a mitochondrial targeting signal (MTS), an N-terminal domain (ND) containing two transmembrane regions (TM), the ATPase (AAA) and proteolytic domain (PD) at the C-terminus resulting in a matrix-facing topology. Sequence alignments (generated by a ClustalW algorithm) are shown for FtsH from *Thermus thermophilus*, Yta10 and Yta12 from bakers yeast and human and murine *m*-AAA protease subunits. Arrows indicate the positions of mutations in the Walker B motif and the proteolytic site in the HExxH motif. WA, Walker A; WB, Walker B; HExxH, canonical metal binding site; PS, proteolytic site. (Accession numbers of the protein sequences are listed in 6.3.)

an effective substrate trapping complex is achieved by mutating the proteolytic site (PS) in all subunits (Tatsuta *et al.*, 2007). These findings immediately illustrate technical difficulties working with the mammalian proteins. Data from yeast suggest that substrates can only be trapped if the complex does not contain any catalytically active subunit. Therefore, a substrate trap approach with proteolytic mutants in a mammalian system would require a mutagenesis of all subunits. Interestingly, it has been shown that coexpression of Yta10 or Yta12 harboring point mutations in the Walker B motif of the AAA ATPase domain (Yta10^{E388Q}, Yta12^{E448Q}, WB see Figure 5) in combination with the wild type form of the respective other subunit did not or only weakly restore growth on non-fermentable carbon sources and the measured ATPase activity of the enzyme (Augustin, 2008, Hersch, 2005 #2199). It was demonstrated that this mutation of the Walker B motif leads to trapping of ATP which inhibits ATP hydrolysis in the neighboring subunit. Additionally, expression of human paraplegin (SPG7) and AFG3L2 subunit variants (SPG7^{E409Q}, AFG3L2^{E408Q}) in yeast leads to similar effects on both hetero- and homo-oligomeric isoenzymes (Steffen Augustin,

manuscript in preparation). These findings indicate a conserved dominant negative effect of this mutation on the holo-enzymatic activity. Moreover, it was possible to co-purify yeast MrpL32 together with the yeast *m*-AAA protease complex that contained one subunit harboring a mutated Walker B motif (Steffen Augustin, personal communication). It is therefore conceivable that dominant negative variants can be used to study defective *m*-AAA proteases in the mammalian system. Therefore, the expression of the respective mutated mammalian *m*-AAA protease subunit in mammalian cells might be a suitable approach to identify putative interaction partners or substrates of mammalian *m*-AAA proteases.

3.2. Generation of stable cell lines expressing mouse or human AFG3L2 variants

3.2.1. The FlpIn T-REx system

For expression of different *m*-AAA protease variants in mammalian cell culture FlpIn T-REx -293 (FITR293) cell lines stably and inducibly overexpressing human AFG3L2 and murine Afg3l2 were generated. An inducible “tet-on”-system was used in order to monitor changes of putative phenotypes upon induction of expression in the respective cell line. The FITR293 cell line expresses the tetracycline repressor under the control of a CMV promoter and contains a blasticidin resistance gene. This human embryonic kidney derived cell line also expresses the *lac Z* gene encoding β -galactosidase which is fused to a Zeocin resistance protein (Figure 6 A) allowing a blue white screening of stable cell clones. Importantly, cells harbor an FRT (Flp-recombinase target) site in their genome enabling Flp (Flippase)-mediated recombination of a gene of interest into this site (Figure 6 A and B) (Andrews *et al.*, 1985; Farley *et al.*, 2000). FITR293 cells can be transiently or stably transfected with pcDNA5 FRT/TO constructs containing the open reading frame of interest and FRT-sites under the control of a tetracycline-inducible promoter. Co-transfection with a Flp recombinase-expressing plasmid allows site-directed recombination and integration into the genome of the FITR293 cells. Cells with correctly inserted construct become hygromycin resistant, Zeocin sensitive and lose their β -galactosidase activity (Figure 6 B). Expression can be induced by addition of tetracycline or doxycycline which suppresses the binding of the tet repressor to the tet operator allowing the RNA-polymerase to bind to the promoter sequence (Figure 6 C). One possible drawback of this system is the low basal expression due to residual tetracycline in the tetracycline-reduced fetal bovine serum and to low binding affinity of the tet repressor, especially if the gene

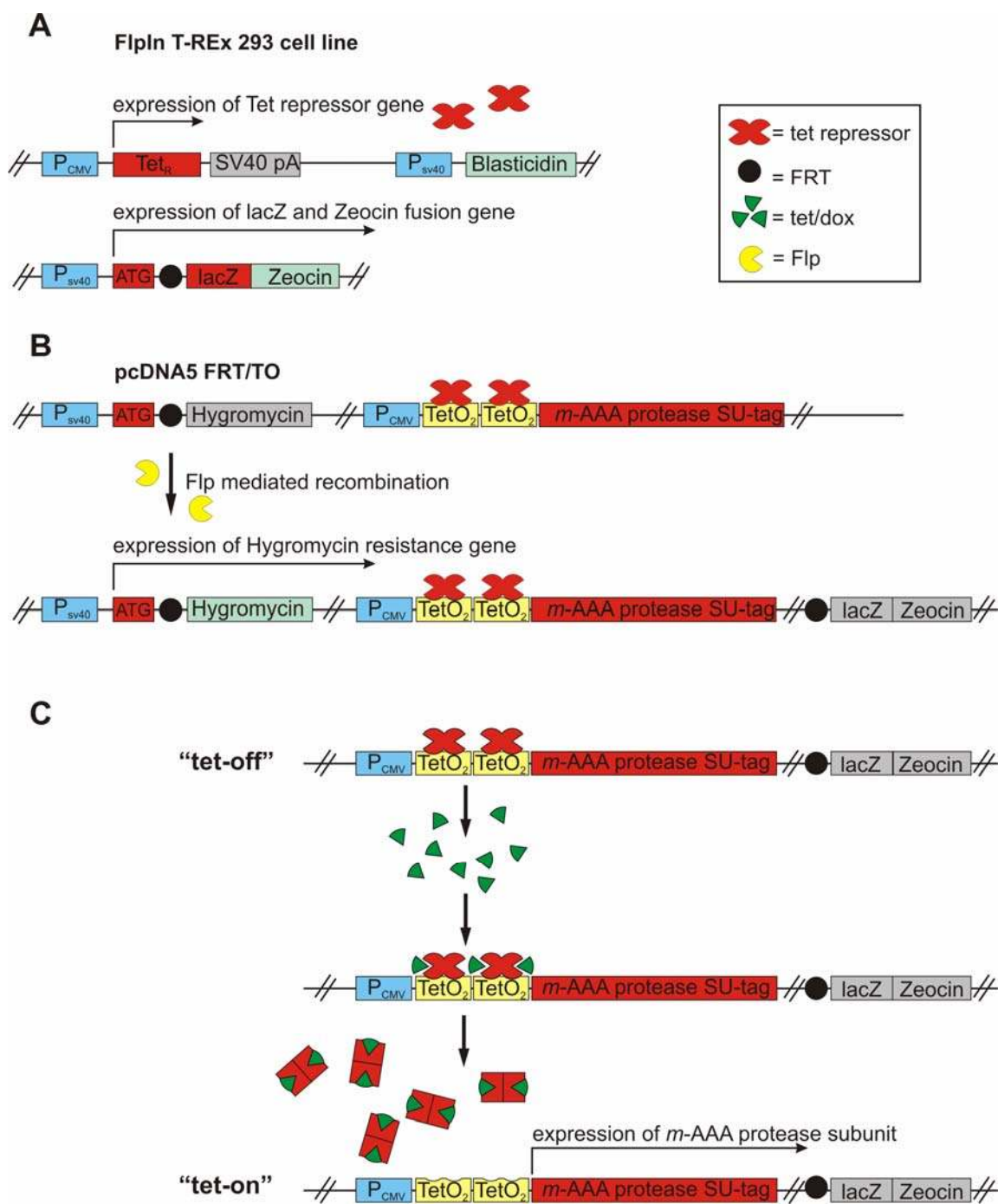


Figure 6: FlpIn T-REx system.

(A) FlpIn T-REx-293 (FITR293) cell line. Stable and inducible expression of target genes is achieved by transfection into the FITR293 cell line which expresses the tetracycline repressor under the control of a CMV promoter. Flp-mediated recombination results in uniform integration and stable expression target genes.

(B) Stable integration by Flp-mediated recombination. pcDNA5 FRT/TO contains an FRT site and the ORF of *m*-AAA protease variants fused with a C-terminal epitope tag for affinity purification under the control of a tetracycline-inducible CMV promoter. Site-directed recombination by Flp causes a switch of the start codon (ATG) from the *lacZ*-*Zeocin* fusion to the *Hygromycin* resistance gene which results in *Hygromycin* resistance, *Zeocin* sensitivity and inactive β -galactosidase.

(C) Tetracycline inducible expression. Expression is turned “on” by adding tetracycline (tet) or doxycycline (dox) to the growth medium. The tet operator is bound by tet repressor homodimers which are released upon tetracycline binding allowing gene expression.

Modified from invitrogen.com. SU; subunit.

codes for a toxic protein. This effect was minimized by using tetracycline reduced serum in the growth medium and by titrating down the concentration of this serum. The benefit of the FlpIn T-REx system is the generation of stable cell lines allowing inducible and, more importantly, uniform expression of a gene of interest enabling direct comparative analysis of cell lines excluding effects of random integrations.

3.2.2. Selection for AFG3L2 overexpressing cell lines

FITR293 cells were transfected with pcDNA5 FRT/TO constructs containing the open reading frames of either murine *Afg3l2* wild type (WT) or Walker B mutant (WB, Afg3l2^{E407Q}), and human *AFG3L2* variants: wild type (WT), the proteolytic site mutant (PS, AFG3L2^{E575Q}) and constructs carrying a mutation in the Walker B motif (WB, AFG3L2^{E408Q}). Murine cDNAs were fused to a C-terminal Strep[®]II-octahistidine epitope tag and human AFG3L2 to a C-terminal hexahistidine tag. Hygromycin resistance allowed positive selection for the insertion into the genome. Growing clones were tested for their β -galactosidase activity (Figure 7 A) and Zeocin sensitivity as described in chapter 2.3.3. Clones lacking β -galactosidase activity and Zeocin resistance were tested for the transgene expression by the addition of tetracycline. A representative immunoblot analysis of total lysates of cells expressing AFG3L2 variants is shown in Figure 7 B. In several clones induction with tetracycline resulted in an increase of AFG3L2 protein levels. However, no size shift was visible of murine Afg3l2 expressing cell lines even in low percentage polyacrylamide gels suggesting a cleavage at the C- or at the N-terminus leading to a loss of the tag. The absence of the epitope tag was confirmed since the binding to either a Strep- or Ni²⁺- specific matrix or the detection using His- or StrepII-tag specific antibodies in Western Blots could not be established. However, human AFG3L2 could be purified via its C-terminal hexahistidine epitope tag (see chapter 3.5.1).

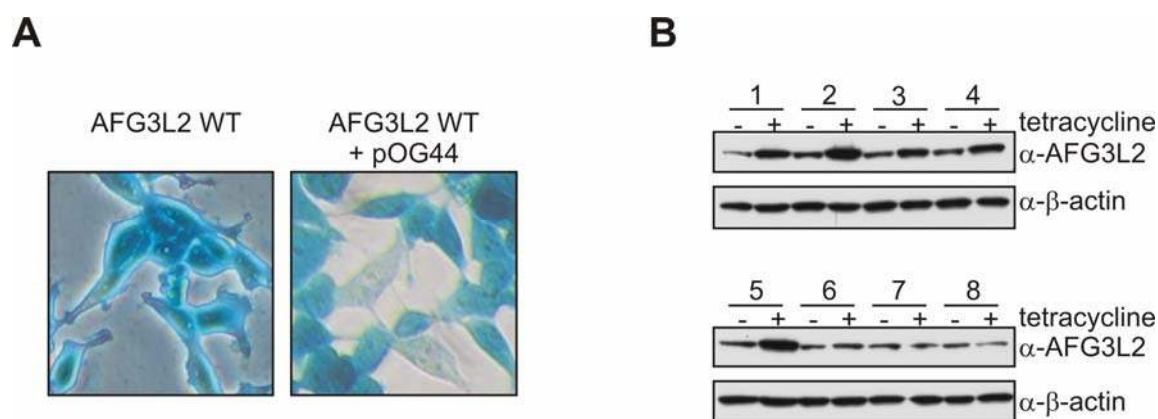


Figure 7: Selection of stable clones inducibly expressing AFG3L2.

(A) β -galactosidase activity staining of FITR293 cells transfected with indicated plasmids. Expression of Fip recombinase from the pOG44 plasmid allows integration of AFG3L2 WT into the genome which was visualized due to the loss of blue staining.

(B) Immunoblot analysis of total cell lysates of 8 clones selected with hygromycin for 3 weeks using antisera directed against human AFG3L2. Expression was induced by addition of tetracycline to the growth medium. Clones 6-8 behaved like untransfected FITR293 cells reflecting endogenous AFG3L2 protein levels. Immunostaining with an antibody directed against β -actin served as a loading control.

3.3. ***Mutation of the Walker B motif has a dominant-negative effect on cell proliferation***

The *m*-AAA protease is part of a large supercomplex together with prohibitins, highly conserved and ubiquitously expressed inner membrane proteins, whose carboxy-terminal domains face the intermembrane space of mitochondria (Tatsuta *et al.*, 2005). This high molecular weight complex of approximately 2 MDa was first described in yeast and later also detected in the mammalian system (Metodieiev, 2005; Steglich *et al.*, 1999). Knockdown experiments on a cellular level revealed an essential function of the prohibitin complex for cell proliferation pointing to a potential role of its assembly partner, the *m*-AAA protease, in this process (Merkwirth *et al.*, 2008; Schleicher *et al.*, 2008). Thus, the cell proliferation of AFG3L2 overexpressing cells was assessed using a colorimetric assay (Figure 8). Treatment of tetracycline had no effect on the growth rate of the parental cell line (Figure 8 A). Furthermore, cells overexpressing AFG3L2/Afg3l2 WT showed no significant difference in proliferation (Figure 8 and B). In contrast, cells expressing the Walker B mutants (AFG3L2 WB or Afg3l2 WB) displayed a strongly reduced cell growth indicating a dominant-negative effect of this mutation on the endogenous protein (Figure 8 A and B). To exclude that the mutation of the Walker B motif interferes with the complex assembly, two-dimensional BN/SDS-PAGE was performed. Immunoblot analysis identified

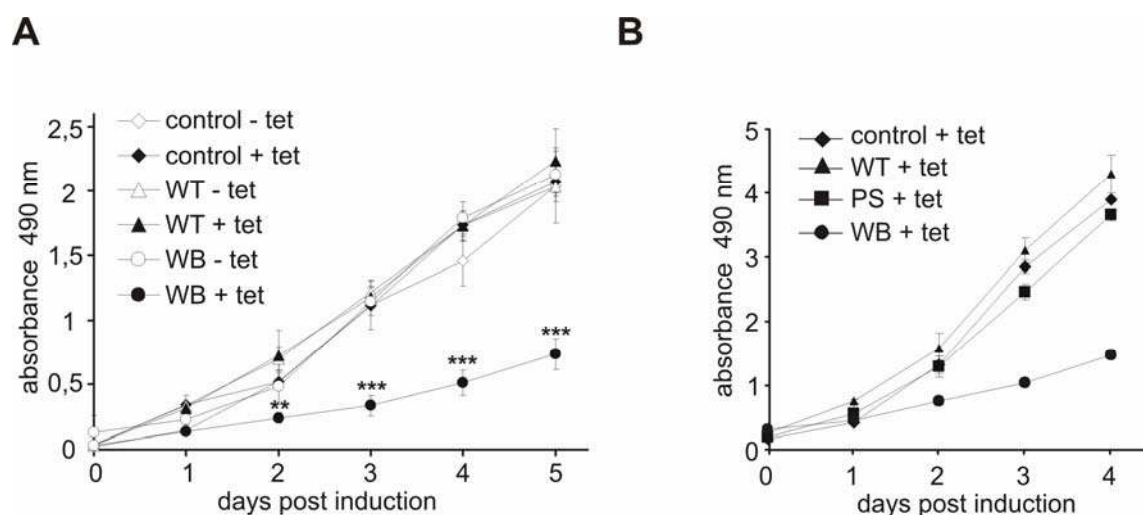


Figure 8: Impaired cell proliferation of Afg3l2/AFG3L2 overexpressing cells harboring a mutation in the Walker B motif.

Colorimetric cell proliferation assay of stable FITR293 clones inducibly expressing murine (A) or human (B) AFG3L2 variants. Conversion of a tetrazolium compound to the formazan product was measured at 490 nm which is directly proportional to the number of living cells in culture. Protein expression was induced with tetracycline and proliferation was assayed daily. Graphs represent means of quadruplicates \pm standard deviation (SD) of one (B) or three independent (A) experiments. **, $p < 0.01$; ***, $p < 0.001$. Filled symbols indicate with and open symbols without tetracycline.

WT, wild type; PS, mutation in the proteolytic site (AFG3L2^{E575Q}); WB, mutation in the Walker B motif (Afg3l2^{E407Q}/AFG3L2^{E408Q}).

m-AAA proteases as part of complexes similar sized as in untransfected cells (see Figure 17 A).

In conclusion, cell proliferation needs the ATPase activity of the *m*-AAA protease. Cells expressing AFG3L2 PS did not show any markedly growth defect and behave like wild type expressing cell lines. However, data from yeast suggest that a putative effect of this mutation is suppressed by endogenous AFG3L2 protein, and, therefore, cannot be excluded (Arlt *et al.*, 1998; Arlt *et al.*, 1996). These findings confirm the results obtained with the yeast protease (Steffen Augustin, manuscript in preparation) suggesting that a mutation in the Walker B motif has a dominant negative effect over the wild type subunits. This indicates a conserved mechanism from yeast to man.

3.4. Mammalian *m*-AAA proteases are required for mitochondrial fusion

Mitochondria are highly dynamic organelles which are actively transported throughout cells to defined subcellular locations. Furthermore, mitochondria vary in size and shape, and their internal structures can change in response to their physiological state (Detmer and Chan, 2007). This adaptation of mitochondria to cellular demands is critical for a number of important processes including calcium signaling, ROS protection, mtDNA maintenance, aging, developmental processes and apoptosis (Balaban *et al.*, 2005; Chen *et al.*, 2003; Szabadkai *et al.*, 2006; Tang *et al.*, 2009; Youle and Karbowski, 2005). To investigate a potential role of the mammalian *m*-AAA proteases in any of these pathways, the structure of the mitochondrial network was monitored, which is regulated by the balance between the antagonistic fusion and fission activities. For this purpose, mitochondrially targeted dsRed was transfected into *m*-AAA protease subunit overexpressing cell lines and mitochondrial morphology was assessed by fluorescence microscopy. Stable FITR293 cell lines inducibly overexpressing AFG3L2 WT and AFG3L2 PS mutant as well as control cells showed a tubular network whereas expression of the dominant negative AFG3L2 WB led to fragmentation in 75 % of the cells (Figure 9 A und B). Additionally, analysis of T-REx-HeLa cells transiently transfected with hexahistidine tagged human AFG3L2 and SPG7 WT, PS and WB confirmed the results observed in FITR293 cells: expression of the dominant-negative mutation of the Walker B motif variant of either SPG7 or AFG3L2 results in fragmentation of mitochondria or a disturbed mitochondrial network (Figure 9 C). These findings are in agreement with siRNA-mediated downregulation of *m*-AAA protease subunits. Loss of functional *m*-AAA protease complexes achieved by depletion of Afg3l2 and Afg3l1 in mouse embryonic fibroblasts caused fragmented mitochondria in more than 80 % of the cells, underscoring a role of mammalian *m*-AAA proteases in the regulation of mitochondrial dynamics (Ehse, 2008). As already described, either stable or transient overexpression of the respective *m*-AAA protease subunit mutated in the proteolytic site did not affect mitochondrial morphology (see chapter 3.3). In summary, a functional ATPase domain of the *m*-AAA protease is necessary to maintain a mitochondrial tubular network, whereas the proteolytic site does not seem to be involved because this mutation is not dominant negative.

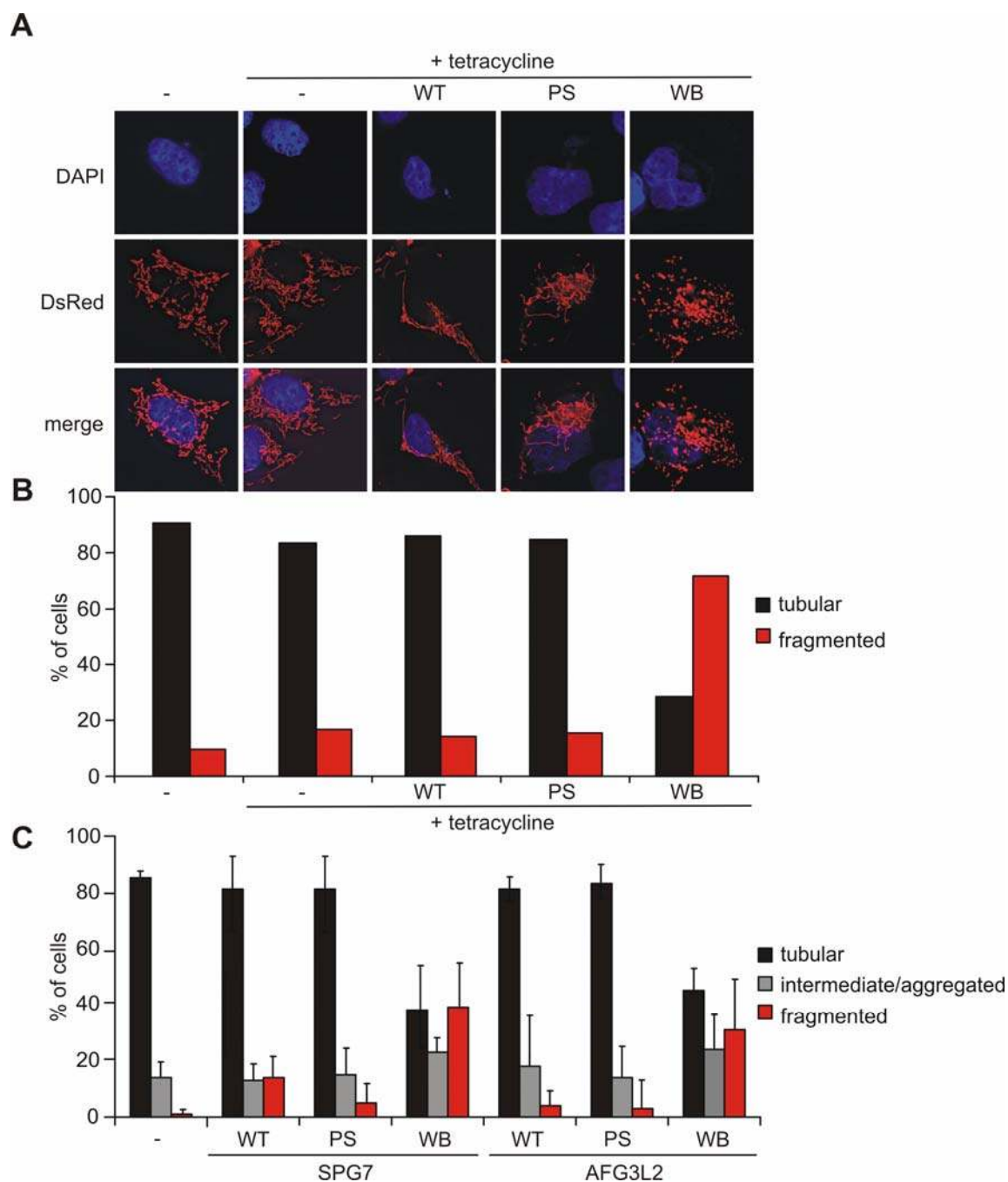


Figure 9: Fragmentation of mitochondria upon expression of SPG7 or AFG3L2 Walker B mutant.

Fluorescence microscopic analysis of mitochondrial morphology of stably transfected FITR293 overexpressing human AFG3L2 variants (**A and B**) and transiently transfected T-REx-HeLa cells inducibly overexpressing human SPG7 or human AFG3L2 variants (**C**). 48 h after transfection with mitochondrial targeted DsRed expression was induced by tetracycline for 24 h and mitochondrial morphology was monitored by fluorescence microscopy. Images were deconvolved. >200 cells were scored and mitochondrial morphology was classified as tubular, intermediate or aggregated, and fragmented. Error bars indicate means \pm standard deviation (SD) of at least three independent experiments.

WT, wild type; PS, mutation in the proteolytic site (SPG7^{E575Q}/AFG3L2^{E575Q}); WB, mutation in the Walker B motif (SPG7^{E409Q}/AFG3L2^{E408Q}).

3.4.1. *m*-AAA proteases regulate the stability of long OPA1 isoforms

In healthy cells, mitochondria form elongated tubules that continuously divide and fuse to form a dynamic interconnected network, which is maintained by a balance between both opposing processes. Therefore, the fragmentation of mitochondria observed in cells expressing the dominant-negative mutation of the Walker B motif, can in principle be explained by two different possibilities: either by an impairment of the fusion machinery or by inducing the fission activity. To distinguish between these possibilities the steady state levels of mitochondrial fusion proteins were monitored. Many of the involved fusion and fission components have been identified and most of them are conserved among species (Hoppins *et al.*, 2007). The antagonistic events – fusion and fission of mitochondrial membranes – are mainly regulated by dynamin-like GTPases (for review (Suen *et al.*, 2008)). Yeast Dnm1 or its human counterpart DRP1, the dynamin-related protein 1, a large GTPase, mediates fission in mammalian cells (Otsuga *et al.*, 1998; Smirnova *et al.*, 1998). DRP1 levels were not affected in AFG3L2 WB overexpressing FITR293 cells (Figure 10 B). In parallel, studies by Sarah Ehses confirmed that mitochondrial fission was not impaired. Transfection of mouse embryonic fibroblasts depleted of murine *m*-AAA protease subunits by siRNA with a dominant-negative variant of DRP1 (DRP1^{K38A}) resulted in fragmentation of mitochondrial tubules due to impaired fusion (Sarah Ehses, personal communication). Wild type cells elongated due to ongoing fusion (James *et al.*, 2003; Smirnova *et al.*, 1998).

Mitochondrial fission is normally counter-balanced by fusion. The mammalian fusion machinery is mainly composed of three dynamin-like GTPases, the mitofusins, Mfn1 and Mfn2, in the outer and OPA1 in the inner mitochondrial membrane (Chen *et al.*, 2003; Olichon *et al.*, 2003; Santel and Fuller, 2001). OPA1 functions in mitochondrial fusion and cristae remodelling (Cipolat *et al.*, 2004; Griparic *et al.*, 2004; Olichon *et al.*, 2003). Alternative splicing of the human OPA1 gene leads to the generation of eight distinct mRNA variants (Delettre *et al.*, 2001; Olichon *et al.*, 2002; Satoh *et al.*, 2003) (see Figure 2). Furthermore, OPA1 protein expression is regulated in a complex manner by post-translational proteolytic cleavages resulting in the accumulation of five apparent isoforms of OPA1 protein (Delettre *et al.*, 2001; Duvezin-Caubet *et al.*, 2007; Ishihara *et al.*, 2006; Olichon *et al.*, 2003; Olichon *et al.*, 2007; Song *et al.*, 2007). Although OPA1 is ubiquitously expressed, mutations in the OPA1 gene lead to autosomal dominant optic atrophy (ADOA) affecting only the optic nerve and retinal ganglion cells (Alexander *et al.*, 2000; Delettre *et al.*, 2000; Johnston *et al.*, 1979). The yeast rhomboid protease Pcp1 has

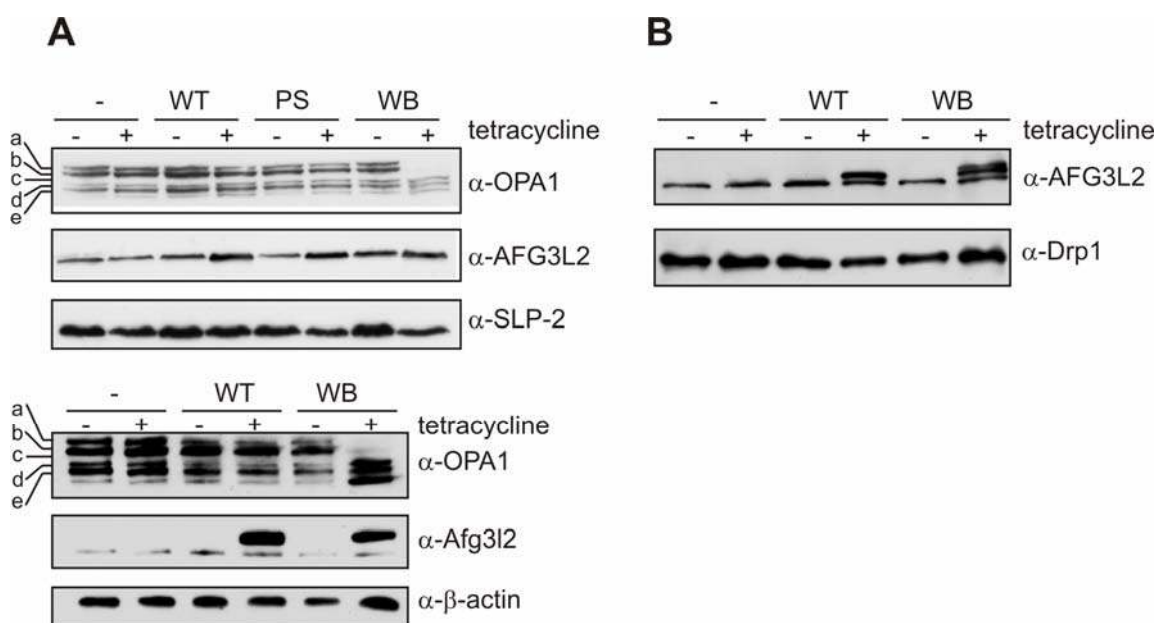


Figure 10: Expression of the Walker B mutants induces processing of OPA1.

(A) Immunoblot analysis of FITR293 cell lysates using antisera specifically recognizing OPA1. After induction with tetracycline stable cell lines inducibly overexpressing human AFG3L2 (upper panel) and murine Afg3l2 (lower panel) variants were harvested, lysed and analyzed by SDS-PAGE and subsequent immunoblotting using antibodies directed against murine Afg3l2 and human AFG3L2. Notably, murine Afg3l2 in FITR runs higher than the human homologue in SDS-PAGE. Immunostaining for β -actin and SLP2 with specific antisera served as loading controls.

(B) Immunoblot analysis of FITR293 cell lysates using antisera specifically recognizing Drp1. Cells expressing murine Afg3l2 were treated as in (A).

(a) and (b) indicate long OPA1 and (c-e) short OPA1 isoforms. WT, wild type; PS, mutation in the proteolytic site (AFG3L2^{E575Q}); WB, mutation in the Walker B motif (Afg3l2^{E407Q}/AFG3L2^{E408Q}).

been shown to cleave the OPA1 homologue Mgm1 (Herlan *et al.*, 2004; Herlan *et al.*, 2003; McQuibban *et al.*, 2003; Sesaki *et al.*, 2003), and its mammalian counterpart PARL was also reported to be involved in OPA1 processing (Cipolat *et al.*, 2006). Similarly, the *m*-AAA protease subunit SPG7 was proposed to cleave OPA1 (Ishihara *et al.*, 2006). However, PARL or SPG7 knockout mouse embryonic fibroblasts produce a normal wild type OPA1 pattern (Duvezin-Caubet *et al.*, 2007; Ehses, 2008; Guillery *et al.*, 2008). Interestingly, reconstituted OPA1 in yeast can be processed by yeast, human or murine *m*-AAA protease isoenzymes identifying OPA1 as a putative substrate of mammalian *m*-AAA proteases (Duvezin-Caubet *et al.*, 2007). Thus, the aim of the following experiments was to clarify the role of mammalian *m*-AAA proteases for the processing of OPA1.

3.4.1.1. Expression of a dominant-negative Walker B mutant leads to an accumulation of short OPA1 isoforms

In order to verify an effect of the tetracycline-inducible overexpression of *m*-AAA protease mutant variants on the accumulation of OPA1 isoforms, FITR293 cell lysates were analyzed by immunoblotting using antibodies directed against OPA1 (Figure 10 A). Five isoforms could be detected in control as well as in Afg3l2 and AFG3L2 WT and PS cell lines. Two long isoforms a and b give rise to three short isoforms c-e which are generated by processing of the long isoforms (Duvezin-Caubet *et al.*, 2007). The observed pattern is similar to those observed in HeLa cells (Duvezin-Caubet *et al.*, 2007; Song *et al.*, 2007). Considering a role for the *m*-AAA protease as processing peptidase, an impaired processing of OPA1 should result in the accumulation of long isoforms. However, interfering with the function of the protease by expressing the dominant-negative mutant variant did not cause an accumulation of long OPA1 isoforms as it was initially suggested (Duvezin-Caubet *et al.*, 2007). In contrast, the long OPA1 isoforms were not detectable while short forms accumulated in cell lines expressing murine Afg3l2 (Figure 10 A, lower panel) or human AFG3L2 WB (Figure 10 A, upper panel). These findings are consistent with data obtained by siRNA mediated downregulation of *m*-AAA protease subunits, although the effect seems to be more prominent in mouse embryonic fibroblasts in which mainly shortest isoform e accumulated (Ehse, 2008).

In summary, lack of functional *m*-AAA proteases obtained by expression of Afg3l2/AFG3L2 WB leads to accelerated processing and/or enhanced degradation of OPA1. The observed effect can be either explained by an induced processing or an increased turnover of l-OPA1 isoforms. These data suggest that OPA1 is not processed or degraded by *m*-AAA proteases. In contrast, *m*-AAA proteases seem to contribute to the stability of l-OPA1 isoforms thereby regulating mitochondrial dynamics.

3.4.1.2. The energy metabolism is not impaired in cells expressing dominant-negative Walker B mutants

Defects in mitochondrial morphology reflect often primary impairments of mitochondrial function. Mitochondrial dysfunction and the dissipation of the membrane potential across the inner membrane can induce OPA1 processing and mitochondrial fragmentation (Duvezin-Caubet *et al.*, 2006; Griparic *et al.*, 2007; Ishihara *et al.*, 2006; Ishihara *et al.*, 2003; Song *et al.*, 2007). It has also been shown that induction of apoptosis and MOMP (mitochondrial outer membrane permeabilization) induce OPA1 cleavage (Guillery *et al.*, 2008; Ishihara *et al.*, 2006). Baricault *et al.* hypothesized that decreased mitochondrial ATP levels, either generated by induction of apoptosis,

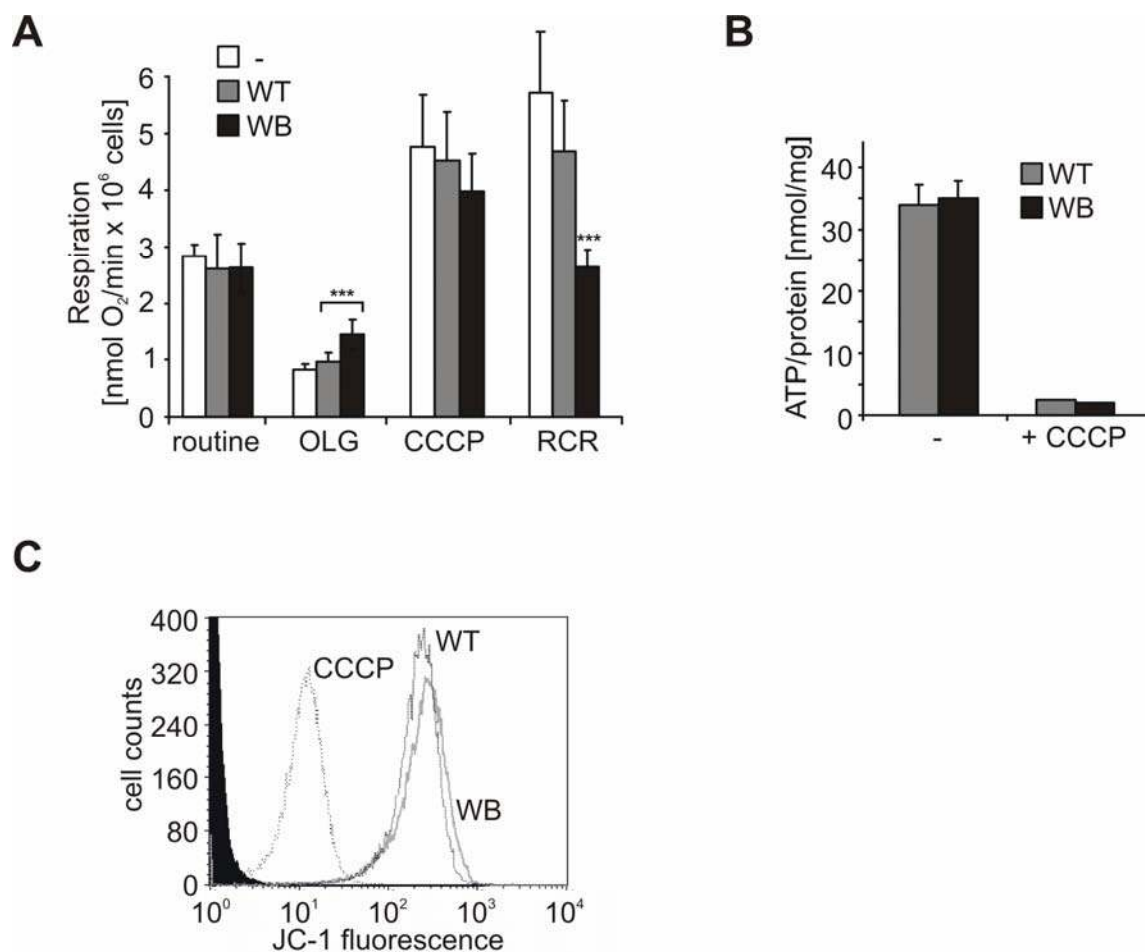


Figure 11: Energy status of FITR293 cells upon expression of dominant negative Afg3l2 variant.

(A) Oxygraph measurements of intact FITR293 cells expressing murine Afg3l2 variants. Respiration was measured under routine conditions, after the addition of 2 μ M oligomycin (OLG) and during titrations with CCCP. Respiratory control ratio (RCR) was determined from the ratio of CCCP-induced to oligomycin-inhibited respiration. Bars represent means \pm standard deviation (SD) of at least three independent experiments. (***) $p < 0.001$.

(B) Determination of cellular ATP levels upon expression of Afg3l2. 48 h before induction of expression standard glucose containing growth medium was changed to medium containing 1 mM galactose. Cells were harvested after 24 h induction with tetracycline and lysed. ATP content was measured by a luciferase assay.

(C) Maintenance of membrane potential upon expression of Afg3l2 WB. FITR293 cells were treated 24 h with tetracycline, stained with JC-1 and analyzed by FACS. To dissipate the membrane potential the uncoupler CCCP was used.

OLG, oligomycin; CCCP, carbonyl cyanide *m*-chlorophenylhydrazone; -, untransfected control cells; WT, wild type; WB, mutation in the Walker B motif (Afg3l2^{E407Q}).

dissipation of the membrane potential or inhibition of the ATP synthase, is the common and crucial stimulus that controls OPA1 processing (Baricault *et al.*, 2007). These results suggest that the ATP-dependent OPA1 processing plays a central role in correlating the energetic metabolism to mitochondrial dynamics. To verify whether the observed changes of organelle morphology were a primary consequence of loss-of fusion activity of OPA1 or a secondary effect due to an impaired energy metabolism, functional analysis of the

FITR293 cell lines were performed. Respiratory activity (Figure 11 A), ATP levels (Figure 11 B) and the mitochondrial membrane potential were monitored (Figure 11 C).

Oxygen consumption in FITR293 cells expressing the Afg3l2 WB revealed normal respiratory activity compared to wild type expressing cells (Figure 11 A). The rate of oxidative phosphorylation is often assumed to be proportional to the rate of respiration, and thus the control of one rate is assumed to be equivalent to the control of the other rate (Brown *et al.*, 1990). However, this is not necessarily the case as the protonmotive force generated by respiration may be consumed by processes other than oxidative phosphorylation, including the passive proton leak or electron slips across the mitochondrial inner membrane (Brown *et al.*, 1990). To monitor these effects, respiration was measured after inhibition of the ATP synthase with oligomycin. Interestingly, treatment with oligomycin revealed a slight but significant higher respiratory rate of Afg3l2 WB expressing cells compared to WT or controls. In contrast, dissipation of the membrane potential using the ionophore CCCP, mimicking maximal respiratory activity, showed lower respiration of the cells (Figure 11 A). The ratio of respiration after CCCP and oligomycin treatment is called the respiratory control ratio and indicates the tightness of the coupling between respiration and phosphorylation. The respiratory control ratio of the Afg3l2 WB cell line was therefore reduced suggesting a proton leak or an electron slip of the respiratory chain. Nevertheless, under normal routine or cell culture conditions respiration was normal.

To assess the mitochondrial membrane potential cells were stained with JC-1, a dye that can selectively enter into mitochondria and reversibly change color as the membrane potential increases (see chapter 2.3.6.2). Fluorescence activated cell sorting revealed no significant alteration in the membrane potential compared to CCCP treatment which was used as a positive control (Figure 11 B). Moreover, cellular ATP levels were not affected by the mutation (Figure 11 C).

In conclusion, FITR293 cells expressing Afg3l2 WB showed a reduced coupling between respiration and phosphorylation. That indicates a putative electron slip or proton leak through the inner mitochondrial membrane (Brand *et al.*, 1994; Brand *et al.*, 1994; Nicholls, 1974). However, under normal cell culture conditions, interference with the ATPase function of *m*-AAA proteases has no effect on respiration or the formation of the membrane potential. Thus, the accelerated processing of OPA1 upon expression of the Walker B mutation is apparently not caused by an impaired membrane potential or respiratory activity.

3.4.1.3. Dominant-negative mutation in Walker B induces destabilization of respiratory chain supercomplexes

The production of ATP requires the coordinated activity of five multi-heteromeric enzyme complexes embedded in the mitochondrial inner membrane and of two mobile electron carriers, ubiquinone (Q) and cytochrome c (see

Figure 1). The electron flow through the respiratory chain is coupled to an active proton translocation across the inner mitochondrial membrane, generated mostly by complexes I, III and IV. The influx of the protons back into the mitochondrial matrix through complex V allows the phosphorylation of ADP into ATP (Torraco *et al.*, 2009). FITR293 cells expressing Afg3l2 WB showed a decreased respiratory activity thereby indicating an effect of *m*-AAA proteases on the respiratory chain. Thus, the aim of the following experiments was to verify the integrity of the respiratory chain through which electrons and protons are transported. To monitor the assembly of respiratory chain subunits BN-PAGE analysis was performed. Expression of the dominant-negative mutant did apparently not impair the complex formation of the respiratory chain (Figure 12 A). The yeast *m*-AAA protease processes MrpL32 which is important for translation of mtDNA (Nolden *et al.*, 2005). Impaired cleavage of MrpL32 results in the disappearance of a subset of the respiratory chain complexes which contain mtDNA encoded subunits (Metodieva, 2005; Nolden *et al.*, 2005). Correlating with BN-PAGE results (Figure 12 A), MRPL32 processing in FITR293 expressing human AFG3L2 variants was only slightly affected (Figure 12 B). Furthermore, in-gel-activity stainings in CN-PAGEs revealed no alteration of the activities of complex I (Figure 12 C) and complex IV (Figure 12 D) upon expression of AFG3L2 WB.

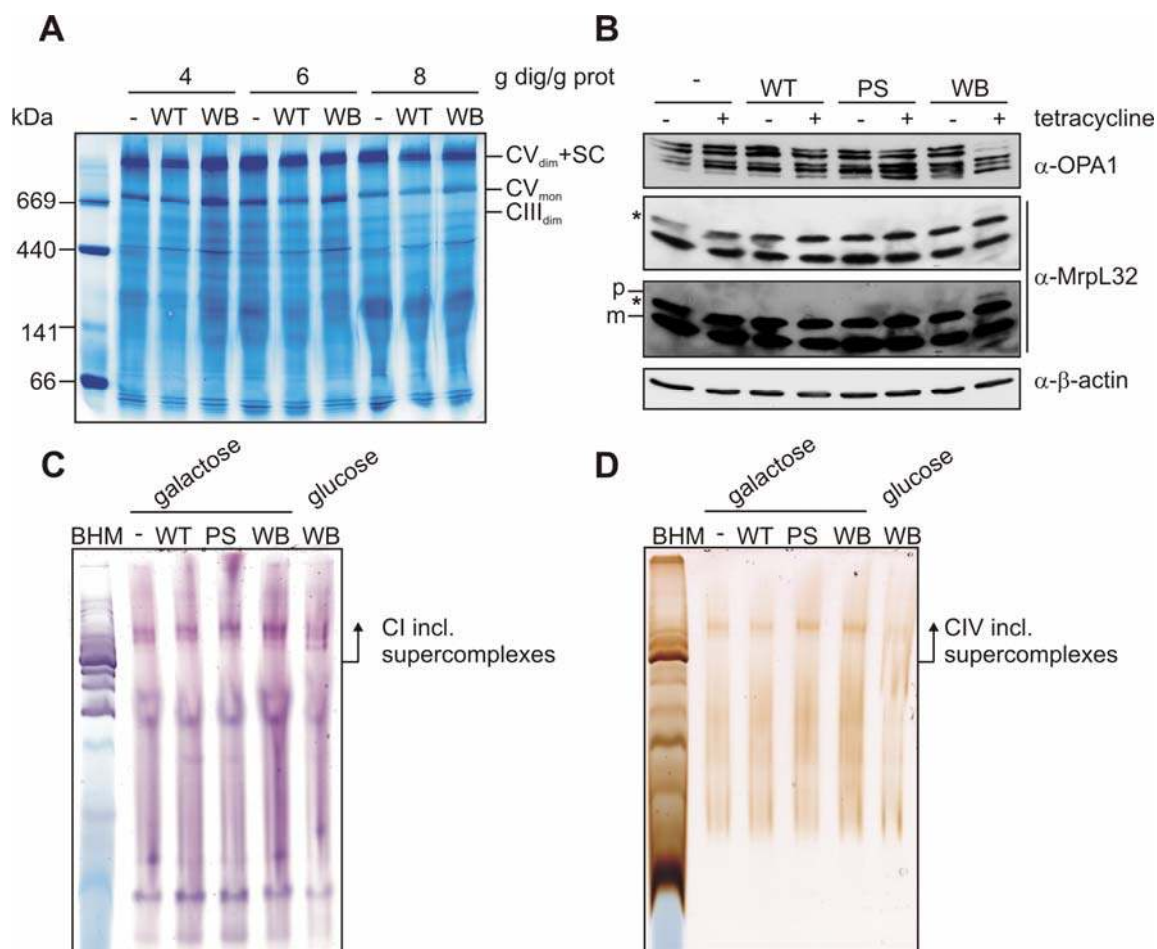


Figure 12: Assembly and activity of the respiratory chain in FITR293 cells expressing dominant-negative mutant variants is apparently not altered.

(A) BN-PAGE analysis of mitochondria isolated from murine Afg3l2 expressing cell lines. The mitochondrial membrane fraction was solubilized using the indicated amounts of digitonin (dig) per g of mitochondrial protein. A 3-11 % [w/v] BN-PAGE was performed and gels were stained with colloidal Coomassie.

(B) Appearance of precursor MrpL32 in immunoblots of total cell lysates from FITR293 cells inducibly overexpressing human AFG3L2 WB. Membranes were stained with antibodies specifically recognizing OPA1 and MrpL32. β-actin served as a loading control. p, precursor; m, mature; *, unspecific crossreaction. The lower film of the MrpL32 immunostaining was exposed longer to visualize the precursor.

(C) In-gel-activity-staining of NADH:ubiquinone oxidoreductase (complex I) of mitochondrial lysates from different FITR293 cell lines. Mitochondria were isolated from cells grown either on glucose or galactose. Digitonin (10 g/g protein) solubilized mitochondrial complexes were separated on a 3-13 % [w/v] CN-PAGE. Bovine heart mitochondria (BHM), solubilized with 8 g dig/g protein, served as positive control. NADH dehydrogenase containing complexes were visualized by a complex I staining.

(D) In-gel-activity-staining of cytochrome c oxidase (complex IV) of solubilized mitochondrial membranes from different FITR293 cell lines. Mitochondria were analyzed as in (C) and gels were stained by a cytochrome c oxidase staining.

CI, NADH:ubiquinone oxidoreductase (complex I); CIV, cytochrome c oxidase (complex IV); BHM, bovine heart mitochondria; SC, supercomplexes; mon, monomeric; dim, dimeric; -, parental cell line control; WT, Afg3l2/AFG3L2 wild type; PS, mutation in the proteolytic site (AFG3L2^{E575Q}); WB, mutation in the Walker B motif (Afg3l2^{E407Q}/AFG3L2^{E408Q}); arrows indicate the appearance of supercomplexes (> 1.5 MDa).

Complexes of the respiratory chain have been shown to form large supramolecular assemblies, termed respiratory supercomplexes or 'respirasomes' (Krause *et al.*, 2004; Marques *et al.*, 2007; Schägger and Pfeiffer, 2000; Wittig *et al.*, 2006). This type of organization was hypothesized to be of high functional importance for optimizing electron transport during respiration (Boekema and Braun, 2007; Schägger, 2001; Schägger, 2002). In mammalian mitochondria, almost all complex I is assembled into supercomplexes comprising complexes I and III and up to four copies of complex IV (Schägger and Pfeiffer, 2000). To monitor the supercomplex composition in Afg3l2 expressing FITR293 cell lines in more detail, immunoblot analysis of a first dimensional BN-PAGE was performed (Figure 13 A). Interestingly, immunostaining with antibodies specifically recognizing subunits of respiratory chain subunits of complexes I, III and IV revealed a slight accumulation of free complexes III and IV and of smaller arrangements which lack complex IV (Figure 13 A). This indicates a reduced stability or higher turnover of these supercomplexes. Intriguingly, this phenomenon is reminiscent of phenotypes observed in Barth Syndrome patients. Isolated mitochondria from these patients harboring mutations in the cardiolipin remodelling enzyme tafazzin show a similarly reduced stability of CI/CIII₂/CIV_{1-n} containing supercomplexes (McKenzie *et al.*, 2006). Earlier, it was hypothesized that the permeability changes of the inner membrane towards protons are caused by changes in the lipid composition of the membrane phospholipids (Brand *et al.*, 1994). This is confirmed by several more recent publications: cardiolipin affects the stability of respiratory chain supercomplexes (Claypool *et al.*, 2008; Jiang *et al.*, 2000; McKenzie *et al.*, 2006; Schägger, 2002; Schlame *et al.*, 2000; Wittig and Schägger, 2009). Deletions of the yeast *m*-AAA protease show decreased phosphatidylethanolamine and cardiolipin levels (Osman *et al.*, 2009). This raised the question whether the mitochondrial phospholipid composition was also altered in mammalian cells expressing dominant-negative AFG3L2 mutants. Therefore, phospholipids of mitochondrial membranes were isolated and analyzed by thin layer chromatography (Figure 13 B). However, cardiolipin levels or the other phospholipids were not significantly affected after 24 h (or 100 h; Sebastian Müller personal communication) induction with tetracycline.

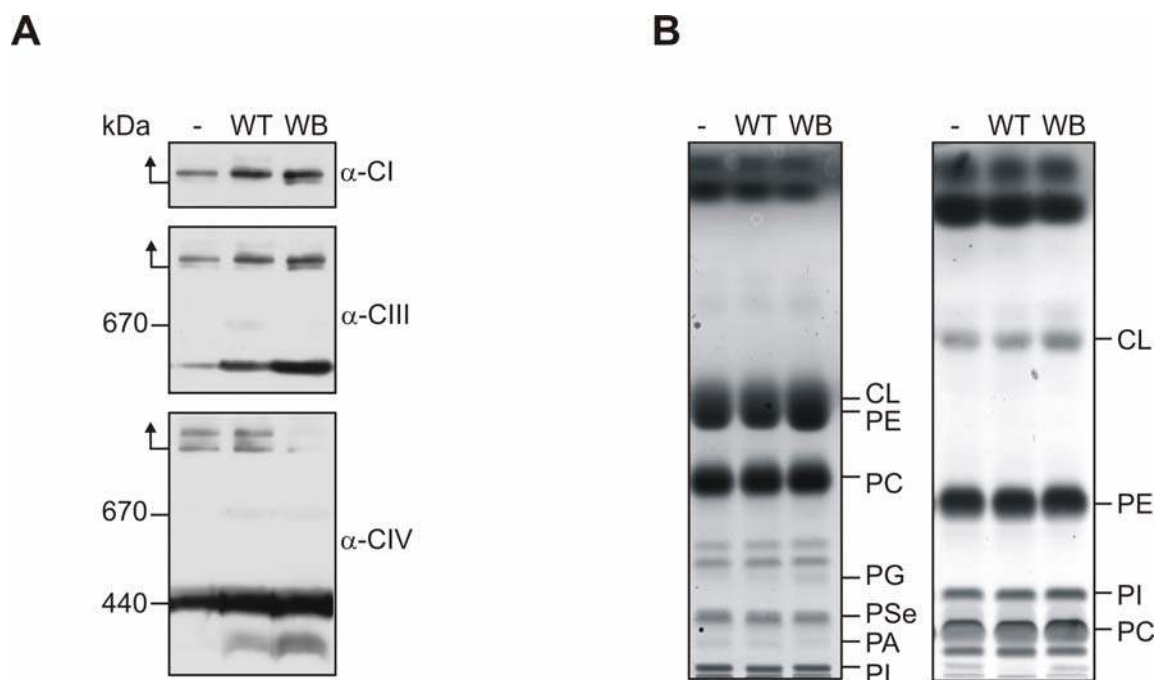


Figure 13: Dominant-negative Walker B mutation affects the stability of supercomplexes but not the phospholipid composition.

(A) Western Blot of BN-PAGE performed with mitochondrial preparations from murine Afg3l2 variant overexpressing cell lines. Expression was induced for 24 h with tetracycline. Immunostaining was performed using antibodies directed against complex I 30 kDa subunit (CI), complex III core 2 subunit (CIII) and complex IV subunit II (CIV). Arrows indicate the appearance of supercomplexes (> 1.5 MDa). (B) Thin layer chromatography (TLC) of isolated phospholipids from FITR293 cells expressing murine Afg3l2. TLC was run with chloroform/methanol/water (left, 65:35:5, v/v/v) and chloroform/ethanol/water/triethylamin (right, 30:35:7:35, v/v/v/v). CL, cardiolipin; PE, phosphatidylethanolamine; PC, phosphatidylcholine; PG, phosphatidylglycerol; PSe, phosphatidylserine; PA, phosphatidic acid; PI, phosphatidylinositol. -, untransfected control cells; WT, wild type Afg3l2; WB, mutation in the Walker B motif (Afg3l2^{E407Q}).

Consistent with these findings, mouse embryonic fibroblasts lacking *m*-AAA protease subunits achieved by siRNA-mediated downregulation showed phospholipid levels compared to wild type cells (Sebastian Müller, personal communication). In summary, functional *m*-AAA proteases are needed for the stability of respiratory chain supercomplexes although the overall assembly is not affected. The reduced stability of the supercomplexes cannot be simply explained by altered phospholipid levels within mitochondria.

3.4.1.4. Induced OPA1 processing at site S1 and increased turnover of non cleavable OPA1 variants

Accelerated OPA1 processing is not induced by an impaired energy metabolism. Membrane potential and ATP levels were not altered (see chapter 3.4.1.2). It has been shown that the induced cleavage takes place at site S1 (Song *et al.*, 2007). The subunit SPG7 of mammalian *m*-AAA proteases has been suggested to cleave OPA1 at site S1. To address the observed phenotype of induced OPA1 processing in cells expressing ATPase mutants of *m*-AAA proteases in more detail, S1 cleavable and non-cleavable variants of rat Opa1 were transfected into Afg3l2 expressing FITR293 cell lines (Figure 14). FLAG-tagged rat Opa1 splice variant 1 (rOpa1 v1; L+S-Opa) (Ishihara *et al.*, 2006) (Figure 14 A) gives rise to a long and a short isoform, and FLAG-tagged rat Opa1 splice variant 1, lacking the cleavage site S1 (rOpa1 v1 Δ S1; L-Opa) (Ishihara *et al.*, 2006) (Figure 14 A), yields only the long isoform. In line with published findings, transfection of rOpa v1 revealed a long and short, whereas v1 Δ S1 a long Opa1 isoform only (Ishihara *et al.*, 2006; Song *et al.*, 2007). Interestingly, cells inducibly expressing Afg3l2 harboring a mutation in the Walker B motif showed an enhanced processing of splice variant 1, illustrated by an accumulation of the short compared to the long isoforms. In contrast, cells expressing rat Opa1 variant 1 lacking cleavage site S1 demonstrated a reduced steady state level of long Opa1 (see Figure 14 C). Quantifications of the immunostaining intensities revealed a drastic change of the ratio of short and long isoforms (Figure 14 B, left panel) as well as to a reduction of long isoforms to 35 % compared to Afg3l2 wild type or control cells (Figure 14 B, right panel).

In summary, these results indicate that a functional ATPase domain of *m*-AAA proteases is necessary to stabilize long-OPA1. In addition, expression of the dominant-negative mutant of Afg3l2 facilitated the processing of a yet unknown protease indicating that *m*-AAA proteases control this processing event in a negative regulatory manner.

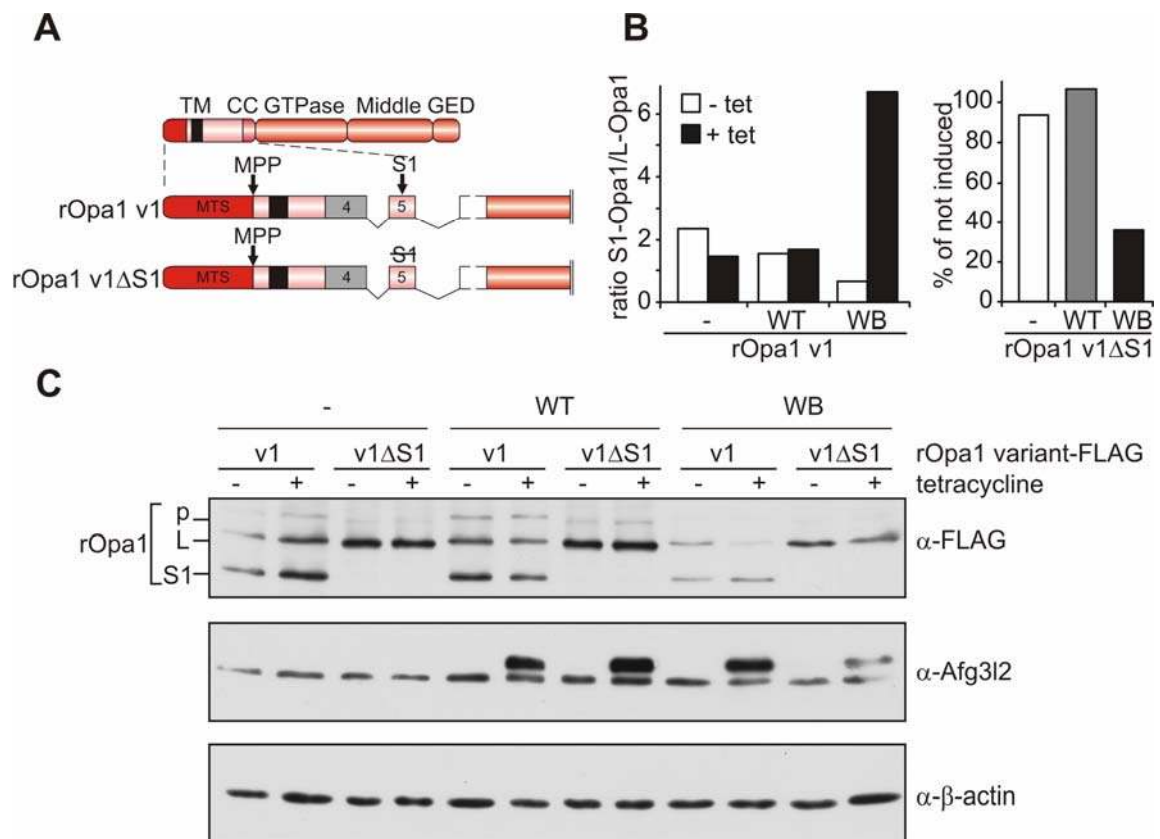


Figure 14: A defective *m*-AAA protease leads to induced processing of OPA1 at site S1 and an increased turnover of long OPA1 isoforms.

(A) Domain structure of C-terminal FLAG tagged rat Opa1 variant 1 (v1) and non-cleavable rOpa1 variant 1 (v1ΔS1) lacking the cleavage site S1. DNA constructs were provided by (Ishihara *et al.*, 2006).

(B) Quantification of the ratio between the short (S1) and the long isoform (L) of rat Opa1 (left panel), and the percentage of visible rOpa1 in cells expressing Afg3l2 WT or WB after transfection with the indicated construct. Murine Afg3l2 expressing FITR293 cell lines were transiently transfected with rat Opa1 splice variant 1-FLAG (v1, left panel) and variant 1-FLAG lacking the processing site S1 (v1ΔS1, right panel). After 24 h, cells were split before induction with tetracycline for 24 h. Cells were lysed and lysates were separated by SDS-PAGE and analyzed by following immunoblotting using FLAG-, murine Afg3l2 and β-actin antibodies. Signals were quantified using ImageQuant TL (GE) software. The intensities of non-cleavable rOpa1 v1 were normalized to the respective β-actin signals.

(C) Western Blot analysis of the experiment described in (B).

TM, transmembrane domain; CC, coiled coil domain; GED, GTPase effector domain; MPP, mitochondrial processing peptidase; tet, tetracycline; r, rat; WT, wild type; WB, mutation in the Walker B motif (Afg3l2^{E407Q}); p, precursor of OPA1; L, long Opa1 isoform; S1, short Opa1 generated by cleavage at site S1.

3.4.1.5. OPA1 co-immunoprecipitates with overexpressed Afg3l2

Obviously, *m*-AAA protease isoenzymes affect the stability of long OPA1 isoforms, but so far the mechanism has remained elusive. Previous experiments suggested an interaction of exogenously expressed SPG7-HA and FLAG tagged OPA1 v1 in HeLa cells (Ishihara *et al.*, 2006). Thus, it is conceivable that also Afg3l2 interacts directly with OPA1. To further investigate this, co-immunoprecipitation experiments were performed.

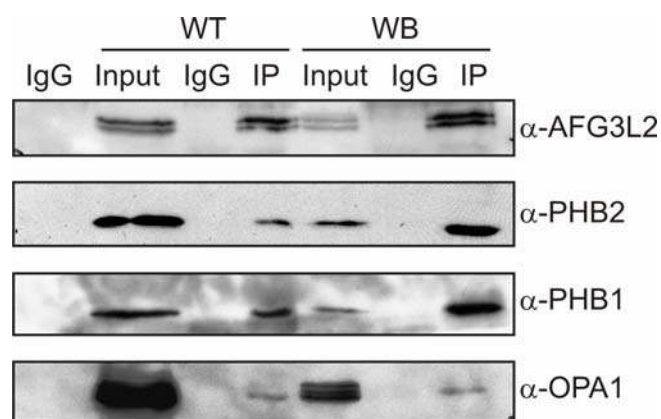


Figure 15: OPA1 isoforms and the prohibitins can be co-immunoprecipitated with overexpressed *m*-AAA protease.

Afg3l2 could be precipitated out of 750 μ g lysed mitochondria from FITR293 inducibly overexpressing murine Afg3l2 WT or WB using antibodies directed against human AFG3L2. Expression was induced for 24 h with tetracycline. Mitochondrial membranes were solubilized using 20 g digitonin/g protein. IgG indicates immunoprecipitation (IP) with preimmune serum which was used as a negative control. IP samples and 10 % of the total input were loaded and analyzed by SDS-PAGE and Western Blot using antisera of human AFG3L2, OPA1, prohibitin 1 and 2 (PHB1 and PHB2).

WT, wild type; WB, Walker B mutant (Afg3l2^{E407Q}).

Immunoprecipitation of endogenous AFG3L2 from digitonin lysed FITR293 mitochondria using a specific antibody revealed a complex composed of the *m*-AAA protease and the prohibitins as previously described for the yeast and murine *m*-AAA proteases (Metodiev, 2005; Steglich *et al.*, 1999). OPA1 could not be detected in the immunoprecipitate (Figure 17 B). However, performing this experiment with mitochondrial lysates from cells inducibly overexpressing murine Afg3l2 WT or WB, both revealed signals of endogenous OPA1 in the immunoprecipitate (Figure 15). However, the interaction was weak compared to that with the prohibitins.

In conclusion, *m*-AAA proteases are in a putative complex with prohibitins and OPA1 the role of which remains to be elucidated. Interestingly, this complex is not affected by the mutation in the Walker B motif.

3.4.1.6. Analysis of the OPA1 complex and apoptotic sensitivity

Besides its role for mitochondrial fusion OPA1 controls apoptotic cristae remodelling (Cipolat *et al.*, 2006; Frezza *et al.*, 2006). Independent of mitofusins it prevents apoptosis by preventing cytochrome c release and mitochondrial dysfunction (Frezza *et al.*, 2006). As mentioned earlier, OPA1 isoforms are generated by alternative splicing as long OPA1 isoforms which reside in the inner mitochondrial membrane (Delettre *et al.*, 2001; Olichon *et al.*, 2002; Satoh *et al.*, 2003). A minor fraction, however, is subjected to proteolytic

processing and gets further released into the intermembrane space which has been suggested to be regulated by the inner membrane rhomboid protease PARL (Cipolat *et al.*, 2006). It is believed that OPA1 oligomers in the intermembrane space are composed of both, transmembrane long and soluble short isoforms. Interestingly, Frezza *et al.* correlated the disassembly of OPA1 oligomers with remodelled cristae (Frezza *et al.*, 2006). For instance, *Parl*^{-/-} mouse embryonic fibroblasts exhibit a reduced amount of oligomeric OPA1 compared to wild type cells (Frezza *et al.*, 2006). Recently, Yamaguchi *et al.* observed that this disassembly is dependent on pro-apoptotic BH3-only proteins or BH3 peptides, and requires the presence of either Bak or Bax in the outer mitochondrial membrane (Yamaguchi *et al.*, 2008). Considering the role of OPA1 on cristae remodelling during apoptosis, the question emerged whether *m*-AAA proteases not only induce the processing and increased turnover of long-OPA1 isoforms but also influence OPA1 complexes and therefore the resistance towards apoptotic stress stimuli.

Therefore, crosslinking of OPA1 as described previously (Frezza *et al.*, 2006; Yamaguchi *et al.*, 2008) was carried out using isolated mitochondria from FITR293 expressing distinct variants of AFG3L2 (Figure 16 A). One distinct band at approximately 160 kDa and also species with a higher molecular weight appeared after crosslinking. Although the dominant-negative mutation in AFG3L2 induced the processing of OPA1, the observed oligomers were formed to a similar extent, indicating that *m*-AAA proteases do not influence the formation of OPA1 complexes (Figure 16 A). To test the sensitivity of FITR293 cells towards apoptotic stimuli, cells were treated with different concentrations of tumor necrosis factor (TNF)- α and cycloheximide. Together they induce the death receptor pathway (Aggarwal, 2003) (Figure 16 B). Cell lysates were analyzed using antibodies against PARP1, a 116 kDa nuclear poly (ADP-ribose) polymerase which appears to be involved in DNA repair in response to environmental stress (Satoh and Lindahl, 1992). This protein is cleaved by caspase-3 *in vivo* and serves as a marker of cells undergoing apoptosis (Nicholson *et al.*, 1995; Oliver *et al.*, 1998; Tewari *et al.*, 1995). Visualizing the activation of caspase-3 by using antibodies specifically recognizing the cleaved form failed since FITR293 cells exhibit low levels of endogenous caspase-3 protein (Eldering *et al.*, 2004). However, expression of dominant-negative Walker B mutant of AFG3L2 had no effect on the sensitivity towards TNF- α and cycloheximide (Figure 16 B).

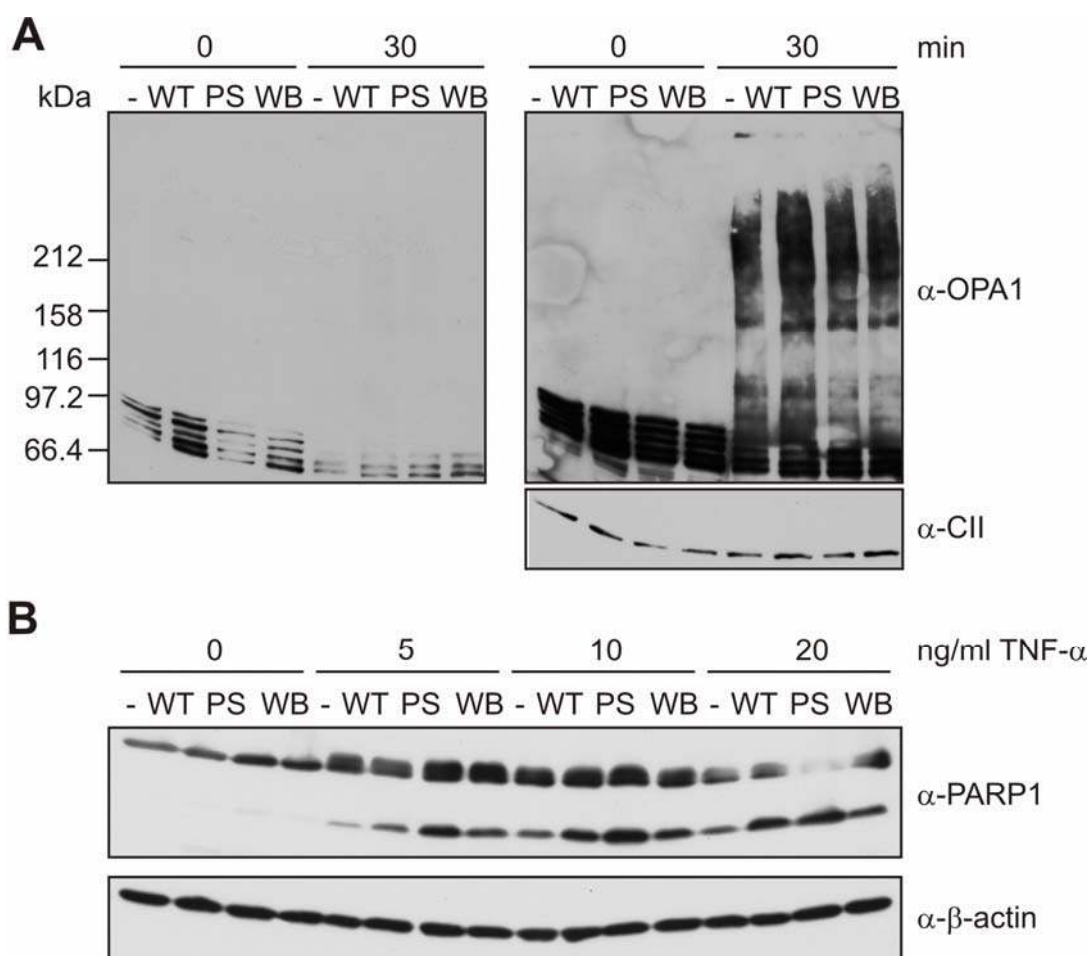


Figure 16: *m*-AAA protease has no apparent effect on the sensitivity of cells towards apoptosis.

(A) OPA1-crosslink showing no effect of the expression of AFG3L2 WB on OPA1 complex formation. Mitochondria isolated from stable FITR293 cells inducibly overexpressing the indicated AFG3L2 variant were incubated with the crosslinker EDC (10 mM/ 1 x PBS) for the indicated time. The reaction was quenched with SDS-loading buffer and complexes were separated on 6-12 % [w/v] Tris-glycine SDS-PAGE and further analyzed by immunoblotting using OPA1 antibodies. (On the right is shown a longer exposure time). Staining with complex II subunit 70 kDa served as loading control.

(B) PARP1 cleavage upon TNF- α induction of apoptosis in cells expressing human AFG3L2 variants. Cells were induced for 24 h with tetracycline and further incubated for 24 h in the presence of 0, 5, 10 and 20 ng/ml TNF- α , 2 μ g/ml cycloheximide and tetracycline. Lysates were analyzed by SDS-PAGE and immunoblotting using antibodies directed against human AFG3L2, PARP1 and β -actin as a loading control.

-, parental cell line control; WT, AFG3L2 wild type; PS, mutation in the proteolytic site (AFG3L2^{E575Q}); WB, mutation in the Walker B motif (AFG3L2^{E408Q}); CII, complex II 70 kDa subunit; PARP1, poly (ADP-ribose) polymerase 1.

To summarize, expressing the dominant-negative mutant of AFG3L2 did not effect the resistance against apoptotic stress induced by TNF- α and cycloheximide. Even though the OPA1 pattern was shifted to the short isoforms, the OPA1 complex formation is not altered, which is in contrast to PARL knockout cells (Frezza *et al.*, 2006). These findings reflect the results of already described co-immunoprecipitation experiments (see chapter 3.4.1.5). The *m*-AAA protease is in a putative complex with OPA1 which is not affected by the Walker B mutation. Therefore, *m*-AAA proteases don't seem to interfere with apoptosis

which is in contradiction to the effects observed in prohibitin 2 knockout cells (Merkwirth *et al.*, 2008), indicating that both proteins exert different functions during apoptosis.

3.4.2. *m*-AAA proteases play a role in stress induced hyperfusion via interaction with Stomatin-like protein 2

m-AAA proteases regulate mitochondrial fusion by stabilizing long OPA1 isoforms. However, the physiological role of mitochondrial fusion and fission in cell function and survival is still poorly understood. It has been reported that mitochondria hyperfuse and form a highly interconnected network in cells exposed to stresses that inhibit cytosolic protein synthesis (Tondera *et al.*, 2009). Stress-induced mitochondrial hyperfusion (SIMH) requires metabolically active mitochondria, leads to mitochondrial ATP production and represents a novel adaptive pro-survival response against stress (e.g. UV irradiation and low concentrations of cycloheximide) (Tondera *et al.*, 2009). It was demonstrated that SIMH is dependent on OPA1, mitofusin1, and on SLP2, also known as Stomatin-like protein 2 (Santel and Fuller, 2001; Tondera *et al.*, 2009). SLP2, like the prohibitins, belongs to the SPFH protein family (Stomatin, Prohibitin, Flotillin and HflK/C) (Tavernarakis *et al.*, 1999). Interestingly, various SPFH-domain-containing proteins are enriched in detergent-resistant membranes suggesting an association with lipid microdomains in several cellular compartments (Browman *et al.*, 2007; Langhorst *et al.*, 2005). SLP2 forms a complex in the mitochondrial inner membrane and was shown to interact specifically with mitofusin 2 which is present in the outer membrane (Hajek *et al.*, 2007; Santel and Fuller, 2001). Interestingly, SLP2 interacts also with prohibitins and contributes to their stability (Da Cruz *et al.*, 2008). To analyze whether SLP2 interacts with the *m*-AAA protease in the inner membrane a 2D-BN/CN-SDS-PAGE was performed to monitor the size of the native complex. Gels were either subjected to immunostaining (BN-SDS-PAGE) or silver staining (CN-SDS-PAGE). Spots from the silver stained gels were picked and analyzed by trypsin digest and subsequent mass spectrometry (see appendix 6.2). SLP2 is present in an abundant protein complex which could be visualized by silver staining (Figure 17 A). Mitofusin 2 proposed to be a binding partner of SLP2 could neither be detected in silver stained protein gels nor in the Western Blot. In FITR293 cells, SLP2 runs at a size of 1-2 MDa, and cofractionates with the prohibitins and the *m*-AAA protease (Figure 17 A). Also prohibitins appeared as very abundant proteins in these experiments underlining an important role within mitochondria and the whole cell (Merkwirth *et al.*, 2008; Merkwirth and Langer, 2009).

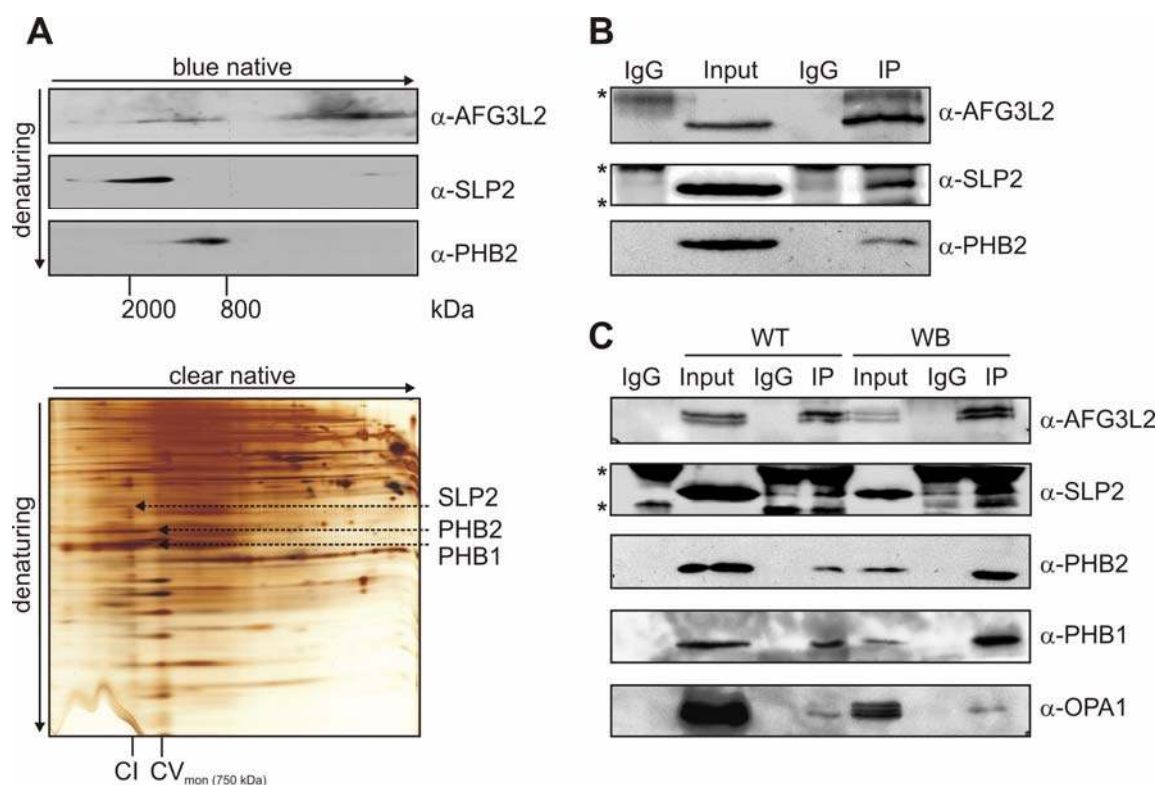


Figure 17: High molecular weight complex containing the prohibitins, SLP2 and AFG3L2.

(A) BN/CN-SDS-PAGE analysis of mitochondria isolated from FITR293 cells. Mitochondrial complexes were solubilized with digitonin at a detergent/protein mass ratio of 6:1 and separated on a 3-11 % [w/v] BN-PAGE and further subjected to a 12 % [w/v] Tris-glycine SDS-PAGE. Gels were analyzed by immunoblotting using antibodies directed against human AFG3L2, prohibitin 2 (PHB2) and SLP2 (upper panel). A 3-13 % [w/v] CN-PAGE was performed with solubilized mitochondria (10 g digitonin/g protein), and the 13 % [w/v] Tris-tricine SDS-PAGE in the second dimension was silver stained (lower panel).

(B) Co-immunoprecipitation (co-IP) of human AFG3L2, SLP2 and prohibitin 2. Human AFG3L2 could be precipitated out of 500 μ g solubilized mitochondria from FITR293 cells with a digitonin/protein ratio of 20:1 using antisera specifically recognizing human AFG3L2. 50 % of the IP samples were loaded. In parallel, an IP in the presence of preimmune serum was used as negative control (IgG). 10 % of the total input was loaded and analyzed by SDS-PAGE and Western Blot using the antisera specified above.

(C) Mitochondria isolated from cells stably overexpressing murine Afg3l2 WT or WB were used for the co-IP which was performed as described in (B). Samples were analyzed with specific antibodies directed against human AFG3L2, PHB1, PHB2, SLP2 and OPA1.

WT, Afg3l2 wild type; WB, Afg3l2 harboring a mutation in the Walker B motif (Afg3l2^{E407Q}); *, crossreactions with immunoglobulins.

However, SLP2 was shown to be important for mitochondrial hyperfusion, thus, a role of prohibitins in hyperfusion, also members of the SPFH domain family, was suggested. Surprisingly, downregulation of prohibitins in mouse embryonic fibroblast revealed that cells lacking prohibitins are still capable to hyperfuse (Tondera *et al.*, 2009). In contrast, cells depleted of *m*-AAA proteases by downregulation cannot undergo SIMH indicating a direct role of *m*-AAA proteases and SLP2 in stress induced hyperfusion (Ehse *et al.*, 2009;

Tondera *et al.*, 2009). Further evidence for a direct interaction of SLP2 and *m*-AAA proteases was revealed by a co-immunoprecipitation (Figure 17 B and C).

Notably, the presence of a high molecular weight complex consisting of AFG3L2, prohibitins and SLP2 could be demonstrated by BN- and CN/SDS-PAGE, and by co-immunoprecipitation (Figure 17). SLP2 and OPA1 could be co-immunoprecipitated together with overexpressed Afg3l2 (Figure 17 C) indicating that *m*-AAA proteases, OPA1 and SLP2 probably act together as one complex in the same pathway.

To conclude, *m*-AAA proteases and prohibitins are crucial for mitochondrial fusion by regulating the stability of long OPA1 isoforms. In addition, *m*-AAA proteases interact with SLP2 which both are required for stress induced mitochondrial hyperfusion suggesting the presence of two functional *m*-AAA protease containing supercomplexes: one fusion-supercomplex containing prohibitins, and another hyperfusion-supercomplex containing SLP2.

3.5. *m*-AAA proteases interact with MIC51

3.5.1. AFG3L2 harboring a mutation in the Walker B motif as a substrate trap

On the cellular level, it could be shown that defective *m*-AAA proteases achieved by the expression of a dominant-negative mutant variant has severe effects on cell proliferation (Figure 8) and mitochondrial morphology (Figure 9) by regulating the stability of long OPA1 isoforms (Figure 10 and 9). However, humans harboring missense mutations, or completely lacking an *m*-AAA protease subunit suffer from neurodegeneration (Cagnoli *et al.*, 2008; DiBella *et al.*, 2008; Ferreirinha *et al.*, 2004; Maltecca *et al.*, 2008) (Casari *et al.*, 1998). On the molecular level the neurodegeneration is barely understood. The yeast *m*-AAA protease was shown to degrade non-assembled and misfolded polypeptides (Koppen and Langer, 2007; Langer, 2000). Besides this quality control function, it also specifically processes MrpL32 (Nolden *et al.*, 2005). Processing of MrpL32 is not markedly affected in cells expressing AFG3L2 WB and can therefore not or only partially explain the observed phenotypes (Figure 12). For mammals, it is hypothesized that an impaired processing of a yet unknown protein causes the observed defects (Koppen and Langer, 2007; Rugarli and Langer, 2006). Thus, identification of substrate proteins of mammalian *m*-AAA proteases might help to unravel the pathogenesis of neurodegeneration. Data from yeast suggest that the dominant negative Walker B mutant can form a substrate trapping complex (Steffen Augustin, personal communication). To identify substrates of mammalian *m*-AAA proteases, the human AFG3L2 variants were fused to a carboxy-terminal hexahistidine tag. Metal affinity chromatography of digitonin solubilized mitochondrial membranes isolated from FTR293 cell lines was performed. Imidazol eluates were size fractionated using a gradient Tris-tricine SDS-PAGE (Figure 18 A). Mitochondria isolated from parental cell lines were used as a negative control to visualize unspecific protein binding. Additional protein bands were cut from the gel and analyzed by mass spectrometry (peptide mass fingerprint) (see chapter 6.2). AFG3L2 and the known assembly partners prohibitin 1 and 2 (PHB1, PHB2) were identified. Interestingly, one additional band appeared in all affinity purifications from AFG3L2 expressing cell lines representing a putative new interacting partner of the *m*-AAA proteases. Mass spectrometry revealed that it is the hypothetical protein of the open reading frame *C2ORF47*. No functional data either for the human or mouse protein is available to date. Two additional bands appeared in the samples expressing the dominant-negative mutant variant only, indicating that these proteins are putative substrate proteins. One band with a molecular mass slightly larger than AFG3L2

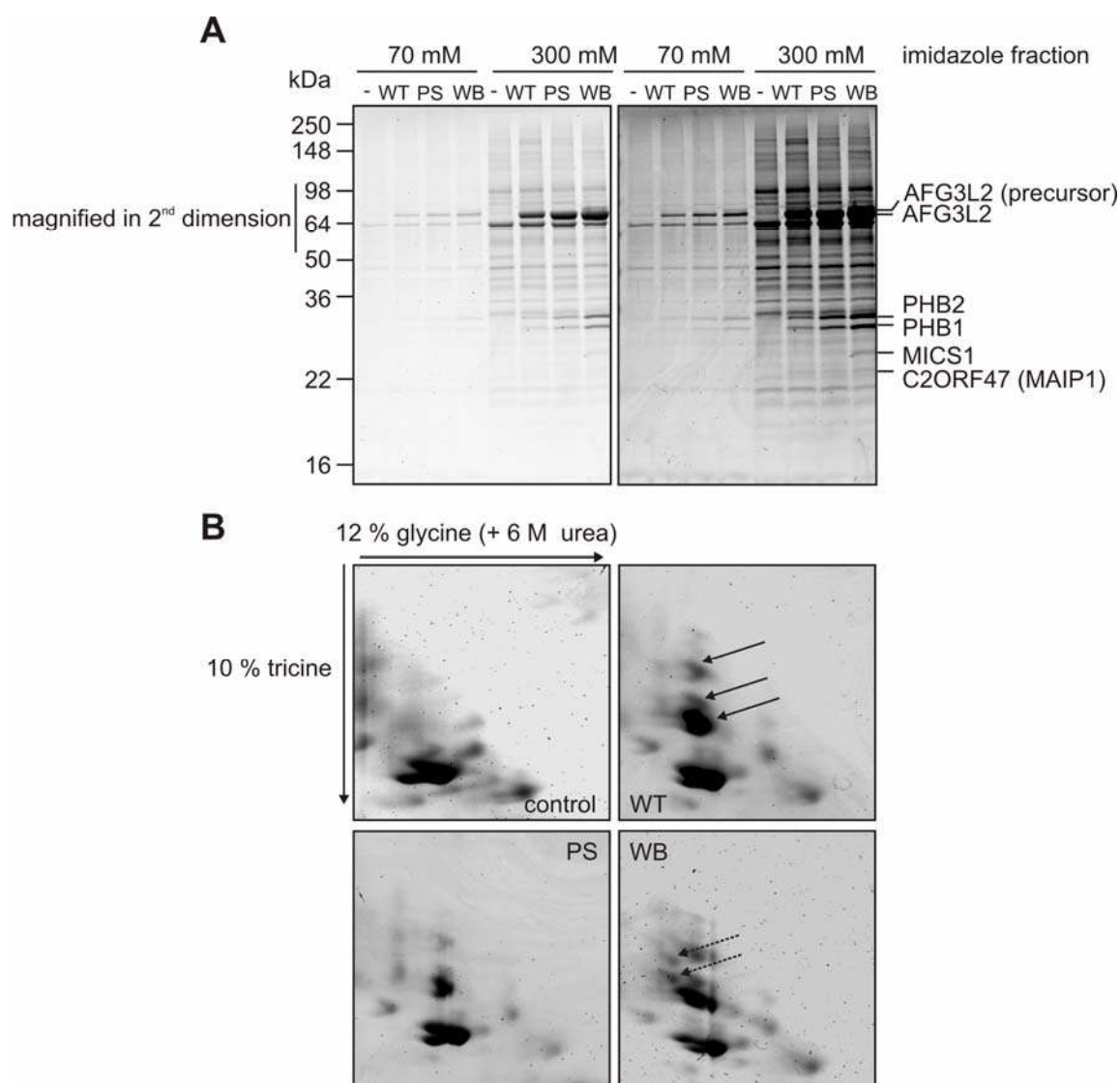


Figure 18: MICS1 and AFG3L2 itself are putative substrates of mammalian *m*-AAA proteases.

(A) Metal affinity chromatography using Ni-NTA to pull down C-terminal hexahistidine tagged human AFG3L2 variants. 5 mg of isolated mitochondria were solubilized (6 g digitonin/g protein) and incubated with Ni-NTA beads, washed and eluted with indicated imidazole concentrations to purify His6-epitope tagged *m*-AAA protease complexes. Fractions were analyzed by a 8-17.5 % [w/v] Tris-tricine SDS-PAGE and stained with colloidal coomassie. Protein bands not visible in the control were cut from the gel and analyzed by mass spectrometry (MS).

(B) Specific spot pattern of AFG3L2 in 2D-SDS-PAGE. Mitochondria were treated as in (A) but run on a 12 % [w/v] Tris-glycine SDS-PAGE containing 6 % [w/v] urea in the first dimension and a 10 % [w/v] Tris-tricine SDS-PAGE in the second dimension. Gels were stained with colloidal coomassie. Visible spots were cut and analyzed by MS. AFG3L2 is marked. Dashed lines indicate AFG3L2 (precursor).

-, parental cell line control; WT, AFG3L2 wild type; PS, mutation in the proteolytic site (AFG3L2^{E575Q}); WB, mutation in the Walker B motif (AFG3L2^{E408Q}); MAIP1, *m*-AAA protease interacting protein 1.

was identified by the peptide spectrum of the peptide mass fingerprint results (see appendix 6.2) as the precursor version of AFG3L2 indicating autocatalytic processing, which recently has been observed for paraplegin (Mirko Koppen, manuscript in preparation) (Ehse, 2008). The second band with a mass smaller than prohibitins could be identified as MICS1, a protein which resides in the inner mitochondrial membrane (see

chapter 1.3.3.3) (Oka *et al.*, 2008). Bands in the other lanes (Figure 18 A, -, PS) were cut and analyzed by peptide mass fingerprint to exclude any presence of MICS1 in the other samples, and indeed, MICS1 was either absent or not detectable by mass spectrometry.

To further investigate a region of low resolution (50-90 kDa) in the Tris-tricine SDS-PAGE, a 2D-SDS-PAGE approach was performed (Figure 18 B). A first dimension using a 12 % [w/v] Tris-glycine SDS-PAGE containing 6 M urea followed by a 10 % Tris-tricine SDS-PAGE was used to analyze the samples from the metal affinity purification. Spots which were not present in the control gel were marked in Figure 18 B and analyzed by mass spectrometry. Spots represent either mature or precursor versions of AFG3L2. Proteins running above the diagonal in this approach represent more hydrophilic proteins (Rais *et al.*, 2004) indicating that the two species of mature and precursor appear less hydrophobic than the main fraction of eluted AFG3L2. Paraplegin could not be detected in any purification followed by a colloidal Coomassie staining. Immunoblotting with a specific antibody revealed the presence of SLP2 specifically in fractions together with AFG3L2 (data not shown). However, it was not visible in protein gels.

To summarize, affinity purification confirmed the results from co-immunoprecipitation experiments. AFG3L2 complexes in the inner mitochondrial membrane interact with prohibitins and to a minor extent with SLP2. Second dimensional SDS-PAGE demonstrated a specific spot pattern of AFG3L2. C2ORF47 was identified as a putative interacting partner of AFG3L2. In addition, MICS1, a highly hydrophobic protein important for cristae organization, and AFG3L2 itself appeared as possible substrates of mammalian *m*-AAA proteases.

3.5.2. MICS1 is not processed by *m*-AAA proteases

Concerning the functions of the yeast *m*-AAA protease (see 1.4.1), MICS1 could be either processed like MrpL32, degraded, or its biogenesis could be affected in a non-proteolytic manner as described for Ccp1 (Leonhard *et al.*, 1996; Nolden *et al.*, 2005; Tatsuta *et al.*, 2007). To clarify the effect of *m*-AAA proteases on MICS1, carboxy-terminally hemagglutinin (HA)-tagged MICS1 (MICS1-4HA) was expressed in AFG3L2 expressing cell lines (Figure 19 A). HA tagged MICS1 was shown to localize to mitochondria (Oka *et al.*, 2008). Co-expression of MICS1-4HA and AFG3L2 variants revealed signals at molecular sizes of 30 kDa in SDS-PAGE visualized by immunoblotting with an antiserum specific for the HA-epitope tag. Interestingly, only one band was detected independent of the co-expression of AFG3L2 WT or WB mutant indicating that

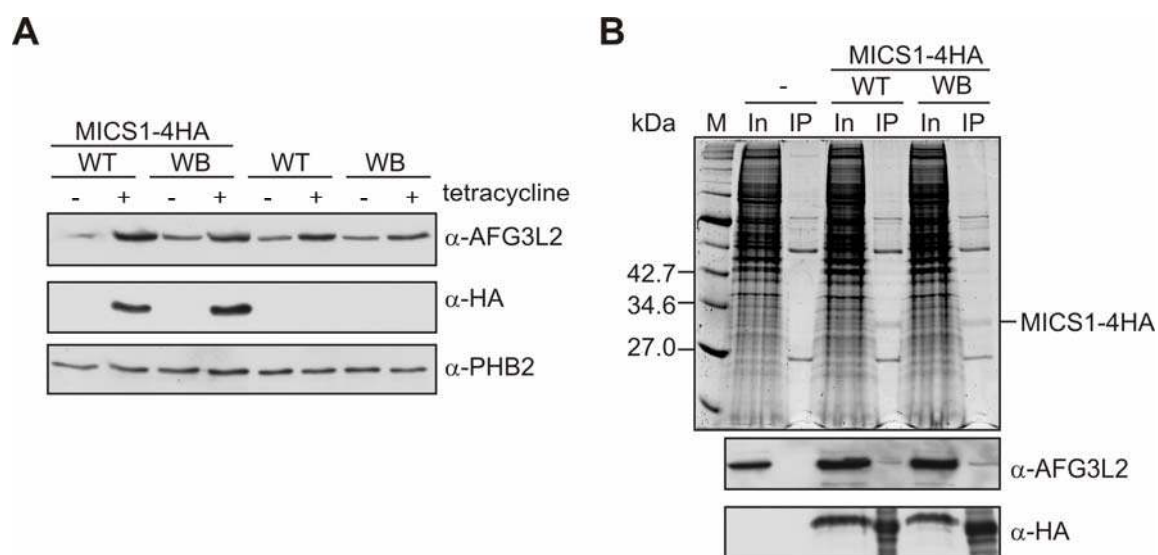


Figure 19: MICS1 binds to but is not processed by *m*-AAA proteases.

(A) No processing defect of MICS1-4HA in cells expressing dominant-negative forms of AFG3L2. MICS1-4HA under a tetracycline-inducible CMV promoter was transiently transfected into FITR293 cells expressing AFG3L2 WT or WB variants two days before induction of expression with tetracycline for 24 h. Cells were harvested and lysed. Samples were size fractionated via SDS-PAGE and analyzed by immunoblotting using antisera directed against AFG3L2, the HA-epitope, and prohibitin 2 as a loading control.

(B) MICS1-4HA physically interacts with AFG3L2. FITR293 expressing indicated AFG3L2 variants and untransfected (-) FITR293 cells were transiently transfected with MICS1-4HA constructs 2 days before induction of expression with tetracycline for 24 h. Cells ($\sim 1 \times 10^8$) were lysed and incubated with HA-antibody-coupled protein G matrix. Elution samples were size fractionated using SDS-PAGE and either analyzed by colloidal coomassie staining (upper panel) or by immunoblotting utilizing antisera recognizing the HA-tag and AFG3L2 (lower panels). 20 % of the IP samples were loaded.

M, protein marker; HA, hemagglutinin epitope; In, 1 % of the input; IP, 20 % of the immunoprecipitation elution fraction; WT, wild type; WB, mutation in the Walker B motif (AFG3L2^{E408Q}).

MICS1-4HA is probably not processed by the *m*-AAA protease, at least not from the N-terminus. Similarly, the band intensity was not significantly changed. However, an effect on the turnover of MICS1 might be mimicked by the overexpression of MICS1. Further experiments are required to examine an effect of *m*-AAA proteases on the stability of MICS1. However, co-immunoprecipitations using the HA-antiserum revealed that AFG3L2 is able to bind MICS1-4HA regardless of the mutation in AFG3L2 indicating a direct role of the *m*-AAA proteases (Figure 19 B).

In conclusion, endogenous MICS1 was co-purified from mitochondria expressing the dominant-negative mutant variant of AFG3L2 which is – based on yeast studies – thought to work as a substrate trap (Tatsuta *et al.*, 2007) (Steffen Augustin, personal comment). Overexpressed HA-tagged MICS1 was not processed by the *m*-AAA protease. Furthermore, exogenously expressed HA-tagged MICS1 can physically bind to the *m*-AAA protease irrespective of a mutation in AFG3L2.

4. Discussion

4.1. ***Dominant-negative Walker B mutation – a novel approach to study mammalian m-AAA proteases***

m-AAA proteases are nuclear-encoded conserved oligomeric metallopeptidases, key components of the mitochondrial protein quality control system with crucial functions in mitochondrial biogenesis (Langer, 2000; Leonhard *et al.*, 2000; Nolden *et al.*, 2005). Yeast cells lacking a functional *m*-AAA protease complex exhibit pleiotropic phenotypes (Arlt *et al.*, 1998; Arlt *et al.*, 1996). Impaired processing of MrpL32, a subunit of the large mitochondrial ribosome, causes the loss of functional complexes of the respiratory chain and respiratory deficiency (Nolden *et al.*, 2005). Processing of this protein enables the full assembly of the ribosome allowing the translation of the mitochondrial genome leading to respiratory activity. To inactivate the proteolytic function of the yeast hetero-oligomeric *m*-AAA protease, all subunits have to be mutated in the proteolytic site (Arlt *et al.*, 1998).

In contrast to the yeast enzyme, which exclusively forms a hetero-oligomeric complex, the mammalian proteases also exist as homo-oligomeric arrangements (Koppen *et al.*, 2007) (Figure 4). Humans harbor homo-oligomeric complexes composed of AFG3L2 and hetero-oligomeric complexes containing SPG7 and AFG3L2. In mice, the expression of the three subunits paraplegin (Spg7), Afg3l2 and Afg3l1 results in the formation of up to six different isoenzymes. Therefore, a complete loss of *m*-AAA protease activity is only achieved by depletion of all subunits. However, siRNA approaches exhibit technical difficulties such as low transfection efficiencies of siRNAs, non-specificity and off-target effects (Svoboda, 2007). Expression of proteolytic inactive subunits, on the other hand, requires mutagenesis of all subunits which is technically difficult to achieve.

In this study, the inducible FlpIn T-REx system was employed to bypass these issues by the overexpression of a dominant negative mutant subunit. Replacement of a glutamate to glutamine in the Walker B motif (WB, see Figure 5) of murine Afg3l2 and human AFG3L2 was identified to cause a dominant negative effect. By the expression of this mutant, crucial functions of mammalian *m*-AAA proteases could be discovered including the control of cell proliferation (see 4.3) and mitochondrial dynamics (chapter 4.4). Notably, the FlpIn T-REx 293 expression system allowed the inducible, stable and uniform overexpression of murine Afg3l2 and human AFG3L2 variants enabling direct comparative analysis of cell lines excluding effects of random integrations. However, expression of the dominant

negative mutant in FITR293 cells has distinct advantages over the RNA interference approach: a high yield of cell material can be produced and used for large scale proteomic analysis. Expression of a subunit mutated in the proteolytic site (PS, see Figure 5) behaved like the expression of wild type subunits indicating that this mutation is not dominant negative and, therefore, not able to inactivate the protease.

The dominant negative Walker B mutation did not affect the formation of *m*-AAA protease prohibitin supercomplexes confirmed by BN-PAGE analysis and metal affinity chromatography (Figure 19). In addition, *m*-AAA protease complexes containing this mutation could be purified together with putative interacting partners and substrates, thereby suggesting that this complex is present in the mitochondrial inner membrane, proteolytically inactive and works as the proposed substrate trapping complex. In line, data from the bacterial homologous ATPase ClpX and the yeast *m*-AAA protease suggests that, during purifications, complexes containing this mutation behave like wild type characterized by the formation of hexameric arrangements (Hersch *et al.*, 2005) (Steffen Augustin, manuscript in preparation). Yeast cells co-expressing wild type and mutant subunits are not able to grow on non-fermentable carbon sources caused by an impaired processing of MrpL32. The mutant yeast complex traps MrpL32 as demonstrated by pulldown experiments (Steffen Augustin, personal communication).

The mutation in the Walker B motif has been studied in yeast and bacteria (Steffen Augustin, manuscript in preparation) (Hersch *et al.*, 2005). It has been shown that specific residues in the pore of the ATPase are in contact with the substrate molecule (Martin *et al.*, 2008). ATP binding and hydrolysis enable the movement of these pore residues, thereby unfolding and pulling the substrate into the proteolytic chamber of the protease (Martin *et al.*, 2008). The glutamate side chain in the Walker B motif is thought to activate a water molecule for attack on the γ -phosphate of bound ATP, and therefore, is important for ATP hydrolysis (Baker and Sauer, 2006; Hersch *et al.*, 2005). However, ATP binding is not affected resulting in a trap of ATP (Hersch *et al.*, 2005). Therefore, the findings of this study suggest that mutation of the critical glutamate inhibits ATP hydrolysis in the respective subunit and additionally in neighboring wild type subunits. Likewise, studies of the yeast *m*-AAA protease showed that this mutation inhibits ATP hydrolysis in the neighboring subunit by trapping of ATP (Steffen Augustin, manuscript in preparation).

In conclusion, this study identified the dominant negative effect of the Walker B mutation in *m*-AAA proteases as a mechanism to inactivate the protease which is conserved from yeast to man.

4.2. ***Mammalian m-AAA proteases affect the stability of respiratory chain supercomplexes***

The mitochondrial inner membrane is the protein-richest cellular membrane, whose functional impairment is associated with aging, myopathies, and neurological disorders in humans (Chan, 2006). It harbors the OXPHOS (oxidative phosphorylation system) complexes which are crucial to produce the general fuel of the cell – ATP (Saraste, 1999). The OXPHOS biogenesis requires a coordinated regulation of two genomes whose translation products have to assemble together with the membrane lipids into fully functional complexes and supercomplexes, the respirasomes [reviewed in (Wittig and Schägger, 2009)]. The yeast *m*-AAA protease is required for the processing of MrpL32 and therefore crucial for mitochondrial translation (Nolden *et al.*, 2005). Expression of AFG3L2 WB in FITR293 cells only modestly impaired MrpL32 processing (Figure 12 B). This is reminiscent of results from *Spg7* deficient mice (Nolden *et al.*, 2005) and from siRNA mediated downregulation of all *m*-AAA protease subunits in mouse embryonic fibroblasts (MEFs) (Ehses, 2008) indicating that mammalian *m*-AAA proteases are able to cleave MrpL32, in general. However, other redundant proteases seem to be active in processing MrpL32.

The overall assembly of the respiratory chain was not affected in FITR293 cells expressing the dominant negative mutant (Figure 12 A). Interestingly, mitochondrial translation is reduced to 50 % in mouse liver mitochondria isolated from *Spg7*^{-/-} mice compared to wild type (Nolden *et al.*, 2005), whereas the translation efficiency in *Spg7* deficient brain or spinal cord is not affected (Ehses, 2008). However, expression of the dominant negative mutation in Afg3l2 did neither alter the oxygen consumption of FITR293 cells (under routine conditions, Figure 11 A) nor the activity of complex I and complex IV (Figure 12 C and D). In line, the respiratory activity in brain, spinal cord and liver mitochondria of *Spg7*^{-/-} mice was comparable to wild type (Ehses, 2008). This suggests that, in liver, though the translation rate is reduced, cells are able to overcome these translation defects resulting in normal respiration. This compensatory mechanism is explained by the generation of respiratory complexes in excess which can be mobilized and attenuated if cells have increased energy requirements [reviewed in (Bernard and Rossignol, 2008)]. However, HSP (see 1.4.3.1) patients which have a deletion in SPG7 showed OXPHOS defects in muscle biopsy (Casari *et al.*, 1998), indicating that effects on OXPHOS might be an important clue but not the primary cause of the disease. Taken together, *m*-AAA proteases are dispensable for respiration in mammals which is in contrast to yeast.

Nevertheless, inhibition of the ATP synthase by oligomycin in cells expressing Afg3l2 WB revealed a slight but significant increase in respiratory activity compared to WT or control cells (Figure 11 A) indicating an electron slip or proton leak of the respiratory chain (Brand *et al.*, 1994; Brand *et al.*, 1994; Brown *et al.*, 1990; Nicholls, 1974). Uncoupling by CCCP treatment revealed a reduced maximal respiratory capacity resulting in the reduction of the respiratory control ratio of up to 40 % compared to Afg3l2 WT expressing cells. A reduced coupling could be explained by a slight decrease in the stability of supercomplexes containing complex IV in cells expressing Afg3l2 WB (Figure 13 A). Similar, mice lacking *Spg7* and one copy of *Afg3l2* (see 1.4.3.1) demonstrate a reduced stability of OXPHOS supercomplexes although the assembly is not affected (Martinelli *et al.*, 2009).

Recently, cytochrome (cyt) *c* has been found to associate with both complex IV and respiratory supercomplexes, providing a potential mechanism for the requirement for cyt *c* in the assembly and/or stability of complex IV and supercomplexes (Vempati *et al.*, 2009). An effect on cyt *c* has not been examined and should be addressed in future experiments.

The reduced stability of respiratory chain supercomplexes was reminiscent of findings from Barth syndrome patients which harbor mutations in the cardiolipin (CL) transacylase tafazzin involved in CL remodeling (McKenzie *et al.*, 2006) (see 1.2.1). Studies have demonstrated a loss of energy coupling efficiency in cellular models of Barth syndrome (Ma *et al.*, 2004; Xu *et al.*, 2005). In addition, Barth syndrome patients have reduced cardiolipin levels (Schlame and Ren, 2006). Interestingly, yeast cells lacking the *m*-AAA protease subunits Yta10 or Yta12 have reduced CL and phosphatidylethanolamine (PE) levels (Osman *et al.*, 2009). However, the phospholipid levels of mitochondria from Afg3l2 WB expressing FITR293 cells (Figure 13 B) and from *m*-AAA protease downregulated MEFs were comparable to wild type cells (Sebastian Müller, personal communication). This suggests that, in contrast to the yeast enzyme, mammalian *m*-AAA proteases do not interfere with CL or PE levels and that the reduced stability of the supercomplexes cannot simply be explained by altered phospholipid levels.

However, the reduced stability may have severe consequences for the organism and in particular for distinct tissues. It is conceivable that OXPHOS becomes limited in tissues with high energy demands. For instance, Barth syndrome affects heart and skeletal muscle and leads to growth retardation (Barth *et al.*, 1983). In line, *m*-AAA proteases have been associated with defects in specific neurons (introduced in chapter 1.4.3.1). Heart, skeletal muscle and brain are tissues with high energy demands (DiMauro, 2004; DiMauro and Schon, 2003).

In conclusion, expression of the dominant negative Walker B mutation in FITR293 cells reduced the maximal respiratory activity of the cells. MrpL32 processing was only

modestly affected and cells comprised an assembled and active respiratory chain. However, expression of the Walker B mutation destabilized the respiratory supercomplexes which cannot simply be explained by an altered mitochondrial phospholipid composition indicating other mechanisms regulated by *m*-AAA proteases.

4.3. The *m*-AAA protease-prohibitin complex is indispensable for cell proliferation

Cells expressing a dominant negative Walker B mutant subunit in yeast poorly grow on non-fermentable carbon sources as the processing of MrpL32 is impaired (Steffen Augustin, manuscript in preparation). However, the growth is normal on glucose containing plates. Expression of Afg3l2/AFG3L2 WB significantly reduced the ability of mammalian cells to proliferate (Figure 8). MrpL32 processing was only slightly affected (Figure 12 B). The integrity of the respiratory chain was maintained, including the membrane potential and ATP levels (Figure 11 and Figure 12), suggesting that mammalian *m*-AAA proteases control cell proliferation independent of a general OXPHOS defect.

The *m*-AAA protease in yeast and the AAA protease in bacteria are part of a large supercomplex containing the protease and SPFH family members, namely prohibitins (Kihara *et al.*, 1996; Steglich *et al.*, 1999) (chapter 1.4.2). The presence of this supercomplex containing both proteins, *m*-AAA protease and prohibitins, could be demonstrated by different approaches (Figure 17 and Figure 18) suggesting that both prohibitins and *m*-AAA proteases act together in one pathway controlling cell proliferation. In fact, these findings are reminiscent of data from mouse embryonic fibroblasts (MEFs) demonstrating an impaired cell proliferation upon Cre-mediated deletion of *Phb2* in *Phb2^{fllox/fllox}* cells leading to the complete loss of prohibitin complexes (Merkwirth *et al.*, 2008). Similar to expression of the Walker B mutants, knockout of *Phb2* results in reduced stability of I-OPA1 and subsequent fragmentation of the mitochondrial network. Expression of a non-cleavable long OPA1 variant revealed only a partial complementation of proliferation, although the tubular shape of mitochondria was restored in up to 60 % of the MEFs (Merkwirth *et al.*, 2008). To summarize, both, defective *m*-AAA proteases or the loss of prohibitins, affect cell proliferation. It remains unclear how the supercomplex of *m*-AAA proteases and prohibitins within the mitochondrial inner membrane interferes with a reduced cell proliferation.

Organisms have evolved mechanisms to prevent cell division under conditions of nutrient deficiencies by cell cycle regulation (Ryan and Hoogenraad, 2007). For instance, a high AMP:ATP ratio of the cell can be sensed by AMP-kinase (AMPK) (Jones *et al.*, 2005;

Ryan and Hoogenraad, 2007). One of the AMPK targets is the tumor suppressor p53 which upon phosphorylation arrests the cell cycle, whereas cellular differentiation and survival are not affected (Jones *et al.*, 2005; Mandal *et al.*, 2005). However, ATP levels in *Phb2* depleted cells (Merkwirth *et al.*, 2008) and cells expressing the WB mutant of Afg3l2 (Figure 11 B) are not altered indicating that the reduced cell proliferation occurs independently of the cellular energy status.

Mitochondria are the major source of reactive oxygen species (ROS) which alone can work as a signaling messenger by blocking cell cycle progression (Finkel, 2003). ROS, principally superoxide anion radical and its hydrogen peroxide, are derived from several sources in mitochondria, e.g. complex I and III. In addition to the physiological ROS, high levels of ROS are especially produced in conditions of mitochondrial dysfunction or altered respiration. PKC β can be activated by these oxidative conditions, and subsequently, phosphorylates the cytosolic P66Shc protein which is then able to translocate to the mitochondrial intermembrane space where it acts as a oxidoreductase transferring electrons directly from cytochrome c to oxygen to generate hydrogen peroxide (Giorgio *et al.*, 2005; Pinton *et al.*, 2007; Pinton and Rizzuto, 2008). Changes of the architecture of OXPHOS supercomplexes have been implicated in elevated ROS levels and the contribution to aging (Dencher *et al.*, 2007). ROS levels in cells expressing the dominant negative mutant variant have to be determined in future experiments.

One of the central regulators of cellular growth are the components of the serine-threonine kinase mTOR (mammalian target of rapamycin) pathway (DeBerardinis *et al.*, 2008; Sarbassov *et al.*, 2005). Inhibition of mTOR results in the stop of cell proliferation and increased autophagy under starvation conditions. Recently, a mitochondrial outer membrane anchored protein, FKBP38, was identified to interact with mTOR and contributes to the activation of the signaling cascade (Bai *et al.*, 2007). However, whether the *m*-AAA protease-prohibitin supercomplex interferes with these pathways or, in particular, with FKBP38 function in the outer membrane is not studied yet. Mitochondrial autophagy, also termed mitophagy, is induced by depolarization of the membrane potential of mitochondria (Twig *et al.*, 2008). The membrane potential of *Phb2* depleted and Afg3l2/AFG3L2 WB mutant expressing cells was comparable to that observed in wildtype cells. However, damaged mitochondria could have been depleted from the cell population by targeting to autophagosomes resulting in reduced mitochondrial mass.

Interestingly, overexpression of the inner membrane protein PNC1 (pyrimidine nucleotide carrier 1, yeast Rim2) has been shown to enhance cell size and proliferation (Floyd *et al.*, 2007). In contrast, lower expression of this six transmembrane spanning-protein results in reduced mitochondrial UTP levels, an increase of ROS and subsequent slower growth, while ATP levels and membrane potential were not affected. Loss of the

prohibitin-*m*-AAA protease complex might interfere with the function or stability of this protein in the membrane which has to be elucidated in the future.

Notably, depletion of prohibitins and *m*-AAA proteases might compromise a similar pathway indicating that a fully active supercomplex containing prohibitins and *m*-AAA proteases is required for cell proliferation. Still, the mechanism linking the loss of functional *m*-AAA protease-prohibitin complexes to cell proliferation is missing. Thus, the experimental identification of signaling mediators controlling this path of communication dependent on prohibitins or *m*-AAA proteases is of great importance.

4.4. *m*-AAA proteases are essential for mitochondrial fusion activity by stabilizing I-OPA1

Mitochondrial fusion is maintained by an equilibrium of both long and short OPA1 isoforms (Delettre *et al.*, 2001; Duvezin-Caubet *et al.*, 2007; Ishihara *et al.*, 2006; Olichon *et al.*, 2003; Olichon *et al.*, 2007; Song *et al.*, 2007). An imbalance leads to subsequent fragmentation of the mitochondrial network (Baricault *et al.*, 2007; Ishihara *et al.*, 2006). The processing of OPA1 needs to be tightly controlled in order to maintain fusion activity (see chapter 1.3.2). In particular, the constitutive processing is highly regulated to generate long and short isoforms, which both are important for mitochondrial fusion (Song *et al.*, 2007). In contrast, the induced processing, which was identified to occur at site S1 is distinct from the constitutive processing (Song *et al.*, 2007). It has been shown that dissipation of the membrane potential ($\Delta\Psi_m$), apoptotic stimuli and mitochondrial outer membrane permeabilization (MOMP) trigger this processing event (Baricault *et al.*, 2007; Griparic *et al.*, 2007; Guillery *et al.*, 2008; Ishihara *et al.*, 2006). In detail, Baricault showed that the primary cause of enhanced OPA1 processing is a decrease in ATP levels (Baricault *et al.*, 2007). An unknown protease cleaves I-OPA1 to generate short isoforms in a deregulated manner (Baricault *et al.*, 2007; Ishihara *et al.*, 2006). Cleavage at site S1 generates short isoforms. However, although not reflecting the *in vivo* situation, OPA1 isoforms which lack the S1 processing site are degraded completely (Griparic *et al.*, 2007; Song *et al.*, 2007). The question is raised what stimulus activates this protease and more importantly, what protease is doing this highly effective job. PARL and paraplegin (Spg7) have been implicated in processing at S1, however MEFs lacking either PARL or paraplegin exhibit a normal wild type like OPA1 pattern (Duvezin-Caubet *et al.*, 2007).

In this study, expression of the dominant-negative Walker B mutant of mammalian *m*-AAA proteases in human FTR293 cells accelerated the processing of OPA1 at site S1 (Figure 14). This resulted in a major punctate mitochondrial network (Figure 9) most

probably due to the imbalance of long and short OPA1 isoforms (Figure 10). Cells respired normal, and ATP-levels and $\Delta\Psi_m$ were not affected (Figure 11) excluding any secondary effect on OPA1 due to an impaired energy metabolism. These findings were consistent with data from siRNA-mediated downregulation experiments (Ehse, 2008). Depletion of the *m*-AAA protease in MEFs results in predominantly fragmented mitochondria and an accelerated processing of l-OPA1. Expression of different OPA1 splice variants lacking either cleavage site S1 or S2 revealed that the induced processing observed in *m*-AAA protease downregulated cells occurs at site S1, not at site S2 (Ehse, 2008).

The lipid environment has been shown to be a crucial regulator of mitochondrial dynamics. Reduced CL levels caused by deletions of *Ups1* (Osman *et al.*, 2009; Sesaki *et al.*, 2006) and decreased PE levels are linked to an inefficient processing of Mgm1 (Osman *et al.*, 2009). Therefore the phospholipid composition, in particular the PE content, might be crucial for efficient Mgm1 cleavage by Pcp1 and mitochondrial cristae morphogenesis (Herlan *et al.*, 2004; Herlan *et al.*, 2003; McQuibban *et al.*, 2003; Meeusen *et al.*, 2006). This study showed, that *m*-AAA proteases interfere with the processing of OPA1. However, neither altered lipid levels nor an accumulation of long OPA1 isoforms were observed in Walker B mutants (Figure 10). Instead, expression of Afg3l2/AFG3L2 WB induced the processing at site S1 (Figure 14) independent of the phospholipid levels (Figure 13 B).

Also other circumstances have been identified to interfere with the stability of long OPA1 isoforms. Depletion of the assembly partner of the *m*-AAA protease, prohibitin, from the inner mitochondrial membrane results in an accumulation of s-OPA1 caused by an enhanced processing of long OPA1 isoforms (Merkwirth *et al.*, 2008). Merkwirth *et al.* concluded that prohibitins are essential for mitochondrial fusion, and importantly, are crucial for cristae morphogenesis in an OPA1 dependent manner. It was hypothesized that mammalian prohibitins like the bacterial homologues HflKC (Kihara *et al.*, 1996) and yeast prohibitins (Steglich *et al.*, 1999) negatively regulate the AAA protease thereby inducing the processing upon depletion of prohibitins (Merkwirth *et al.*, 2008; Merkwirth and Langer, 2009).

Taken together, these findings suggest that mammalian *m*-AAA proteases and prohibitins control the induced processing of OPA1 and, therefore, regulate the stability of l-OPA1. The molecular mechanism underlying this regulation is unclear.

The question remains whether mammalian *m*-AAA proteases are involved in the constitutive processing of OPA1. Several evidence point to a proteolytic function of mammalian *m*-AAA proteases on OPA1. Firstly, this study demonstrated that mammalian *m*-AAA proteases can interact, when overexpressed, with endogenous OPA1 suggesting OPA1 as a putative substrate (Figure 15). This was also shown by crosslinking of

exogenously expressed SPG7 and OPA1 (Ishihara *et al.*, 2006). Secondly, Ishihara showed that exogenously expressed SPG7 triggers the cleavage of OPA1 (Ishihara *et al.*, 2006), and finally, demonstrated by heterologous expression in yeast, *m*-AAA proteases are able to cleave OPA1. Two models are proposed, model A suggests a direct proteolytic function of *m*-AAA proteases on OPA1, model B excludes the *m*-AAA protease of this function.

Model A: Three proteases are active in the processing of OPA1 (irrespective of MPP and the caspase-cleavage site) (model A, Figure 20). The *i*-AAA protease has been linked to the processing at site S2 (Griparic *et al.*, 2007; Song *et al.*, 2007). The constitutive processing at site S1 is presumably performed by mammalian *m*-AAA proteases, which together with the *i*-AAA protease generate the balanced equilibrium required for mitochondrial fusion activity. However, upon low ATP conditions or in the absence of *m*-AAA proteases, a yet unknown protease is activated to cleave OPA1.

Model B: A second model excludes *m*-AAA proteases from a proteolytic function on OPA1, resulting in the cleavage by an unknown protease in constitutive and induced processing events which are negatively regulated by a functional supercomplex of prohibitins and *m*-AAA proteases (model B, Figure 20). A decrease of the ATP levels stimulate the induced processing (Baricault *et al.*, 2007). This envisions a situation that the ATP-dependent metallopeptidase upon the reduction of ATP is less active thereby producing a certain stress stimulus, which leads to the subsequent activation of the unknown protease.

It could be possible that an unknown protein inhibiting the cleavage at S1 is activated by *m*-AAA proteases. By mutating *m*-AAA proteases this inhibitory protein cannot prevent the processing of OPA1. Excluding the protease of a direct function on OPA1 raises the question why OPA1 and *m*-AAA proteases interact with each other. This could be explained by the presence of large fusion complexes or organized domains in the mitochondrial inner membrane, which promote sterical contacts of fusion components and the lipids. It is likely, that these complexes exist. Considering the hypothesis that the

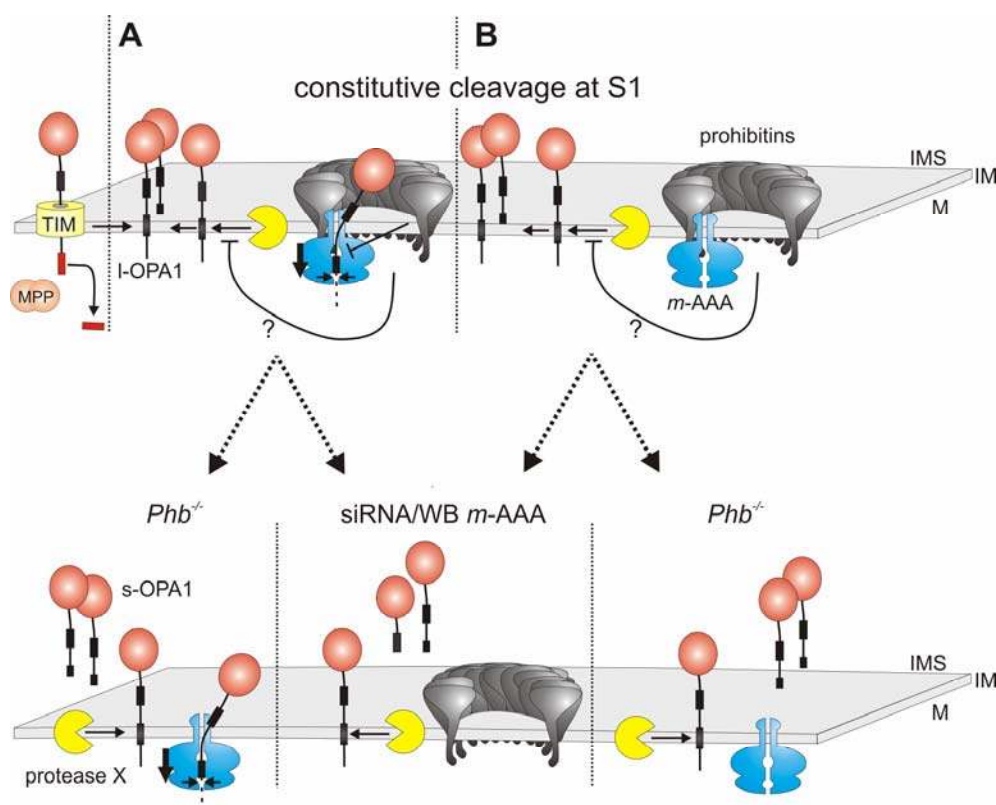


Figure 20: Model of OPA1 processing at the mitochondrial inner membrane.

The mitochondrial targeting sequence of OPA1 is cleaved off by MPP upon import into mitochondria (Ishihara *et al.*, 2006).

(A) *m*-AAA protease is involved in OPA1 processing. *m*-AAA protease and/or protease X cleave OPA1 at S1, which is negatively regulated by the prohibitins and/or the supercomplex. Loss of functional supercomplex leads to induced processing performed by protease X and/or *m*-AAA protease (if present). **(B)** *m*-AAA protease-prohibitin-supercomplex negatively regulates OPA1 processing by protease X. Loss of *m*-AAA proteases or prohibitins activates protease X.

TIM, translocase of the mitochondrial inner membrane; MPP, mitochondrial processing peptidase; IMS, intermembrane space; IM, inner membrane; M, matrix.

prohibitins work as membrane organizers or scaffold proteins (Merkwirth and Langer, 2009), it is possible that the *m*-AAA protease-prohibitin-supercomplex organize these large complexes thereby allowing membrane fusion. In fact, *m*-AAA protease, prohibitins, OPA1 and SLP2 (discussed in the next chapter 4.5.1) were detected in a putative complex (Figure 15).

This interaction does not necessarily have to be direct. In the past, the major part of novel protein-protein interactions identified in the mitochondrial morphology field was demonstrated by co-IP experiments with the addition of crosslinkers, and thus, might not represent physiological conditions. However, by using crosslinkers several fusion and fission proteins were demonstrated to physically interact like the mitofusins and OPA1 (Guillery *et al.*, 2008). In addition, Mfn2 could be crosslinked to SLP2 (Hajek *et al.*, 2007), and SLP2 to prohibitins (Da Cruz *et al.*, 2008). If *m*-AAA proteases interact with prohibitins

and SLP2 (Figure 17), and SLP2 interacts with Mfn2 which binds to OPA1, do the *m*-AAA proteases interact with OPA1? Clearly, further experiments are necessary to answer this question. It should be emphasized that the observed interaction of OPA1 and AFG3L2 was very weak and one binding partner was overexpressed. However, the co-IP was performed without the addition of crosslinkers.

In summary, mammalian *m*-AAA proteases and prohibitins were identified as crucial components of mitochondrial fusion by stabilizing I-OPA1. However, the molecular mechanism is still not fully understood. The identification of the protease inducibly cleaving at site S1 upon expression of Afg3L2/AFG3L2 WB and low ATP levels could unravel the understanding of this regulatory mechanism of OPA1 processing. In addition, analysis of this protease could further clarify if mammalian *m*-AAA proteases are involved in OPA1-processing or not, or if the *m*-AAA protease-prohibitin-supercomplex plays a role in organizing the large fusion complex by preventing the induced cleavage of OPA1.

4.5. Identification of novel interacting partners or putative substrates of mammalian *m*-AAA proteases

This study was initiated to identify substrates and interacting partners of mammalian *m*-AAA proteases in order to unravel molecular functions of the proteases. For this purpose, co-immunoprecipitation, 2-dimensional blue- or clear- native PAGEs and metal affinity chromatography experiments were performed. Prohibitins, SLP2, and MAIP1 could be identified as novel interacting partners. Using the substrate trapping approach discussed in chapter 4.1 the precursor of AFG3L2 and MICS1 appeared as potential substrates of mammalian *m*-AAA proteases thereby linking *m*-AAA proteases to new roles within mitochondria.

4.5.1. *m*-AAA proteases and SLP2 are crucial for mitochondrial hyperfusion

Co-immunoprecipitation experiments using antibodies directed against AFG3L2 revealed a complex of *m*-AAA proteases, PHB1, PHB2 and SLP2 (Figure 17 B). In addition, SLP2 was identified in *m*-AAA protease pulldown experiments although to a lower extent as prohibitins (Figure 18 A). BN- and CN-SDS-PAGE analysis of mitochondria isolated from human FITR293 cells demonstrated that SLP2, *m*-AAA proteases, prohibitin complexes co-migrated at approximately 1-2 MDa. SLP2 was present in complexes which migrated at

higher molecular weights when compared to prohibitins (Figure 17 A). Like prohibitins, SLP2 was very abundant and visible in silver stained CN-SDS-PAGE.

SLP2 or Stomatin like protein 2 is a member of the SPFH family, a large group of proteins including prohibitins and HflKC (chapter 1.4.2) (Browman *et al.*, 2007; Tavernarakis *et al.*, 1999). SLP2 was recently identified as a mitochondrial protein (Hajek *et al.*, 2007). Within mitochondria SLP2 is suggested to be anchored to the inner membrane facing the intermembrane space (Da Cruz *et al.*, 2008; Hajek *et al.*, 2007). SLP2 binds to prohibitins and contributes to their stability (Da Cruz *et al.*, 2008). Downregulation of SLP2 induces a metalloprotease dependent turnover of prohibitin 1, subunits of respiratory complex IV and complex I. Additionally, SLP2 together with prohibitin 1 is upregulated upon inhibition of mitochondrial protein synthesis by chloramphenicol (Da Cruz *et al.*, 2008). However, the physiological functions of SLP2 are barely understood.

Recently, Tondera *et al.* discovered the phenomenon of mitochondrial hyperfusion which is believed to be a cellular stress response and therefore termed SIMH (stress induced mitochondrial hyperfusion) (Tondera *et al.*, 2009). Treatment of mammalian cells with UV irradiation or low concentrations of cycloheximide (CHX) results in the hyperfusion of mitochondria generating a highly elongated interconnected network in combination with elevated ATP levels in the cell. Tondera discovered that SIMH is dependent on its key players, namely Mfn1, OPA1 and, interestingly, SLP2. It is claimed that long OPA1 isoforms are necessary for mitochondrial hyperfusion. However, *Phb2* depleted MEFs, which accumulate only short OPA1 isoforms, are competent for hyperfusion (Tondera *et al.*, 2009). Upon shRNA mediated downregulation of SLP2, OPA1 processing at site S1 is modestly elevated, whereas processing at S2 was slightly inhibited. However, treatment with CHX leads to an enhanced processing of l-OPA1, in particular at S1. It should be emphasized that expression of a non-cleavable OPA1 variant lacking the S1 cleavage site was stable, which was also observed in *Phb2* depleted MEFs (Merkwirth *et al.*, 2008). These results are distinct from findings obtained in this study. While non-functional *m*-AAA protease induced the processing at S1, non-cleavable OPA1 isoforms lacking the processing site S1 were degraded indicating that defective *m*-AAA proteases induce the turnover of l-OPA1 (Figure 14). It is suggested that the protease which mediates this turnover requires the presence of prohibitins and/or SLP2, possibly for organizing protein and lipid domains which allow efficient degradation in close proximity. In addition, SLP2 negatively affects the processing at S1 upon SIMH, indicating that SLP2 stabilizes l-OPA1 during stress induced hyperfusion. These findings lead to the hypothesis

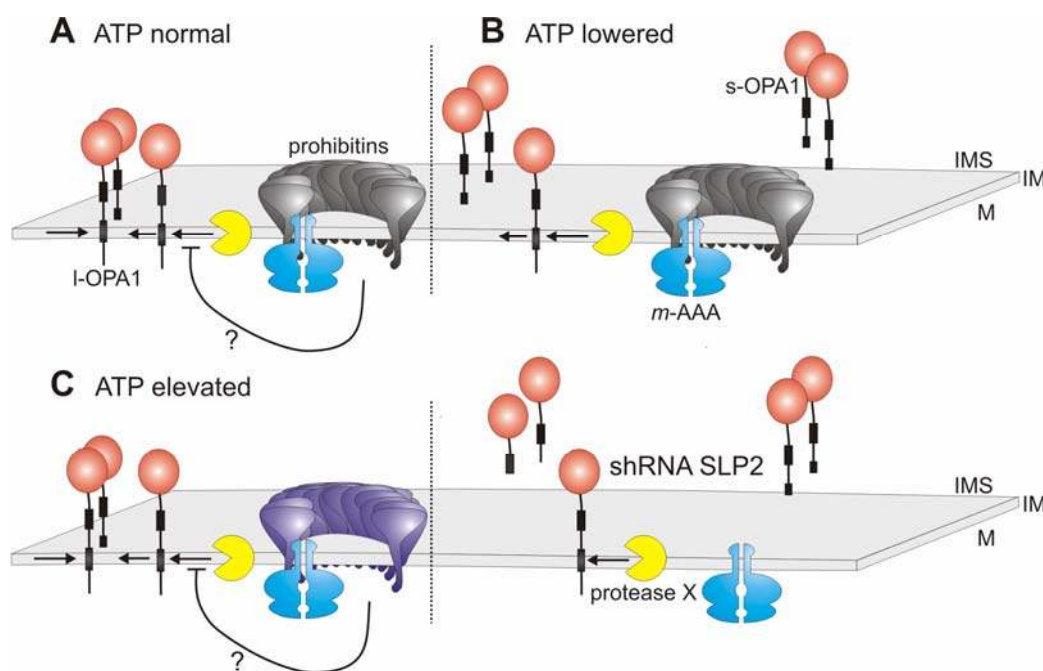


Figure 21: Dependence of mitochondrial fusion events on ATP levels.

To simplify the model, *m*-AAA proteases were excluded of any proteolytic function on OPA1.

(A) Constitutive processing of OPA1 at normal ATP levels. The supercomplex containing *m*-AAA proteases and prohibitins negatively regulates the cleavage by the protease X.

(B) Induced processing caused by lower ATP levels. The processing is deregulated leading to enhanced cleavage at site S1 and increased turnover of I-OPA1.

(C) SLP2 and *m*-AAA proteases containing supercomplexes inhibit the cleavage of I-OPA1 upon elevated ATP levels. Loss of SLP2 under hyperfusion conditions leads to induced processing of I-OPA1 at S1 by protease X.

that *m*-AAA proteases are required under both conditions: for prohibitin dependent mitochondrial fusion and for SLP2 dependent hyperfusion (Ehse, 2008; Tondera *et al.*, 2009).

It is concluded that during hyperfusion, ATP levels increase, and that this subsequently inhibits the processing of OPA1 in an ATP and SLP2 dependent manner thereby allowing hyperfusion. The ATP-dependent inhibition presumably is performed by the *m*-AAA protease which negatively regulates the cleavage at S1 (discussed in chapter 4.4) (Figure 21). These findings point to an interesting dichotomy: both SLP2 and *m*-AAA proteases are required for SIMH, whereas for fusion, *m*-AAA proteases and PHBs are necessary. Considering the co-migration of the *m*-AAA protease with both SLP2 and PHB2 containing complexes in BN-SDS-PAGE (Figure 17 A), and the fact that the interaction of endogenous prohibitins and SLP2 could be crosslinked to each other (Da Cruz *et al.*, 2008), it is conceivable that the interaction of prohibitins and SLP2 is not direct but rather mediated by *m*-AAA proteases. This possibility has to be proven in future experiments e.g. by downregulation of *m*-AAA proteases and subsequent co-immunoprecipitation of SLP2 and

prohibitins. Furthermore, another more striking model predicts two distinct *m*-AAA protease containing supercomplexes, one active in hyperfusion including SLP2, and another more abundant fusion supercomplex containing prohibitins (Figure 21).

In conclusion, SLP2 and mammalian *m*-AAA proteases form a high molecular weight complex in the inner mitochondrial membrane which is crucial for mitochondrial hyperfusion. It is hypothesized that elevated ATP levels prevent the enhanced processing of I-OPA1 which is negatively regulated by *m*-AAA proteases and SLP2. The degradation of non-cleavable I-OPA1 is controlled in an ATP-dependent process, presumably by mammalian *m*-AAA proteases. However, the exact molecular mechanism of hyperfusion and the protein machineries involved remain elusive.

4.5.2. *m*-AAA proteases interact with MAIP1 (*m*-AAA protease interacting protein 1)

In metal affinity chromatography experiments C2ORF47 co-eluted with AFG3L2 indicating that C2ORF47 (chromosome 2 open reading frame 47) is an interaction partner of mammalian *m*-AAA proteases (Figure 19 A). Therefore, it was named MAIP1 (***m*-AAA protease interacting protein 1**). The open reading frame of MAIP1 encodes for a protein that was predicted to target to mitochondria. The apparent molecular weight of mature MAIP1 is 22 kDa, which fits to the calculated molecular mass of the identified protein (Figure 18 A). MAIP1 carries a 100 amino acid long aminoterminal mitochondrial targeting sequence (MitoProt). The program HMMTOP (Tusnady and Simon, 2001) predicts one transmembrane domain in the N-terminal region, and a topology that the C-terminal part of the protein exposes the intermembrane space (sequence analysis in the appendix 6.3.2). Evolutionary conserved homologues of MAIP1 could not be identified in bacteria or yeast, but in other vertebrates and a more distantly related protein in insects. To date, there are no functional data on the vertebrate protein, but the insect homologue of MAIP1 is known as juvenile hormone esterase (JHE) binding protein 29 (Liu *et al.*, 2007). Juvenile hormone (JH) disperses throughout the hemolymph and act on responsive tissues. JHE is critical for the appropriate regulation and degradation of JH during insect development. MAIP1 identified as a binding protein of JHE has been shown to localize to mitochondria but its function is not understood (Liu *et al.*, 2007; Liu *et al.*, 2008). Based on the localization and detection of the esterase within mitochondria, it was hypothesized that the homologue of MAIP1 chaperones the esterase into and/or out of the mitochondria. Whether JHE functions in the mitochondria, or is stored there is unknown (Liu *et al.*, 2007; Liu *et al.*, 2008; Liu *et al.*, 2007). JHE is homologous to esterases and lipases, e.g. carboxyl esterase lipases or cholesterol esterases, proteins which mediate the hydrolysis and mobilization of

lipids in cells. However, a role of the interaction of MAIP1 with the *m*-AAA protease and a link to cholesterol esterases remains speculative.

4.5.3. AFG3L2 is autocatalytically processed

Ectopically expressed AFG3L2 was affinity purified via a C-terminal hexa-histidine tag. In 2D-gelelectrophoresis a set of spots were detected and evaluated by mass spectrometric analysis, all were identified as human AFG3L2 (Figure 18 B). In the 2D-SDS-PAGE approach used in this study, hydrophobic proteins run below the diagonal (Rais *et al.*, 2004). The minor fraction of AFG3L2 spots migrated above the diagonal indicating less hydrophobicity of the corresponding protein possibly reflecting distinct charge variants of AFG3L2. This could be a result of conformational protein variants, existing in an equilibrium during sample preparation and Tris-tricine gel-electrophoresis and therefore not caused from heterogeneity in the primary structure of the protein. This has been previously demonstrated in a Lectin protein rViscumin (Lutter *et al.*, 2001). No molecular differences like common chemical or post-translational modifications or nonenzymatic deamidation were found to cause the different charge values of the separated spots. The spot pattern was observed even under high urea concentration (Lutter *et al.*, 2001), such as those which were used in this study. However, a post-translational modification of AFG3L2 cannot be excluded and will be examined in future experiments.

Interestingly, the precursor of AFG3L2 was detected upon purification of AFG3L2 WB (Figure 19 A). Considering that the WB variant functions as a substrate trap, the precursor itself might be a substrate of the protease leading to autocatalytic cleavage. Similar results were obtained from murine fibroblasts (Mirko Koppen, manuscript in preparation) indicating a conserved mechanism in mouse and human. Briefly, cells downregulated of Afg3l1 and Afg3l2 accumulate precursors of paraplegin. Import of radioactively labeled lysate into isolated mitochondria lacking various subunit combinations revealed that Afg3l2 and paraplegin are processed by Afg3l1 and/or Afg3l2 during import. This two-step processing of paraplegin and Afg3l2 reminds of other mitochondrial inner membrane and intermembrane space proteins, like Mgm1 or Ccp1 whose intramitochondrial sorting is ensured by bipartite presequences (Neupert and Herrmann, 2007). Also Lon, a AAA⁺ protease soluble in the matrix and FtsH can cleave itself (Akiyama, 1999; Wagner *et al.*, 1997). It remains unclear which factors determine the specificity of the protease resulting in either degradation or proteolytic processing of its substrate. Studies with other ATP-dependent proteases indicate that stable proteolytic fragments are generated if the protein contains tightly folded structures that prevent the complete degradation of the protein (Piwko and Jentsch, 2006). A tightly folded domain may interrupt processive degradation

by *m*-AAA proteases initiated from the N-terminus resulting in the release of the matured protein like MrpL32, AFG3L2 or OPA1. This hypothesis is likely since AAA proteases like FtsH are poor unfoldases compared to other AAA⁺ proteases such as ClpXP (Herman *et al.*, 2003; Ito and Akiyama, 2005).

4.5.4. MICS1 is a putative substrate of mammalian *m*-AAA proteases

MICS1 co-eluted with hexa-histidin tagged AFG3L2 which harbors the mutation in the Walker B motif indicating that MICS1 is a putative substrate of mammalian *m*-AAA proteases. MICS1 was recently identified as a 23-26 kDa mitochondrial membrane protein (Oka *et al.*, 2008). MICS1 has seven transmembrane domains and resides in the mitochondrial inner membrane facing its carboxy-terminal region into the intermembrane space. Due to the induction of mitochondrial fragmentation in up to 55 % of the cells and the disorganization of mitochondrial cristae upon siRNA mediated downregulation, the so far unknown protein was named MICS1 (for mitochondrial morphology and cristae structure) (see chapter 1.3.3.3) (Oka *et al.*, 2008). The interaction with AFG3L2 WB can be explained by several hypotheses: MICS1 might be processed by mammalian *m*-AAA proteases resulting in an accumulation of a precursor version, like it was observed for MrpL32 or AFG3L2 itself (Figure 12 and Figure 18) (Nolden *et al.*, 2005). Secondly, MICS1, like other yeast inner membrane proteins, could be degraded by *m*-AAA proteases (Arlt *et al.*, 1998; Arlt *et al.*, 1996; Langer *et al.*, 1997; Pajic *et al.*, 1994). Finally, *m*-AAA proteases may affect the import of MICS1, rather than its turnover, as it was shown for cytochrome *c* peroxidase (Esser *et al.*, 2002; Tatsuta *et al.*, 2007).

Downregulation of MICS1 rendered the cells more susceptible towards apoptotic stimuli (Oka *et al.*, 2008). Instead, overexpression of MICS1 inhibits apoptosis and crosslinking experiments showed a physical interaction with cytochrome *c* pointing to a protective role of MICS1 to help cells to survive under unhealthy conditions. Expression of Afg3L2/AFG3L2 WB had apparently no effect on the sensitivity of cells to apoptosis (Figure 16), which is in contrast to *Phb2* knockout MEFs (discussed in chapter 4.6). Thus, a negative effect of the inactivation of AFG3L2 on MICS1 is unlikely, pointing to either a degradation or dislocation function of mammalian *m*-AAA proteases. To investigate these issues, FITR293 cells were transfected with HA-tagged MICS1. In SDS-PAGE, MICS1 ran at the estimated size which corresponds to a mature version of MICS1 with cleaved mitochondrial presequence (Figure 18 A). A precursor band of MICS1-4HA did not accumulate in cells expressing AFG3L2 WB (Figure 19 A) excluding MICS1 as a

proteolytically processed substrate of mammalian *m*-AAA proteases. MICS1 did not accumulate in cells expressing AFG3L2 WB when compared to WT.

Interestingly, sequence analysis revealed distant homology to a bacterial membrane protein YccA which is degraded by FtsH. YccA spans the membrane seven times and, when overexpressed, is FtsH-dependently degraded with a half-life of 15 min. (Kihara *et al.*, 1998). YccA in wild-type cells can be crosslinked with FtsH, and its level increases by shortening of the N-terminally located cytosolic tail which is believed to be the degradation initiation region (see chapter 1.4.4). The physiological function of YccA is unclear. These findings even more propose that *m*-AAA proteases are linked to MICS1. Furthermore, due to its homology to YccA, it can be speculated that MICS1 is degraded dependent on *m*-AAA proteases. MICS1 accumulates and binds to the substrate trapping WB complex. To confirm the interaction of MICS1, co-IPs using the HA-antibody were performed, and surprisingly, overexpressed MICS1 could also bind to the AFG3L2 wild type version (Figure 19 B). This might be caused by the overexpression of MICS1 resulting in the accumulation on *m*-AAA proteases indicating that MICS1 could be a quality control substrate of mammalian *m*-AAA proteases. However, endogenous MICS1 co-eluted only with WB in pulldown experiments.

To summarize, endogenous MICS1 co-eluted with the putative substrate trapping *m*-AAA protease complex, however the processing of overexpressed MICS1 was not affected and an accumulation of MICS1 in FITR293 cells expressing AFG3L2 WB was not observed. It should be mentioned that Ccp1, a yeast protein which is dislocalized by the *m*-AAA protease was never trapped in pulldown experiments (Takashi Tatsuta, personal communication). However, in IP samples of HA-tagged MICS1, also AFG3L2 was present further underlining that *m*-AAA proteases are linked to MICS1.

Interestingly, MEFs depleted of the *m*-AAA protease by siRNA-mediated downregulation show an aberrant cristae morphology (Sarah Eheses, manuscript in preparation). MICS1 is a likely candidate to link *m*-AAA proteases and cristae organization, however, Walker B expressing cells exhibit also destabilized respiratory supercomplexes. There are good indications that the bends in membranes induced by ATP synthase dimers are responsible for shaping the inner membranes and forming the cristae (see chapter 1.3.3 and 1.3.3.1) [reviewed in (Zick *et al.*, 2009)]. Thus, the organisation of complex V appears to play a structural role. However, an effect on the ATP synthase was not observed in cells expressing the Walker B variant. Mitochondrial morphology may also have an effect on or be affected by cristae morphology (Vonck and Schäfer, 2009). Up to now it is unclear if, once a supercomplex is formed, it persists until degradation, or if there is a permanent transition between individual complexes floating in the membrane and supercomplexes

(Vonck and Schäfer, 2009). The question remains “what comes first”: unstable supercomplexes or disorganized cristae?

Considering the suggested role of MICS1 in cristae organization and apoptosis, mammalian *m*-AAA proteases might contribute to these functions of MICS1 by regulating the steady state levels of MICS1. To investigate this, the stability of MICS1 in cells expressing the Walker B mutant compared to wild type has to be determined, e.g. with chase experiments.

4.6. *m*-AAA proteases and prohibitins – highly conserved complexes with overlapping functions?

Prohibitins and *m*-AAA proteases are crucial for cell proliferation (discussed in chapter 4.3). Deletions or mutations in prohibitins and *m*-AAA proteases results in an impaired cell proliferation indicating that the supercomplex is required to maintain cell growth. In addition, both have been demonstrated to be important for the stabilization of I-OPA1 (see 4.4). It was concluded that the supercomplex containing prohibitins and *m*-AAA proteases regulates the induced processing of OPA1 at the processing site S1 in a negative regulatory manner. Finally, deletions of prohibitins or *m*-AAA proteases have been shown to alter the cristae morphogenesis (4.5.4).

Yet, phenotypes are not completely similar. Firstly, inactivation of *m*-AAA proteases induces the turnover of non-cleavable OPA1 isoforms which were stable upon depletion of *Phb2* in MEFs (see 4.4). Secondly, prohibitins are dispensable for mitochondrial hyperfusion, whereas *m*-AAA proteases are necessary to allow fusion under hyperfusion conditions (discussed in chapter 4.5.1). Interestingly, *Phb*^{-/-} MEFs are more susceptible to apoptosis (Merkwirth *et al.*, 2008). Although major analysis of apoptosis in cells expressing the Walker B mutant is missing, there is evidence that WB cells behave different from *Phb2* knockout cells. Treatment with TNF- α and cycloheximide, an inducer of the extrinsic pathway, had no significant effect on the sensitivity towards apoptosis (Figure 16). In addition, siRNA-mediated downregulation of *m*-AAA proteases in MEFs revealed that MEFs were not more sensitive, instead they seemed modestly protected against etoposide, an inducer of the intrinsic apoptotic pathway (Sarah Ehses, personal communication).

Besides fusion, OPA1 has an important role for inner membrane dynamics, cristae organization and apoptosis (Cipolat *et al.*, 2006; Frezza *et al.*, 2006) (introduced in chapters 1.3.3.2 and 1.3.3.3). The question is raised why the resistance towards apoptosis upon deletion of prohibitins or *m*-AAA proteases is distinct though depletion of both leads

to an accumulation of s-OPA1. The disassembly of OPA1 complexes has been shown to be an important step during mitochondrial dependent apoptosis (Yamaguchi *et al.*, 2008).

For instance, PARL deficient MEFs show reduced amounts of crosslinked OPA1 oligomers (Frezza *et al.*, 2006). In line, PARL knockout cells are more susceptible to apoptotic stimuli (Cipolat *et al.*, 2006). However, in FITR293 cells expressing AFG3L2 WB, OPA1 complex accumulated comparable to wild type. This indicates, though less long isoforms present, the expression of the dominant negative mutant did apparently not affect complex formation of OPA1. Prohibitins were linked to apoptosis. Whether the loss of prohibitins affects the OPA1 complex is unclear and has to be determined. Since apoptosis is linked to the disassembly of OPA1 complexes, it can be assumed that this might be the cause of the increased sensitivity towards apoptosis of prohibitin depleted cells.

However, the formation of OPA1 complexes might not be the only phenotypical difference in apoptosis resistance between *m*-AAA protease and *Phb2* deficient cells. The identification of MICS1 may be the key to understand this phenomenon. MICS1 has been demonstrated to bind cyt c and upon overexpression to increase the resistance to apoptosis due to a delay in cyt c release (Oka *et al.*, 2008). Thus, an impaired degradation would necessarily result in the accumulation of MICS1 protecting *m*-AAA protease mutant cells to release cyt c. In contrast, *Phb2*^{-/-} MEFs lack the inhibitory function of prohibitins on the protease (Merkwirth and Langer, 2009). This results in an increased activity of *m*-AAA proteases which subsequently decreases MICS1 levels in the inner membrane resulting in disorganized cristae and increased sensitivity towards apoptotic stress. Although this model appears attractive, it should be considered that observed cristae phenotypes of the *Phb2* depletion, siRNA of *m*-AAA proteases and MICS1 are not completely similar. Instead, *Phb2*^{-/-} cells show more vesicular cristae which are comparable to those which was termed the stage 2 after inducing apoptosis (Sun *et al.*, 2007). Stage 2 is characterized by a release of cyt c but membrane potential is maintained.

It will be of interest to compare the cristae morphology in MICS1 and *m*-AAA protease depleted cells in different physiological conditions.

4.7. Translating cellular phenotypes to neurodegenerative diseases

Human AFG3L2 and SPG7 are associated with distinct neurodegenerative diseases, spinocerebellar ataxia (SCA) (Cagnoli *et al.*, 2006; Cagnoli *et al.*, 2008; DiBella *et al.*, 2008) and hereditary spastic paraplegia (HSP) (Casari *et al.*, 1998), respectively. The question remains whether the observed phenotypes in the cell culture system reflect the

physiological situation in humans. This is difficult to judge, since the dominant negative Walker B mutation is deleterious to the activity of the protease. It appears likely that humans or mice expressing this mutation in one subunit die or exhibit more severe defects than observed in SCA and HSP patients. Considering that expression of SPG7 WB in T-REx-HeLa cells resulted in fragmentation of the mitochondrial network (Figure 9 C) it is assumed that the mutation in *SPG7* is also dominant negative over the activity of the protease. In line, an *SPG7* Walker B disease mutation in HSP patients could not be identified so far (Elleuch *et al.*, 2006). The diseases do not resemble the deletion phenotype rather representing nuances of a functional state of the proteases considering tissue-specific expression of *m*-AAA protease subunits (Martinelli *et al.*, 2009). Interestingly, *Spg7*-deficient mice show a rather mild phenotype with neuronal degeneration restricted to regions in the longest motoneurons (Ferreirinha *et al.*, 2004). *Spg7*^{-/-} mice additionally lacking one copy of *Afg3l2* demonstrate severe degeneration of the cerebellum and the hippocampus (Martinelli *et al.*, 2009) indicating that these tissues particularly require *Afg3l2* function. This observation is reminiscent of the CMT2A pathogenesis linked to mitofusin 2 (Züchner *et al.*, 2006). A low expression of *Mfn1* explains the susceptibility of Purkinje cells in CMT2A pathogenesis. A conditional knockout of mitofusins in the cerebellum of mice revealed a requirement of *Mfn2* but not of *Mfn1* for Purkinje cells (Chen *et al.*, 2007). In fact, *Afg3l2* is strongly expressed in Purkinje cells. While *Spg7* expression appeared confined to Purkinje cells and specific neurons, *Afg3l1* transcript was instead poorly detected in the brain. These findings suggest that reduced expression levels of the subunits result in a lower abundance of active subunits. This subsequently triggers the degeneration Purkinje cells and the cerebellum. However, it cannot be excluded that differences in the enzymatic properties or substrate specificities of *m*-AAA protease isoenzymes or even different substrate proteins exist which explain the tissue specific defects observed in HSP or SCA patients.

Notably, mitochondrial dysfunction is an early event in virtually all common neurodegenerative diseases, including Huntington's disease (HD), Parkinson's disease (PD) and Alzheimer's disease (AD) (Lin and Beal, 2006). Interestingly, respiratory deficiency occurs late in mice lacking *Spg7* and one allele of *Afg3l2* (Martinelli *et al.*, 2009) indicating that this is not the primary cause of neurodegeneration. This study revealed crucial functions of *m*-AAA proteases for the regulation of mitochondrial morphology suggesting dysfunctions of mitochondrial dynamics as the primary cause of the diseases. In fact, research suggests that many of the mitochondrial defects associated with HD, PD and AD could result, at least in part, from disruption of the fusion/fission mechanism indicating mitochondrial fragmentation as a hallmark of neurodegenerative diseases (Knott and Bossy-Wetzel, 2008).

But why are in particular neurons prone for mitochondrial dysfunctions? Neurons are highly specialized cells. They have a huge energy demand and extremely long processes with axons extending up to one meter in motor neurons, indicating that energy has to be transmitted across long distances. Finally, their major function is communication which suggests a tightly regulated signalling system that relies on balances of ions in synapses and efficient functioning of ion channels, receptors and pumps (Chan, 2006; Chen and Chan, 2006; Detmer and Chan, 2007; Knott and Bossy-Wetzel, 2008; Knott *et al.*, 2008). For instance, due to the extremely long axons, or to their remarkable dendritic tree Purkinje cells can be a preferential target when mitochondrial dynamics, transport, and function are even slightly perturbed. Interestingly, Purkinje cell mitochondria from mice lacking *Spg7* and one allele of *Afg3l2* were giant and contained swollen cristae (Martinelli *et al.*, 2009). This might be explained by a lack of mitochondrial fusion, and implies that dysfunctional giant mitochondria cannot restore their function by fusing and exchanging their contents with fully functional mitochondria (Navratil *et al.*, 2008). Martinelli *et al.* observed that mitochondria in these mice tend to lose mitochondrial DNA (Martinelli *et al.*, 2009) which is attributed as a secondary effect of the loss of fusion activity (Hoppins *et al.*, 2007).

Therefore, the observed phenotypes in HSP, SCA or CMT2A are presumably caused by a decreased fusion activity resulting in the loss of mtDNA and later to reduced OXPHOS activities. In addition, the compensatory mechanisms of OXPHOS might reduce with age thereby explaining the progressive disease pathogenesis (Bernard and Rossignol, 2008).

In conclusion, this study identified key functions of mammalian *m*-AAA protease in cell proliferation and mitochondrial morphogenesis. In addition, MICS1 was discovered to interact with mammalian *m*-AAA proteases suggesting that MICS1 might be a potential substrate or regulatory binding partner of the proteases. Moreover, the identification of MICS1 could contribute to the understanding of the observed phenotypes associated with mutations of *m*-AAA protease subunits in human and mice. The presence of swollen cristae in synaptic terminals of *Spg7^{-/-}* mice might be caused by an impaired function of MICS1. Although those cells might exhibit an increased resistance towards apoptosis, OXPHOS supercomplexes could be destabilized resulting in a reduced maximal respiratory capacity. This effect may also contribute to mitochondrial dysfunction especially in neuronal cells. However, the role of this interaction is yet unclear, therefore further experiments will aim to analyze the stability of MICS1 in cells expressing dominant negative mutant AFG3L2. Future experiments will also focus on putative signaling events which are involved in the maintenance of cell proliferation by mitochondrially localized proteases. Finally, the identification of the protease which cleaves OPA1 in an inducible manner might help to elucidate molecular details of the fusion process. This protease could be a therapeutic

target against diseases associated with dysfunctions in mitochondrial dynamics due to an impaired energy metabolism.

5. References

- Acehan, D., Y. Xu, D.L. Stokes, and M. Schlame. 2007. Comparison of lymphoblast mitochondria from normal subjects and patients with Barth syndrome using electron microscopic tomography. *Lab. Invest.* 87:40-8.
- Aggarwal, B.B. 2003. Signalling pathways of the TNF superfamily: a double-edged sword. *Nat. Rev. Immunol.* 3:745-56.
- Akiyama, Y. 1999. Self-processing of FtsH and its implication for the cleavage specificity of this protease. *Biochemistry.* 38:11693-11699.
- Aldridge, J.E., T. Horibe, and N.J. Hoogenraad. 2007. Discovery of genes activated by the mitochondrial unfolded protein response (mtUPR) and cognate promoter elements. *PLoS ONE.* 2:e874.
- Alexander, C., M. Votruba, U.E. Pesch, D.L. Thiselton, S. Mayer, A. Moore, M. Rodriguez, U. Kellner, B. Leo-Kottler, G. Auburger, et al. 2000. OPA1, encoding a dynamin-related GTPase, is mutated in autosomal dominant optic atrophy linked to chromosome 3q28. *Nat. Genet.* 26:211-215.
- Alley, M.C., D.A. Scudiero, A. Monks, M.L. Hursey, M.J. Czerwinski, D.L. Fine, B.J. Abbott, J.G. Mayo, R.H. Shoemaker, and M.R. Boyd. 1988. Feasibility of drug screening with panels of human tumor cell lines using a microculture tetrazolium assay. *Cancer Res.* 48:589-601.
- Amati-Bonneau, P., M.L. Valentino, P. Reynier, M.E. Gallardo, B. Bornstein, A. Boissiere, Y. Campos, H. Rivera, J.G. de la Aleja, R. Carroccia, et al. 2008. OPA1 mutations induce mitochondrial DNA instability and optic atrophy 'plus' phenotypes. *Brain.* 131:338-51.
- Amiott, E.A., P. Lott, J. Soto, P.B. Kang, J.M. McCaffery, S. DiMauro, E.D. Abel, K.M. Flanigan, V.H. Lawson, and J.M. Shaw. 2008. Mitochondrial fusion and function in Charcot-Marie-Tooth type 2A patient fibroblasts with mitofusin 2 mutations. *Exp. Neurol.* 211:115-27.
- Andrews, B.J., G.A. Proteau, L.G. Beatty, and P.D. Sadowski. 1985. The FLP recombinase of the 2 micron circle DNA of yeast: interaction with its target sequences. *Cell.* 40:795-803.
- Arlt, H., G. Steglich, R. Perryman, B. Guiard, W. Neupert, and T. Langer. 1998. The formation of respiratory chain complexes in mitochondria is under the proteolytic control of the *m*-AAA protease. *EMBO J.* 17:4837-4847.
- Arlt, H., R. Tauer, H. Feldmann, W. Neupert, and T. Langer. 1996. The YTA10-12-complex, an AAA protease with chaperone-like activity in the inner membrane of mitochondria. *Cell.* 85:875-885.
- Arnold, I., and T. Langer. 2002. Membrane protein degradation by AAA proteases in mitochondria. *Biochim. Biophys. Acta.* 1592:89-96.
- Atorino, L., L. Silvestri, M. Koppen, L. Cassina, A. Ballabio, R. Marconi, T. Langer, and G. Casari. 2003. Loss of *m*-AAA protease in mitochondria causes complex I deficiency and increased sensitivity to oxidative stress in hereditary spastic paraplegia. *J. Cell. Biol.* 163:777-787.
- Augustin, S. 2008. Struktur und Funktionsmechanismus der mitochondrialen *m*-AAA-Protease aus *S. cerevisiae*. Institute for Genetics. University of Cologne, Cologne.
- Augustin, S., M. Nolden, S. Müller, O. Hardt, I. Arnold, and T. Langer. 2005. Characterization of peptides released from mitochondria: evidence for constant proteolysis and peptide efflux. *J. Biol. Chem.* 280:2691-2699.

- Bai, X., D. Ma, A. Liu, X. Shen, Q.J. Wang, Y. Liu, and Y. Jiang. 2007. Rheb activates mTOR by antagonizing its endogenous inhibitor, FKBP38. *Science*. 318:977-980.
- Baker, T.A., and R.T. Sauer. 2006. ATP-dependent proteases of bacteria: recognition logic and operating principles. *Trends. Biochem. Sci.* 31:647-653.
- Balaban, R.S., S. Nemoto, and T. Finkel. 2005. Mitochondria, oxidants, and aging. *Cell*. 120:483-95.
- Banfi, S., M.T. Bassi, G. Andolfi, A. Marchitello, S. Zanotta, A. Ballabio, G. Casari, and B. Franco. 1999. Identification and characterization of AFG3L2, a novel paraplegin-related gene. *Genomics*. 59:51-8.
- Baricault, L., B. Segui, L. Guegan, A. Olichon, A. Valette, F. Larminat, and G. Lenaers. 2007. OPA1 cleavage depends on decreased mitochondrial ATP level and bivalent metals. *Exp Cell Res*. 313:3800-8.
- Barth, P.G., H.R. Scholte, J.A. Berden, J.M. Van der Klei-Van Moorsel, I.E. Luyt-Houwen, E.T. Van 't Veer-Korthof, J.J. Van der Harten, and M.A. Sobotka-Plojhar. 1983. An X-linked mitochondrial disease affecting cardiac muscle, skeletal muscle and neutrophil leucocytes. *J. Neurol. Sci.* 62:327-355.
- Bateman, J.M., M. Iacovino, P.S. Perlman, and R.A. Butow. 2002. Mitochondrial DNA instability mutants of the bifunctional protein Ilv5p have altered organization in mitochondria and are targeted for degradation by Hsp78 and the Pim1p protease. *J. Biol. Chem.* 277:47946-47953.
- Behrens, M., G. Michaelis, and E. Pratje. 1991. Mitochondrial inner membrane protease 1 of *Saccharomyces cerevisiae* shows sequence similarity to the *Escherichia coli* leader peptidase. *Mol. Gen. Genet.* 228:167-176.
- Benedetti, C., C.M. Haynes, Y. Yang, H.P. Harding, and D. Ron. 2006. Ubiquitin-like protein 5 positively regulates chaperone gene expression in the mitochondrial unfolded protein response. *Genetics*. 174:229-239.
- Bernard, G., and R. Rossignol. 2008. Ultrastructure of the mitochondrion and its bearing on function and Bioenergetics. *Antioxidants and Redox Signaling*. 10:1313-1342.
- Beyer, A. 1997. Sequence analysis of the AAA protein family. *Protein Sci.* 6:2043-2058.
- Blum, H., H. Beier, and H.J. Gross. 1987. Improved silver staining of plant proteins, RNA and DNA in polyacrylamide gels. *Electrophoresis*. 8:93-99.
- Boekema, E.J., and H.P. Braun. 2007. Supramolecular structure of the mitochondrial oxidative phosphorylation system. *J Biol. Chem.* 282:1-4.
- Bornhvd, C., F. Vogel, W. Neupert, and A.S. Reichert. 2006. Mitochondrial membrane potential is dependent on the oligomeric state of F₁F₀-ATP synthase supracomplexes. *J. Biol. Chem.* 281:13990-13998.
- Bossy-Wetzell, E., M.J. Barsoum, A. Godzik, R. Schwarzenbacher, and S.A. Lipton. 2003. Mitochondrial fission in apoptosis, neurodegeneration and aging. *Curr. Opin. Cell. Biol.* 15:706-716.
- Brand, M.D., L.F. Chien, E.K. Ainscow, D.F. Rolfe, and R.K. Porter. 1994. The causes and functions of mitochondrial proton leak. *Biochim. Biophys. Acta.* 1187:132-9.
- Brand, M.D., L.F. Chien, and P. DiDio. 1994. Experimental discrimination between proton leak and redox slip during mitochondrial electron transport. *Biochem. J.* 297 (Pt 1):27-9.
- Brandner, K., D.U. Mick, A.E. Frazier, R.D. Taylor, C. Meisinger, and P. Rehling. 2005. Taz1, an outer mitochondrial membrane protein, affects stability and assembly of inner membrane protein complexes: implications for Barth Syndrome. *Mol. Biol. Cell.* 16:5202-5214.

- Breckenridge, D.G., M. Stojanovic, R.C. Marcellus, and G.C. Shore. 2003. Caspase cleavage product of BAP31 induces mitochondrial fission through endoplasmic reticulum calcium signals, enhancing cytochrome c release to the cytosol. *J. Cell Biol.* 160:1115-1127.
- Broadley, S.A., and F.U. Hartl. 2008. Mitochondrial stress signaling: a pathway unfolds. *Trends Cell Biol.* 18:1-4.
- Browman, D.T., M.B. Hoegg, and S.M. Robbins. 2007. The SPFH domain-containing proteins: more than lipid raft markers. *Trends Cell Biol.* 17:394-402.
- Brown, G.C., P.L. Lakin-Thomas, and M.D. Brand. 1990. Control of respiration and oxidative phosphorylation in isolated rat liver cells. *Eur. J. Biochem.* 192:355-362.
- Brown, J.H., C. Cohen, and D.A. Parry. 1996. Heptad breaks in alpha-helical coiled coils: stutters and stammers. *Proteins.* 26:134-145.
- Brunner, M., C. Klaus, and W. Neupert. 1994. The mitochondrial processing peptidase. R.G. Landes Comp., Austin.
- Cagnoli, C., C. Mariotti, F. Taroni, M. Seri, A. Brussino, C. Michielotto, M. Grisoli, D. Di Bella, N. Migone, C. Gellera, et al. 2006. SCA28, a novel form of autosomal dominant cerebellar ataxia on chromosome 18p11.22-q11.2. *Brain.* 129:235-242.
- Cagnoli, C., G. Stevanin, A. Durr, P. Ribai, S. Forlani, A. Brussino, P. Pappi, L. Pugliese, M. Barberis, R.L. Margolis, et al. 2008. Mutations in AFG3L2 gene (SCA28) in autosomal dominant cerebellar ataxias. In Annual meeting of the American Society of Human Genetics, Philadelphia, Pennsylvania.
- Campuzano, V., L. Montermini, Y. Lutz, L. Cova, C. Hindelang, S. Jiralerspong, Y. Trottier, S.J. Kish, B. Faucheux, P. Trouillas, et al. 1997. Frataxin is reduced in Friedreich ataxia patients and is associated with mitochondrial membranes. *Hum. Mol. Genet.* 6:1771-1780.
- Campuzano, V., L. Montermini, M.D. Molto, L. Pianese, M. Cossee, F. Cavalcanti, E. Monros, F. Rodius, F. Duclos, A. Monticelli, et al. 1996. Friedreich's ataxia: autosomal recessive disease caused by an intronic GAA triplet repeat expansion. *Science.* 271:1423-1727.
- Carelli, V., C. La Morgia, L. Iommarini, R. Carroccia, M. Mattiazzi, S. Sangiorgi, S. Farne, A. Maresca, B. Foscari, L. Lanzi, et al. 2007. Mitochondrial optic neuropathies: how two genomes may kill the same cell type? *Biosci. Rep.* 27:173-84.
- Casari, G., M. De-Fusco, S. Ciarmatori, M. Zeviani, M. Mora, P. Fernandez, G. DeMichele, A. Filla, S. Coccozza, R. Marconi, et al. 1998. Spastic paraplegia and OXPHOS impairment caused by mutations in paraplegin, a nuclear-encoded mitochondrial metalloprotease. *Cell.* 93:973-983.
- Cereghetti, G.M., A. Stangherlin, O. Martins de Brito, C.R. Chang, C. Blackstone, P. Bernardi, and L. Scorrano. 2008. Dephosphorylation by calcineurin regulates translocation of Drp1 to mitochondria. *Proc. Natl. Acad. Sci. U S A.* 105:15803-15808.
- Cerveney, K.L., Y. Tamura, Z. Zhang, R.E. Jensen, and H. Sesaki. 2007. Regulation of mitochondrial fusion and division. *Trends Cell Biol.* 17:563-9.
- Chan, D.C. 2006. Mitochondria: dynamic organelles in disease, aging, and development. *Cell.* 125:1241-1252.
- Chang, C.R., and C. Blackstone. 2007. Cyclic AMP-dependent protein kinase phosphorylation of Drp1 regulates its GTPase activity and mitochondrial morphology. *J. Biol. Chem.* 282:21583-21587.
- Chen, H., and D.C. Chan. 2006. Critical dependence of neurons on mitochondrial dynamics. *Curr. Opin. Cell Biol.* 18:453-459.
- Chen, H., A. Chomyn, and D.C. Chan. 2005. Disruption of fusion results in mitochondrial heterogeneity and dysfunction. *J. Biol. Chem.* 280:26185-26192.

- Chen, H., S.A. Detmer, A.J. Ewald, E.E. Griffin, S.E. Fraser, and D.C. Chan. 2003. Mitofusins Mfn1 and Mfn2 coordinately regulate mitochondrial fusion and are essential for embryonic development. *J. Cell. Biol.* 160:189-200.
- Chen, H., J.M. McCaffery, and D.C. Chan. 2007. Mitochondrial fusion protects against neurodegeneration in the cerebellum. *Cell.* 130:548-62.
- Choi, S.Y., P. Huang, G.M. Jenkins, D.C. Chan, J. Schiller, and M.A. Frohman. 2006. A common lipid links Mfn-mediated mitochondrial fusion and SNARE-regulated exocytosis. *Nat Cell Biol.* 8:1255-62.
- Cipolat, S., O. Martins de Brito, B. Dal Zilio, and L. Scorrano. 2004. OPA1 requires mitofusin 1 to promote mitochondrial fusion. *Proc. Natl. Acad. Sci. U S A.* 101:15927-15932.
- Cipolat, S., T. Rudka, D. Hartmann, V. Costa, L. Serneels, K. Craessaerts, K. Metzger, C. Frezza, W. Annaert, L. D'Adamio, et al. 2006. Mitochondrial rhomboid PARL regulates cytochrome c release during apoptosis via OPA1-dependent cristae remodeling. *Cell.* 126:163-75.
- Claypool, S.M., P. Boonthung, J.M. McCaffery, J.A. Loo, and C.M. Koehler. 2008. The Cardiolipin Transacylase, Tafazzin, Associates with Two Distinct Respiratory Components Providing Insight into Barth Syndrome. *Mol. Biol. Cell.*
- Cohen, M.M., G.P. Leboucher, N. Livnat-Levanon, M.H. Glickman, and A.M. Weissman. 2008. Ubiquitin-Proteasome-dependent Degradation of a Mitofusin, a Critical Regulator of Mitochondrial Fusion. *Mol Biol Cell.* 19:2457-64.
- Coonrod, E.M., M.A. Karren, and J.M. Shaw. 2007. Ugo1p is a multipass transmembrane protein with a single carrier domain required for mitochondrial fusion. *Traffic.* 8:500-511.
- Cribbs, J.T., and S. Strack. 2007. Reversible phosphorylation of Drp1 by cyclic AMP-dependent protein kinase and calcineurin regulates mitochondrial fission and cell death. *EMBO Rep.* 8:939-944.
- Da Cruz, S., P.A. Parone, P. Gonzalo, W.V. Bienvenut, D. Tondera, A. Jourdain, M. Quadroni, and J.C. Martinou. 2008. SLP-2 interacts with prohibitins in the mitochondrial inner membrane and contributes to their stability. *Biochim. Biophys. Acta.* 1783:904-11.
- de Brito, O.M., and L. Scorrano. 2008. Mitofusin 2 tethers endoplasmic reticulum to mitochondria. *Nature.* in press.
- DeBerardinis, R.J., J.J. Lum, G. Hatzivassiliou, and C.B. Thompson. 2008. The biology of cancer: metabolic reprogramming fuels cell growth and proliferation. *Cell Metab.* 7:11-20.
- Delettre, C., J.M. Griffoin, J. Kaplan, H. Dollfus, B. Lorenz, L. Faivre, G. Lenaers, P. Belenguer, and C.P. Hamel. 2001. Mutation spectrum and splicing variants in the *OPA1* gene. *Hum. Genet.* 109:584-591.
- Delettre, C., G. Lenaers, J.M. Griffoin, N. Gigarel, C. Lorenzo, P. Belenguer, L. Pelloquin, J. Grosgeorge, C. Turc-Carel, E. Perret, et al. 2000. Nuclear gene *OPA1*, encoding a mitochondrial dynamin-related protein, is mutated in dominant optic atrophy. *Nat. Genet.* 26:207-210.
- Delettre, C., G. Lenaers, L. Pelloquin, P. Belenguer, and C.P. Hamel. 2002. OPA1 (Kjer type) dominant optic atrophy: a novel mitochondrial disease. *Mol. Genet. Metab.* 75:97-107.
- Dencher, N.A., M. Frenzel, N.H. Reifschneider, M. Sugawa, and F. Krause. 2007. Proteome alterations in rat mitochondria caused by aging. *Ann. N. Y. Acad. Sci.* 1100:291-298.
- Depienne, C., G. Stevanin, A. Brice, and A. Durr. 2007. Hereditary spastic paraplegias: an update. *Curr. Opin. Neurol.* 20:674-80.
- Detmer, S.A., and D.C. Chan. 2007. Complementation between mouse Mfn1 and Mfn2 protects mitochondrial fusion defects caused by CMT2A disease mutations. *J. Cell. Biol.* 176:405-414.

- Detmer, S.A., and D.C. Chan. 2007. Functions and dysfunctions of mitochondrial dynamics. *Nat. Rev. Mol. Cell Biol.* 8:870-9.
- Diaz, F., H. Fukui, S. Garcia, and C.T. Moraes. 2006. Cytochrome c oxidase is required for the assembly/stability of respiratory complex I in mouse fibroblasts. *Mol. Cell. Biol.* 26:4872-81.
- DiBella, D., F. Lazzaro, A. Brusco, G. Battaglia, P. A., A. Finardi, V. Fracasso, M. Plumari, C. Cagnoli, F. Tempia, et al. 2008. AFG3L2 mutations cause autosomal dominant ataxia SCA28 and reveal an essential role of the m-AAA AFG3L2 homocomplex in the cerebellum. *In Annual meeting of the American Society of Human Genetics, Philadelphia, Pennsylvania.*
- DiMauro, S. 2004. Mitochondrial diseases. *Biochim. Biophys. Acta.* 1658:80-88.
- DiMauro, S., and G. Davidzon. 2005. Mitochondrial DNA and disease. *Ann. Med.* 37:222-32.
- DiMauro, S., and E.A. Schon. 2003. Mitochondrial respiratory-chain diseases. *N. Engl. J. Med.* 348:2656-2668.
- DiMauro, S., and E.A. Schon. 2008. Mitochondrial disorders in the nervous system. *Annu. Rev. Neurosci.* 31:91-123.
- Dimmer, K.S., F. Navoni, A. Casarin, E. Trevisson, S. Ende, A. Winterpacht, L. Salviati, and L. Scorrano. 2008. LETM1, deleted in Wolf-Hirschhorn syndrome is required for normal mitochondrial morphology and cellular viability. *Hum. Mol. Genet.* 17:201-214.
- Dudkina, N.V., S. Sunderhaus, H.P. Braun, and E.J. Boekema. 2006. Characterization of dimeric ATP synthase and cristae membrane ultrastructure from *Saccharomyces* and *Polytomella* mitochondria. *FEBS Lett.* 580:3427-3432.
- Duvezin-Caubet, S., R. Jagasia, J. Wagener, S. Hofmann, A. Trifunovic, A. Hansson, A. Chomyn, M.F. Bauer, G. Attardi, N.G. Larsson, et al. 2006. Proteolytic processing of OPA1 links mitochondrial dysfunction to alterations in mitochondrial morphology. *J. Biol. Chem.* 281:37972-37979.
- Duvezin-Caubet, S., M. Koppen, J. Wagener, M. Zick, L. Israel, A. Bernacchia, R. Jagasia, E.I. Rugarli, A. Imhof, W. Neupert, et al. 2007. OPA1 processing reconstituted in yeast depends on the subunit composition of the m-AAA protease in mitochondria. *Mol. Biol. Cell.* 18:3582-90.
- Ehse, S. 2008. Functional analysis of mammalian m-AAA proteases. *In Institute for Genetics. University of Cologne, Cologne.*
- Eldering, E., W.J. Mackus, I.A. Derks, L.M. Evers, E. Beuling, P. Teeling, S.M. Lens, M.H. van Oers, and R.A. van Lier. 2004. Apoptosis via the B cell antigen receptor requires Bax translocation and involves mitochondrial depolarization, cytochrome C release, and caspase-9 activation. *Eur. J. Immunol.* 34:1950-60.
- Elleuch, N., C. Depienne, A. Benomar, A.M. Hernandez, X. Ferrer, B. Fontaine, D. Grid, C.M. Tallaksen, R. Zemmouri, G. Stevanin, et al. 2006. Mutation analysis of the paraplegin gene (SPG7) in patients with hereditary spastic paraplegia. *Neurology.* 66:654-659.
- Ende, S., M. Fuhry, S.J. Pak, B.U. Zabel, and A. Winterpacht. 1999. LETM1, a novel gene encoding a putative EF-hand Ca(2+)-binding protein, flanks the Wolf-Hirschhorn syndrome (WHS) critical region and is deleted in most WHS patients. *Genomics.* 60:218-225.
- Escobar-Henriques, M., B. Westermann, and T. Langer. 2006. Regulation of mitochondrial fusion by the F-box protein Mdm30 involves proteasome-independent turnover of Fzo1. *J. Cell Biol.* 173:645-650.
- Esser, K., E. Pratje, and G. Michaelis. 1996. SOM 1, a small new gene required for mitochondrial inner membrane peptidase function in *Saccharomyces cerevisiae*. *Mol. Gen. Genet.* 252:437-445.

- Esser, K., B. Tursun, M. Ingenhoven, G. Michaelis, and E. Pratje. 2002. A novel two-step mechanism for removal of a mitochondrial signal sequence involves the mAAA complex and the putative rhomboid protease Pcp1. *J. Mol. Biol.* 323:835-43.
- Falkenberg, M., N.G. Larsson, and C.M. Gustafsson. 2007. DNA replication and transcription in mammalian mitochondria. *Annu. Rev. Biochem.* 76:679-99.
- Farley, F.W., P. Soriano, L.S. Steffen, and S.M. Dymecki. 2000. Widespread recombinase expression using FLPeR (flipper) mice. *Genesis.* 28:106-110.
- Ferre, M., P. Amati-Bonneau, Y. Tourmen, Y. Malthiery, and P. Reynier. 2005. eOPA1: an online database for OPA1 mutations. *Hum. Mutat.* 25:423-428.
- Ferreirinha, F., A. Quattrini, M. Priozi, V. Valsecchi, G. Dina, V. Broccoli, A. Auricchio, F. Piemonte, G. Tozzi, L. Gaeta, et al. 2004. Axonal degeneration in paraplegin-deficient mice is associated with abnormal mitochondria and impairment of axonal transport. *J. Clin. Invest.* 113:231-242.
- Fichera, M., M. Lo Giudice, M. Falco, M. Sturnio, S. Amata, O. Calabrese, S. Bigoni, E. Calzolari, and M. Neri. 2004. Evidence of kinesin heavy chain (KIF5A) involvement in pure hereditary spastic paraplegia. *Neurology.* 63:1108-1110.
- Finkel, T. 2003. Oxidant signals and oxidative stress. *Curr. Opin. Cell Biol.* 15:247-254.
- Floyd, S., C. Favre, F.M. Lasorsa, M. Leahy, G. Trigiante, P. Stroebel, A. Marx, G. Loughran, K. O'Callaghan, C.M. Marobbio, et al. 2007. The insulin-like growth factor-I-mTOR signaling pathway induces the mitochondrial pyrimidine nucleotide carrier to promote cell growth. *Mol. Biol. Cell.* 18:3545-3555.
- Fontanesi, F., I.C. Soto, and A. Barrientos. 2008. Cytochrome c oxidase biogenesis: new levels of regulation. *IUBMB Life.* 60:557-568.
- Frank, S., B. Gaume, E.S. Bergmann-Leitner, W.W. Leitner, E.G. Robert, F. Catez, C.L. Smith, and R.J. Youle. 2001. The role of dynamin-related protein 1, a mediator of mitochondrial fission, in apoptosis. *Dev. Cell.* 1:515-525.
- Frey, T.G., C.W. Renken, and G.A. Perkins. 2002. Insight into mitochondrial structure and function from electron tomography. *Biochim. Biophys. Acta.* 1555:196-203.
- Frezza, C., S. Cipolat, O. Martins de Brito, M. Micaroni, G.V. Beznoussenko, T. Rudka, D. Bartoli, R.S. Polishuck, N.N. Danial, B. De Strooper, et al. 2006. OPA1 controls apoptotic cristae remodeling independently from mitochondrial fusion. *Cell.* 126:177-89.
- Fritz, S., D. Rapaport, E. Klanner, W. Neupert, and B. Westermann. 2001. Connection of the mitochondrial outer and inner membranes by Fzo1 is critical for organellar fusion. *J. Cell Biol.* 152:683-692.
- Fritz, S., N. Weinbach, and B. Westermann. 2003. Mdm30 is an F-box protein required for maintenance of fusion-competent mitochondria in yeast. *Mol. Biol. Cell.* 14:2303-2313.
- Gasteiger, E., C. Hoogland, A. Gattiker, S. Duvaud, M.R. Wilkins, R.D. Appel, and A. Bairoch. 2005. Protein Identification and Analysis Tools on the ExPASy Server. In *The Proteomics Protocols Handbook*. J.M. Walker, editor. Humana Press, Inc., Totowa, NJ. 571-607.
- Germain, M., J.P. Mathai, H.M. McBride, and G.C. Shore. 2005. Endoplasmic reticulum BIK initiates DRP1-regulated remodeling of mitochondrial cristae during apoptosis. *EMBO J.* 24:1546-1556.
- Gietz, R.D., and A. Sugino. 1988. New yeast-*Escherichia coli* shuttle vectors constructed with *in vitro* mutagenized yeast genes lacking six-base pair restriction sites. *Gene.* 74:527-534.
- Gilkerson, R.W., J.M. Selker, and R.A. Capaldi. 2003. The cristal membrane of mitochondria is the principal site of oxidative phosphorylation. *FEBS Lett.* 546:355-8.

- Giorgio, M., E. Migliaccio, F. Orsini, D. Paolucci, M. Moroni, C. Contursi, G. Pelliccia, L. Luzi, S. Minucci, M. Marcaccio, et al. 2005. Electron transfer between cytochrome c and p66Shc generates reactive oxygen species that trigger mitochondrial apoptosis. *Cell*. 122:221-233.
- Gonzalvez, F., Z.T. Schug, R.H. Houtkooper, E.D. MacKenzie, D.G. Brooks, R.J. Wanders, P.X. Petit, F.M. Vaz, and E. Gottlieb. 2008. Cardiolipin provides an essential activating platform for caspase-8 on mitochondria. *J. Cell Biol.* 183:681-696.
- Graef, M., and T. Langer. 2006. Substrate specific consequences of central pore mutations in the *i*-AAA protease Yme1 on substrate engagement. *J. Struct. Biol.* 151:101-108.
- Graef, M., G. Seewald, and T. Langer. 2007. Substrate recognition by AAA+ ATPases: distinct substrate binding modes in ATP-dependent protease Yme1 of the mitochondrial intermembrane space. *Mol. Cell Biol.* 27:2476-2485.
- Graham, F.L., J. Smiley, W.C. Russell, and R. Nairn. 1977. Characteristics of a human cell line transformed by DNA from human adenovirus type 5. *J. Gen. Virol.* 36:59-74.
- Green, D.R., and G. Kroemer. 2004. The pathophysiology of mitochondrial cell death. *Science*. 305:626-629.
- Griffin, E.E., and D.C. Chan. 2006. Domain interactions within Fzo1 oligomers are essential for mitochondrial fusion. *J. Biol. Chem.* 281:16599-16606.
- Griparic, L., T. Kanazawa, and A.M. van der Blik. 2007. Regulation of the mitochondrial dynamin-like protein Opa1 by proteolytic cleavage. *J Cell Biol.* 178:757-64.
- Griparic, L., N.N. van der Wel, I.J. Orozco, P.J. Peters, and A.M. van der Blik. 2004. Loss of the intermembrane space protein Mgm1/OPA1 induces swelling and localized constrictions along the lengths of mitochondria. *J. Biol. Chem.* 279:18792-18798.
- Guélin, E., M. Rep, and L.A. Grivell. 1996. Afg3p, a mitochondrial ATP-dependent metalloprotease, is involved in the degradation of mitochondrially-encoded Cox1, Cox3, Cob, Su6, Su8 and Su9 subunits of the inner membrane complexes III, IV and V. *FEBS Lett.* 381:42-46.
- Guillery, O., F. Malka, T. Landes, E. Guillou, C. Blackstone, A. Lombes, P. Belenguer, D. Arnoult, and M. Rojo. 2008. Metalloprotease-mediated OPA1 processing is modulated by the mitochondrial membrane potential. *Biol Cell.* 100:315-25.
- Hajek, P., A. Chomyn, and G. Attardi. 2007. Identification of a novel mitochondrial complex containing mitofusin 2 and stomatin-like protein 2. *J. Biol. Chem.* 282:5670-81.
- Hales, K.G., and M.T. Fuller. 1997. Developmentally regulated mitochondrial fusion mediated by a conserved, novel, predicted GTPase. *Cell.* 90:121-129.
- Hansen, J.J., A. Dürr, C.-R. I., C. Georgopoulos, D. Ang, M.N. Nielson, C.S. Davoine, A. Brice, B. Fontaine, N. Gregersen, et al. 2002. Hereditary spastic paraplegia SPG13 is associated with a mutation in the gene encoding the mitochondrial chaperonin Hsp60. *Am. J. Hum. Genet.* 70:1328-1332.
- Hanson, P.I., and S.W. Whiteheart. 2005. AAA+ proteins: have engine, will work. *Nat. Rev. Mol. Cell Biol.* 6:519-529.
- Harding, A.E. 1982. The clinical features and classification of the late onset autosomal dominant cerebellar ataxias. A study of 11 families, including descendants of the 'the Drew family of Walworth'. *Brain.* 105:1-28.
- Helms, V. 2002. Attraction within the membrane. Forces behind transmembrane protein folding and supramolecular complex assembly. *EMBO Rep.* 3:1133-8.
- Herlan, M., C. Bornhvd, K. Hell, W. Neupert, and A.S. Reichert. 2004. Alternative topogenesis of Mgm1 and mitochondrial morphology depend on ATP and a functional import motor. *J. Cell Biol.* 165:167-173.

- Herlan, M., F. Vogel, C. Bornhövd, W. Neupert, and A.S. Reichert. 2003. Processing of Mgm1 by the rhomboid-type protease Pcp1 is required for maintenance of mitochondrial morphology and of mitochondrial DNA. *J. Biol. Chem.* 278:27781-27788.
- Herman, C., S. Prakash, C.Z. Lu, A. Matouschek, and C.A. Gross. 2003. Lack of a robust unfoldase activity confers a unique level of substrate specificity to the universal AAA protease FtsH. *Mol. Cell.* 11:659-669.
- Hermann, G.J., J.W. Thatcher, J.P. Mills, K.G. Hales, M.T. Fuller, J. Nunnari, and J.M. Shaw. 1998. Mitochondrial fusion in yeast requires the transmembrane GTPase Fzo1p. *J. Cell Biol.* 143:359-373.
- Hersch, G.L., R.E. Burton, D.N. Bolon, T.A. Baker, and R.T. Sauer. 2005. Asymmetric interactions of ATP with the AAA+ ClpX6 unfoldase: allosteric control of a protein machine. *Cell.* 121:1017-1027.
- Hinshaw, J.E., and S.L. Schmid. 1995. Dynamin self-assembles into rings suggesting a mechanism for coated vesicle budding. *Nature.* 374:190-192.
- Hollenbeck, P.J., and W.M. Saxton. 2005. The axonal transport of mitochondria. *J. Cell Sci.* 118:5411-5419.
- Hoppins, S., J. Horner, C. Song, J.M. McCaffery, and J. Nunnari. 2009. Mitochondrial outer and inner membrane fusion requires a modified carrier protein. *J. Cell Biol.* 184:569-581.
- Hoppins, S., L. Lackner, and J. Nunnari. 2007. The machines that divide and fuse mitochondria. *Annu. Rev. Biochem.* 76:751-780.
- Hoppins, S., and J. Nunnari. 2009. The molecular mechanism of mitochondrial fusion. *Biochim. Biophys. Acta.* 1793:20-26.
- Ingerman, E., E.M. Perkins, M. Marino, J.A. Mears, J.M. McCaffery, J.E. Hinshaw, and J. Nunnari. 2005. Dnm1 forms spirals that are structurally tailored to fit mitochondria. *J. Cell Biol.* 170:1021-7.
- Isaya, G., D. Miklos, and R.A. Rollins. 1994. *MIP1*, a new yeast gene homologous to the rat mitochondrial intermediate peptidase gene, is required for oxidative metabolism in *Saccharomyces cerevisiae*. *Mol. Cell. Biol.* 14:5603-5616.
- Ishihara, N., Y. Eura, and K. Mihara. 2004. Mitofusin 1 and 2 play distinct roles in mitochondrial fusion reactions via GTPase activity. *J. Cell Sci.* 117:6535-46.
- Ishihara, N., Y. Fujita, T. Oka, and K. Mihara. 2006. Regulation of mitochondrial morphology through proteolytic cleavage of OPA1. *EMBO J.* 25:2966-2977.
- Ishihara, N., A. Jofuku, Y. Eura, and K. Mihara. 2003. Regulation of mitochondrial morphology by membrane potential, and DRP1-dependent division and FZO1-dependent fusion reaction in mammalian cells. *Biochem. Biophys. Res. Commun.* 301:891-898.
- Ito, K., and Y. Akiyama. 2005. Cellular functions, mechanism of action, and regulation of FtsH protease. *Annu. Rev. Microbiol.* 59:211-31.
- Ito, K., and Y. Akiyama. 2005. Cellular functions, mechanism of action, and regulation of FtsH protease. *Ann. Rev. Microbiol.* 59:211-231.
- Jahani-Asl, A., and R.S. Slack. 2007. The phosphorylation state of Drp1 determines cell fate. *EMBO Rep.* 8:912-913.
- James, D.I., P.A. Parone, Y. Mattenberger, and J.C. Martinou. 2003. hFis1, a novel component of the mammalian mitochondrial fission machinery. *J. Biol. Chem.* 278:36373-9.
- Jensen, R.E., A.E. Hobbs, K.L. Cerveny, and H. Sesaki. 2000. Yeast mitochondrial dynamics: fusion, division, segregation, and shape. *Microsc. Res. Tech.* 51:573-583.

- Jiang, F., M.T. Ryan, M. Schlame, M. Zhao, Z. Gu, M. Klingenberg, N. Pfanner, and M.L. Greenberg. 2000. Absence of cardiolipin in the *crd1* null mutant results in decreased mitochondrial membrane potential and reduced mitochondrial function. *J Biol. Chem.* 275:22387-94.
- John, G.B., Y. Shang, L. Li, C. Renken, C.A. Mannella, J.M. Selker, L. Rangell, M.J. Bennett, and J. Zha. 2005. The mitochondrial inner membrane protein mitofilin controls cristae morphology. *Mol. Biol. Cell.* 16:1543-1554.
- Johnston, P.B., R.N. Gaster, V.C. Smith, and R.C. Tripathi. 1979. A clinicopathologic study of autosomal dominant optic atrophy. *Am J Ophthalmol.* 88:868-75.
- Jones, R.G., D.R. Plas, S. Kubek, M. Buzzai, J. Mu, Y. Xu, M.J. Birnbaum, and C.B. Thompson. 2005. AMP-activated protein kinase induces a p53-dependent metabolic checkpoint. *Mol. Cell.* 18:283-293.
- Kalousek, F., G. Isaya, and L.E. Rosenberg. 1992. Rat liver mitochondrial intermediate peptidase (MIP): purification and initial characterization. *EMBO J.* 11:2803-2809.
- Kambacheld, M., S. Augustin, T. Tatsuta, S. Muller, and T. Langer. 2005. Role of the novel metallopeptidase Mop112 and saccharolysin for the complete degradation of proteins residing in different subcompartments of mitochondria. *J Biol Chem.* 280:20132-9.
- Karata, K., T. Inagawa, A.J. Wilkinson, T. Tatsuta, and T. Ogura. 1999. Dissecting the role of a conserved motif (the second region of homology) in the AAA family of ATPases. Site-directed mutagenesis of the ATP-dependent protease FtsH. *J. Biol. Chem.* 274:26225-26232.
- Karata, K., C.S. Verma, A.J. Wilkinson, and T. Ogura. 2001. Probing the mechanism of ATP hydrolysis and substrate translocation in the AAA protease FtsH by modelling and mutagenesis. *Mol. Microbiol.* 39:890-903.
- Karbowski, M., Y.J. Lee, B. Gaume, S.Y. Jeong, S. Frank, A. Nechushtan, A. Santel, M. Fuller, C.L. Smith, and R.J. Youle. 2002. Spatial and temporal association of Bax with mitochondrial fission sites, Drp1, and Mfn2 during apoptosis. *J. Cell Biol.* 159:931-938.
- Karbowski, M., A. Neutzner, and R.J. Youle. 2007. The mitochondrial E3 ubiquitin ligase MARCH5 is required for Drp1 dependent mitochondrial division. *J. Cell Biol.* 178:71-84.
- Karbowski, M., K.L. Norris, M.M. Cleland, S.Y. Jeong, and R.J. Youle. 2006. Role of Bax and Bak in mitochondrial morphogenesis. *Nature.* 441:658-662.
- Kent, C. 1995. Eukaryotic phospholipid biosynthesis. *Annu Rev Biochem.* 64:315-43.
- Kihara, A., Y. Akiyama, and K. Ito. 1996. A protease complex in the *Escherichia coli* plasma membrane: HflKC (HflA) forms a complex with FtsH (HflB), regulating its proteolytic activity against SecY. *EMBO J.* 15:6122-6131.
- Kihara, A., Y. Akiyama, and K. Ito. 1998. Different pathways for protein degradation by the FtsH/HflKC membrane-embedded protease complex: an implication from the interference by a mutant form of a new substrate protein, YccA. *J. Mol. Biol.* 279:175-188.
- Knott, A.B., and E. Bossy-Wetzel. 2008. Impairing the mitochondrial fission and fusion balance: a new mechanism of neurodegeneration. *Ann. N. Y. Acad. Sci.* 1147:283-292.
- Knott, A.B., G. Perkins, R. Schwarzenbacher, and E. Bossy-Wetzel. 2008. Mitochondrial fragmentation in neurodegeneration. *Nat. Rev. Neurosci.* 9:505-18.
- Kooijman, E.E., V. Chupin, B. de Kruijff, and K.N. Burger. 2003. Modulation of membrane curvature by phosphatidic acid and lysophosphatidic acid. *Traffic.* 4:162-174.
- Koppen, M., and T. Langer. 2007. Protein degradation within mitochondria: versatile activities of AAA proteases and other peptidases. *Crit. Rev. Biochem. Mol. Biol.* 42:221-42.

- Koppen, M., M.D. Metodiev, G. Casari, E.I. Rugarli, and T. Langer. 2007. Variable and Tissue-Specific Subunit Composition of Mitochondrial *m*-AAA Protease Complexes Linked to Hereditary Spastic Paraplegia. *Mol. Cell. Biol.* 27:758-767.
- Korbel, D., S. Wurth, M. Käser, and T. Langer. 2004. Membrane protein turnover by the *m*-AAA protease in mitochondria depends on the transmembrane domains of its subunits. *EMBO Rep.* 5:698-703.
- Kozlovsky, Y., L.V. Chernomordik, and M.M. Kozlov. 2002. Lipid intermediates in membrane fusion: formation, structure, and decay of hemifusion diaphragm. *Biophys. J.* 83:2634-2651.
- Krause, F. 2007. Oxidative phosphorylation supercomplexes in various eukaryotes: A paradigm change gains critical momentum. In *Complex I and Alternative Dehydrogenases*. M.I. González Siso, editor. Transworld Research Network. 179-213.
- Krause, F., C.Q. Scheckhuber, A. Werner, S. Rexroth, N.H. Reifschneider, N.A. Dencher, and H.D. Osiewacz. 2004. Supramolecular organization of cytochrome c oxidase- and alternative oxidase-dependent respiratory chains in the filamentous fungus *Podospora anserina*. *J. Biol. Chem.* 279:26453-61.
- Krause, F., and H. Seelert. 2008. Detection and analysis of protein-protein interactions of organellar and prokaryotic proteomes by blue native and colorless native gel electrophoresis. *Curr. Protoc. Protein Sci.* Chapter 19:Unit 19 18.
- Kremmidiotis, G., A.E. Gardner, C. Settasatian, A. Savoia, G.R. Sutherland, and D.F. Callen. 2001. Molecular and functional analyses of the human and mouse genes encoding AFG3L1, a mitochondrial metalloprotease homologous to the human spastic paraplegia protein. *Genomics.* 76:58-65.
- Kunau, W.H., A. Beyer, T. Franken, K. Gotte, M. Marzioch, J. Saidowsky, A. Skaletz-Rorowski, and F.F. Wiebel. 1993. Two complementary approaches to study peroxisome biogenesis in *Saccharomyces cerevisiae*: forward and reversed genetics. *Biochimie.* 75:209-224.
- Kuonen, D.R., P.J. Roberts, and I.R. Cottingham. 1986. Purification and analysis of mitochondrial membrane proteins on nondenaturing gradient polyacrylamide gels. *Anal Biochem.* 153:221-6.
- Kwon, M., S. Chong, S. Han, and K. Kim. 2003. Oxidative stresses elevate the expression of cytochrome c peroxidase in *Saccharomyces cerevisiae*. *Biochim. Biophys. Acta.* 1623:1-5.
- Lackner, L.L., and J.M. Nunnari. 2009. The molecular mechanism and cellular functions of mitochondrial division. *Biochim. Biophys. Acta.*
- Laemmli, U.K. 1970. Cleavage of structural proteins during the assembly of the head of bacteriophage T4. *Nature.* 227:680-5.
- Langer, T. 2000. AAA proteases - cellular machines for degrading membrane proteins. *Trends Biochem. Sci.* 25:207-256.
- Langer, T. 2000. AAA proteases: cellular machines for degrading membrane proteins. *Trends Biochem. Sci.* 25:247-51.
- Langer, T., M. Käser, C. Klanner, and K. Leonhard. 2001. AAA proteases of mitochondria: quality control of membrane proteins and regulatory functions during mitochondrial biogenesis. *Biochemical Society Transactions.* 29:431-436.
- Langer, T., K. Leonhard, H. Arlt, R. Perryman, and W. Neupert. 1997. Degradation of membrane proteins by AAA proteases in mitochondria. IOS Press, Amsterdam.
- Langhorst, M.F., A. Reuter, and C.A. Stuermer. 2005. Scaffolding microdomains and beyond: the function of reggie/flotillin proteins. *Cell Mol Life Sci.* 62:2228-40.

- Lee, Y.J., S.Y. Jeong, M. Karbowski, C.L. Smith, and R.J. Youle. 2004. Roles of the mammalian mitochondrial fission and fusion mediators Fis1, Drp1, and Opa1 in apoptosis. *Mol. Biol. Cell.* 15:5001-5011.
- Legesse-Miller, A., R.H. Massol, and T. Kirchhausen. 2003. Constriction and Dnm1p recruitment are distinct processes in mitochondrial fission. *Mol. Biol. Cell.* 14:1953-1963.
- Lemaire, C., P. Hamel, J. Velours, and G. Dujardin. 2000. Absence of the mitochondrial AAA protease Yme1p restores Fo-ATPase subunit accumulation in an *oxa1* deletion mutant of *Saccharomyces cerevisiae*. *J. Biol. Chem.* 275:23471-23475.
- Leonhard, K., B. Guiard, G. Pellechia, A. Tzagoloff, W. Neupert, and T. Langer. 2000. Membrane protein degradation by AAA proteases in mitochondria: extraction of substrates from either membrane surface. *Mol. Cell.* 5:629-638.
- Leonhard, K., J.M. Herrmann, R.A. Stuart, G. Mannhaupt, W. Neupert, and T. Langer. 1996. AAA proteases with catalytic sites on opposite membrane surfaces comprise a proteolytic system for the ATP-dependent degradation of inner membrane proteins in mitochondria. *EMBO J.* 15:4218-4229.
- Leonhard, K., A. Stiegler, W. Neupert, and T. Langer. 1999. Chaperone-like activity of the AAA domain of the yeast Yme1 AAA protease. *Nature.* 398:348-351.
- Lill, R., Z. Fekete, K. Sipos, and C. Rotte. 2005. Is there an answer? Why are mitochondria essential for life? *IUBMB Life.* 57:701-3.
- Lill, R., and U. Muhlenhoff. 2008. Maturation of iron-sulfur proteins in eukaryotes: mechanisms, connected processes, and diseases. *Annu Rev Biochem.* 77:669-700.
- Lin, M.T., and M.F. Beal. 2006. Mitochondrial dysfunction and oxidative stress in neurodegenerative diseases. *Nature.* 443:787-95.
- Lindquist, S. 1986. The heat-shock response. *Annu. Rev. Biochem.* 55:1151-1191.
- Liu, Z., L. Ho, and B. Bonning. 2007. Localization of a *Drosophila melanogaster* homolog of the putative juvenile hormone esterase binding protein of *Manduca sexta*. *Insect Biochem. Mol. Biol.* 37:155-163.
- Liu, Z., X. Li, J.R. Prasifka, R. Jurenka, and B.C. Bonning. 2008. Overexpression of *Drosophila* juvenile hormone esterase binding protein results in anti-JH effects and reduced pheromone abundance. *Gen. Comp. Endocrinol.* 156:164-172.
- Liu, Z., N. Pal, and B.C. Bonning. 2007. Potential ligands of DmP29, a putative juvenile hormone esterase binding protein of *Drosophila melanogaster*. *Insect Biochem. Mol. Biol.* 37:838-846.
- Loucks, F.A., E.K. Schroeder, A.E. Zommer, S. Hilger, N.A. Kelsey, R.J. Bouchard, C. Blackstone, J.L. Brewster, and D.A. Linseman. 2009. Caspases indirectly regulate cleavage of the mitochondrial fusion GTPase OPA1 in neurons undergoing apoptosis. *Brain Res.* 1250:63-74.
- Lowell, B.B., and G.I. Shulman. 2005. Mitochondrial dysfunction and type 2 diabetes. *Science.* 307:384-7.
- Lutter, P., H.E. Meyer, M. Langer, K. Witthohn, W. Dormeyer, A. Sickmann, and M. Bluggel. 2001. Investigation of charge variants of rViscumin by two-dimensional gel electrophoresis and mass spectrometry. *Electrophoresis.* 22:2888-2897.
- Ma, L., F.M. Vaz, Z. Gu, R.J. Wanders, and M.L. Greenberg. 2004. The human TAZ gene complements mitochondrial dysfunction in the yeast *taz1Delta* mutant. Implications for Barth syndrome. *J. Biol. Chem.* 279:44394-44399.
- Malka, F., O. Guillery, C. Cifuentes-Diaz, E. Guillou, P. Belenguer, A. Lombes, and M. Rojo. 2005. Separate fusion of outer and inner mitochondrial membranes. *EMBO Rep.* 6:853-9.

- Maltecca, F., A. Aghaie, D.G. Schroeder, L. Cassina, B.A. Taylor, S.J. Phillips, M. Malaguti, S. Previtali, J.L. Guenet, A. Quattrini, *et al.* 2008. The mitochondrial protease AFG3L2 is essential for axonal development. *J. Neurosci.* 28:2827-36.
- Mandal, S., P. Guptan, E. Owusu-Ansah, and U. Banerjee. 2005. Mitochondrial regulation of cell cycle progression during development as revealed by the tenured mutation in *Drosophila*. *Dev. Cell.* 9:843-854.
- Mannella, C.A. 2006. Structure and dynamics of the mitochondrial inner membrane cristae. *Biochim. Biophys. Acta.* 1763:542-8.
- Mannella, C.A., D.R. Pfeiffer, P.C. Bradshaw, Moraru, II, B. Slepchenko, L.M. Loew, C.E. Hsieh, K. Buttle, and M. Marko. 2001. Topology of the mitochondrial inner membrane: dynamics and bioenergetic implications. *IUBMB Life.* 52:93-100.
- Mariotti, C., A. Brusco, D. Di Bella, C. Cagnoli, M. Seri, C. Gellera, S. Di Donato, and F. Taroni. 2008. Spinocerebellar ataxia type 28: a novel autosomal dominant cerebellar ataxia characterized by slow progression and ophthalmoparesis. *Cerebellum.* 7:184-8.
- Marques, I., N.A. Dencher, A. Videira, and F. Krause. 2007. Supramolecular organization of the respiratory chain in *Neurospora crassa* mitochondria. *Eukaryot Cell.* 6:2391-405.
- Martin, A., T.A. Baker, and R.T. Sauer. 2008. Diverse pore loops of the AAA+ ClpX machine mediate unassisted and adaptor-dependent recognition of ssrA-tagged substrates. *Mol. Cell.* 29:441-50.
- Martinelli, P., V. La Mattina, A. Bernacchia, R. Magnoni, F. Cerri, G. Cox, A. Quattrini, G. Casari, and E. Rugarli. 2009. Genetic interaction between *m*-AAA protease isoenzymes reveals novel roles in cerebellar degeneration. *Hum. Mol. Genet.*
- Martinus, R.D., G.P. Garth, T.L. Webster, P. Cartwright, D.J. Naylor, P.B. Hoj, and N.J. Hoogenraad. 1996. Selective induction of mitochondrial chaperones in response to loss of the mitochondrial genome. *Eur. J. Biochem.* 240:98-103.
- McKenzie, M., M. Lazarou, D.R. Thorburn, and M.T. Ryan. 2006. Mitochondrial respiratory chain supercomplexes are destabilized in Barth Syndrome patients. *J. Mol. Biol.* 361:462-9.
- McQuibban, G.A., S. Saurya, and M. Freeman. 2003. Mitochondrial membrane remodelling regulated by a conserved rhomboid protease. *Nature.* 423:537-541.
- Meeusen, S., R. DeVay, J. Block, A. Cassidy-Stone, S. Wayson, J.M. McCaffery, and J. Nunnari. 2006. Mitochondrial inner-membrane fusion and crista maintenance requires the dynamin-related GTPase Mgm1. *Cell.* 127:383-395.
- Meeusen, S., J.M. McCaffery, and J. Nunnari. 2004. Mitochondrial fusion intermediates revealed in vitro. *Science.* 305:1747-1752.
- Meglei, G., and G.A. McQuibban. 2009. The Dynamin-Related Protein Mgm1p Assembles into Oligomers and Hydrolyzes GTP To Function in Mitochondrial Membrane Fusion (dagger). *Biochemistry.* 48:1774-1784.
- Merkwirth, C., S. Dargazanli, T. Tatsuta, S. Geimer, B. Lower, F.T. Wunderlich, J.C. von Kleist-Retzow, A. Waisman, B. Westermann, and T. Langer. 2008. Prohibitins control cell proliferation and apoptosis by regulating OPA1-dependent cristae morphogenesis in mitochondria. *Genes Dev.* 22:476-88.
- Merkwirth, C., and T. Langer. 2009. Prohibitin function within mitochondria: Essential roles for cell proliferation and cristae morphogenesis. *Biochim. Biophys. Acta.* 1793:27-32.
- Metodiev, M.D. 2005. Role of prohibitins for proteolysis in yeast and murine mitochondria. University of Cologne.

- Minauro-Sanmiguel, F., S. Wilkens, and J.J. Garcia. 2005. Structure of dimeric mitochondrial ATP synthase: novel F₀ bridging features and the structural basis of mitochondrial cristae biogenesis. *Proc. Natl. Acad. Sci. U S A.* 102:12356-12358.
- Mishra, S., L.C. Murphy, and L.J. Murphy. 2006. The prohibitins: emerging roles in diverse functions. *J. Cell. Mol. Med.* 10:353-63.
- Mogk, A., D. Dougan, J. Weibezahn, C. Schlieker, K. Turgay, and B. Bukau. 2004. Broad yet high substrate specificity: the challenge of AAA+ proteins. *J. Struct. Biol.* 146:90-98.
- Mogk, A., T. Haslberger, P. Tessarz, and B. Bukau. 2008. Common and specific mechanisms of AAA+ proteins involved in protein quality control. *Biochem. Soc. Trans.* 36:120-125.
- Mootha, V.K., J. Bunkenborg, J.V. Olsen, M. Hjerrild, J.R. Wisniewski, E. Stahl, M.S. Bolouri, H.N. Ray, S. Sihag, M. Kamal, et al. 2003. Integrated analysis of protein composition, tissue diversity, and gene regulation in mouse mitochondria. *Cell.* 115:629-40.
- Mozdy, A.D., J.M. McCaffery, and J.M. Shaw. 2000. Dnm1p GTPase-mediated mitochondrial fission is a multi-step process requiring the novel integral membrane component Fis1p. *J. Cell. Biol.* 151:367-380.
- Munnich, A., P. Rustin, A. Rotig, D. Chretien, J.P. Bonnefont, C. Nuttin, V. Cormier, A. Vassault, P. Parvy, J. Bardet, et al. 1992. Clinical aspects of mitochondrial disorders. *J. Inherit. Metab. Dis.* 15:448-55.
- Nakai, T., T. Yasuhara, Y. Fujiki, and A. Ohashi. 1995. Multiple genes, including a member of the AAA family, are essential for the degradation of unassembled subunit 2 of cytochrome c oxidase in yeast mitochondria. *Mol. Cell. Biol.* 15:4441-4452.
- Navratil, M., A. Terman, and E.A. Arriaga. 2008. Giant mitochondria do not fuse and exchange their contents with normal mitochondria. *Exp. Cell Res.* 314:164-172.
- Naylor, K., E. Ingerman, V. Okreglak, M. Marino, J.E. Hinshaw, and J. Nunnari. 2006. Mdv1 interacts with assembled dnm1 to promote mitochondrial division. *J. Biol. Chem.* 281:2177-2183.
- Nebauer, R., I. Schuiki, B. Kulterer, Z. Trajanoski, and G. Daum. 2007. The phosphatidylethanolamine level of yeast mitochondria is affected by the mitochondrial components Oxa1p and Yme1p. *FEBS J.* 274:6180-6190.
- Neuhoff, V., R. Stamm, I. Pardowitz, N. Arold, W. Ehrhardt, and D. Taube. 1990. Essential problems in quantification of proteins following colloidal staining with coomassie brilliant blue dyes in polyacrylamide gels, and their solution. *Electrophoresis.* 11:101-117.
- Neupert, W., and J.M. Herrmann. 2007. Translocation of proteins into mitochondria. *Annu. Rev. Biochem.* 76:723-49.
- Neutzner, A., and R.J. Youle. 2005. Instability of the mitofusin Fzo1 regulates mitochondrial morphology during the mating response of the yeast *Saccharomyces cerevisiae*. *J. Biol. Chem.* 280:18598-18603.
- Neuwald, A.F., L. Aravind, J.L. Spouge, and E.V. Koonin. 1999. AAA+: A class of chaperone-like ATPases associated with the assembly, operation, and disassembly of protein complexes. *Genome Res.* 9:27-43.
- Nicholls, D.G. 1974. The influence of respiration and ATP hydrolysis on the proton-electrochemical gradient across the inner membrane of rat-liver mitochondria as determined by ion distribution. *Eur. J. Biochem.* 50:305-15.
- Nicholson, D.W., A. Ali, N.A. Thornberry, J.P. Vaillancourt, C.K. Ding, M. Gallant, Y. Gareau, P.R. Griffin, M. Labelle, Y.A. Lazebnik, et al. 1995. Identification and inhibition of the ICE/CED-3 protease necessary for mammalian apoptosis. *Nature.* 376:37-43.

- Niederquell, M. 2008. Comparative gel-based analysis of mitochondrial proteomes in *Saccharomyces cerevisiae*. University of Cologne.
- Niemann, A., M. Ruegg, V. La Padula, A. Schenone, and U. Suter. 2005. Ganglioside-induced differentiation associated protein 1 is a regulator of the mitochondrial network: new implications for Charcot-Marie-Tooth disease. *J. Cell. Biol.* 170:1067-1078.
- Nijtmans, L.G., L. de Jong, M. Artal Sanz, P.J. Coates, J.A. Berden, J.W. Back, A.O. Muijsers, H. van der Spek, and L.A. Grivell. 2000. Prohibitins act as a membrane-bound chaperone for the stabilization of mitochondrial proteins. *EMBO J.* 19:2444-51.
- Nijtmans, L.G.J., M. Artal Sanz, L.A. Grivell, and P.J. Coates. 2002. The mitochondrial PHB complex: roles in mitochondrial respiratory complex assembly, ageing and degenerative disease. *Cell. Mol. Life Sci.* 59:143-155.
- Niwa, H., D. Tsuchiya, H. Makyio, M. Yoshida, and K. Morikawa. 2002. Hexameric ring structure of the ATPase domain of the membrane-integrated metalloprotease FtsH from *Thermus thermophilus* HB8. *Structure (Camb)*. 10:1415-1423.
- Nolden, M., S. Ehses, M. Koppen, A. Bernacchia, E.I. Rugarli, and T. Langer. 2005. The *m*-AAA protease defective in hereditary spastic paraplegia controls ribosome assembly in mitochondria. *Cell.* 123:277-289.
- Nolden, M., B. Kisters-Woike, T. Langer, and M. Graef. 2006. Quality control of proteins in the mitochondrion. *Topics in Current Genetics.* 16:119-147.
- Ogura, T., K. Inoue, T. Tatsuta, T. Suzaki, K. Karata, K. Young, L.-H. Su, C.A. Fierke, J.E. Jackman, C.R.H. Raetz, et al. 1999. Balanced biosynthesis of major membrane components through regulated degradation of the committed enzyme of lipid A biosynthesis by the AAA protease FtsH (HflB) in *Escherichia coli*. *Mol. Microbiol.* 31:833-844.
- Ogura, T., S.W. Whiteheart, and A.J. Wilkinson. 2004. Conserved arginine residues implicated in ATP hydrolysis, nucleotide-sensing, and inter-subunit interactions in AAA and AAA+ ATPases. *J. Struct. Biol.* 146:106-112.
- Ogura, T., and A.J. Wilkinson. 2001. AAA+ superfamily of ATPases: common structure-diverse function. *Genes to Cells.* 6:575-597.
- Oka, T., T. Sayano, S. Tamai, S. Yokota, H. Kato, G. Fujii, and K. Mihara. 2008. Identification of a novel protein MICS1 that is involved in maintenance of mitochondrial morphology and apoptotic release of cytochrome c. *Mol. Biol. Cell.* 19:2597-608.
- Olichon, A., L. Baricault, N. Gas, E. Guillou, A. Valette, P. Belenguer, and G. Lenaers. 2003. Loss of OPA1 perturbs the mitochondrial inner membrane structure and integrity, leading to cytochrome c release and apoptosis. *J. Biol. Chem.* 278:7743-7746.
- Olichon, A., G. Elachouri, L. Baricault, C. Delettre, P. Belenguer, and G. Lenaers. 2007. OPA1 alternate splicing uncouples an evolutionary conserved function in mitochondrial fusion from a vertebrate restricted function in apoptosis. *Cell Death Differ.* 14:682-92.
- Olichon, A., L.J. Emorine, E. Descoins, L. Pelloquin, L. Brichese, N. Gas, E. Guillou, C. Delettre, A. Valette, C.P. Hamel, et al. 2002. The human dynamin-related protein OPA1 is anchored to the mitochondrial inner membrane facing the inter-membrane space. *FEBS Lett.* 523:171-176.
- Oliver, F.J., G. de la Rubia, V. Rolli, M.C. Ruiz-Ruiz, G. de Murcia, and J.M. Murcia. 1998. Importance of poly(ADP-ribose) polymerase and its cleavage in apoptosis. Lesson from an uncleavable mutant. *J. Biol. Chem.* 273:33533-9.
- Osman, C., M. Haag, C. Potting, J. Rodenfels, P.V. Dip, F.T. Wieland, B. Brügger, B. Westermann, and T. Langer. 2009. The genetic interactome of prohibitins: coordinated control of cardiolipin and phosphatidylethanolamine by conserved regulators in mitochondria. *J. Cell Biol.*

- Otsuga, D., B.R. Keegan, E. Brisch, J.W. Thatcher, G.J. Hermann, W. Bleazard, and J.M. Shaw. 1998. The dynamin-related GTPase, Dnm1p, controls mitochondrial morphology in yeast. *J. Cell Biol.* 143:333-349.
- Pajic, A., R. Tauer, H. Feldmann, W. Neupert, and T. Langer. 1994. Yta10p is required for the ATP-dependent degradation of polypeptides in the inner membrane of mitochondria. *FEBS Lett.* 353:201-206.
- Pearce, D.A., and F. Sherman. 1995. Degradation of cytochrome oxidase subunits in mutants of yeast lacking cytochrome c and suppression of the degradation by mutation of *yme1*. *J. Biol. Chem.* 270:1-4.
- Perkins, D.N., D.J. Pappin, D.M. Creasy, and J.S. Cottrell. 1999. Probability-based protein identification by searching sequence databases using mass spectrometry data. *Electrophoresis.* 20:3551-3567.
- Petroski, M.D., and R.J. Deshaies. 2005. Function and regulation of cullin-RING ubiquitin ligases. *Nat. Rev. Mol. Cell Biol.* 6:9-20.
- Pfeiffer, K., V. Gohil, R.A. Stuart, C. Hunte, U. Brandt, M.L. Greenberg, and H. Schagger. 2003. Cardiolipin stabilizes respiratory chain supercomplexes. *J Biol Chem.* 278:52873-80.
- Piao, L., Y. Li, S.J. Kim, K.C. Sohn, K.J. Yang, K.A. Park, H.S. Byun, M. Won, J. Hong, G.M. Hur, et al. 2009. Regulation of OPA1-mediated mitochondrial fusion by leucine zipper/EF-hand-containing transmembrane protein-1 plays a role in apoptosis. *Cell. Signal.*
- Pinton, P., C. Giorgi, R. Siviero, E. Zecchini, and R. Rizzuto. 2008. Calcium and apoptosis: ER-mitochondria Ca²⁺ transfer in the control of apoptosis. *Oncogene.* 27:6407-18.
- Pinton, P., A. Rimessi, S. Marchi, F. Orsini, E. Migliaccio, M. Giorgio, C. Contursi, S. Minucci, F. Mantovani, M.R. Wieckowski, et al. 2007. Protein kinase C beta and prolyl isomerase 1 regulate mitochondrial effects of the life-span determinant p66Shc. *Science.* 315:659-663.
- Pinton, P., and R. Rizzuto. 2008. p66Shc, oxidative stress and aging: importing a lifespan determinant into mitochondria. *Cell Cycle.* 7:304-308.
- Piwko, W., and S. Jentsch. 2006. Proteasome-mediated protein processing by bidirectional degradation initiated from an internal site. *Nat. Struct. Mol. Biol.* 13:691-697.
- Praefcke, G.J., and H.T. McMahon. 2004. The dynamin superfamily: universal membrane tubulation and fission molecules? *Nat. Rev. Mol. Cell Biol.* 5:133-147.
- Rainey, R.N., J.D. Glavin, H.W. Chen, S.W. French, M.A. Teitell, and C.M. Koehler. 2006. A New Function in Translocation for the Mitochondrial *i*-AAA Protease Yme1: Import of Polynucleotide Phosphorylase into the Intermembrane Space. *Mol. Cell. Biol.* 26:8488-8497.
- Rais, I., M. Karas, and H. Schagger. 2004. Two-dimensional electrophoresis for the isolation of integral membrane proteins and mass spectrometric identification. *Proteomics.* 4:2567-71.
- Rak, M., X. Zeng, J.J. Briere, and A. Tzagoloff. 2009. Assembly of F₀ in *Saccharomyces cerevisiae*. *Biochim. Biophys. Acta.* 1793:108-116.
- Rapaport, D., M. Brunner, W. Neupert, and B. Westermann. 1998. Fzo1p is a mitochondrial outer membrane protein essential for the biogenesis of functional mitochondria in *Saccharomyces cerevisiae*. *J. Biol. Chem.* 273:20150-20155.
- Rawlings, N.D., and A.J. Barrett. 1995. Evolutionary families of metallopeptidases. *Methods Enzymol.* 248:183-228.
- Reichert, A.S., and W. Neupert. 2002. Contact sites between the outer and inner membrane of mitochondria-role in protein transport. *Biochim. Biophys. Acta.* 1592:41-9.

- Rojo, M., F. Legros, D. Chateau, and A. Lombes. 2002. Membrane topology and mitochondrial targeting of mitofusins, ubiquitous mammalian homologs of the transmembrane GTPase Fzo. *J. Cell Sci.* 115:1663-1674.
- Ron, D., and P. Walter. 2007. Signal integration in the endoplasmic reticulum unfolded protein response. *Nat. Rev. Mol. Cell Biol.* 8:519-529.
- Röttgers, K., N. Zufall, B. Guiard, and W. Voos. 2002. The ClpB homolog Hsp78 is required for the efficient degradation of proteins in the mitochondrial matrix. *J. Biol. Chem.* 277:45829-45837.
- Rouser, G., S. Fkeischer, and A. Yamamoto. 1970. Two dimensional thin layer chromatographic separation of polar lipids and determination of phospholipids by phosphorus analysis of spots. *Lipids.* 5:494-6.
- Rugarli, E.I., and T. Langer. 2006. Translating *m*-AAA protease function in mitochondria to hereditary spastic paraplegia. *Trends Mol. Med.* 12:262-269.
- Ryan, M.T., and N.J. Hoogenraad. 2007. Mitochondrial-nuclear communications. *Annu. Rev. Biochem.* 76:701-722.
- Salvioli, S., A. Ardizzoni, C. Franceschi, and A. Cossarizza. 1997. JC-1, but not DiOC6(3) or rhodamine 123, is a reliable fluorescent probe to assess delta psi changes in intact cells: implications for studies on mitochondrial functionality during apoptosis. *FEBS Lett.* 411:77-82.
- Santel, A., and M.T. Fuller. 2001. Control of mitochondrial morphology by a human mitofusin. *J Cell Sci.* 114:867-74.
- Santel, A., and M.T. Fuller. 2001. Control of mitochondrial morphology by a human mitofusin. *J. Cell Sci.* 114:867-874.
- Saraste, M. 1999. Oxidative phosphorylation at the fin de siècle. *Science.* 283:1488-1493.
- Saraste, M., P.R. Sibbald, and A. Wittinghofer. 1990. The P-loop - a common motif in ATP- and GTP-binding proteins. *Trends Biochem. Sci.* 15:430-434.
- Sarbassov, D.D., S.M. Ali, and D.M. Sabatini. 2005. Growing roles for the mTOR pathway. *Curr. Opin. Cell Biol.* 17:596-603.
- Satoh, M., T. Hamamoto, N. Seo, Y. Kagawa, and H. Endo. 2003. Differential sublocalization of the dynamin-related protein OPA1 isoforms in mitochondria. *Biochem. Biophys. Res. Commun.* 300:482-493.
- Satoh, M.S., and T. Lindahl. 1992. Role of poly(ADP-ribose) formation in DNA repair. *Nature.* 356:356-8.
- Sauer, R.T., D.N. Bolon, B.M. Burton, R.E. Burton, J.M. Flynn, R.A. Grant, G.L. Hersch, S.A. Joshi, J.A. Kenniston, I. Levchenko, et al. 2004. Sculpting the proteome with AAA(+) proteases and disassembly machines. *Cell.* 119:9-18.
- Schägger, H. 2001. Respiratory chain supercomplexes. *IUBMB Life.* 52:119-28.
- Schägger, H. 2002. Respiratory chain supercomplexes of mitochondria and bacteria. *Biochim. Biophys. Acta.* 1555:154-9.
- Schägger, H. 2006. Tricine-SDS-PAGE. *Nat Protoc.* 1:16-22.
- Schägger, H., W.A. Cramer, and G. von Jagow. 1994. Analysis of molecular masses and oligomeric states of protein complexes by blue native electrophoresis and isolation of membrane protein complexes by two-dimensional native electrophoresis. *Anal Biochem.* 217:220-30.

- Schägger, H., R. de Coo, M.F. Bauer, S. Hofmann, C. Godinot, and U. Brandt. 2004. Significance of respirasomes for the assembly/stability of human respiratory chain complex I. *J. Biol. Chem.* 279:36349-53.
- Schägger, H., and K. Pfeiffer. 2000. Supercomplexes in the respiratory chains of yeast and mammalian mitochondria. *EMBO J.* 19:1777-83.
- Schägger, H., and G. von Jagow. 1987. Tricine-sodium dodecyl sulfate-polyacrylamide gel electrophoresis for the separation of proteins in the range from 1 to 100 kDa. *Anal Biochem.* 166:368-79.
- Schägger, H., and G. von Jagow. 1991. Blue native electrophoresis for isolation of membrane protein complexes in enzymatically active form. *Anal. Biochem.* 199:223-231.
- Scheffler, I.E. 1999. Mitochondria. Wiley & Sons, New York.
- Schlame, M. 2008. Cardiolipin synthesis for the assembly of bacterial and mitochondrial membranes. *J. Lipid Res.* 49:1607-1620.
- Schlame, M., and M. Ren. 2006. Barth syndrome, a human disorder of cardiolipin metabolism. *FEBS Lett.* 580:5450-5455.
- Schlame, M., D. Rua, and M.L. Greenberg. 2000. The biosynthesis and functional role of cardiolipin. *Prog. Lipid Res.* 39:257-88.
- Schleicher, M., B.R. Shepherd, Y. Suarez, C. Fernandez-Hernando, J. Yu, Y. Pan, L.M. Acevedo, G.S. Shadel, and W.C. Sessa. 2008. Prohibitin-1 maintains the angiogenic capacity of endothelial cells by regulating mitochondrial function and senescence. *J. Cell Biol.* 180:101-12.
- Schlickum, S., A. Moghekar, J.C. Simpson, C. Steglich, R.J. O'Brien, A. Winterpacht, and S.U. Endele. 2004. LETM1, a gene deleted in Wolf-Hirschhorn syndrome, encodes an evolutionarily conserved mitochondrial protein. *Genomics.* 83:254-261.
- Schmidt, T.G., J. Koepke, R. Frank, and A. Skerra. 1996. Molecular interaction between the Strep-tag affinity peptide and its cognate target, streptavidin. *J. Mol. Biol.* 255:753-66.
- Schneider, H., T. Sollner, K. Dietmeier, C. Eckerskorn, F. Lottspeich, B. Trulzsch, W. Neupert, and N. Pfanner. 1991. Targeting of the master receptor MOM19 to mitochondria. *Science.* 254:1659-62.
- Schrader, M. 2006. Shared components of mitochondrial and peroxisomal division. *Biochim. Biophys. Acta.* 1763:531-541.
- Scorrano, L., M. Ashiya, K. Buttle, S. Weiler, S.A. Oakes, C.A. Mannella, and S.J. Korsmeyer. 2002. A distinct pathway remodels mitochondrial cristae and mobilizes cytochrome c during apoptosis. *Dev. Cell.* 2:55-67.
- Sesaki, H., C.D. Dunn, M. Iijima, K.A. Shepard, M.P. Yaffe, C.E. Machamer, and R.E. Jensen. 2006. Ups1p, a conserved intermembrane space protein, regulates mitochondrial shape and alternative topogenesis of Mgm1p. *J. Cell Biol.* 173:651-8.
- Sesaki, H., and R.E. Jensen. 2001. *UGO1* encodes an outer membrane protein required for mitochondrial fusion. *J. Cell Biol.* 152:1123-1134.
- Sesaki, H., and R.E. Jensen. 2004. Ugo1p links the Fzo1p and Mgm1p GTPases for mitochondrial fusion. *J. Biol. Chem.* 279:28298-28303.
- Sesaki, H., S.M. Southard, A.E. Hobbs, and R.E. Jensen. 2003. Cells lacking Pcp1p/Ugo2p, a rhomboid-like protease required for Mgm1p processing, lose mtDNA and mitochondrial structure in a Dnm1p-dependent manner, but remain competent for mitochondrial fusion. *Biochem. Biophys. Res. Commun.* 308:276-83.

- Sesaki, H., S.M. Southard, M.P. Yaffe, and R.E. Jensen. 2003. Mgm1p, a dynamin-related GTPase, is essential for fusion of the mitochondrial outer membrane. *Mol. Biol. Cell.* 14:2342-2356.
- Sever, S., A.B. Muhlberg, and S.L. Schmid. 1999. Impairment of dynamin's GAP domain stimulates receptor-mediated endocytosis. *Nature.* 398:481-486.
- Shah, Z.H., V. Migliosi, S.C. Miller, A. Wang, T.B. Friedman, and H.T. Jacobs. 1998. Chromosomal locations of three human nuclear genes (RPSM12, TUFM, and AFG3L1) specifying putative components of the mitochondrial gene expression apparatus. *Genomics.* 48:384-388.
- Shevchenko, A., H. Tomas, J. Havlis, J.V. Olsen, and M. Mann. 2006. In-gel digestion for mass spectrometric characterization of proteins and proteomes. *Nat. Protoc.* 1:2856-2860.
- Smeitink, J.A., M. Zeviani, D.M. Turnbull, and H.T. Jacobs. 2006. Mitochondrial medicine: A metabolic perspective on the pathology of oxidative phosphorylation disorders. *Cell Metab.* 3:9-13.
- Smirnova, E., D.L. Shurland, E.D. Newman-Smith, B. Pishvaee, and A.M. van der Bliek. 1999. A model for dynamin self-assembly based on binding between three different protein domains. *J. Biol. Chem.* 274:14942-7.
- Smirnova, E., D.L. Shurland, S.N. Ryazantsev, and A.M. van der Bliek. 1998. A human dynamin-related protein controls the distribution of mitochondria. *J. Cell Biol.* 143:351-8.
- Snider, J., and W.A. Houry. 2008. AAA+ proteins: diversity in function, similarity in structure. *Biochem. Soc. Trans.* 36:72-7.
- Song, Z., H. Chen, M. Fiket, C. Alexander, and D.C. Chan. 2007. OPA1 processing controls mitochondrial fusion and is regulated by mRNA splicing, membrane potential, and Yme1L. *J. Cell Biol.* 178:749-55.
- Steglich, G., W. Neupert, and T. Langer. 1999. Prohibitins regulate membrane protein degradation by the m-AAA protease in mitochondria. *Mol. Cell. Biol.* 19:3435-3442.
- Strauss, M., G. Hofhaus, R.R. Schroder, and W. Kuhlbrandt. 2008. Dimer ribbons of ATP synthase shape the inner mitochondrial membrane. *EMBO J.* 27:1154-1160.
- Suen, D.F., K.L. Norris, and R.J. Youle. 2008. Mitochondrial dynamics and apoptosis. *Genes Dev.* 22:1577-90.
- Sun, M.G., J. Williams, C. Munoz-Pinedo, G.A. Perkins, J.M. Brown, M.H. Ellisman, D.R. Green, and T.G. Frey. 2007. Correlated three-dimensional light and electron microscopy reveals transformation of mitochondria during apoptosis. *Nat. Cell Biol.* 9:1057-1065.
- Suppanz, I.E., C.A. Wurm, D. Wenzel, and S. Jakobs. 2009. The m-AAA protease processes cytochrome c peroxidase preferentially at the inner boundary membrane of mitochondria. *Mol. Biol. Cell.* 20:572-80.
- Svoboda, P. 2007. Off-targeting and other non-specific effects of RNAi experiments in mammalian cells. *Curr. Opin. Mol. Ther.* 9:248-257.
- Szabadkai, G., K. Bianchi, P. Várnai, D. De Stefani, M.R. Wieckowski, D. Cavagna, A.I. Nagy, T. Balla, and R. Rizutto. 2006. Chaperone-mediated coupling of endoplasmic reticulum and mitochondrial Ca²⁺ channels. *J. Cell. Biol.* 175:901-911.
- Taguchi, N., N. Ishihara, A. Jofuku, T. Oka, and K. Mihara. 2007. Mitotic phosphorylation of dynamin-related GTPase Drp1 participates in mitochondrial fission. *J. Biol. Chem.* 282:11521-11529.
- Tamai, S., H. Iida, S. Yokota, T. Sayano, S. Kiguchiya, N. Ishihara, J. Hayashi, K. Mihara, and T. Oka. 2008. Characterization of the mitochondrial protein LETM1, which maintains the mitochondrial tubular shapes and interacts with the AAA-ATPase BCS1L. *J. Cell. Sci.* 121:2588-2600.

- Tang, S., P.K. Le, S. Tse, D.C. Wallace, and T. Huang. 2009. Heterozygous Mutation of Opa1 in *Drosophila* Shortens Lifespan Mediated through Increased Reactive Oxygen Species Production. *PLoS ONE*. 4:e4492.
- Tatsuta, T., S. Augustin, M. Nolden, B. Friedrichs, and T. Langer. 2007. *m*-AAA protease-driven membrane dislocation allows intramembrane cleavage by rhomboid in mitochondria. *EMBO J*. 26:325-335.
- Tatsuta, T., and T. Langer. 2008. Quality control of mitochondria: protection against neurodegeneration and ageing. *EMBO J*. 27:306-14.
- Tatsuta, T., K. Model, and T. Langer. 2005. Formation of membrane-bound ring complexes by prohibitins in mitochondria. *Mol. Biol. Cell*. 16:248-259.
- Tavernarakis, N., M. Driscoll, and N.C. Kypides. 1999. The SPFH domain: implicated in regulating targeted protein turnover in stomatins and other membrane-associated proteins. *Trends Biochem. Sci*. 24:425-427.
- Tebbe, A., C. Klein, B. Bisle, F. Siedler, B. Scheffer, C. Garcia-Rizo, J. Wolfertz, V. Hickmann, F. Pfeiffer, and D. Oesterhelt. 2005. Analysis of the cytosolic proteome of *Halobacterium salinarum* and its implication for genome annotation. *Proteomics*. 5:168-79.
- Tewari, M., L.T. Quan, K. O'Rourke, S. Desnoyers, Z. Zeng, D.R. Beidler, G.G. Poirier, G.S. Salvesen, and V.M. Dixit. 1995. Yama/ CPP32 beta, a mammalian homolog of CED-3, is a CrmA-inhibitable protease that cleaves the death substrate poly(ADP-ribose) polymerase. *Cell*. 81:801-9.
- Thomas, P.E., D. Ryan, and W. Levin. 1976. An improved staining procedure for the detection of the peroxidase activity of cytochrome P-450 on sodium dodecyl sulfate polyacrylamide gels. *Anal Biochem*. 75:168-76.
- Thorsness, P.E., and T.D. Fox. 1993. Nuclear mutations in *Saccharomyces cerevisiae* that affect the escape of DNA from mitochondria to the nucleus. *Genetics*. 134:21-28.
- Tondera, D., S. Grandemange, A. Jourdain, M. Karbowski, Y. Mattenberger, H. S., S. Da Cruz, P. Clerc, I. Raschke, C. Merkwirth, et al. 2009. SLP-2 is required for stress-induced mitochondrial hyperfusion. *EMBO J*. 28:1589-1600.
- Torraco, A., F. Diaz, U.D. Vempati, and C.T. Moraes. 2009. Mouse models of oxidative phosphorylation defects: powerful tools to study the pathobiology of mitochondrial diseases. *Biochim. Biophys. Acta*. 1793:171-80.
- Towbin, H., T. Staehelin, and J. Gordon. 1979. Electrophoretic transfer of proteins from polyacrylamide gels to nitrocellulose sheets: procedure and some applications. *Proc. Natl. Acad. Sci. U S A*. 76:4350-4.
- Tusnady, G.E., and I. Simon. 2001. The HMMTOP transmembrane topology prediction server. *Bioinformatics*. 17:849-850.
- Twig, G., A. Elorza, A.J. Molina, H. Mohamed, J.D. Wikstrom, G. Walzer, L. Stiles, S.E. Haigh, S. Katz, G. Las, et al. 2008. Fission and selective fusion govern mitochondrial segregation and elimination by autophagy. *EMBO J*. 27:433-446.
- Twig, G., B. Hyde, and O.S. Shirihai. 2008. Mitochondrial fusion, fission and autophagy as a quality control axis: the bioenergetic view. *Biochim. Biophys. Acta*. 1777:1092-1097.
- Vaden, D.L., V.M. Gohil, Z. Gu, and M.L. Greenberg. 2005. Separation of yeast phospholipids using one-dimensional thin-layer chromatography. *Anal. Biochem*. 338:162-4.
- Vempati, U.D., X. Han, and C.T. Moraes. 2009. Lack of cytochrome c in mouse fibroblasts disrupts assembly/stability of respiratory complexes I and IV. *J. Biol. Chem*. 284:4383-91.

- Vereb, G., J. Szollosi, J. Matko, P. Nagy, T. Farkas, L. Vigh, L. Matyus, T.A. Waldmann, and S. Damjanovich. 2003. Dynamic, yet structured: The cell membrane three decades after the Singer-Nicolson model. *Proc. Natl. Acad. Sci. U S A.* 100:8053-8.
- Voelker, D.R. 1997. Phosphatidylserine decarboxylase. *Biochim. Biophys. Acta.* 1348:236-44.
- Vogel, F., C. Bornhvd, W. Neupert, and A.S. Reichert. 2006. Dynamic subcompartmentalization of the mitochondrial inner membrane. *J. Cell Biol.* 175:237-47.
- Vonck, J., and E. Schäfer. 2009. Supramolecular organization of protein complexes in the mitochondrial inner membrane. *Biochim. Biophys. Acta.* 1793:117-124.
- Wagner, I., H. Arlt, L. van Dyck, T. Langer, and W. Neupert. 1994. Molecular chaperones cooperate with PIM1 protease in the degradation of misfolded proteins in mitochondria. *EMBO J.* 13:5135-5145.
- Wagner, I., L. Van Dyck, A. Savel'ev, W. Neupert, and T. Langer. 1997. Autocatalytic processing of the ATP-dependent PIM1 protease: Crucial function of a pro-region for sorting to mitochondria. *EMBO J.* 16:7317-7325.
- Walker, J.E., M. Saraste, M.J. Runswick, and N.J. Gay. 1982. Distantly related sequences in the alpha- and beta-subunits of ATP synthase, myosin, kinases and other ATP-requiring enzymes and a common nucleotide binding fold. *EMBO J.* 1:945-51.
- Wallace, D.C. 2005. A mitochondrial paradigm of metabolic and degenerative diseases, aging, and cancer: a dawn for evolutionary medicine. *Annu. Rev. Genet.* 39:359-407.
- Wasiak, S., R. Zunino, and H.M. McBride. 2007. Bax/Bak promote sumoylation of DRP1 and its stable association with mitochondria during apoptotic cell death. *J. Cell Biol.* 177:439-450.
- Waterham, H.R., J. Koster, C.W. van Roermund, P.A. Mooyer, R.J. Wanders, and J.V. Leonard. 2007. A lethal defect of mitochondrial and peroxisomal fission. *N. Engl. J. Med.* 356:1736-1741.
- Weber, E.R., T. Hanekamp, and P.E. Thorsness. 1996. Biochemical and functional analysis of the *YME1* gene product, an ATP and zinc-dependent mitochondrial protease from *S. cerevisiae*. *Mol. Biol. Cell.* 7:307-317.
- Weber, E.R., R.S. Rooks, K.S. Shafer, J.W. Chase, and P.E. Thorsness. 1995. Mutations in the mitochondrial ATP synthase gamma subunit suppress a slow-growth phenotype of *yme1* yeast lacking mitochondrial DNA. *Genetics.* 140:435-442.
- Westermann, B. 2008. Molecular machinery of mitochondrial fusion and fission. *J. Biol. Chem.* 283:13501-5.
- White, K.E., V.J. Davies, V.E. Hogan, P.P. Nichols, D.M. Turnbull, and M. Votruba. 2009. OPA1 deficiency is associated with increased autophagy in retinal ganglion cells in a murine model of dominant optic atrophy. *Invest. Ophthalmol. Vis. Sci.*
- Willems, A.R., M. Schwab, and M. Tyers. 2004. A hitchhiker's guide to the cullin ubiquitin ligases: SCF and its kin. *Biochim. Biophys. Acta.* 1695:133-170.
- Wittig, I., R. Carozzo, F.M. Santorelli, and H. Schägger. 2006. Supercomplexes and subcomplexes of mitochondrial oxidative phosphorylation. *Biochim. Biophys. Acta.* Epub ahead of print.
- Wittig, I., and H. Schägger. 2009. Supramolecular organization of ATP synthase and respiratory chain in mitochondrial membranes. *Biochim. Biophys. Acta.*
- Wong, E.D., J.A. Wagner, S.W. Gorsich, J.M. McCaffery, J.M. Shaw, and J. Nunnari. 2000. The dynamin-related GTPase, Mgm1p, is an intermembrane space protein required for maintenance of fusion competent mitochondria. *J. Cell Biol.* 151:341-352.

- Wong, E.D., J.A. Wagner, S.V. Scott, V. Okreglak, T.J. Holewinski, A. Cassidy-Stone, and J. Nunnari. 2003. The intramitochondrial dynamin-related GTPase, Mgm1p, is a component of a protein complex that mediates mitochondrial fusion. *J. Cell. Biol.* 160:303-311.
- Wurm, C.A., and S. Jakobs. 2006. Differential protein distributions define two sub-compartments of the mitochondrial inner membrane in yeast. *FEBS Lett.* 580:5628-34.
- Xu, Y., J.J. Sutachan, H. Plesken, R.I. Kelley, and M. Schlame. 2005. Characterization of lymphoblast mitochondria from patients with Barth syndrome. *Lab. Invest.* 85:823-830.
- Yamaguchi, R., L. Lartigue, G. Perkins, R.T. Scott, A. Dixit, Y. Kushnareva, T. Kuwana, M.H. Ellisman, and D.D. Newmeyer. 2008. Opa1-mediated cristae opening is Bax/Bak and BH3 dependent, required for apoptosis, and independent of Bak oligomerization. *Mol. Cell.* 31:557-69.
- Yamaguchi, R., and G. Perkins. 2009. Dynamics of mitochondrial structure during apoptosis and the enigma of Opa1. *Biochim. Biophys. Acta.*
- Yoneda, T., C. Benedetti, F. Urano, S.G. Clark, H.P. Harding, and D. Ron. 2004. Compartment-specific perturbation of protein handling activates genes encoding mitochondrial chaperones. *J. Cell. Sci.* 117:4055-4066.
- Youle, R.J., and M. Karbowski. 2005. Mitochondrial fission in apoptosis. *Nat. Rev. Mol. Cell. Biol.* 6:657-63.
- Yu, A.Y., and W.A. Houry. 2007. ClpP: a distinctive family of cylindrical energy-dependent serine proteases. *FEBS Lett.* 581:3749-3757.
- Zhang, Y., and D.C. Chan. 2007. New insights into mitochondrial fusion. *FEBS Lett.* 581:2168-2173.
- Zhao, Q., J. Wang, I.V. Levichkin, S. Stasinopoulos, M.T. Ryan, and N.J. Hoogenraad. 2002. A mitochondrial specific stress response in mammalian cells. *EMBO J.* 21:4411-4419.
- Zick, M., R. Rabl, and A.S. Reichert. 2009. Cristae formation-linking ultrastructure and function of mitochondria. *Biochim. Biophys. Acta.* 1793:5-19.
- Zollino, M., R. Lecce, R. Fischetto, M. Murdolo, F. Faravelli, A. Selicorni, C. Butte, L. Memo, G. Capovilla, and G. Neri. 2003. Mapping the Wolf-Hirschhorn syndrome phenotype outside the currently accepted WHS critical region and defining a new critical region, WHSCR-2. *Am. J. Hum. Genet.* 72:590-597.
- Züchner, S., P. De Jonghe, A. Jordanova, K.G. Claey's, V. Guergueltcheva, S. Cherninkova, S.R. Hamilton, G. Van Stavern, K.M. Krajewski, J. Stajich, et al. 2006. Axonal neuropathy with optic atrophy is caused by mutations in mitofusin 2. *Ann. Neurol.* 59:276-281.
- Züchner, S., I.V. Mersiyanova, M. Muglia, N. Bissar-Tadmouri, J. Rochelle, E.L. Dadali, M. Zappia, E. Nelis, A. Patitucci, J. Senderek, et al. 2004. Mutations in the mitochondrial GTPase mitofusin 2 cause Charcot-Marie-Tooth neuropathy type 2A. *Nat. Genet.* 36:449-451.
- Züchner, S., and J.M. Vance. 2005. Emerging pathways for hereditary axonopathies. *J. Mol. Med.* 83:935-943.
- Zunino, R., A. Schauss, P. Rippstein, M. Andrade-Navarro, and H.M. McBride. 2007. The SUMO protease SENP5 is required to maintain mitochondrial morphology and function. *J. Cell Sci.* 120:1178-1188.

6. Appendix

6.1. List of abbreviations

AAA	ATPases associated with a variety of cellular activities
ADOA	autosomal dominant optic atrophy
ADP	adenosine diphosphate
Afg3l1	ATPase family gene 3-like 1
Afg3l2	murine ATPase family gene 3-like 2
AFG3L2	human ATPase family gene 3-like 2
AMP	adenosine monophosphate
APS	ammoniumperoxo disulfate
ATP	adenosine triphosphate
Bcl-2	B-cell lymphoma 2
BN	blue native
bp	base pairs
CCCP	carbonyl cyanide <i>m</i> -chlorophenyl hyradzone
cDNA	complementary DNA
CMT2A/4A	Charcot-Marie-Tooth type 2A/4A
CMV	cytomegalo-virus
CN	colorless/clear native
Co-IP	co-immunoprecipitation
C-terminal	carboxy-terminal
C-terminus	carboxy-terminus
DMSO	dimethyl sulfoxide
DNA	deoxyribonucleic acid
<i>E. coli</i>	<i>Escherichia coli</i>
EDTA	ethylene diamine tetraacetic acid
FITR293	FlpIn T-REx-293 cell line
g	gram
g	gravity
GTP	guanosine triphosphate
h	hour(s)
HA	hemagglutinin
HCl	hydrochloric acid
HEPES	N-2-hydroxyethylpiperazine-N'-2-ethanesulfonic-acid
His/6His/8His	histidine/hexa-histidine/octa-histidine
HSP	hereditary spastic paraplegia
IP	immunoprecipitation
JHEbp29	juvenile hormone esterase binding protein 29
K	potassium
kb	kilobase pairs
KCl	potassium chloride
kDa	kilodalton
KOH	potassium hydroxide
m	meter
M	molar (mole per liter)
MDa	megadalton
Mg	magnesium
μ g	microgram
μ l	microliter
mg	milligram

min	minute(s)
ml	milliliter
mM	millimolar
MOMP	mitochondrial outer membrane permeabilization
MPP	mitochondrial processing peptidase
mRNA	messenger RNA
mtDNA	mitochondrial DNA
MTS	mitochondrial targeting sequence
NaCl	sodium chloride
NAD ⁺	nicotinamide adenine dinucleotide (oxidized form)
NADH	nicotinamide adenine dinucleotide (reduced form)
nDNA	nuclear DNA
N-terminal	aminoterminal
N-terminus	amino terminus
Oligo	oligonucleotide
ORF	open reading frame
PA	phosphatic acid
PAGE	polyacrylamide gel electrophoresis
PBS	phosphate buffered saline
PC	phosphatidylcholine
PCR	polymerase chain reaction
PE	phosphatidylethanolamine
PG	phosphatidylglycerol
PI	phosphatidylinositol
PMSF	phenylmethylsulphonyl fluoride
PS	<i>m</i> -AAA protease subunit variant harboring mutation in the proteolytic site
PSe	phosphatidylserine
PVDF	polyvinylidene fluoride
RNA	ribonucleic acid
ROS	reactive oxygen species
rpm	rounds per minute
RT	room temperature
s	second(s)
SDS	sodium dodecyl sulfate
SPG	spastic paraplegia gene
SPG7	Spastic Paraplegia 7, human paraplegin
Sp _g 7	Spastic Paraplegia 7, murine paraplegin
SRH	second region of homology
TBS	Tris buffered saline
TIM	translocase of the inner membrane
TM	transmembrane domain
Tris	2-amino-2-(hydroxymethyl)-1,3-propanediol
U	unit(s)
V	volt(s)
v/v	volume per volume
w/v	weight per volume
WB	<i>m</i> -AAA protease subunit variant harboring mutation in the Walker B motif within the ATPase domain
WT	wild type

6.2. Mass spectrometric analysis

Bands from 1D and 2D gels were subjected to a gel digestion according to (Shevchenko *et al.*, 2006) with slight modifications. MS analyses were performed using a MALDI-TOFTOF instrument (4800 *Plus*, Applied Biosystems) and α -cyano-4-hydroxycinnamic acid as matrix. Proteins were identified comparing the NCBI.nr-protein sequence database of *Homo sapiens* (human) with the MALDI-MS spectra of tryptic peptides by using the MOWSE algorithm as implemented in the MS search engine MASCOT (Matrix Science, London, UK) (Perkins *et al.*, 1999). The analyses were performed at the Proteomics Mass Spectrometry Facility of the CECAD (Cologne – Excellent in Aging Research) by Dr. rer. nat. Tobias Lamkemeyer.

Results are depicted in the following tables. Abbreviations in the tables: Acc No, accession number; MW_{pred} , predicted mass; MW_{exp} , experimental mass; MW_{theor} , theoretical mass corresponding to the mass of mature proteins (containing the mitochondrial targeting sequences); $MW_{theor+tags}$, theoretical mass including epitope tags [predicted with the ProtParam tool (Gasteiger *et al.*, 2005)]; Seq-cov, sequence coverage; No PMF, number of matched masses.

Table 5: MASCOT results of AFG3L2 precursor (Figure 18 B).

Acc No	MW_{pred} [kDa]	MW_{exp} [kDa]	MW_{theor} [kDa]	$MW_{theor+tags}$ [kDa]	Score*	Seq-cov [%]	No PMF
Q9Y4W6	88.528	~85	88.584	89.407	136	32	30

Matched peptides of AFG3L2 precursor shown in **Bold Red**.

```

1 MAHRCLRLW RGGCWPRGLQ QLLVPGGVGP GEQPCLRTLY RFVTTQARAS
51 RNSLLTDIIA AYQRFCSRPP KGFKEYFPNG KNGKKASEPK EVMGEKKESK
101 PAATTRSSGG GGGGGGKRG KKDDSHWWSR FQKGDIPWDD KDFRMFFLWT
151 ALFWGGVMFY LLLKRSGREI TWKDFVNNYL SKGVVDRLEV VNKRFVRVTF
201 TPGKTPVDGQ YVWFNIGSVD TFERNLETLQ QELGIEGENR VPVYIAESD
251 GSFLLSMLPT VLIIAFLLYT IRRGPAGIGR TGRGMGGLFS VGETTAKVLK
301 DEIDVKFKDV AGCEEAKLEI MEFVNFLKNP KQYQDLGAKI PKGAILTGPP
351 GTGKTLLAKA TAGEANVPFI TVSGSEFLEM FVGVGPARVR DLFALARKNA
401 PCILFIDEID AVGRKRGRGN FGGQSEQENT LNQLLVEMDG FNTTTNVVIL
451 AGTNRPDILD PALLRPGRFD RQIFIGPPDI KGRASIFKVH LRPLKLDSTL
501 EKDKLARKLA SLTPGFSGAD VANVCNEAAL IAARHLSDSI NQKHFEQAIE
551 RVIGGLEKKT QVLQPEEKKT VAYHEAGHAV AGWYLEHADP LLKVSIIIPRG
601 KGLGYAQYLP KEQYLYTKEQ LLDRMCMTLG GRVSEEIFFG RITGAQDDL
651 RKVTQSAYAQ IVQFGMNEKV GQISFDLPRQ GDMVLEKPYS EATARLIDDE
701 VRILINDAYK RTVALLTEKK ADVEKVALLL LEKEVLDKND MVELLGPRPF
751 AEKSTYEEFV EGTGSLDEDT SLPEGLKDOWN KEREKEKEEP PGEKVAN

```

Table 6: MASCOT results of AFG3L2 (Figure 18 B).

Acc No	MW _{pred} [kDa]	MW _{exp} [kDa]	MW _{theor} [kDa]	MW _{theo+tags} [kDa]	Score*	Seq-cov [%]	No PMF
EAX01551	84.392	~ 75	88.584	89.407	126	26	24

Matched peptides of AFG3L2 shown in **Bold Red**.

1 LYRFVTTQAR ASRNSLLTDI IAAYQRFCSR PPKGFEKYFP NGKNGKKASE
 51 PKEVMGEKKE SKPAATTRSS GGGGGGGGKR GGK**KDDSHWW SR**FQK**GDIPW**
 101 **DDKDFR**MFFL WTALFWGGVM FYLLLKRSGR **EITWKDFVNN YLSK**GVVDRL
 151 EVVNRKRVV TFTP GKTPVD GQYVWFNIGS VDTFERN**LET LQOELGIEGE**
 201 **NRVPV**YIAE SDGSFLLSML PTVLIIAFL YTI**R**RG**PAGI GR**TGRGM**GGL**
 251 **FSVGETTAKV** LKDEIDVKFK DVAGCEEAKL EIMEFVNF**LK NPKQYQDLGA**
 301 KIPKGAILTG PPGTGKTLA KATAGEANVP FITVSGSEFL EMFVGVGPAR
 351 **VRDLFALARK** NAPCILFIDE IDAVGRKRGR GNFGGQSEQE NTLNQLLVEM
 401 DGFNTTTNVV ILAGTNRPI LDPALLRPGR FDR**QIFIGPP DIKGR**ASIFK
 451 **VHLRPLKIDS TLEK**DKLARK LASLTPGFSG ADVANVCNEA ALIAARHLSD
 501 SINQK**HFEQA IERV**IGGLEK KTQVLQPEEK KTVAYHEAGH AVAGWYLEHA
 551 DPLLKVSIIIP RGK**GLGYAQY LPKEQYLYTK EQLLDR**MCMT LGGR**VSEEIF**
 601 **FGRIT**TGAQD DLR**KVTQ**SAY **AQIVQFGMNE KVGQISFDLP RQGD**MVLEKP
 651 **YSEATAR**LID DEVR**ILLINDA YKR**TVALLTE KKADVEKVAL LLEKEVLDK
 701 NDMVELLGR PFAEKSTYEE FVEGTGSLDE DTSLPEGLKD WNKEREKEKE
 751 EPPGEKVAN

Table 7: MASCOT results of MICS1 (Figure 18 A).

Acc No	MW _{pred} [kDa]	MW _{exp} [kDa]	MW _{theor} [kDa]	MW _{theo+tags} [kDa]	Score*	Seq-cov [%]	No PMF
CAH72661	35.259	~ 28	35.282	-	101	51	16

Matched peptides of MICS1 shown in **Bold Red**.

1 MLAARLVCLR TLPSRVFHPA FTKASPVVKN SITKNQWLLT PSREYATKTR
 51 IGIRRGRT**QO ELKEAALEPS MEKIFKIDQM GR**WVAGGAI EK**AVIWPQYV**
 101 **KDRIHSTYMY LAGSIGLTAL SAIAISRTPV LMNFMMRGSW VTIGVTFAAM**
 151 **VGAGMLVRSI PYDQSPGPKH** LAWLLHSGVM GAVVAPL**TIL GG**PLLIR**AAW**
 201 **YTAGIVGGLS TVAMCAPSEK** FLNMGAPLGV GLGLV**FVSSL GSM**FLPPTTV
 251 AGATLYSVAM YGGLVLF**SMF LLYDTQKVIK RAEVSPMYGV QKYDPINSML**
 301 **SIYMDTLNIF MRVATMLATG GNR**KK

Table 8: MASCOT results of MAIP1 (Figure 18 A).

Acc No	MW _{pred} [kDa]	MW _{exp} [kDa]	MW _{theor} [kDa]	MW _{theo+tags} [kDa]	Score*	Seq-cov [%]	No PMF
Q8WWC4	32.524	~ 25	32.545	-	91	50	12

Matched peptides of MAIP1 shown in **Bold Red**.

1 MALAARLLPQ FLHSRSLPCG AVRLR**TPAVA EVR**LPSATLC YFCRCRLGLG
 51 AALFPRSARA LAASALPAQG SRWPVLSSPG LPAAFASFPA CPQRSYSTEE
 101 KPQQHQK**TKM IVLGFSNPIN WVR**TRIK**AFI IWAYFDKEFS I**TEFSE**GAQO**
 151 **AFAHVSKLLS QCKFDLLEEL VAK**EVLHALK EKVTSLPDNH **KNALAA**NIDE
 201 **IVFTSTGDIS IYYDEKGRKE VNILMCFWYL TSANIPSETL RGASV**FQV**KL**
 251 GNQNVETK**QL LSAS**YEF**QRE FTQGVKPDWT IAR**IEH**SKLL E**

Table 9: MASCOT results of PHB1 (Figure 18 A).

Acc No	MW _{pred} [kDa]	MW _{exp} [kDa]	MW _{theor} [kDa]	MW _{theo+tags} [kDa]	Score*	Seq-cov [%]	No PMF
NP_002625	29.787	~ 30	32.972	-	239	86	22

Matched peptides of prohibitin 1 shown in **Bold Red**

1 MAAKVFESIG **KFGLALAVAG GVN**SALY**NV DAGHRA**VIFD **RFRGVQ**DIVV
 51 **GEGTHFLIPW VQKPIIFDCR** SRPR**NV**VI**T GSKDLQ**NVNI **TLRILFRP**VA
 101 **SQLPRIFTSI GEDYDERVLP** **SITTEILK**SV VAR**FDAGELI TQRE**LVSR**QV**
 151 **SDDLTERAAT FGLILDDVSL** **THLTFGKEFT EAVEAKQVAQ** **QEAERAR**FVV
 201 EKAEQQK**AA IISAEG**SKA **AELIAN**SLAT **AGDGLIELRK** **LEAAEDIAYQ**
 251 **LSRSRNITYL PAGQSVLLQL** **PQ**

Table 10: MASCOT results of PHB2 (Figure 18 A).

Acc No	MW _{pred} [kDa]	MW _{exp} [kDa]	MW _{theor} [kDa]	MW _{theo+tags} [kDa]	Score*	Seq-cov [%]	No PMF
NP_009204	33.276	~ 32	33296.3	-	234	82	28

Matched peptides of prohibitin 2 shown in **Bold Red**

1 MAQNL**KDLAG RLPAGPR**GMG TALK**LLL**GAG **AVAYGVRESV** **FTVEGGHRAI**
 51 **FFNRIGGVQQ DTILA**EGLHF **RIPWFQYPII** YDIR**ARPRKI** **SSPTGSKDLQ**
 101 **MVNISLRVLS RPNAQELPSM** **YQRLGLDYEE RVLPSIVNEV** **LKS**SV**AKFNA**
 151 **SQLITQRAQV SLLIRRE**ELTE **RAKDFSLILD DVAITELSFS** **REYTA**AVEAK
 201 **QVAQQEAQRA QFLVEKAKQE** **QRQKIVQ**AEG **EAEAAKMLGE** **ALSKNPGYIK**
 251 L**RKIRAAQNI SKTIATSQNR** **IYLTADNLVL NLQDES**FTRG **SDSLIK**GKK

Search Parameters

Type of search:	Peptide Mass Fingerprint
Enzyme:	trypsin
Variable modifications:	oxidation (M)
Mass values:	monoisotopic
Protein mass:	unrestricted
Peptide mass Tolerance:	± 50 ppm
Peptide charge state:	1+
Max missed cleavages:	1
(*)	Protein score is $-10 \cdot \log(P)$, where P is the probability that the observed match is a random event. Protein scores greater than 66 are significant ($p < 0.05$).

6.3. Protein sequence analysis

All sequence alignments were generated by the ClustalW program. Accession numbers used were the following:

FtsH (<i>Thermus thermophilus</i>)	BAA96090
Yta12 (<i>Saccharomyces cerevisiae</i>)	CAA56953
Yta10 (<i>Saccharomyces cerevisiae</i>)	NP_013807
Spg7 (<i>Mus musculus</i>)	AAN03852
Afg3l2 (<i>Mus musculus</i>)	Q8JZQ2
Afg3l1 (<i>Mus musculus</i>)	NP_473411
SPG7 (<i>Homo sapiens</i>)	Q9UQ90
AFG3L2 (<i>Homo sapiens</i>)	NP_006787
MICS1 (<i>Homo sapiens</i>)	NP_055209
YccA (<i>Escherichia coli</i>)	P0AAC6
C2ORF47/MAIP1 (<i>Homo sapiens</i>)	Q8WWC4
JHEbp29 (<i>Drosophila melanogaster</i>)	AAF47306

6.3.1. m-AAA proteases

Table 11: Sequence identities/similarities of human compared to other m-AAA protease subunits.

-	Yta10	Yta12	Afg3l2	Afg3l1	Spg7
AFG3L2	46% / 57%	44% / 55%	92% / 94%	69% / 78%	39% / 51%
SPG7	39% / 52%	37% / 50%	39% / 51%	38% / 51%	87% / 91%

	1	50
FtsH (Th. th.)	(1) -----	-----
Yta12 (S. c.)	(1) ---MLLSWSRIATKVVRRPVRFRSYY-CLTHIKSLHTQYRLNRLQENK	
Yta10 (S. c.)	(1) -----MMWQRYARGAPRS-----LTSLSFGK	
Spg7 (M. m.)	(1) --MAAALLLRCLRPPEPRPRRLWGLLSGRGPGPLSSGAGARRPYAARGT	
Afg3l2 (M. m.)	(1) MAHRCLLWSRGGCR-RCLPPLLVP--CCLGPDRRPCLRTLTYQYATVQT	
Afg3l1 (M. m.)	(1) ---MLRLVGAAGSRALWPFSLWRCGCAGSGGTVWSSVRACGIALOG	
SPG7 (H. s.)	(1) --MAVLLILLRALRCPGPPRPLWGPAPAWSPGFPARPGRGRPYMASRP	
AFG3L2 (H. s.)	(1) MAHRCRLWGRGGCWPRRLQQLLVP---CGVGPGEQPCLRTLTYRFVITDA	
	51	100
FtsH (Th. th.)	(1) -----	-----
Yta12 (S. c.)	(47) SGNKEDNEDAKLNKEIPTDEEVEAIRKQVEKYIEQTKNNTIPANWKEQ	
Yta10 (S. c.)	(23) AS-----RISTVKPVLRSRMPVHQRILQTLISGLATRNTIHRSTQIR	
Spg7 (M. m.)	(49) PV-----GPAANGGHAPOSLRLRLTSPFEGISGLLLKQHIVP	
Afg3l2 (M. m.)	(48) ASSRR-----SLLRDVIAAYQFCSRPPKGFKEYFPNGKNGK	
Afg3l1 (M. m.)	(48) HLGRC-----QQLALQGKITSFSPRLYSKPPRCFEKFFKNNKNRK	
SPG7 (H. s.)	(49) PG-----DLAENGGRALQSLQLRLTPTFEINGLLKQHLVQ	
AFG3L2 (H. s.)	(48) RASRN-----SLLTDLIAAYQFCSRPPKGFKEYFPNGKNGK	

		101		150	
FtsH (Th. th.)	(1)	-----	-----	-----	
Yta12 (S. c.)	(97)	KRKIDESIRRL	EDAVLKQESNRIQ	EEERKEK-----EEENGPSKAKSNR	
Yta10 (S. c.)	(63)	S-----	FHISWTRLNENRPNK-----	EGEGKNNGNKDN	
Spg7 (M. m.)	(87)	NAVR-----	LWPLSGSTLYFN	TSRMKQKNK-----DNK--PKGKTPE	
Afg312 (M. m.)	(85)	KASE-----	-----PKEAVG	EKKKEPQPSGPQ-PSGAGGGGKRRG	
Afg311 (M. m.)	(89)	SAS-----	PGNSVPPKKEPK-----	NAGPGGGGNRGG	
SPG7 (H. s.)	(87)	NPVR-----	LWQLLGGTFYFN	TSRLKQKNK-----EKDK--SKGKAPE	
AFG3L2 (H. s.)	(85)	KASE-----	-----PKEVMG	EKKKESKPAATTRSSGGGGGGKRRG	
		151		200	
FtsH (Th. th.)	(1)	-----	-----	-----MPRAPFSILALVGLA	
Yta12 (S. c.)	(140)	TKEQGYFE	GNNSRNIPPPPPPPPKP	FLNDPS-NPVSKNVNLFQIGLTFE	
Yta10 (S. c.)	(92)	SNKE---	DGKDKRNE-----	FGSLSEYFRSKEFANTMFTITIGFTII	
Spg7 (M. m.)	(123)	DDEE---	E-KRRKER-----	EDQMY-RERLRTLFTIALVMSLL	
Afg312 (M. m.)	(120)	KKEDSHW	WSRFQKGD-----	F-PWDDKDFRMYFLWLTALFWGGVMY	
Afg311 (M. m.)	(117)	KGDDFPW	WRMQKGE-----	F-PWDDKDFRSLAVLGAAGVAGFLYF	
SPG7 (H. s.)	(123)	EDEE---	E-FRRRER-----	DLQMY-RERLRTLLVIAVMSLL	
AFG3L2 (H. s.)	(121)	KKDDSHW	WSRFQKGD-----	I-PWDDKDFRMFFLWLTALFWGGVMY	
		201		250	
FtsH (Th. th.)	(17)	FLAWP	SASRGTVGAPSGT	VNYTTFLEDLKA	GRVKEVVRAGDTRIQGVLE
Yta12 (S. c.)	(189)	LLSFLDLLNS	SLEEQS-EITWQDF	REKLAKGYAKLI	VVNKSMVKVMLN
Yta10 (S. c.)	(130)	ETLLTPSSN	SGDSDSNRVLTF	QDFKTKYLEKGLV	SKIYVNVKFLVEAELV
Spg7 (M. m.)	(156)	NLSLTS---	-----GGSTSW	ADFFVNEMLAKGEV	QVRVQVPESDVVEVYL
Afg312 (M. m.)	(160)	FVFKSS---	-----GREITW	KDFVNNYLSKGV	VDRLEVVNKRFRVRFIT
Afg311 (M. m.)	(157)	YFRDP-----	-----GKEITW	KHFVQYYLARGL	VDRLEVVNKQFVRVIPV
SPG7 (H. s.)	(156)	NALSLS---	-----GGSTSW	NDFFVHEMLAKGEV	QVRVQVPESDVVEVYL
AFG3L2 (H. s.)	(161)	LLLKRS---	-----GREITW	KDFVNNYLSKGV	VDRLEVVNKRFRVRFIT
		251		300	
FtsH (Th. th.)	(67)	DG-----	-----SAFTTYA	ASPPLNATLEGW	MARGVSVRVEPP
Yta12 (S. c.)	(238)	DNGKNQADN	-YGRNFYVFTIGS	IDSFEHKLQKAQ	DELIDKDFRIPVLYV
Yta10 (S. c.)	(180)	N-----	TKQVSEFTIGS	VDFEEDQIQD	LLNIPPRDRIPIKYI
Spg7 (M. m.)	(197)	HPGAVVFG	RPRALMYRMQ	VANIDKFEKLR	AAEDELNIEAKDRIPVSYK
Afg312 (M. m.)	(201)	PKGTP-----	VDGOYVWFN	IGSVDTFERN	LETLOQELGIEGENRVPVYI
Afg311 (M. m.)	(197)	PGTT-----	SERFVWFN	IGSVDTFERN	LESAQWELGIEPTNQAAVYI
SPG7 (H. s.)	(197)	HPGAVVFG	RPRALMYRMQ	VANIDKFEKLR	AAEDELNIEAKDRIPVSYK
AFG3L2 (H. s.)	(202)	PKGTP-----	VDGOYVWFN	IGSVDTFERN	LETLOQELGIEGENRVPVYI
		301		350	
FtsH (Th. th.)	(100)	QGQNALG	FLWPLLLVGLL	LIGALYFYSR	NG-----RAGPSDSA
Yta12 (S. c.)	(287)	QEGNWAK	AMFQILPTVLM	IAGTIWITRRS	-----AQAGGS
Yta10 (S. c.)	(220)	ERSSPF	FLFPFLPTI	ILLGGLYFITR	KINSSPPNANGGGGGLGGMFNV
Spg7 (M. m.)	(247)	RTGFFGN	ALYALGMTA	GLAILWYVFL	LAG----MTGREGG-FSAFNQL
Afg312 (M. m.)	(246)	AESD-GS	FLSMLPTVLI	IAFLLYTIRG	----PACIGRTGRMGGLFSV
Afg311 (M. m.)	(240)	TESD-GS	FLRSLVPTL	VLVSILLYAM	RRG----PMGTGRGGRG-GGLFSV
SPG7 (H. s.)	(247)	RTGFFGN	ALYALYVGMT	AGLAILWYVFL	LAG----MTGREGG-FSAFNQL
AFG3L2 (H. s.)	(247)	AESD-GS	FLSMLPTVLI	IAFLLYTIRG	----PACIGRTGRMGGLFSV
		351		400	
FtsH (Th. th.)	(140)	TKSRARV	LTEAPKVT--	FKDVAGAE	EAKLEIKIVEFLKNE
Yta12 (S. c.)	(330)	SRSKAK	KFNTEIDV	KIKFDVAGC	DEAKLEIMEFVSLKNE
Yta10 (S. c.)	(270)	GKSRAK	LFNKETDI	KISFNVAGC	DEAKLEIMEFVHFLKNE
Spg7 (M. m.)	(291)	KMARFT	LVDGKTG	KGSFQDV	AGMHEAKLEVREFV
Afg312 (M. m.)	(291)	GETTAK	VLKDEIDV	K--FKDVAGC	EEAKLEIMEFVNF
Afg311 (M. m.)	(284)	GETTAK	LKNNIDV	R--FADVAGC	EEAKLEIMEFVNF
SPG7 (H. s.)	(291)	KMARFT	LVDGKM	GKGSFQDV	AGMHEAKLEVREFV
AFG3L2 (H. s.)	(292)	GETTAK	VLKDEIDV	K--FKDVAGC	EEAKLEIMEFVNF
		401		450	
FtsH (Th. th.)	(188)	IPKGVLL	VGGPPGVG	TKTHLARA	VAGEARVPFITASGSD
Yta12 (S. c.)	(380)	IPRGAIL	SGPPGTG	TKTLAKA	TAGEAGVPFYFVSGSEF
Yta10 (S. c.)	(320)	IPRGAIL	SGPPGTG	TKTLAKA	TAGEANVPFLSVSGSEF
Spg7 (M. m.)	(341)	VPKGAIL	LGPPCG	TKTLAKA	VATEAQPFLAMAGPEF
Afg312 (M. m.)	(339)	IPKGAILT	GPPGTG	TKTLAKA	TAGEANVPFITVSGSEF
Afg311 (M. m.)	(332)	IPKGAILT	GPPGTG	TKTLAKA	TAGEANVPFITVNGSEF
SPG7 (H. s.)	(341)	VPKGAIL	LGPPCG	TKTLAKA	VATEAQPFLAMAGPEF
AFG3L2 (H. s.)	(340)	IPKGAILT	GPPGTG	TKTLAKA	TAGEANVPFITVSGSEF

		Walker B	
		451	500
FtsH (Th. th.)	(238)	RDLFETAKRHAPCIVFIDEIDAVGRKRGSG--VGGNDEEREC	TLNQLLVE
Yta12 (S. c.)	(430)	RDLFKTARENAPSIVFIDEIDAIGKARQKG-NFSGANDERE	NTLNQMLVE
Yta10 (S. c.)	(370)	RDLFTQARSMAPSIIFIDEIDAIGKERGKGGALGGANDERE	ATLNQLLVE
Spg7 (M. m.)	(391)	RSLFKEARARAPCIVYIDEIDAVGKKRSTSMGFSNTEE-	EOTLNQLLVE
Afg312 (M. m.)	(389)	RDLFALARKNAPCILFIDEIDAVGRKRG-NFGGQSEQ-	ENTLNQLLVE
Afg311 (M. m.)	(382)	RDMFAMARKHAPCILFIDEIDAIGRKRGRG-HLGGQSEQ-	ENTLNQMLVE
SPG7 (H. s.)	(391)	RSLFKEARARAPCIVYIDEIDAVGKKRSTTMSGFSNTEE-	EOTLNQLLVE
AFG3L2 (H. s.)	(390)	RDLFALARKNAPCILFIDEIDAVGRKRG-NFGGQSEQ-	ENTLNQLLVE
		501	550
FtsH (Th. th.)	(286)	MDGF EKDIAIVVMAATNRPDILDPALLRPGRFDRQIAIDAFD	VVKGREQITL
Yta12 (S. c.)	(479)	MDGFTPADHVVVLAGTNRPDILDKALLRPGRFDRHINIDKPE	LEGRKATIF
Yta10 (S. c.)	(420)	MDGFTTSDQVVVLAGTNRPDVLDNALMRPGFRDRHIQIDSE	FDVNGRQQIY
Spg7 (M. m.)	(440)	MDGMGTTDHSVIVLASTNRADVLDNALMRPGFRDRHVFIDLE	FTIQERREIF
Afg312 (M. m.)	(437)	MDGFNTTINVVILAGTNRPDILDPALLRPGFRDRQIFIGP	EDIKGRASIF
Afg311 (M. m.)	(430)	MDGFN SSTNVVLAGTNRPDILDPALTRPGFRDRQIYIGP	EDIKGRSSIF
SPG7 (H. s.)	(440)	MDGMGTTDHSVIVLASTNRADILDGALMRPGRDRHVFIDLE	FTIQERREIF
AFG3L2 (H. s.)	(438)	MDGFNTTINVVILAGTNRPDILDPALLRPGFRDRQIFIGP	EDIKGRASIF
		551	600
FtsH (Th. th.)	(336)	RIHARGKPLAEDVDLAL-----AKRT-PGFVGADLENILNEA	ALLAARE
Yta12 (S. c.)	(529)	AVHLHHLKILAGEIFDLKN----RLAALTPGFSGADIANVCNEA	ALLAARS
Yta10 (S. c.)	(470)	LVHLKRLNLDPLLTDMMNLSGKLATLTPGFTGADIANACNEA	ALLAARH
Spg7 (M. m.)	(490)	EQHLKGLKITQPSSFYSQ----RLAELTPGFSGADIANICNEA	ALLHAARE
Afg312 (M. m.)	(487)	KVHLRPLKLD SALEKDKLAR--KLASLTPGFSGADVAVNCNEA	ALLAARH
Afg311 (M. m.)	(480)	KVHLRPLKLDGSLSKDALSR--KLAALTPGFTGADISVNCNEA	ALLAARH
SPG7 (H. s.)	(490)	EQHLKSLKITQSSTFYSQ----RLAELTPGFSGADIANICNEA	ALLHAARE
AFG3L2 (H. s.)	(488)	KVHLRPLKLDSTLEKDKLAR--KLASLTPGFSGADVAVNCNEA	ALLAARH
		proteolytic site	
		601	650
FtsH (Th. th.)	(380)	GRRKITMKDLEEAADRVMMGPAKKSLLVLSFRDRRITAYHEA	GHALAAHFL
Yta12 (S. c.)	(575)	DEDAVKLNHFEOAIERVIGGVERKSKLLSPEEKKVVAYHEA	GHAVCGWYL
Yta10 (S. c.)	(520)	NDPYLTIHHEFOAIERVIGLEKKTIVLSKEEKRSVAYHEA	GHAVCGWYL
Spg7 (M. m.)	(536)	GHTSVHTFNFEYAVERVLAGTAKKSKILLSKEEQRVAVFHE	SGHALVGMWL
Afg312 (M. m.)	(535)	LSDAINEKHFEEOAIERVIGGLEKKTQVLOPEEKKTVAYHEA	GHAVAGWYL
Afg311 (M. m.)	(528)	LSPSVQERHFEEOAIERVIGGLEKKTQVLOPESEKTTVAYHEA	GHAVVCGWYL
SPG7 (H. s.)	(536)	GHTSVHTLNFEYAVERVLAGTAKKSKILLSKEEQKVAVFHE	SGHALVGMWL
AFG3L2 (H. s.)	(536)	LSDSINQKHFEEOAIERVIGGLEKKTQVLOPEEKKTVAYHEA	GHAVAGWYL
		651	700
FtsH (Th. th.)	(430)	EHADGVHKVTIVPRGR-ALGFMMPPRREMLHWSRKRILLQILA	VALAGRAA
Yta12 (S. c.)	(625)	KYADPLLKVSIIPRGGALGYAQYLPGLIFLLTEQQLKDRMTMS	LGGRVS
Yta10 (S. c.)	(570)	KYADPLLKVSIIPRGGALGYAQYLPDQYLISEEQFRHRMIMAL	LGGRVS
Spg7 (M. m.)	(586)	EHTEAVMKVSIAPRTNALGFSQLPRDQYIFLTKEQLFERMCMA	LGGRAS
Afg312 (M. m.)	(585)	EHADPLLKVSIIPRGG-GLGYAQYLPKEQYLYTKEQLDRMCM	TLGGRVS
Afg311 (M. m.)	(578)	EHADPLLKVSIIPRGG-GLGYAQYLPREQFLYTREQLFORMCM	MLGGRVA
SPG7 (H. s.)	(586)	EHTEAVMKVSIIPRTNALGFALQMLPRDQHLFTKEQLFERMCMA	LGGRAS
AFG3L2 (H. s.)	(586)	EHADPLLKVSIIPRGG-GLGYAQYLPKEQYLYTKEQLDRMCM	TLGGRAS
		701	750
FtsH (Th. th.)	(479)	EEIVFDDVTTGAENDFRQATELARRMTTEWGMHPEFGPVAY	AVREDTYLG
Yta12 (S. c.)	(675)	EELHFPSVTSGASDDFKKVTSMATAMVTELGMSDKIGWVNY	QKRD----D
Yta10 (S. c.)	(620)	EELHFPSVTSGAHDDFKKVTQMANAMVTSLGMSPKIGYLSFD	QNDG---N
Spg7 (M. m.)	(636)	EAISFSRVTSGAQDDLKRVTRIAYSMVKQFGMAPSIGPVSEF	PEAQEG-LM
Afg312 (M. m.)	(634)	EEIFFGRIITGAQDDLKRVTSAYAQIVQFGMNEKVGQISFD	LPRQ--GD
Afg311 (M. m.)	(627)	EQLFFGQITGAQDDLKRVTSAYAQIVQFGMSEKLGQVSFD	FPRQ--GE
SPG7 (H. s.)	(636)	EALSFNEVTSGAQDDLKRVTRIAYSMVKQFGMAPGIGPISF	PEAQEG-LM
AFG3L2 (H. s.)	(635)	EEIFFGRIITGAQDDLKRVTSAYAQIVQFGMNEKVGQISFD	LPRQ--GD

		751		800
FtsH (Th. th.)	(529)	G Y D V R Q Y S E E T A K R I D E A V R L I E E Q Y Q R V K A L L L E K R E V L E R V A E T L L E		
Yta12 (S. c.)	(721)	S D L T K P F S D E T G D I I D S E V Y R I V Q E C H D R C T K L L K E K A F D V E K I A Q V L L K		
Yta10 (S. c.)	(667)	F K V N K P F S N K T A R T I D L E V K S I V D D A H F A C T E L L T K N L K V D L V A K E L L R		
Spg7 (M. m.)	(685)	G I G R R P F S Q G L Q Q M M D H E A K I L V A K A Y R H T E K V L L D N L D K L Q A L A N A L L E		
Afg312 (M. m.)	(682)	M V L E K P Y S E A T A R M I D D E V R I L I S D A Y R R T V A L L T E K K A D V E K V A L L L L E		
Afg311 (M. m.)	(675)	T M V E K P Y S E A T A Q L I D E V R C L V R S A Y N R T L E L L T Q C R E Q V E K V G R R L L E		
SPG7 (H. s.)	(685)	G I G R R P F S Q G L Q Q M M D H E A R I L V A K A Y R H T E K V L Q D N L D K L Q A L A N A L L E		
AFG3L2 (H. s.)	(683)	M V L E K P Y S E A T A R L I D D E V R I L I N D A Y K R T V A L L T E K K A D V E K V A L L L L E		
		801		850
FtsH (Th. th.)	(579)	R E T L T A E E F Q R V V E G L P L E A P E E A R E E E P P R ----- V P K V K P G G		
Yta12 (S. c.)	(771)	K E V L T R E D M I D L L G K R P P - E R N D A F D K Y L N D Y -- E T E --- K I R K E E E K N		
Yta10 (S. c.)	(717)	K E A I T R E D M I R L L G P R P F K - E R N E A F E K Y L D P ----- K S N		
Spg7 (M. m.)	(735)	K E V I N Y E D I E A L I G P P P H G P K K M I A P Q K W I D A E ----- K E R Q A S G E		
Afg312 (M. m.)	(732)	K E V L D K N D M V L L G P R P F T - E K S - T Y E E F V E G T G S L D E D T S L P E G L Q D W N		
Afg311 (M. m.)	(725)	K E V L E K A D M I E L L G P R P F A - E K S - T Y E E F V E G T G S L E D T S L P E G L K D W N		
SPG7 (H. s.)	(735)	K E V I N Y E D I E A L I G P P P H G P K K M I A P Q R W I D A Q ----- R E K Q D L G E		
AFG3L2 (H. s.)	(733)	K E V L D K N D M V E L L G P R P F A - E K S - T Y E E F V E G T G S L D E D T S L P E G L K D W N		
		851		873
FtsH (Th. th.)	(620)	A L G G A -----		
Yta12 (S. c.)	(815)	E K R N E P ----- K P S T N ---		
Yta10 (S. c.)	(751)	T E P P E A ----- P A A T N ---		
Spg7 (M. m.)	(776)	E E A P A P -----		
Afg312 (M. m.)	(780)	K E R E K E E K K E K E K E E P L N E K V V S		
Afg311 (M. m.)	(773)	K G R E E G G ----- T E R G L Q E S P V -		
SPG7 (H. s.)	(776)	E E T E E T Q Q P P L G G E E P T W P K ---		
AFG3L2 (H. s.)	(781)	K E R E K E ----- K E E P P G E K V A N		

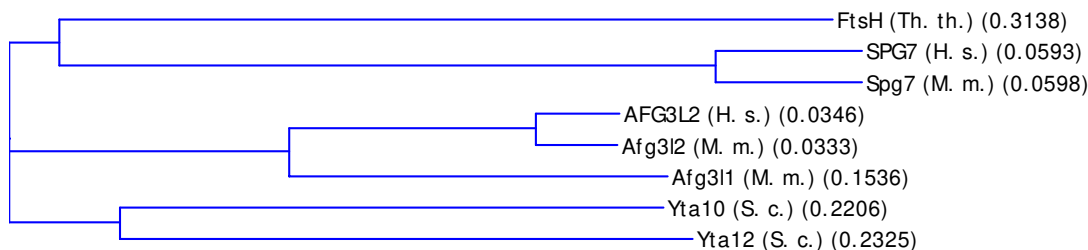


Figure 22: Phylogenetic dendrogram showing the relationship of *m*-AAA protease subunits.

The phylogenetic tree is based on the ClustalW alignment shown above and generated with the AlignX program of Vector NTI (Invitrogen).

6.3.2. MAIP1 and JHEbdp29

MAIP1 and juvenile hormone binding protein 29 share 18 % sequence identity and 32 % similarity.

JHEbp29 (D. m.)	(1)	1	-----	50
C2ORF47 (H. s.)	(1)	MALAARLLPQFLHSRSLPCGAVRLRTPAVA	EVRLPSATL	CYFCRCR
JHEbp29 (D. m.)	(13)	51	RISLMR	LQPRPTV
C2ORF47 (H. s.)	(51)	AALFPR	SARALAA	SA
JHEbp29 (D. m.)	(63)	101	ESLNRLPRLMDFPE	IV
C2ORF47 (H. s.)	(99)	EEKPQQHQKTKMIV	LG	SNP
JHEbp29 (D. m.)	(113)	151	AKQA	LQV
C2ORF47 (H. s.)	(148)	AKQA	FAH	VS
JHEbp29 (D. m.)	(163)	201	ES	DI
C2ORF47 (H. s.)	(198)	IDE	IV	FT
JHEbp29 (D. m.)	(211)	251	-EIPWN	M
C2ORF47 (H. s.)	(244)	SVFQVK	L	GNQNVETKQ
JHEbp29 (D. m.)	(260)	301	NETI	
C2ORF47 (H. s.)	(292)	----		

6.3.3. MICS1 and YccA

MICS1 and YccA have 11% sequence identity and 25% similarity.

YccA (E. c.)	(1)	1	-----	50
MICS1 (H. s.)	(1)	MLAARLVCLRTLPSRVFHPAFTKASP	VVKNSITKNQWLLTPSREYATKTR	
YccA (E. c.)	(1)	51	-----	100
MICS1 (H. s.)	(51)	IGIRRGRTGQELKEAALEPSMEKIF	KIDQMGRWFVAGGA	VGLGALCYYG
YccA (E. c.)	(1)	101	---MDR	IV
MICS1 (H. s.)	(101)	LGLSNE	IG	AEKAVIWPQYVKDRIHS
YccA (E. c.)	(48)	151	PSPGL	L
MICS1 (H. s.)	(151)	LMNF	MM	RGSWVTI
YccA (E. c.)	(91)	201	GP	IL
MICS1 (H. s.)	(201)	GAVV	APL	TIL
YccA (E. c.)	(141)	251	G	IV
MICS1 (H. s.)	(251)	GL	GL	V
YccA (E. c.)	(186)	301	G	ETN
MICS1 (H. s.)	(301)	RA	EV	SPMYGVQKYDP

7. Zusammenfassung

Mitochondrien besitzen ein Qualitätskontrollsystem für Proteine, das aus verschiedenen Proteasen unterschiedlicher Lokalisation besteht, um falsch gefaltete und nicht assemblierte Proteine abzubauen. Ein wichtiger Bestandteil dieses Systems in der inneren Mitochondrienmembran ist die *m*-AAA Protease, die als ATP-abhängige oligomere Metalloprotease ihr aktives Zentrum zur Matrix exponiert. Die *m*-AAA Proteasen im Menschen bilden sowohl hetero- als auch homo-oligomere Komplexe aus den Untereinheiten AFG3L2 und SPG7 aus. Eine dritte Untereinheit in Mäusen (Afg3l1) resultiert in einer Vielzahl möglicher Isoenzyme in der inneren Mitochondrienmembran. Mutationen oder Deletionen verschiedener Untereinheiten der humanen *m*-AAA Proteasen führen zu Neurodegenerationen in unterschiedlichen Regionen des zentralen aber auch peripheren Nervensystems. Somit scheint eine bestimmte Zusammensetzung von aktiven Isoenzymen in unterschiedlichen Gewebe vor allem aber in Neuronen erforderlich ist. Eine weitere Funktion der *m*-AAA Protease – zumindest in Hefe – ist die spezifische Prozessierung von Proteinen. Welche Aktivität zur Pathogenese der assoziierten Krankheiten beiträgt ist unklar, weil die Funktion der menschlichen *m*-AAA Proteasen auf zellulärer und molekularer Ebene und damit auch der Hintergrund der verschiedenen Krankheitszustände nicht bekannt sind. Die Säuger *m*-AAA Proteasen wurden mit der Prozessierung der Dynamin-ähnlichen GTPase OPA1 in Verbindung gebracht. Dies impliziert eine Rolle der *m*-AAA Proteasen bei der mitochondrialen Fusion. Um die Funktion der *m*-AAA Proteasen innerhalb der Mitochondrien vollständig zu entschlüsseln ist es nötig weitere Substrate der Proteasen zu identifizieren.

In dieser Arbeit konnte eine dominant negative Mutation im Walker B Motiv der ATPase Domäne in der *m*-AAA Protease Untereinheit AFG3L2/Afg3l2 identifiziert werden. Die Expression dieser dominant negativen Mutation in humanen Zelllinien ermöglichte die Generierung eines *m*-AAA Protease Komplexes, der als Substratfalle fungierte. Mit Hilfe dieses Ansatzes konnten mögliche neue Bindungspartner und Substrate der Protease identifiziert und damit auch die molekulare Funktion der Protease geklärt werden. So befinden sich die *m*-AAA Proteasen mit den Prohibitinen in der inneren Mitochondrienmembran in einem Superkomplex, der Zellwachstum und durch die Stabilisierung von langen OPA1 Isoformen die mitochondriale Fusion kontrolliert. Gleichzeitig interagieren die Proteasen mit SLP2 und regulieren möglicherweise in einem weiteren Superkomplex stress-induzierte Hyperfusion. Unreifes AFG3L2 (mit mitochondrialer Präsequenz) und MICS1 ein Protein in der inneren

Mitochondrienmembran, konnten als mögliche Substrate identifiziert werden. MICS1 ist essentiell für die Cristae Morphogenese und soll bei Apoptose eine Rolle spielen.

Mit Hilfe dieser Arbeit konnten *m*-AAA Proteasen mit zellulären Funktionen wie mitochondriale Morphologie, Cristae Organisation und Apoptose in Zusammenhang gebracht werden. Diese Arbeit könnte daher dazu beitragen, die molekularen Ursachen von Neurodegenerationen, die mit Mutationen von humanen *m*-AAA Protease Unterheiten assoziiert sind, aufzudecken.

8. Danksagung

Dank sagen möchte ich vor allem Prof. Dr. Thomas Langer, dafür dass er mich während dieser Arbeit unterstützt, gefördert aber auch gefordert hat. Vielen Dank für die vielen Anregungen und Freitag-Morgen-Diskussionen. Aber auch sonst „stand die Tür für mich immer offen“!

Ganz besonderen Dank an meinen 2. Gutachter und ehemaligen Diplomarbeitsbetreuer Prof. Dr. Mats Paulsson für seine Bereitschaft, mir auch während dieser Arbeit mit wissenschaftlichen Ratschlägen zur Seite zu stehen.

Prof. Dr. Guenter Schwarz danke ich, daß er sich bereit erklärt hat, den Prüfungsvorsitz zu übernehmen.

Des Weiteren möchte ich mich bei Dr. Andrea Bernacchia und Prof. Dr. Elena Rugarli für die gute Zusammenarbeit und die Messungen der mitochondrial Respiration herzlichst bedanken.

Ich danke auch den Korrektoren, die ein wenig mehr Ordnung in diese Arbeit gebracht haben, allen voran Gerrit (fürs „Mittwochs-Schwimmen“ und dafür, dass wir so gute Freunde geworden sind), Julia H. (für die vielen wissenschaftlichen Ratschläge und die Freundschaft), Casi (der immer hilft), Sarah (für Griechenland) und Claudia (für das „Wilmes-Lachen“).

Ich danke meinen jetzigen und ehemaligen Sport- und Kletterfreunden Christof (fürs Aushalten neben mir im Labor), Sascha und Julia F. (Euch beiden ganz besonders für immer ein offenes Ohr), Tanja (fürs gemeinsam Durchstehen und die schönen Yogastunden), Marion, Daniela G., Anke, und natürlich allen ehemaligen und jetzigen Mitgliedern der Arbeitsgruppe von Thomas Langer für das tolle Zusammenarbeiten und die gute Stimmung im Labor: Anne, Christoph, Metodi, Daniela T., Takashi, Mafalda, GuZi, Kami, Sebastian, Mirko, Mark, Thorsten, Biesi, Marina, Florian G., Steffen, Dominik, Isabell, Olaf, Joanna, Fabian, Florian B., Sabrina, Justus, Oliver, Brigitte und zu guter Letzt Susanne Scheffler, die mich immer mit allem versorgt hat, was ich brauchte: Briefmarken, Chemikalien und Gespräche. Ich danke allen von der zweiten Etage für die gruppenübergreifende tolle und bestmögliche Arbeitsatmosphäre.

Zuletzt danke ich meiner Familie und meinen Freunden, die mir während dieser ganzen Zeit beigestanden haben und den Abschluss dieser Arbeit ermöglicht haben.

9. Eidesstattliche Erklärung

Ich versichere, dass ich die von mir vorgelegte Dissertation selbständig angefertigt, die benutzten Quellen und Hilfsmittel vollständig angegeben und die Stellen der Arbeit – einschließlich Tabellen, Karten und Abbildungen –, die anderen Werken im Wortlaut oder dem Sinn nach entnommen sind, in jedem Einzelfall als Entlehnung kenntlich gemacht habe; dass diese Dissertation noch keiner anderen Fakultät oder Universität zur Prüfung vorgelegen hat; dass sie – abgesehen von unten angegebenen Teilpublikationen – noch nicht veröffentlicht worden ist sowie, dass ich eine solche Veröffentlichung vor Abschluss des Promotionsverfahrens nicht vornehmen werde. Die Bestimmungen der Promotionsordnung sind mir bekannt. Die von mir vorgelegte Dissertation ist von Herrn Prof. Dr. Thomas Langer betreut worden.

Köln, im März 2009

Ines Raschke

Teilpublikationen im Rahmen dieser Arbeit:

Ehse, S., **I. Raschke**, A. Bernacchia, S. Geimer, D. Tondera, J.-C. Martinou, B. Westermann, E. I. Rugarli, and T. Langer. Regulation of OPA1 processing and mitochondrial fusion by *m*-AAA protease isoenzymes and OMA1. *J. Cell Biol.* accepted.

Tondera, D., S. Grandemange, A. Jourdain, M. Karbowski, Y. Mattenberger, S. Herzig, S. Da Cruz, P. Clerc, **I. Raschke**, C. Merkwirth, et al. 2009. SLP-2 is required for stress-induced mitochondrial hyperfusion. *EMBO J.* 28:1589-1600.

10. Lebenslauf

■ Persönliche Daten

Name und Anschrift: Ines Raschke, Remscheider Str. 18a, 51103 Köln
Geburtsdaten: 16.04.1980 in Hildesheim
Staatsangehörigkeit: deutsch
Familienstand: ledig

■ Schule und Studium

seit 2004 wissenschaftliche Angestellte am Institut für Genetik der Universität zu Köln, bei Prof. Dr. Thomas Langer
Promotion zum Thema „*Mammalian m-AAA Proteases as Key Regulators of Mitochondrial Function – Analysis of Dominant Negative Mutant Variants*“
angestrebter Abschluss: Dr. rer. nat.
(Disputation 15. Mai 2009)

1999 – 2004 Studium der Biologie an der Universität zu Köln
Schwerpunkte: Biochemie, Genetik und Pharmakologie
Diplomarbeit zum Thema „Klonierung und Charakterisierung eines neuen extrazellulären Matrixproteins der EC-Domänenfamilie“, bei Prof. Mats Paulsson, Institut für Biochemie II, Medizinische Fakultät der Universität zu Köln
Abschluss: Diplom

1992 – 1999 Goethegymnasium Hildesheim
Abschluss: Allgemeine Hochschulreife

1990 – 1992 Orientierungsstufe Bad Salzdettfurth

1986 – 1990 Grundschule Bodenburg

■ Publikationen

Ehses, S., **I. Raschke**, A. Bernacchia, S. Geimer, D. Tondera, J.-C. Martinou, B. Westermann, E. I. Rugarli, and T. Langer. Regulation of OPA1 processing and mitochondrial fusion by *m-AAA* protease isoenzymes and OMA1. *J. Cell Biol.* accepted.

Tondera, D., S. Grandemange, A. Jourdain, M. Karbowski, Y. Mattenberger, S. Herzig, S. Da Cruz, P. Clerc, **I. Raschke**, C. Merkwirth, et al. 2009. SLP-2 is required for stress-induced mitochondrial hyperfusion. *EMBO J.* 28:1589-1600.